# Adigrat Sandstone in Northern and Central Ethiopia:
## Stratigraphy, Facies, Depositional Environments and Palynology

Vorgelegt von
Diplom-Geowissenschaftler
Dawit Lebenie Enkurie

Von der Fakultät VI – Planen Bauen Umwelt
der Technischen Universität Berlin
zur Erlangung des akademischen Grades

"Doktor der Naturwissenschaften"

(Dr. rer. nat.)

genehmigte Dissertation

Promotionsausschuss:

Vorsitzender: Prof. Dr. rer. nat. Gerhard Franz
Berichter: Prof. Dr. rer. nat. Wilhelm Dominik
Berichter: Prof. Dr. rer. nat. Eberhard Klitzsch
Berichter: Dr. Robert Bussert

Tag der wissenschaftlichen Aussprache: 04. Mai 2010

**Berlin 2010**

**D 83**

# Adigrat Sandstone in Northern and Central Ethiopia: Stratigraphy, Facies, Depositional Environments and Palynology*

**von**

**Dawit Lebenie Enkurie****

## Zusammenfassung

In Nord- und Zentral-Äthiopien sind bis zu 430 m mächtige, kontinentale und flachmarine klastische Sedimentfolgen aufgeschlossen, die als 'Adigrat-Sandstein' bezeichnet werden. In der vorliegenden Arbeit wurde auf Grundlage detaillierter stratigraphischer, sedimentfazieller und palynologischer Untersuchungen dieser Schichtenfolgen im Mekelle- und Blauen-Nil-Becken ein umfassendes Bild des zeitlichen und räumlichen Aufbaus der 'Adigrat-Sandsteine' erarbeitet, wobei auch neue Erkenntnisse über die Entwicklungsgeschichte dieser Sedimentbecken gewonnen wurden. Darüber hinaus wurde die stratigraphische Stellung der Sedimentfolge mit Hilfe von Palynomorphen geklärt.

Die Schichtenfolge des 'Adigrat-Sandsteins' (Obertrias–Mitteljura) wird in drei durch Diskordanzen (Hiaten) voneinander getrennte stratigraphische Einheiten gegliedert. Die unterste Einheit (*Einheit I*) wurde im Keuper (oberstes Karn–unterstes Rhät) unter tidal-ästuarinen und sturm-dominierten Bedingungen flachmarin abgelagert. Die Transport-richtungen der Sedimente und die nach Nordosten hin zunehmende Mächtigkeit des keilförmigen Sedimentkörpers weisen darauf hin, dass die Sedimente in einem weiträumigen, flachen, nach Nordosten zur Neotethys hin geöffneten Golf abgelagert wurden. Dies bedeutet, dass sich in der Obertrias von Nordosten her ein flacher Meeresgolf über die arabische Plattform und Nord-Äthiopien höchstwahrscheinlich bis nach Zentral-Äthiopien hinein erstreckt hat. Diese sich in der oberen Trias über Südarabien bis nach Äthiopien erstreckende Meeresbucht der Neotethys ist eine wesentliche Neuerkenntnis zur Paläogeographie der Region.

Die nächstjüngere stratigraphische Einheit (*Einheit II*) wurde im Untertoarcium abgelagert. In Bezug auf Sedimentfazies und Ablagerungssysteme besteht diese Einheit im Mekelle-Becken aus fluvio-deltaischen Sedimenten, die in einem aktiven Riftbecken abgelagert wurden. Im Blauen-Nil-Becken bestehen die Sedimente dagegen aus Ablagerungen von Barriere-Inseln und Gezeitenkanälen eines ‚*barrier/inlet-spit*'-Systems. Die gleichbleibende Transportrichtung der Schichtenfolge der Einheit II in den voneinander getrennten Sedimentbecken belegt einen generell nach Südosten geneigten Kontinentalrand. Die Änderung der nach Nordosten gerichteten Sedimentschüttungen nach Südosten deutet auf den Einfluß des beginnenden Riftings zwischen Ost- und Westgondwana während des Toarciums und eine lokale Beckeninversion hin.

---

* Von der Fakultät VI – Planen Bauen Umwelt der Technischen Universität Berlin zur Erlangung des akademischen Grades "Doktor der Naturwissenschaften" (Dr. rer. nat.) genehmigte dissertation (D 83).
Tag der wissenschaftlichen Aussprache: 04. May 2010
Vorsitzender: Prof. Dr. G. Franz
Berichter: Prof. Dr. W. Dominik, Prof. Dr. E. Klitzsch und Dr. R. Bussert
** Anschrift des Verfassers: Explorationsgeologie, TU Berlin, Sekr. ACK 1-1, Ackerstraße 76, 13355 Berlin

Die oberste stratigraphische Einheit (*Einheit III*) - die nur im Mekelle-Becken ausgebildet ist - wurde im Obertoarcium–Untercallovium abgelagert, während sich im Blauen-Nil-Becken in dieser Zeit Evaporite bildeten. Die zu dieser Zeit einsetzende Entwicklung eines transgressiven Barrieren-Lagunen-Systems im Mekelle-Becken steht vermutlich in Verbindung mit dem fortschreitenden Rifting zwischen Ost- und West-gondwana. Der Wechsel von einem 'Gilbert-Typ'-Delta zu einem Barrieren-Lagunen-System deutet darauf hin, dass hierbei ein störungskontrolliertes, sich rasch vertiefendes Becken in eine Meeresstraße mit einem geringen Küstengradienten überging. Die landwärtige Verlagerung der Barrieren-Lagunen-Komplexe wird auf die von Südosten her vorgreifende Transgression zurückgeführt, wobei vermutlich der Meeresspiegelanstieg die Sedimentzufuhr überstieg. Mit dem danach erneut einsetzenden relativen Abfall des Meeresspiegels wurden die zuvor abgelagerten barriere-formenden Sandsteine zunehmend durch zahlreiche Gezeitenkanäle eingeschnitten. Gleichzeitig entstanden daneben progradierende Gezeiten- und Strandebenen.

Pollen und Sporen aus 16 produktiven Oberflächenproben des 'Adigrat-Sandsteins' wurden drei informellen Sporomorph-Vergesellschaftungen zugeordnet. In aufsteigender Reihenfolge sind dies die Vergesellschaftungszonen AZ I: Obertrias (oberstes Karn–unterstes Rhät); AZ II: später Unterjura (Untertoarcium) und AZ III: später Unterjura–Mitteljura (Obertoarcium–Untercallovium). Die wesentliche Merkmale der AZ I sind die Dominanz von 'non-taeniaten', bisaccaten Gymnospermen-Pollen (hauptsächlich *Falcisporites*), der niedrigere Anteil von Pteridophyten-Sporen und das Fehlen von Pollen der 'taeniaten' bisaccaten- und Araucariaceae-Typen. AZ II wird durch die Vorherrschaft von inaperturaten Gymnospermen-Pollen (*Classopollis*, *Araucariacites* und *Callialasporites*) und laevigaten trileten Pteridophyten-Sporen charakterisiert. AZ III wird von trileten Sporen dominiert, die eine vielgestaltige Skulptur besitzen (*Ischyosporites*, *Klukisporites*, *Converrucosisporites* und *Neoraistrikia*). Trilete Sporen mit striaten Skulpturen (z.B. *Cicatricosisporites*) fehlen. Mit diesem Ergebnis konnte erstmals palynologisch eine stratigraphische Gliederung der Sedimentabfolge erzielt werden.

## Abstract

In northern and central Ethiopia, continental to shallow-marine siliciclastic sediments of up to 430 m thick are exposed. These sediments are referred to as the 'Adigrat Sandstone'. This study provides a detailed investigation of the stratigraphy, sedimentary facies, depositional environments and palynology of the 'Adigrat Sandstone' succession in the Mekelle and Blue Nile basins in order to obtain a complete picture of the large-scale spatial/temporal stacking patterns of depositional systems, whereby a new knowledge of the mode of evolution of the basins and the mechanisms controlling their formation can be obtained. The study also provides a more reliable stratigraphic position for the sandstone succession based on palynological data.

Three unconformity bounded stratigraphic units have been identified within the Late Triassic to Middle Jurassic 'Adigrat Sandstone' succession. *Unit I* that represents the lower stratigraphic unit in both basins is Late Triassic (Late Carnian–Early Rhaetian) in age. It is composed of transgressive tide-dominated estuarine and prograding storm-dominated shoreface deposits. The overall northeastward-thickening wedge-shaped geometry of the depositional body and the palaeocurrent patterns in both basins suggest that the sediments accumulated on a vast slowly subsiding passive continental margin in a shallow gulf, which extended northeast into the Neotethys. This indicates that the Late Triassic shallow gulf, which encroached into the Arabian platform from the northeast, had most probably reached the northern and central parts of Ethiopia. A Neotethyan seaway through Saudi Arabia into

Ethiopia has an important bearing on the palaeotectonic and palaeogeographic scenario of the region at that time.

The second stratigraphic unit (*Unit II*) is Late Liassic (Early Toarcian) in age. No direct similarity can be inferred regarding facies successions and depositional systems within *Unit II* in the two basins. In the Mekelle Basin, the unit is composed of coarse-grained sandstones and conglomerates of fluvial and deltaic origin whereas in the Blue Nile Basin the unit is of barrier/inlet-spit origin. The fluvio-deltaic deposits in the Mekelle Basin have been accumulated in an active rift basin. The key similarity in the strata of *Unit II* in both basins is their similar palaeocurrent patterns, indicating deposition on a SE-dipping divergent continental margin. The abandonment of the previously existing NE-dipping continental margin and its replacement by a SE-dipping one can be best explained by rifting and basin inversion, which is most probably associated with the break-up of East and West Gondwana that commenced during the Toarcian.

The uppermost stratigraphic unit (*Unit III*), which is recognised only in the Mekelle Basin, is Middle Jurassic (Late Toarcian to Early Callovian) in age. This phase corresponds to delta abandonment and the inception of transgressive barrier-lagoon system, which is most probably related to the continuous crustal thinning and subsidence along the evolving rift between East and West Gondwana. The transition from a 'Gilbert-type' delta to a barrier-lagoon system suggests that the basin has evolved from a possibly fault-controlled, broadly downwarping basin to a cratonic seaway characterised by a low gradient coastal to nearshore profile. The landward migration of the barrier-lagoon complex is attributed to the marine transgression progressing from the southeast as the rate of sea level rise exceeds the rate of sediment supply. As relative sea level started to fall, the elongate shoestring sand bodies of the uppermost barrier were destructed and cannibalised by a number of tidal inlet channels, which cut through them. Barrier destruction was concomitantly accompanied by the establishment of prograding open-coast tidal flats and strandplains.

Based on 16 productive samples collected at different stratigraphic levels, three informal palynological assemblage zones have been identified within the Adigrat Sandstone succession in the Mekelle and Blue Nile basins. These assemblage zones, in ascending order, are: AZ I, Late Triassic (Late Carnian–Early Rhaetian); AZ II, latest Early Jurassic (Early Toarcian); and AZ III, latest Early–Middle Jurassic (Late Toarcian–Early Callovian). The principal characteristics of AZ I are the dominance of non-taeniate disaccate gymnospermous pollen, mainly belonging to *Falcisporites*, the low proportion of pteridophyte spores and the absence of taeniate disaccate and Araucariaceae-type pollen. AZ II is characterised by the predominance of inaperturate gymnospermous pollen (*Classopollis*, *Araucariacites* and *Callialasporites*) and of pteridophyte spores (mainly laevigate trilete spores). Disaccate pollen grains, which dominated AZ I, become extremely rare and are represented by few specimens of *Alisporites*. AZ III is dominated by trilete spores that possess extremely diverse sculptural types, amongst which *Ischyosporites*, *Klukisporites*, *Converrucosisporites* and *Neoraistrikia* are the most prominent forms. Trilete spores with striate sculpture (e.g., *Cicatricosisporites*) and disaccate pollen are entirely absent. These palynological results allow for the first time a better biostratigraphic subdivision of the Adigrat Sandstone succession and its correlation with equivalent units in the region.

**Acknowledgements**

This research work would have never been successfully undertaken without the unreserved support of Dr. Robert Bussert and Prof. Dr. Wilhelm Dominik. I would like to express my deepest gratitude to Dr. Robert Bussert for his regorous interest and willingness to accompany me during my fieldwork and for sharing me his profound knowledge and experience of geological fieldwork. His continued discussion and critical comments helped me a lot to improve and refine the final draft of the thesis. His overall support over the past four years has been an outstanding measure of friendship and professionalism.

I am deeply indebted to Prof. Dr. Wilhelm Dominik for his willingness to supervise my thesis, for his uninterupted encouragement, intelectual advice and financial support. Special thanks are due to Dr. Eckart Schrank for his valuable guidance regarding my palynological work and to Dr. Peter Luger for his assistance in my micropalaeontological investigation.

Financial support for the fieldwork was partly provided to me by the Deautsche Akademische Austauch Dienst (DAAD), for which I am very thankful. I want to acknowledge Addis Ababa University and Mekelle University in general and Dr. Balemwal Atnafu and Dr. Nata Tadesse in partucular for providing me all the necessary support letters that were very vital for the successful completion of my fieldwork.

During my laboratory work, I received enormous assistance from Ms. Conni von Engelhardt and Ms. Cordelia Lange, for which I am very grateful. During my graphic works and overall computer related difficulties, I received considerable help from Mr. Manfred Thiel which I would like to appreciate. Mr. Bernd Kleeberg is thanked for helping me with phtographic works.

Lastly, my special thanks go to all my family Mam and Dad, my children Lilli and Lucy and my sister Lakech for their longlasting support, patience and understanding.

# Contents

# 1. Introduction

## 1.1 Geographic features

The main geomorphologic features of Ethiopia, a part of East Africa (also called the 'Horn of Africa'), are the Northwestern Plateau (NWP) and the Southeastern Plateau (SEP) that are separated by the Ethiopian Rift Valley (ERV) (Fig. 1a). The study was conducted in two areas located in the northern and central parts of the Northwestern Plateau, which are referred to as the Mekelle and the Blue Nile areas respectively.

The first study area lies between latitudes 13°00' to 14°00' N and longitudes 39°00 to 40°00' E, in and around Mekelle (Fig. 1b), the capital of the Tigrai Province. The area, which is also informally known as 'the Mekelle Outlier', is bounded in the west and north by the Tigre Plateau and in the east by the western escarpment of the Danakil Depression, occupying an area of about 12,000 square kilometers (Beyth 1972b). Accessibility to the Mekelle area is possible through an asphalted highway to the north that extends from the capital Addis Ababa up to Asmara, the capital of Eritrea. The other important roads, which are significant to the accessibility of the sedimentary outcrops, are interconnected all-weather gravel roads that bifurcate from the highway. These include the Mekelle-Abiadi, Mekelle-Samre, Abiadi-Samre, Wukro-Megab and Mekelle-Berhale roads. Most of the areas between these roads are inaccessible to four-wheel drive vehicles. However, numerous interweaved footpaths and stream beds provide additional access during the field work.

The second study area is situated in the Blue Nile canyon of central western Ethiopia, between latitudes 08°45' to 10°30' N and longitudes 36°30 to 39°00' E (Fig. 1c) and covers an area of 55,000 square kilometers. Easy access to the study area is possible through two asphalted highways radiating to the west and northwest from the capital Addis Ababa, the latter crosses the Dejen area. The sedimentary outcrops, which are mainly located in the central part of the canyon (i.e., Fincha, Dedu, Yejube, Amuru and Bekotabo areas), are accessible through all-weather gravel roads that branch from the two highways. The most important ones are the Gedo-Fincha, Bako-Amuru-Bekotabo and Debre Markos-Yejube roads.

In the Mekelle area, the altitude ranges from 1200 m in the southeast and southwest to 2900 m in the north (at Atsbi), whereas in the Blue Nile canyon it ranges from 900 m in the central part to more than 4000 m in the north. This extreme variation in topography, together with the country's location in the tropical zone, controls the climate of the study area. The highlands with altitudes in excess of 2500 m are characterised by mean annual temperatures generally below 15° C and receive rainfall throughout most of the year. In contrast, in lowland areas with altitudes below 1500 m mean annual temperature is higher than 25° C and rainfall is often in short. In the intermediate areas with altitudes between 1500–2500 m temperature falls within the range of 15°–25° C and rainfall is seasonal, with rainy seasons between June–September and between February–March.

The drainage system of the study areas is generally controlled by the gradient of the Northwestern Plateau that gently dips towards the northwest and west. The Giva, Tsaliet, Werii and Arekwa rivers and their tributaries that drain westerly into the Tekeze River are the major elements of the drainage system in the Mekelle area. The Guder, Muger, Fincha, Chemoga, Bir and Jema rivers, all draining into the Blue Nile River (locally called Abay River), constitute the important ones in the drainage system of the Blue Nile canyon.

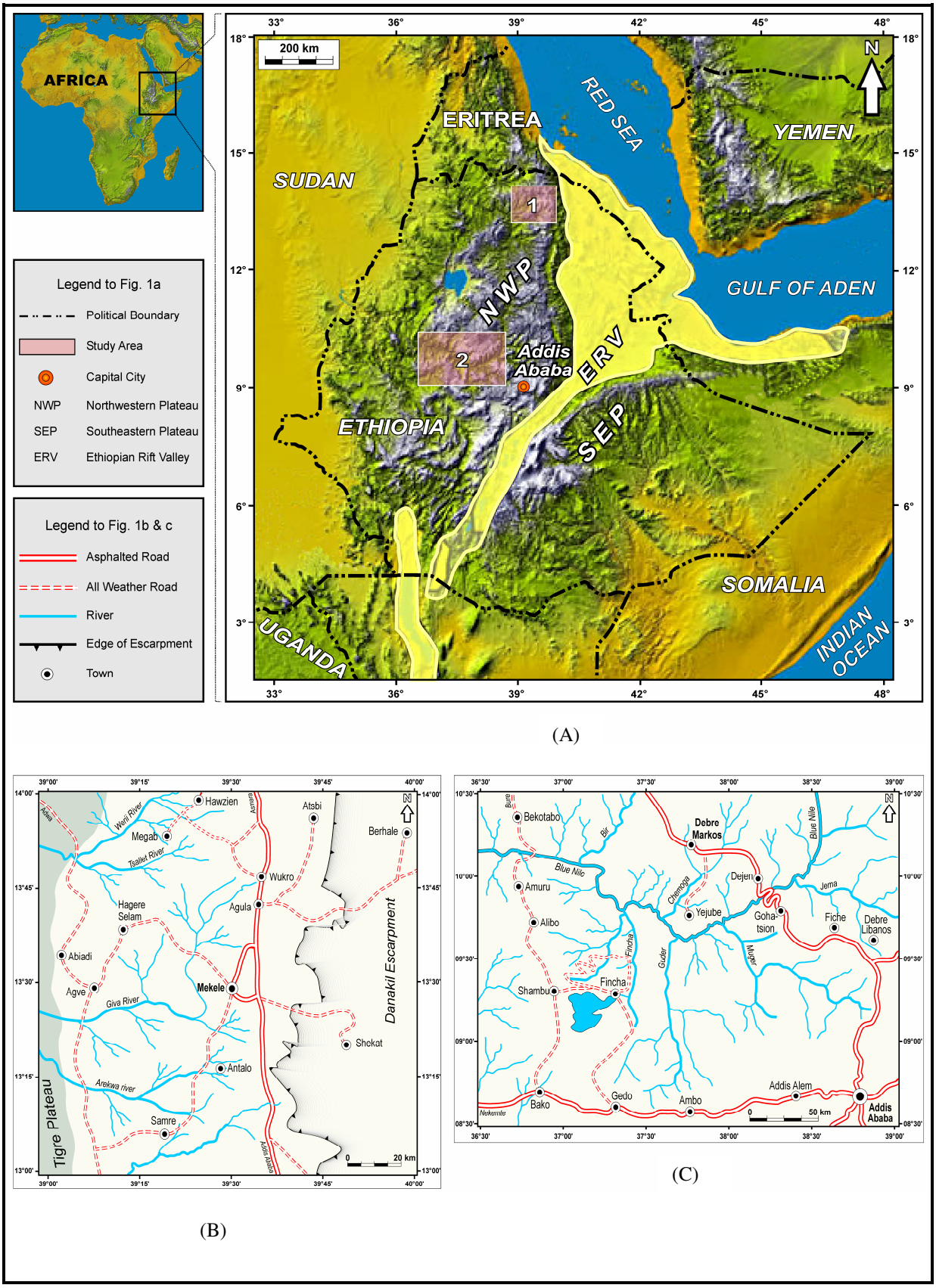


Fig. 1. The geographical setting of the study area. A. Locations of the study area within the framework of the main geomorphologic features of Ethiopia, i.e., the Northwestern Plateau (NWP), the Southeastern Plateau (SEP) and the Ethiopian Rift Valley (ERV). Study areas: 1 – Mekelle Basin; 2 – Blue Nile Basin. B & C. Road accessibilities and major drainage systems of the Mekelle area (left) and the Blue Nile area (right).

## 1.2. Previous work

Geological studies in Ethiopia started in the second half of the 19th century with the first scientific expedition called the 'Napier Expedition' conducted between 1867 and 1868 by W.T. Blanford and his team. The results were published in Blanford (1869, 1870), in which he established the well-known five-fold subdivision of the geology of northern Ethiopia into Basement, Adigrat Sandstone, Antalo Limestone, Upper Sandstone and Trap Series. This was followed by Aubry (1886) and Futterer (1894). Both studies were of reconnaissance nature and did not reach beyond a very schematic description and classification of rock successions.

The most important geological studies started to emerge at the beginning of the 20th century. The first systematic mapping of the region was conducted by Dainelli & Marineli (1912), Krenkel (1925) and Merla & Minucci (1938). A couple of years later, Dainelli (1943) published in Italian language a standard reference work not only for Ethiopia but also for the whole of East Africa. In this work the author made the earliest attempt to explain the sedimentary history of East Africa, including Ethiopia, as the result of a single transgressive-regressive episode. A valuable compilation in English derived mainly from Dainelli's book but also including the observations of Jespen & Athearn (1961, 1962) was made by Mohr (1963) in the form of a textbook called "The Geology of Ethiopia".

Systematic mapping and more detailed description of rocks in specific regions continued throughout the 1970s, which includes the works of Levitte (1970), Arkin et al. (1971), Beyth (1972a) and Garland et al. (1978) in northern Ethiopia and that of Dainelli (1970) in the Blue Nile area. Levitte (1970) compiled a geological map of the Mekelle area at a scale of 1:50,000 with a detailed explanatory report, which has been subsequently modified by Arkin et al. (1971). Garland et al. (1978) and Garland (1980) published a detailed report of the geology of the Adigrat area, including a map of the area at a scale of 1:250,000. Kazmin (1973, 1975) compiled the first geological map at a scale of 1:2,000,000 that covers the whole Ethiopia whereas Merla et al. (1979) compiled a map that covers Ethiopia and Somalia. Tefera et al. (1996) from the Ethiopian Geological Survey attempted to combine the information from Kazmin (1973) and Merla et al. (1979) in one map but they produced a map which is by far of less quality and less informative than the two maps.

Specific studies that focus only on the Palaeozoic and/or Early Mesozoic siliciclastic sediments in northern and central Ethiopia include those of Ficcarelli (1968), Shumburo (1968), Dow et al. (1971), Beyth (1972b, 1973), Canuti & Pirini Radrizzani (1975), Beauchamp (1977), Assefa (1979, 1981, 1991), Saxena & Assefa (1983), Bosellini (1997), Russo et al. (1994), Geletu & Wille (1998), Atnafu (2003), Wolela (1997, 2008), Bussert & Dawit (2009a,b) and Dawit & Bussert (2009). Wolela (1997, 2008) attempted to study the sedimentology of the 'Adigrat Sandstone' in the Blue Nile Basin but he failed to provide new results except reiterating what has already been said by previous workers.

## 1.3. Objective and scope of the present work

The formation of sedimentary basins and the large-scale stacking patterns of depositional systems within their fills are generally controlled by a combination of regional to global causal factors (i.e., allogenic processes that include tectonics, climate and eustasy (Beerbower 1964)) and modifying local environmental processes (i.e., autocyclic processes including local differences in subsidence, supply and composition of sediments). Extensive research is currently being conducted by the petroleum industry and scientific institutions in order to distinguish and understand the relative roles of these factors and to document the larger-scale stratigraphic architecture of sedimentary basin fills. Particular reference has been given to the development of transgressive-regressive facies cycles in response to changes in the rate of sea

level compared to changes in the rate of sedimentation (e.g., Van Wagoner et al. 1990, Posamentier & Allen 1999, Embry 2001, Catuneanu 2002). This method of stratigraphic analysis is immensely valuable to hydrocarbon exploration because it provides the platform for the predictability of facies that are directly relevant to hydrocarbon source rocks, reservoirs, traps and seals. Analysing sedimentary facies where outcrop and subsurface data are available, and predicting facies and depositional trends where these data are lacking, are the basic steps in the workflow of many petroleum companies.

In the case of Ethiopia, hydrocarbon shows have been reported between the Mekelle and the Blue Nile areas (e.g., around Were-Ilu area, Tadesse & Keller 2006). The area is mostly covered by a thick (≥ 2000 m) succession of flood basalts of Tertiary age, making exploration activities difficult. However, the area lies between northern and central Ethiopia where outcrops of Palaeozoic and Mesozoic sedimentary rocks are widespread (Fig. 2.1a & 2.2a). Despite the enormous potential of these outcrops in predicting facies and depositional trends between northern and central Ethiopia, including the areas with oil-shows, the stratigraphic position, the sedimentary facies architecture and depositional environments of these sedimentary rocks are poorly known, as well as the structural evolution of the depositional basins. The results obtained from previous studies provide a contradictory and complex picture. These contrarieties are outlined below.

Regarding the structural evolution, Bosellini (1989, 1997) and Russo et al. (1994) proposed that the Mekelle and Blue Nile basins represent failed arms (aulacogen-like basins) of a multi-branched rift system associated with the break-up of Gondwanaland. In contrast, Beyth (1972b) postulated an intramontane origin for the Mekelle Basin that was formed by the rise of two east-west-trending structural highs, one around 13° N, and another one around 14° N latitudes. Moreover, according to Schandelmeier et al. (1997), the Blue Nile Basin represents a transtensional opening formed by the dextral strike-slip movement along two sub-parallel transcontinental shear zones during severe intraplate deformation of NE Africa. However, Woldetinsae (2005) and Hautot et al. (2006) hypothesised that the basins are simply synclinal structures that reflect the basement topography. Detailed structural and sedimentological investigations are still lacking in order to support or confute these contrasting hypotheses.

The thickness, facies architecture and depositional environments of the 'Adigrat Sandstone' succession are poorly constrained. According to Krenkel (1925), Beyth (1972a, 1972b), Beauchamp (1977), Garland (1980), Bosellini (1989), Russo et al. (1994) and Bosellini et al. (1997), the succession is of purely continental nature deposited in fluvial and/or lacustrine-deltaic environments, whereas Dainelli (1943) hypothesised a transgressive shallow marine depositional environment. A shallow marine origin for the Adigrat Sandstone was also favoured by Merla & Minucci (1938) and Mohr (1962). Merla et al. (1979) even believed that the environment of deposition is marine throughout. Concerning the thickness of the 'Adigrat Sandstone' in the Blue Nile Basin, Russo et al. (1994) measured about 300 m south of Dejen. In contrast, more recently Wolela (2008) gave an account of a 800 m thick continental (alluvial) succession that overlies basement, which he called 'the Triassic–Jurassic Adigrat Sandstone Formation'.

The stratigraphic position of the 'Adigrat Sandstone' succession is mainly based on regional correlation and/or based on the ages of the underlying and overlying formations. In the Blue Nile Basin, a Triassic–Lower Jurassic age was hypothesised for the sandstone succession by Jespen & Athearn (1961, 1964), Mohr (1962, 1963) and Russo et al. (1994), whilst Beauchamp & Lemoigne (1974) assigned a Permo-Triassic age. In the Mekelle basin, the succession was supposed to be of Triassic–Middle Jurassic age (Merla & Minucci 1938, Beyth 1972b). Although the absence of age diagnostic fossils formed a major impediment, no attempts have ever been made to solve these controversial age assignments through a detailed palynological investigation.

Controversial is also the tectonic-palaeogeographic relationships of the Mekelle and Blue Nile basins with adjacent basins in NE Africa and Arabia. Questionable is, on the one hand, the possible genetic relationships of the two basins with 'Karoo' basins of East Africa (i.e., the Ogaden, Mandera-Lugh, Mudugh, Berbera/Borema, Ahl Mado basins, Anza and Lamu grabens), which are supposed to have been formed by intracontinental rifting associated with the break-up of Gondwana (Cannon et al. 1981, Bosellini 1989, Hankel 1993, Wopfner 1993, Russo et al. 1994). On the other hand, a possible genetic relationship might have existed with sedimentary basins in southwestern Ethiopia and southeastern Sudan (i.e., Melut-Gambela, and Muglad-Sudd basins) (Schandelmeier et al. 1997).

Therefore, the main objectives of the geological investigation in the Mekelle and Blue Nile basins during the present work are:

I. to elucidate the facies architecture and depositional environments of the 'Adigrat Sandstone' succession in the two basins;

II. to document the large-scale spatial/temporal stacking patterns of depositional systems within the two basins;

III. to understand the mechanisms controlling the formation of the basins principally from the stratigraphic architectures, so as to constrain the mode of evolution of the basins;

IV. to provide a more reliable stratigraphic position for the 'Adigrat Sandstone' succession based on palynological data;

V. to reconstruct the palaeogeography of the region during the deposition of the sandstone succession and to assess its possible tectonic-palaeogeographic relationships with adjacent regions in NE Africa and Arabia.

## 1.4. Methods

### 1.4.1. Field methods

Four field trips were carried out during this study to investigate the 'Adigrat Sandstone' succession in the Mekelle and Blue Nile areas: September–November 2006; February–April 2007; Februry–March 2008 and March–May 2009. During these field campaigns, a number of detailed sedimentologic sections were logged bed-by-bed to document the facies architecture, the variations in grain-size, physical and biogenic sedimentary structures, degree of bioturbation and type of trace fossils, and contents of body fossils. Furthermore, palaeocurrent directions were recorded using a geologic compass (Freiberger 'Gefügekompass'). The number of measured sections is limited (i.e., twelve sections) due to difficulties arising from the steepness of the outcrop walls, the broad areal extent of the study areas and the protracted length of the sedimentary sections, i.e., usually in excess of 400 m. 370 samples were collected from the various lithologies for laboratory investigation. Sampling intervals are 10–20 m for parts of successions with little or no lithologic changes. In facies successions with rapid lithologic changes, sampling intervals are as narrow as 0.1–0.5 m. Geological traverses and orientations in the field were supported by topographic maps of 1:50,000 scale produced by the Ethiopian Mapping Agency. Locations and thicknesses of measured sections were controlled additionally by GPS-measurements using *Garmin Geko 201* GPS instrument.

### 1.4.2. Laboratory methods

Laboratory investigations were conducted on collected samples to support the macroscopic analysis of field data. These include petrographical analyses, palynological analyses and micropalaeontological analyses, all of which were carried out in the laboratory of the Exploration Geology Department at the Technical University of Berlin. In addition, macrofossils and vertebrate remains including teeth, bone fragments, tooth plates and different kinds of coprolites embedded in firm sandstones were extracted in the laboratory of the Natural Science Museum of Berlin. Taxonomic identifications of the vertebrate fauna were performed with the help of palaeontologists from the museum.

**Petrographic analyses** have been performed under the microscope on 74 selected samples to study the mineralogical composition, grain-size, degree of sorting and roundness, and other features indicative of a particular depositional environment. Analysis of grain-size and mineralogical composition by point-counting and size distribution statistics has brought no meaningful results since, on the one hand, most of the sandstones were found to be compositionally matured quartzarenites, and on the other hand, no significant textural deviations could be seen from the results obtained in the field using a hand lens. However, some thin-sections were particularly useful in assisting the identification of specific depositional environments and sediment sources. For instance, glauconite grains found in some thin-sections indicated a shallow marine depositional environment. Similarly, the presence of heavy mineral lags in association with high degree of grain sorting and roundness observed in thin-sections suggested deposition in a beach foreshore environment.

**Palynological analyses** have been conducted with the primary objective of determining the stratigraphic position of the sedimentary succession. Due to the absence of stratigraphically meaningful fossils, biostratigraphic control has been lacking for the 'Adigrat Sandstone' succession in the Mekelle and Blue Nile basins. Palynological investigation has been carried out on 92 selected mudstone samples collected at different stratigraphic levels of the studied sections. From each sample, 10 grams of sediment was taken and subjected to standard rock maceration procedures involving: (i) manual crushing and mixing of the sediment; (ii) treatment with dilute (10%) HCl-solution to remove carbonate components and subsequent neutralisation with distilled water; (iii) treatment with concentrated (38%) HF-solution to remove the silicate components and subsequent neutralisation with distilled water; (iv) boiling of the residue in a concentrated (37%) HCl-solution to remove fluoride crystals formed during the HF-treatment; (v) sieving of the remaining residue using a 15 µm nylon sieve; (vi) mounting a drop of the residue on glass slides; and (vii) adding glycerine jelly and pressuring a thin cover glass against the slides. Productive slides were screened out under the microscope and then examined to determine the taxa and distribution of palynomorphs. Out of 92 samples processed, only 16 samples were productive. 5 samples were of moderate to low yield and 11 samples yielded rich pollen and spore assemblages, as well as abundant phytoclasts and cuticles. The remaining 76 samples were found to be barren. Photomicrographs of well-preserved and representative pollen and spores were taken by using analogue Camera (Wild Leitz MPS 52) mounted on a petrographic microscope.

**Micropalaeontological analyses** have been performed on 46 selected greenish gray mudstone samples with the purpose of assisting the biostratigraphic age determinations established by means of palynological data, as well as in the interpretation of depositional environments. The extraction of microfossils involved the following preparation steps: (i) disintegration of the samples by saturating with dilute $H_2O_2$-solution, (ii) removing the fine

fraction through sieving with a 0.063 mm sieve, (iii) drying the residue, and (iv) hand-picking the fossils under a binocular microscope. Out of 52 samples processed, 14 samples were found to contain agglutinated foraminifera, predominantly *Ammodiscus* and rarely scolecodont fragments. Photomicrographs of well-preserved fossils were taken by using analogue Camera (Wild Leitz MPS 52) mounted on a binocular microscope.

## 2. Regional geological setting

### 2.1. Introduction

The African continent has experienced a complex history of suturing and rifting during cyclical assembly and dispersal of supercontinents. The geology of Ethiopia, as part of today's Horn of Africa, is the result of this complex orogenic evolution that involves: (i) terrane accretion and collision of Precambrian cratons and mobile belts during the late Neoproterozoic and early Cambrian Pan-African Orogeny (900–550 Ma) (Unrug 1992, Stern 1994), (ii) a relatively tectonic quiescence and associated peneplanation during the Mid-Cambrian to Mid-Ordovician times, (iii) severe regional glaciation and subsequent marine incursions from the Palaeotethys in the Late Ordovician to Early Silurian times, (iv) intracontinental rifting and break-up of Gondwana, which began in the Late Carboniferous and continued until late Cretaceous times (Cannon et al. 1981, Fairbridge 1982, Wopfner 1994), and (v) Tertiary continental flood basalt volcanism, plateau uplift and formation of the East African Rift System (EARS), which was largely related to the evolution of a mantle hot spot underneath the Ethiopian plateau, and the separation of Arabia from northeast Africa (Ebinger et al. 1993, Hofmann et al. 1997, George et al. 1998). Within the global plate-tectonic framework, each of these mega-events, their global causes, their ages and their distribution in space and time impart a distinct stratigraphic signature in the geological evolution of Ethiopia and adjacent regions in East Africa.

The geology of northern and central Ethiopia is characterised by the Precambrian crystalline basement, Palaeozoic and Mesozoic sedimentary successions and the Tertiary continental flood basalts (Trap series) (Fig. 2.1 & 2.2). In the following sections, the crystalline basement and the Trap basalts will be described together for the northern and central Ethiopia since each of them are basically similar in composition and age in the two regions. However, due to conflicting data and stratigraphic subdivisions for the Palaeozoic and Mesozoic sedimentary successions in northern and central Ethiopia a detailed reevaluation of the biostratigraphic data was found to be compelling. Consequently, the sedimentary successions are described separately for the two regions.

### 2.2. The Precambrian Basement

The Precambrian basement of Ethiopia forms a transition zone between the low-grade volcano-sedimentary succession and mafic-ultramafic complexes of the Arabian Nubian Shield (ANS) and the high-grade multiply metamorphosed and deformed schists and gneisses, migmatites, ophiolite fragments and granulites of the Mozambique Belt (MB) (Worku 1996, Stern & Abdelsalam 1998, Tadesse et al. 2000, Braathen et al. 2001, Yiabas et al. 2002, Miller et al. 2003, Stern et al. 2004). Based on field relations, structural style and metamorphic grade, Gilboy (1970) and Kazmin et al. (1978, 1979) classified the Precambrian rocks of Ethiopia into three groups: i) the Lower Complex (Archean cratonic basement), which is composed of the multiply deformed and metamorphosed high-grade gneisses, migmatites and associated granulites, ii) the Middle Complex (Palaeo- to Mesoproterozoic platform cover), which consists of psammitic and pelitic metasediments, and iii) the Upper

Complex (Neoproterozoic mobile belt), which constitutes low-grade rocks of island arc-ophiolite association. According to these authors, the Lower and Middle Complexes correspond to the MB and the Upper Complex to the ANS. This interpretation has been refuted later by the geochronological data of Ayalew et al. (1990) and Worku (1996), who revealed that some of the previously assumed Archean rocks show the same ages as the arc and back-arc complexes of the ANS (ca. 950 to 550 Ma). This traditional classification was, therefore, modified and a two-fold classification was adopted: i) the reworked pre-Pan-African crust and ii) the Pan-African juvenile crust.

Apart from limited geochronological data, there are no isotopic data available to outline the age limit of the reworked pre-Pan-African crust in Ethiopia and to characterize its evolution. Ages of about 2500 Ma in eastern Ethiopia and about 1600 Ma in southern Ethiopia have been recorded from xenolitic zircons from granites, but ages older than Pan-African has not yet been determined in western Ethiopia (Ayalew & Gichile 1990, Ayalew et al. 1990, Teklay et al. 1993, Braathen et al. 2001).

In contrast, the Pan-African juvenile crust is formed between 830 and 650 Ma and was followed by deformation, metamorphism and intensive plutonism that continued until 520 Ma (Worku 1996, Stern & Abdelsalam 1998, Tadesse et al. 2000, Braathen et al. 2001, Yiabas et al. 2002, Miller et al. 2003, Stern et al. 2004). The Ethiopian basement can generally be characterized by the juxtaposition and tectonic intercalation of the low-grade rocks related to the arc-back-arc complexes of the ANS (northeast African ororgenic belt) with those of the high-grade ones related to the MB (southeast African ororgenic belt). These two orogenic belts combined to form the East African Orogen (Stern 1994), that extends from southern Israel and Egypt in the north to Mozambique and Madagascar in the south for more than 5000 km along strike (Stern & Dawoud 1991).

## 2.3. Palaeozoic and Mesozoic Sedimentary Successions

### 2.3.1. Northern Ethiopia

According to Blanford (1869, 1870), Dow et al. (1971) and Beyth (1972a, b), the stratigraphy of northern Ethiopia can be divided into seven units: Basement, Enticho Sandstone, Edaga Arbi Glacials, Adigrat Sandstone, Antalo Limestone, Upper Sandstone (Amba Aradam Formation of Shumburo (1968)) and Trap series (Fig. 2.1). More refinements have been made later by other workers and these will be included in the description and age constraints of each unit, which is outlined below.

#### Enticho Sandstone

The Enticho Sandstone is named after its type section in the town Enticho (N 14°16′/E 39°09′) in northern Ethiopia (Dow et al. 1971). It overlies Neoproterozoic basement rocks with an angular unconformity and has a thickness of up to 200 m in northern Ethiopia. The Sandstone succession, which is predominantly composed of quartzarenites, was interpreted to represent the arenaceous facies of the Edaga Arbi Glacials (Dow et al. 1971, Beyth 1972 a, b, Garland 1980). More recently, however, Bussert & Dawit (2009b) and Dawit & Bussert (2009) recognised a lower subunit of glaciomarine origin and an upper subunit deposited in a shallow-marine environment.

The glaciomarine deposits, as described by Bussert & Dawit (2009b), overlay the Neoproterozoic basement and range in thickness from 70–100 m. They are composed of massive to large-scale trough cross-bedded sandstones and conglomeratic channel fills, interpreted as subaqueous meltwater deposits. In part, diamictites occur in association with

brittle and ductile soft-sediment deformation structures, which are thought to represent shallow marine push-moraine/grounding-line fan complexes. Other indicators of glacigenic depositional conditions include the occurrence of striated surfaces and polymict clast assemblages. Micro crag and tails and the orientation of glacitectonic deformation structures indicate NE-directed glacier flow.

The upper part of the Enticho Sandstone, as described by Dawit & Bussert (2009), represents a slightly northward (seaward) thickening clastic wedge deposited in a shallow epicontinental sea along the southern margin of the Palaeotethys. It overlies Late Ordovician (Hirnantian) glacigenic sediments and is partly overlain by Permo–Carboniferous glacigenic deposits. The thickness ranges from around 80 m in the South to more than 100 m in the North. The sandstone succession is composed of four upward-coarsening units. The lower three progradational units contain successive cross-bed sets, which exhibit bipolar foreset dip directions that resemble large-scale herringbone-type cross-bedding suggesting deposition in a tide-dominated shelf setting. The uppermost unit consists of cross-bed sets with unimodal foresets oriented constantly towards the North, indicating deposition most likely in braid plains and/or braid deltas. The fine-grained sediments in the lower parts of the upward-coarsening units contain traces including *Arthrophycus alleganhensis, Arthrophycus leniares, Scolicia, Didymaulichnus* and rare *Zoophycos* indicating *Cruziana* Ichnofacies. Towards the top of each unit scattered vertical burrows are present that may belong to *Skolithos* Ichnofacies.

Based on fossil siphonoromid impressions, Saxena & Assefa (1983) assigned an Ordovician age for the Enticho Sandstone in general. Bussert & Dawit (2009) assigned a Late Ordovician (Hirnantian) age for the glacigenic lower part because of their similarity with other Hirnantian glacigenic sediments widespread in North Africa and on the Arabian Peninsula. Some of the trace fossils mentioned above, esp. *Arthrophycus alleganhensis*, indicates an Early Silurian age for the overlying shallow marine sediments (Dawit & Bussert 2009). Hence, the succession correlates with other post-glacial (post-Hirnantian) shallow marine sequences in North Africa and the Arabian Peninsula. Its presence in northern Ethiopia suggests that the post-Hirnantian transgression had extended farther southward into Gondwana than thought before.

**Edaga Arbi Glacials**

Dow et al. (1971) first recognised the glacigenic character of the sediments in the lower part of the basal siliciclastic deposits, which they termed as “Edaga Arbi Tillite”. After erecting a type section near the town Edaga Arbi (N 14°02′/E 39°04′) in northern Ethiopia, Beyth (1972 a, 1972b, 1973) named these glacigenic sediments as “Edaga Arbi Glacials”. The Edaga Arbi Glacials consist predominantly of grey, black or purple clay- and siltstones that often contain dispersed pebbles or boulders up to 6 m in diameter (Beyth 1972a). The thickness of the succession is highly variable but attains a maximum thickness of 150 m near its type section.

Based on lithofacies associations, Bussert & Dawit (2009a) subdivided the Edaga Arbi Glacials into two laterally interfingering subunits: (i) a fine-grained lithofacies association composed predominantly silt- and claystones of in part “varve-like” or with dispersed clasts (dropstones) that are interpreted to represent deposition from suspension settling in a glaci-lacustrine environment. The intercalated massive to crudely stratified clast-rich diamictites represent meltout and/or lodgement tills. (ii) a coarse-grained lithofacies association composed of lenses of clast-supported massive to crudely horizontally bedded conglomerates with clasts of up to 30 cm in diameter and trough cross-bedded sandstones. The former represents glacifluvial channel fills and/or glacideltaic deposits whereas the latter is deposited in lake margin settings and in small lacustrine deltas. In conclusion, the Edaga Arbi Glacials are deposited in N-S trending glacial troughs and valleys up to several kilometres wide and

tens of meters deep that are incised into Precambrian basement and into Early Palaeozoic sediments.

Based on recent palynological investigations, latest Carboniferous to Early Permian age has been assigned to the Edaga Arbi Glacials by Bussert & Schrank (2007), which was confirmed by new palynological findings from a number of additional sections. Therefore, the Edaga Arbi Glacials in northern Ethiopia seem to be correlative with similar glacigenic sediments known in many parts of Gondwana deposited during the well-known Permo-Carboniferous Gondwanan glaciation. Correlative equivalents were described in Saudi Arabia (e.g., McClure 1980, 1988) and in Yemen (Kruck & Thiele 1983, El-Nakhal et al. 2002), as well as in Egypt and Sudan (Klitzsch 1983).

**Adigrat Sandstone**

The Adigrat Sandstone, which is the main focus of the present study, was named after the town Adigrat (N 14°16′/E 39°28′) by Blanford (1869). It was later redefined by Levitte (1970), Dow et al. (1971) and Beyth (1972a, b) to include only the upper part of the previous Adigrat Sandstone with its type section near the town Abiadi. The succession is described below according to the information given by these authors. The thickness reaches up to 670 m, thinning westward over a short distance to about 80 m above the Tekeze River and disappearing north of Adigrat-Axum road. The continuation towards the Danakil depression is not yet clear. The succession is divided in to four members: Unit 1 forms a gentle slop at the base of the section and units 2-4 form a cliff above the slope. Unit 1 is composed of white and yellow to brown, well-sorted, fine- to medium-grained sandstones. Bed thickness ranges from 1–15 m and the sandstones contain abundant quart pebbles. Cross-bedding is minor. Unit 2 is composed of poorly sorted medium- to fine-grained reddish sandstones with abundant quartz pebbles. Cross-bedding is common and the sandstones contain ferruginous wood fragments. Unit 3 is made up of friable, medium- to coarse-grained, cross-bedded white quartz sandstones with well-distributed lenses of ferruginous silt that show turbidity structures. Unit 4 consists of fine- to medium-grained yellow to red sandstones interbedded with variegated silt- and claystones. Most of the sandstones in all units are composed of very mature sand, thus they are probably the result of several erosional cycles.

Based on the absence of any trace of fauna, the abundance of ferruginous/lateritic beds and the presence of fossil wood fragments, Beyth (1972a, b) interpreted the sandstones as have been deposited either in estuarine, lacustrine-deltaic or continental environments in a basin, which was frequently subaerial. Similarly, Garland (1980) and Bosellini et al. (1997) suggested a continental depositional environment in a piedmont area or in an intramontane basin. In contrast, Dainelli (1912, 1943), Merla & Minucci (1938) and Merla et al. (1979) proposed a shallow marine origin.

The stratigraphic position of the Adigrat Sandstone in northern Ethiopia is poorly constrained. Only the upper age limit is reasonably well-established by a fairly rich foraminifera fauna (e.g., *Nauitiloculina oolithica*, *Praekurnubia crusei*, *Valvulina* gr. *negeoni*, *Kurnubia palestiniensis*, *Trochamina* sp. and *Cylindroporella* sp.) found at the basal part of the overlying Antalo Limestone to be Late Callovian (?)–Early Oxfordian (Bosellini et al. 1997). The lower boundary is thought to be diachronous (Mohr 1962, Bosellini et al. 1997) and considered by Bosellini et al. (1997) to be “practically impossible to date”. Others (e.g., Merla & Minucci 1938, Beyth 1972b) hypothesised a broadly Triassic age for the lower boundary.

Fig. 2.1. A. Generalised geological map of the Mekelle area (modified after Arkin et al. 1971). B. A schematic cross-section across the Mekelle Basin (not to scale). C. The stratigraphy of northern Ethiopia (See text about the relationship between Antalo Limestone and Agula Shale).

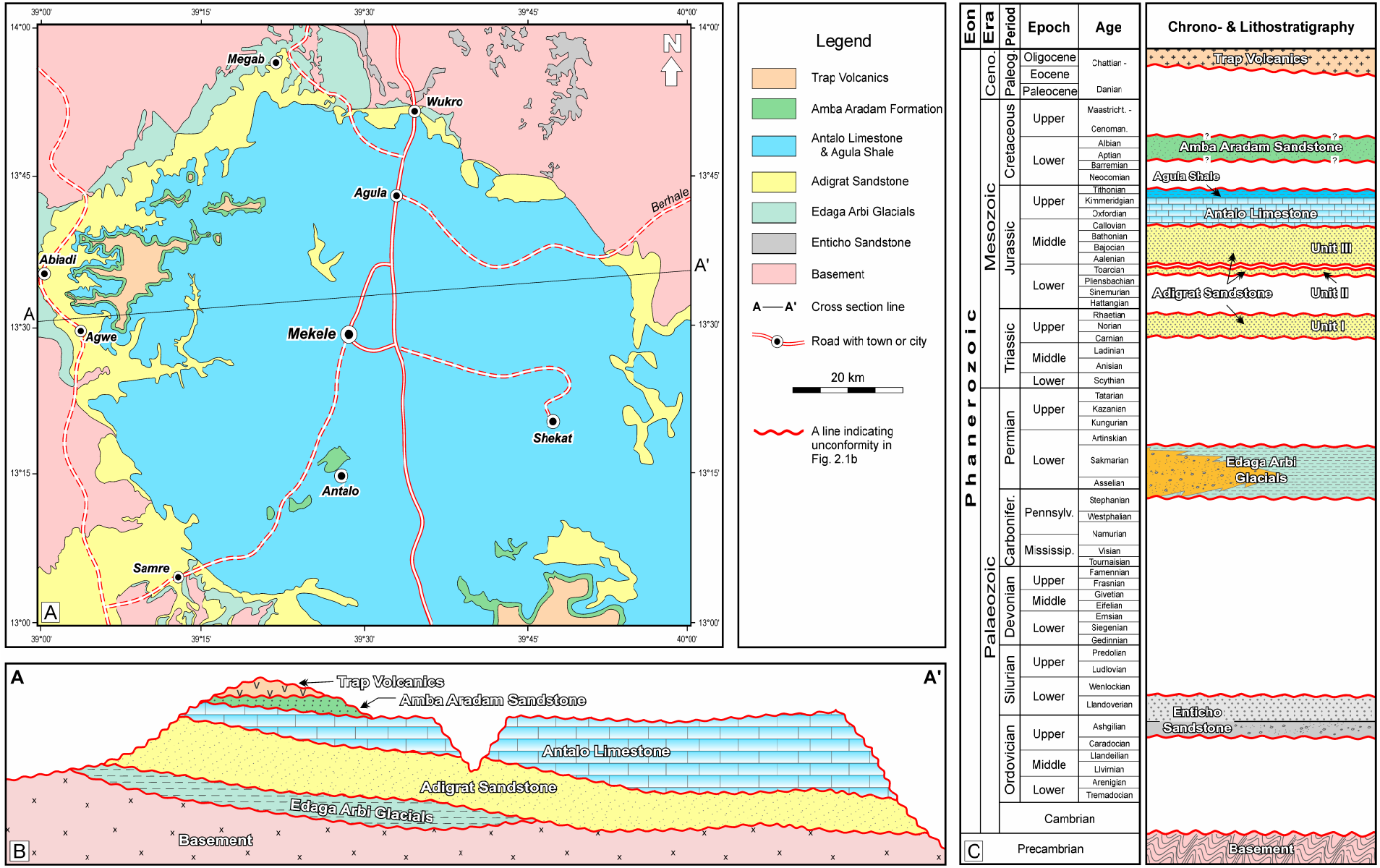
39°00'
39°15'
39°30'
39°45'
40°00'
14°00'
13°45'
13°30'
13°15'
13°00'
N
Megab
Wukro
Agula
Berhale
Abiadi
A
A'
Agwe
Mekele
Shekat
Antalo
Samre
A
Legend
Trap Volcanics
Amba Aradam Formation
Antalo Limestone & Agula Shale
Adigrat Sandstone
Edaga Arbi Glacials
Enticho Sandstone
Basement
A — A' Cross section line
Road with town or city
20 km
A line indicating unconformity in Fig. 2.1b
A
A'
Trap Volcanics
Amba Aradam Sandstone
Antalo Limestone
Adigrat Sandstone
Edaga Arbi Glacials
Basement
B
Eon
Era
Period
Epoch
Age
Phanerozoic
Ceno.
Paleog.
Oligocene
Eocene
Paleocene
Chattian -
Danian
Mesozoic
Cretaceous
Upper
Lower
Maastricht. -
Cenoman.
Albian
Aptian
Barremian
Neocomian
Jurassic
Upper
Middle
Lower
Tithonian
Kimmeridgian
Oxfordian
Callovian
Bathonian
Bajocian
Aalenian
Toarcian
Pliensbachian
Sinemurian
Hettangian
Triassic
Upper
Middle
Lower
Rhaetian
Norian
Carnian
Ladinian
Anisian
Scythian
Palaeozoic
Permian
Upper
Lower
Tatarian
Kazanian
Kungurian
Artinskian
Sakmarian
Asselian
Carboniifer.
Pennsylv.
Mississip.
Stephanian
Westphalian
Namurian
Visian
Tournaisian
Devonian
Upper
Middle
Lower
Famennian
Frasnian
Givetian
Eifelian
Emsian
Siegenian
Gedinnian
Silurian
Upper
Lower
Predolian
Ludlovian
Wenlockian
Llandoverian
Ordovician
Upper
Middle
Lower
Ashgilian
Caradocian
Llandeilian
Llvirnian
Arenigian
Tremadocian
Cambrian
C
Precambrian
Chrono- & Lithostratigraphy
Trap Volcanics
Amba Aradam Sandstone
Agula Shale
Antalo Limestone
Unit III
Adigrat Sandstone
Unit II
Unit I
Edaga Arbi Glacials
Enticho Sandstone
Basement

## Antalo Limestone

The Antalo Limestone was first named by Blanford (1869, 1870) after the town Antalo (N 13°18′/E 39°19′) in northern Ethiopia. The unit was well-described by Levitte (1970), Beyth (1972a, b), Merla et al. (1979), Bosellini et al. (1997) and Matire et al. (2000). According to Beyth (1972a, b), the thickness of the succession ranges from 300 m in the west to 800 m in the east. He identified four different facies, which are briefly outlined, from bottom to top, as follows: (i) a cross-bedded sandy oolite and coquina with minor amount of marl and a few chert beds, with microfauna including mainly corals, gastropods, and echinoids, (ii) interbedding of marl and lithographic limestone with abundant brachiopods and some algal and chert beds, (iii) cliffs of coral and algal reef limestones interbedded with marl and biostromes, and (iv) black to grey microcrystalline limestone interbedded with marl. Bosellini et al. (1997) attempted to subdivided the limestone unit into four depositional sequences (A1 to A4), which are composed of thickening and shallowing up cycles. However, he excluded the lower 30 m thick barrier-lagoon deposits (i.e., his "Transition Beds") from his sequence stratigraphic analysis. These deposits may represent the transgressive part of his "A1 sequence" (sensu Tucker 1996). The limestone succession was deposited in a homoclinal ramp or on a wide cratonic margin gently dipping to the southeast (Bosellini et al. 1997).

A Late Callovian to Kimmeridgian age has been assigned to the Antalo Limestone by Bosellini et al. (1997) based on a rich benthic foraminifera fauna. However, Matire et al. (2000) proposed an Oxfordian to Kimmeridgian age for the unit based on ammonite fauna. By assuming that the Adigrat Sandstone succession was entirely nonmarine, Bosellini (1989) and Bosellini et al. (1997) believed the Jurassic sea first reached the Tigrai province in the Late Callovian. It is yet to see in the present work if that hold true. The Antalo Limestone can be correlated with the limestone unit in the Blue Nile Basin and the Urandab Formation in the Ogaden basin.

## Agula Shale

The "Agula Shale" named after the town Agula (N 13°41′/E 39°35′) in northern Ethiopia after Beyth (1972a) identified a shaly unit at the upper part of the Antalo Limestone. Nonetheless, Bosellini et al. (1997) included the shaly unit to his "Antalo Supersequence". The thickness of the unit may reach up to 300 m. It is composed, from bottom to top, of well-sorted, festoon cross-bedded fine quartzarenites (tidal bars), laminated black shales and mudstones, dolomites and gypsum beds with nodular or chickenwire structures, and oolitic or coquinoid limestones (storm beds) with small gastropods and pelecypods. These facies association is interpreted to represent peritidal, lagoonal and sabkha environments (Beyth 1972a, b, Bosselini et al. 1997). The latter authors reported a fauna including *Modiolus* cfr. *intricatus, Palaeonucula, Corbulomima* and *Placunopsis* and assigned a Late Kimmeridgian age for the unit. The succession is, in places, extensively intruded and dismembered by the Mekelle Dolerites. The presence of carbonate breccia may probably be related to fault systems, which were active towards the end of the Jurassic that might have created some rocky shores or carbonate cliffs (Bosellini et al. 1997). The Agula Shale represents, according to Bosellini (1989), the last regression which led to a general withdrawal of the Jurassic sea from northern Ethiopia, and most probably from the entire east Africa.

## Amba Aradam Formation

This formation, previously known as the Upper Sandstone (Blanford 1869), was named after its type section near the town Amba Aradam (N 13°20′/E 39°34′) in northern Ethiopia (Shumburo 1968). The Amba Aradam Formation is up to 200 m thick and rests with angular

unconformity on carbonates and claystones of the Agula Shale (Bosellini et al. 1997). It consists of white or red sandstones with interbedded purple to violet silt- and mudstones, lateritic paleosols and lenses of conglomerates. The sandstones are often cross-bedded and form fining-upward sequences, which are interpreted by Bosellini et al. (1997) as "point bar sequences" deposited in a fluvial meandering river system. The lower- and uppermost parts of the succession are intensively lateritised. Bosellini et al. (1997) described the presence of eolian sediments at the base of the formation.

Despite the absence of age diagnostic fossils, the formation is believed to be correlative of the Debre Libanos Sandstone in the Blue Nile Basin (Assefa 1991) and the Aptian–Albian Upper Sandstone Unit in the Harar region of southeastern Ethiopia (Assefa 1991, Bosellini et al. 1997). It also seems to correlate in part with the Yesomma Sandstone in western Somalia (Bosellini 1989), with the lower part of the Tisje Formation in northern Somalia (Luger et al. 1994) and with the Tawilah Sandstone (Kruck et al. 1996) or Ghiras Formation (the lower part of the Tawilah Group; Al Subbary et al. 1993) in Yemen.

### 2.3.2. Central Ethiopia

The Blue Nile Basin of central Ethiopia consists of up to 2600 m thick Palaeozoic and Mesozoic sedimentary succession, which is exposed in the Blue Nile River canyon (Fig. 2.2a & b). Based on this study and the data reported by Mohr (1963), Assefa (1991) and Russo et al. (1994), the complete succession in the Blue Nile Basin can informally be grouped into eight stratigraphic units: pre-Adigrat I, pre-Adigrat II, pre-Adigrat III, Adigrat Sandstone, Gohatsion Formation, Antalo Limestone, Muger Mudstone and Debre Libanos Sandstone (Fig. 2.2). These units are briefly described below.

#### Pre-Adigrat I

In the Blue Nile basin, the oldest sedimentary succession that overlies the crystalline basement, referred to here as "Pre-Adigrat I" is up to 50 m thick and occur in small isolated outcrops between Bekotabo and Amuru (Fig. 2.2a & b). The succession, which was neither reported nor described before, is composed of poorly sorted, massive to cross-bedded medium- to coarse-grained white sandstones and conglomerates. The presence of ductile soft-sediment deformation structures, large-scale trough cross-bedding, crude horizontal bedding and channel-type cut and fill structures impart a closer similarity with the lower glacigenic part of the Enticho Sandstone in northern Ethiopia. However, other indicators of glacigenic depositional conditions including striated surfaces, diamictites and polymict clast assemblages have not yet been observed. Fossil conulariids, i.e., marine metazoans with phosphatic skeleton (e.g., *Climacoconus* sp. and *Eoconularia* sp.) that have been reported from the Fincha valley (Mesfin 1989) were supposed to indicate the presence of Ordovician to Silurian age sediments in that area but no conclusive evidence was provided as to whether they come from the Per-Adigrat I succession. If the fossils are from this unit, the succession would be correlative to the upper shallow marine part of the Enticho Sandstone in northern Ethiopia.

#### Pre-Adigrat II

Pre-Adigrat II sediments are widespread in the Blue Nile basin and reach a maximum thickness of 400 m in the Fincha valley of central Ethiopia. These sediments are not confined to north-south trending channels, as indicated by Jespen & Athearn (1961) and Mohr (1963). The succession unconformably overlies either the Precambrian basement or pre-Adigrat I. In the northwest (e.g., in Bekotabo area, around 40 km south of Bure), it reaches up to 200 m in

thickness. It consists of lateral accretion deposits, floodplain fines, crevasse splays, playa-lake and eolian dune sediments. The main sediment transport direction is to the west. The spatial distribution of lithofacies, the presence of numerous mud-filled abandoned channels, the widespread occurrence of oxisol-like paleosols, along with the associated ´probable` eolian facies, may point to a seasonal, semi-arid to arid palaeoclimate and a low-relief alluvial flood basin that consisted of continuously shifting ephemeral rivers and of temporary lakes that were fringed by vast sub-aerially exposed mud-flats. The extension of these sediments towards northern and eastern Ethiopia is not yet clear, as well as is their age. Jespen & Athearn (1961) assumed a Triassic age for this unit. Recent attempts to date these sediments failed, since the collected samples were barren of palynomorphs. However, a pre-Late Carboniferous age can tentatively be assigned, based on the age of the overlying unit.

**Pre-Adigrat III**

Pre-Adigrat III succession ranges in thickness from 350 m in Fincha and Dedu areas to less than 100 m in Fuliya and Dejen areas. The succession pinches out after a short distance west of Amuru between pre-Adigrat II succession and Adigrat Sandstone (Fig 2.2a). It is composed of three successive cycles of stacked, multi-storey sheet sandstone bodies that are capped by overbank fines and crevasse splay deposits. Leaf imprints, coaly streaks and palynomorphs are abundant, indicating favourable conditions of preservation on the floodplain, such as permanent water saturation and poor drainage. The abundance of relatively unstable detrital minerals, like feldspars and micas, points to source proximity, little reworking and rapid rate of deposition. These features may suggest a deposition in alluvial plains and/or lacustrine-deltaic environment.

The basal part of the Pre-Adigrat III succession contains *Punctatisporites gretensis, Microbaculispora tentula, Retusotriletes diversiformis, Horriditriletes tereteangulatus, Potonieisporites nuvicus, Florinites eremus, Striatopodocarpites fusus, Plicatipollenites sp, Tiwariasporites simplex, Vittatina faciolata, V. scutata, Waylandites magmus* and *Cycadopites cymbatus,* indicating a latest Carboniferous to Early Permian age (cf. Anderson 1977, Kemp et al. 1977, Price 1983, Stephenson et al. 2003). The top of the succession is dominated by *Staurosaccites quadrifidus* and *Ovalipollis ovalis*, which indicates a Middle Triassic age (cf. Dolby & Balme, 1976, Geletu & Wille 1998). In southwestern Ethiopia, these sediments were palynologically dated as Early to Late Permian in age (Davidson & McGregor, 1976). Pre-Adigrat III succession can be correlated with fluvial and lacustrine synrift sediments, often referred to as 'Karoo sediments', which are widespread in eastern and southern Africa. In the Ogaden Basin of southeastern Ethiopia, age equivalent successions are known as the Bohk Shale and the Gumburu Sandstone (Worku & Astin 1992).

**Adigrat Sandstone**

The Adigrat Sandstone, which is the main focus of this study, is supposed to reach up to 300 m in thickness and is composed, in its lower part, of subhorizontal layers of fine-grained sandstones that are intercalated with reddish shales and siltstones (Russo et al. 1994). The succession grades upwards into planar cross-bedded medium- to coarse-grained sandstones with some reactivation surfaces. In the upper part, the unit is made up of several fining-upward sequences with reddish coarse-grained sandstones at the base and siltstones at the top. Russo et al. (1994) also reported several channels that contain pebbles and rare wood fragments at their base and oriented mainly towards the SE. The succession was interpreted as having been deposited in a fluvial environment (Mohr 1962, Beauchamp 1977, Russo et al. 1994, Wolela 1997, 2008).

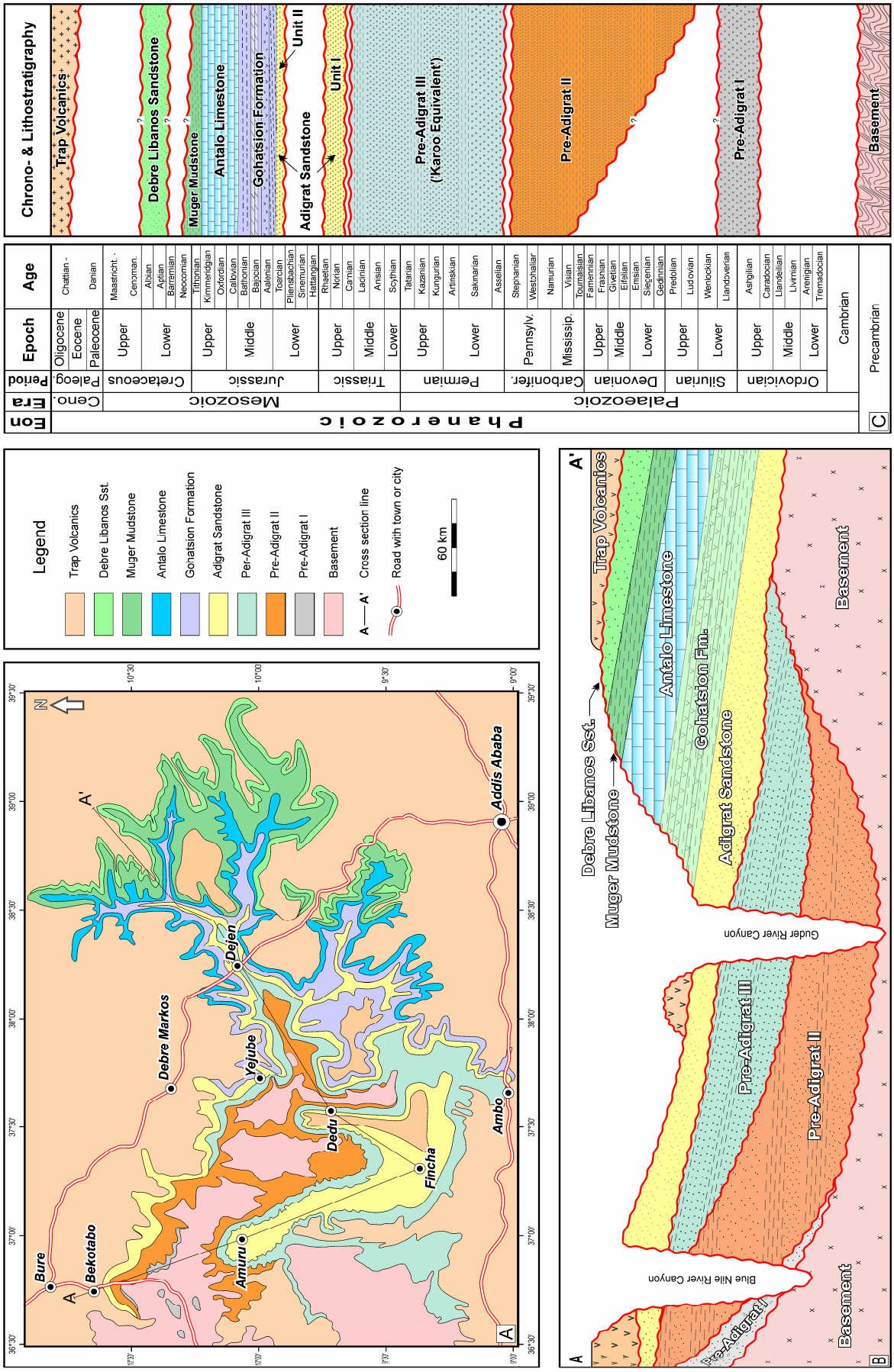


Fig. 2.2. A. Generalised geological map of the Blue Nile canyon (modified after Kazmin 1972). B. A schematic cross-section across the Blue Nile Basin (not to scale). C. The stratigraphy of central Ethiopia.

The stratigraphic position and the thickness distribution of the Adigrat Sandstone succession in the Blue Nile Basin remain controversial. The inconsistent usage of the name "Adigrat Sandstone" by different authors in the region also created serious confusions. Triassic to Early Jurassic age has been hypothesised by Jespen & Athearn (1961) and Mohr (1962). Beauchamp & Lamoigne (1975) assigned a Permo-Triassic age for this unit, whereas Kazmin (1975) assumed a broad interval of Carboniferous–Mesozoic age.

**Gohatsion Formation**

The Formation was previously known as Abbei Beds (Krenkel 1926, Mohr 1962) or as the Shale and Gypsum Unit (Jespen & Athearn 1961). Later, it was renamed by Assefa (1981) after its type section in the town Gohatsion in central Ethiopia. The succession reaches up to 450 m in thickness. According to Assefa (1981) and Russo et al. (1994), it consists of a cyclic repetition of facies successions that are composed, from bottom to top, of alternating dolostones, marlstones and shales, bioturbated mudstones with thin siltstone intercalations, fine-grained coquinoid cross-laminated sandstones and thick beds of gypsum. The presence of scattered small bivalves and gastropods (*Corbiculinae*, *Lucinids*, *Arcomytilus*, *Protocerithium*) suggests a peritidal environment with associated lagoonal and pond water bodies (Russo et al. 1994).

Regarding the stratigraphic position of the Gohatsion Formation, Mohr (1962) assigned a Bajocian age, whereas Assefa (1981) has given a Liassic to Bathonian age. In the Ogaden Basin of southeastern Ethiopia, the equivalent Hamanlei Formation was dated as Pliensbachian to Bathonian (Geletu 1998).

Russo et al. (1994) proposed that the Gohatsion Formation corresponds to the initial flooding of the craton, which is largely related to rifting and subsidence of the future African continental margin.

**Antalo Limestone**

The term Antalo Limestone, though originally assigned by Blanford (1870) to the limestone unit in northern Ehiopia, was sebsequentely extended to the limestone unit of the Blue Nile basin. The 420 m thick carbonate succession, as described by Russo et al. (1994) and Atnafu (2003), conformably overlies the Gohatsion Formation and can be subdivided into three parts. The lower part (180 m thick) is composed of burrowed mudstones that grade upwards into oolitic and coquinoid limestones with or without intercalated marl beds, and then into massive limestones with scattered patches of corals, nerineids and stromatoporoids, for which a shallow water environment was inferred. The middle part (200 m thick) consists of highly fossiliferous interbedding of marly limestones and marls. The presence of ammonite fauna (e.g., *Lithacoceras* sp. and *Subplanites spathi*), in association with brachiopods (e.g., *Terebratula pelagica and Nanogyra*) and other infaunal siphone feeders (*Anisocardia*, *Venilicardia* and *Somalirhynchia somalica* and *Zeillleria latifrons*) suggests a shelf to open marine environment (Russo et al. 1994, Atnafu 2003). The upper part (50 m thick) comprises planar laminated oolitic and refal limestones, which was interpreted to indicate the return of shallow water conditions.

The presence of *Pfenderina* sp. and *Nautiloculina oolithica* at the base of the limestone unit points to a Callovian age (Russo et al. 1994). *Kurnubia palestiniensis*, *Parurgonina caelinensis*, *Conikurnubia* sp. and *Salpingoporella annulata* at the top of the unit indicates a Kimmeridgian age (Turi et al. 1990, Atnafu 1991, 2003, Russo et al. 1994). The Antalo Limestone in the Blue Nile basin is considered to be correlative with the Urandab Formation of the Ogaden Basin, the Garura and Gedaara Formatios of northern Somalia, the Amran Series of Yemen and the Twaiq Mountaine Limestone and the Hanifa Formation of

Saudi Arabia. According to Bosellini (1989), Russo et al. (1994) and Bosellini et al. (1997), the limestone unit represents a major Callovian-Early Oxfordian drowning of the craton that was related to the commencement of Gondwana drifting and the formation of the African continental margin. Despite their prediction of a major drift-related continental flooding, they pointed out a conformable transition between the Antalo Limestone and the underlying Gohatsion Formation. However, major continental flooding cycles of regional extent are believed to result in unconformity bounded units (e.g., cf. Embry 1995, Catuneanu 2006). In any case, the flooding event appears to coincide broadly with the onset of sea-floor spreading, which was constrained by the age of the oldest oceanic crust flanking Somalia and Madagascar (dated as 151–159 Ma (Coffin and Rabinowitz, 1988)) and a global eustatic sea level highstand (Haq et al. 1987).

**Muger Mudstone**

The unit was previously known as the "Upper Gypsum" (Aubry 1886, Merla et al. 1979). The name "Muger Mudstone" was adapted after a type section was erected by Assefa (1991) along the bank of the Muger River (N 09°37'/E 38°24) in the eastern part of the Blue Nile canyon. The succession is 15 m in the Gohatsion area but thickens eastwards to reach up to 320 m in the Jema river valley. In its type locality, it is 260 m thick and conformably overlies the Antalo Limestone. Based on lithology, Assefa (1991) and Russo et al. (1994) subdivided the unit into two parts. The lower part (15 m thick) is composed of alternating beds of nodular and vein-filling gypsum, dolomites, and shales, for which the authors assigned a supratidal and lagoonal environment. Estuarine environment has been proposed by Goodwine et al. (1999, 2006). The rest of the succession (240 m thick) is characterised by interbedded sand-, silt and mudstones with local occurrences of lignite layers and scattered plant fragments. This siliciclastic succession was interpreted by Assefa (1991) to represent deposits of a meandering river system.

Regarding the stratigraphic position of the Muger Mudstone, Assefa (1991) assumed a broad interval of post-Kimmeridgian to pre-Middle Eocene age. Based on the presence of microflora (e.g., *Classopollis*, *Cicatricosisporites*, *Callialasporites trilobatus*, *Krauselisporites*, *Neoraistrickia*, *Crybelosporites* cf. *C. striatus* and *Gleicheniidites*) and dinoflagellates (e.g., *Chytroeisphaeridia* and *Leptodinium acneum*) as well as the acritarch *Micrhystridium*, Goodwine et al. (1999) assigned a Tithonian age for the base of the unit. An Early Cretaceous age was proposed for the upper part of the formation, on the basis of the occurrence of tooth plates of *Neoceralodus africanus* (also referred to *Asiotoceratodus tiguidensis),* teeth of the batoid *Rhinobatos* sp., shell fragments of pelomedusoid turtles, and teeth of sauropods (Wood et al. 1993, Werner 1995, Schmidt & Werner 1998). These biostratigraphic evidences appear to contradict with the attempt made by Assefa (1991) to correlate the unit with the Agula Shale of northern Ethiopia, which was dated as "not older than Kimmeridgian" (Bossellini et al. 1997).

**Debre Libanos Sandstone**

The sandstone unit, which was previously referred to as the "Upper Sandstone" (Merla et al. 1979), was renamed by Assefa (1991) after its type section near the village of Debre Libanos (N 09°44'/E 38°52') of central Ethiopia. In its type locality it is 172 m thick but the variation in thickness west to east is extreme as it ranges from few meters to up to 280 m. The lower boundary is marked by a change from alternating beds of mudstone and fine-grained sandstone that form gentle slopes (Muger Mudstone) to a generally massive, cliff-forming coarse-grained sandstone. The upper boundary is unconformable as it is overlain by the Tertiary flood basalts. The succession is characterised by cross-bedded pebbly sandstones and

fine conglomerates with rare occurrences of mudstones. A braided fluvial depositional environment was inferred for the unit (Assefa 1991). Fossils were not yet discovered apart from silicified wood fragments. Based on lithologic similarities, a broad correlation with the Amba Aradam Formation of northern Ethiopia and the Upper Sandstone of southeastern Ethiopia has been hypothesised by the above-cited workers.

### 2.2.3. The Tertiary Trap Series

The Tertiary Trap Series of Ethiopia occur near the triple junction of the Red Sea, the Gulf of Aden and the East African Rift System, and have long been associated with the Afar hotspot (Richards et al. 1989). Prolific outpourings of mainly basalts have built a subaerial pile, which originally covered an area in excess of 500,000 square km, with total thickness locally exceeding 2,000 m (Hofmann et al. 1997). The northwestern traps consist of a series of Late Eocene and Oligocene fissure basalts, covered by Miocene shield volcanoes. Conventional K/Ar ages measured in basalts, rhyolites and ignimbrites from the plateau to the north of Addis Ababa range from 14 to 40 Myr (Merla et al. 1979). Berhe et al. (1987) have distinguished three prolonged stages of volcanism at 50–40, 40–30 and 30–21 Myr ago, whereas Ebinger et al. (1993) and George et al. (1998) have proposed that the main phase of volcanism occurred between 45 and 35 Myr ago in the southern part of the Ethiopian rift. In contrast, the geochronological and palaeomagnetic results of Hofmann et al. (1997) suggest that flood basalt eruptions in Ethiopia occurred in two pulses, beginning shortly before 30 Myr and ending before 29 Myr, possibly lasting <1 Myr. The classification of the trap series, including their petrology and geochemistry, has been addressed in a number of studies (e.g., Hofmann et al. 1997, Pik et al. 1998, 1999, Beccaluva et al. 2007).

The age, duration and location of Ethiopian trap volcanism have potential significance for continental breakup, global climate change and mass extinctions. Emplacement of the Ethiopian traps has been linked to the extinction event that defines the boundary between the Eocene and Oligocene epochs in the Cenozoic era (Courtillot et al. 1997). Other workers (e.g., Hofmann et al. 1997) argue that it is tempting to relate the disrupted world climate around 30 Myr ago to the eruption of the Ethiopian traps.

## 3. Nomenclature and Definitions – an overwiew of terminologies

Over the years, many different methods and concepts have been used in the study of sedimentary rocks. In the understanding of modern and ancient depositional environments, however, a common approache that appears to premeate is an attempt to subdivide a rock body into constituent building blocks, i.e., '*facies*'. The most useful modern working definition of facies, which will be used throughout this study, was that given by Walker (1992), as 'a particular combination of lithology, structure and textural attributes that characterises features different from other rock bodies'. Facies units that are closely related will ultimately be given an environmental interpretation. As used herein, *facies association* refers to a group of facies genetically related to one another and have some environmental significance (Collinson 1969). A *depositional system* refers to a three-dimensional assemblage of process-related sedimentary facies that record a particular palaeogeomorphic element, i.e., a particular *depositional environment* (Galloway 1989). Linkages of contemporaneous depositional systems that are bounded by unconformities build stratigraphic units (i.e., allostratigraphic units, NACSN 1983), and if related to cycles of sea level fluctuation, depositional sequences (Michum 1977, Van Wagoner et al. 1990). Relationships between

facies, facies associations, depositional systems and environments as well as the stratigraphic units or sequences they form are illustrated in Fig 3.1. Facies analysis refers to a method of characterising bodies of rocks with unique lithological, physical and biological attributes relative to all adjacent deposits. In this study, the analysis is exclusively based on outcrops because any kind of subsurface data is lacking.

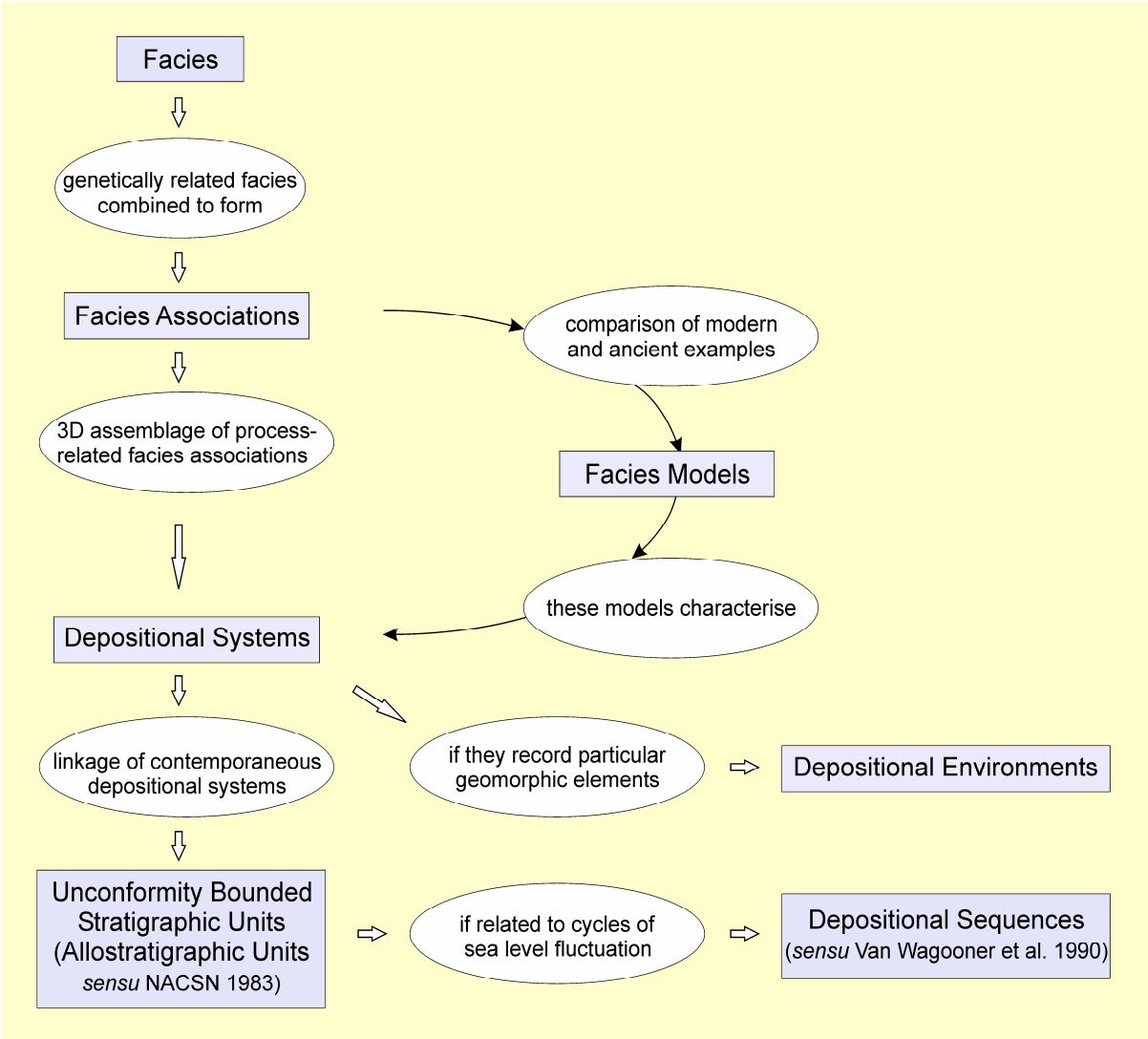


Fig. 3.1. Relationships between facies, facies associations, depositional systems and sequences. Modified after Walker (1984).

The Adigrat Sandstone of northern and central Ethiopia reflects a complex arrangement of facies units deposited in a variety of depositional environments ranging from continental to shallow-marine settings. This section presents a brief account of the definitions, nomenclatures and classifications of the main siliciclastic depositional systems that have bearing on sedimentary successions of the study area. The continental to shallow-marine siliciclastic deposits in the Adigrat Sandstone succession may be catagorised into six depositional systems; namely, the fluvial, estuarine, deltaic, barrier-lagoon, strandplain and tidal flat systems.

## 3.1. The Fluvial System

Fluvial systems represent an important member of nonmarine siliciclastic depositional systems. A number of criteria have been used to classify and differentiate fluvial systems. The most classical ones are those of Rust (1978) and Schumm (1968). Based on the degree of channel sinuosity and braiding, Rust (1978) classified fluvial systems into straight, braided meandering, and anastomosing. In contrast, Schumm (1968) identified three types of river systems on the basis of width/depth ratio of channels and the mode of sediment transport. These are bed-load, mixed-load and suspended-load-dominated systems. Miall (1987) criticised both classification schemes as 'inadequate' to describe the highly variable natural spectrum of channel systems, which he referred to as 'a continuum of channel patterns'. Miall (1996) identified 16 different types of river systems. Even though the author stressed the existance of many transitional forms between his systems, his classification appears to be based on the combination of parameters used by Rust (1978) and Schumm (1968).

The fundamental components of any fluvial system are channel fills, channel bars, natural levees, crevasse splays and flood plains. These architectural elements are products of variable combinations of smaller scale bedforms such as ripples, dunes, antidunes, plane beds and associated stratasets. The origin, geometry, and migration of these bedforms and their associated sedimentary structures are well-summarized by Allen (1982) and Middleton & Southard (1984).

Fluvial deposits generally fine upward, reflecting progressively weaker flows during filling, and also fine downchannel as water flow decelerates in that direction. They consist, from bottom to top, of poorly sorted, structureless coarse sand, gravel and/or mud clasts (lag deposits) that grade upward to planar or cross-bedded stratasets. Planar- and/or ripple-laminated suspended-load and organic matter drape over existing bed topography as the angle of divergence between the enlarging channel and the filling channel increases. Paleocurrent orientations recorded in fluvial deposits are broadly parallel to the mean orientation of structures such as channel axis, pebble imbrication and/or foreset dip directions of various scales of cross strata that generally correspond with local water flow directions.

## 3.2. The Estuarine System

Estuaries, as defined geologically here, are transgressive depositional systems that receive sediments from both fluvial and marine sources (Fig. 3.3) and commonly occupy the seaward portion of a drowned valley (Dalrymple et al. 1992). They contain facies influenced by tide, wave, and fluvial processes, and are considered to extend from the landward limit of tidal facies at their heads to the seaward limit of coastal facies at their mouths. Other environments that are closely associated with estuaries are incised valleys. An incised-valley system is defined as a fluvially eroded, elongate topographic low that is characteristically larger than a single channel, and is marked by an abrupt seaward shift of depositional facies across a regionally mappable unconformity (Zaitlin et al. 1994). Estuarine deposits exhibit generally a retrogradational stacking of facies and a tripartite zonation reflecting the interaction of marine and fluvial processes (Boyd et al. 2006, Fig. 3.2). These tripartite zones are: (i) an outer zone dominated by marine processes (waves and/or tidal currents), (ii) a relatively low-energy central zone, where marine energy and river currents are approximately equal in strength in the long term, and (3) an inner, river-dominated zone.

Based on the relative power of wave and tidal processes, estuaries can be divided into two main types, wave-dominated and tide-dominated estuaries (Fig. 3.2). ***Wave-dominated estuaries*** consist of a marine sand body (barrier, tidal inlets, ebb and flood tidal deltas) that

accumulates in the area of high wave energy at the mouth, a low-energy central part (the "central basin") and a bayhead delta (Nichol 1991, Rahmani 1988, Zaitlin and Shultz 1990). ***Tide-dominated estuaries*** are composed of elongate sand bars at the mouth that grade updip into upper flow regime plane beds. The central mixed-energy (tidal–fluvial meanders) and inner river-dominated portions of the estuary are characterized by tidal channel deposits that are flanked by brackish-water marsh sediments (Dalrymple & Zaitlin 1989, Woodroffe et al. 1989). Tidal estuarine deposits can be differentiated from their wave-dominated counterparts by the predominance of tidal structures such as mud drapes on foresets, tidal bundles and opposite palaeocurrent directions. The main difference to tidal flat deposits is the presence of clearly defined, "tripartite" distribution of lithofacies (coarse-fine-coarse) with the central zone characterised by an area of net bedload convergence (Roy et al. 1980).

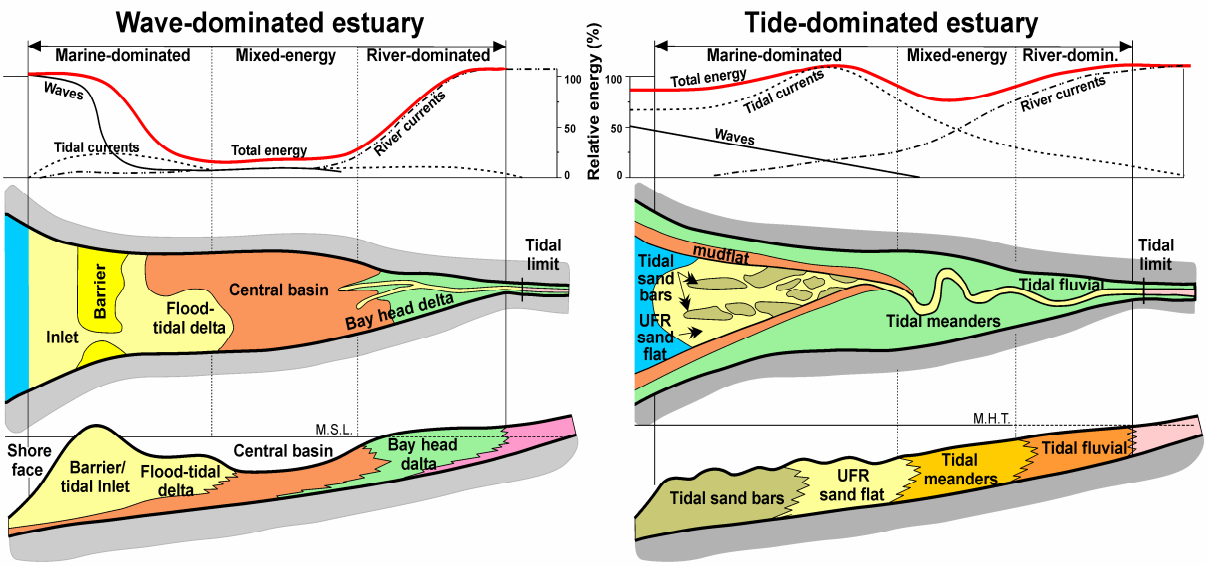


Fig. 3.2. Morphological components, sedimentary facies and distribution of energy types in the tripartite zonation of a wave- and a tide-dominated estuary (modified after Dalrymple et al. 1992).

## 3.3. The Deltaic System

As defined by Elliot (1986), deltas are progradational sediment bodied formed when a river supplies sediment more rapidly than it can be redistributed by basinal processes, such as waves and tides. The morphology and facies architecture of a delta is controlled by the proportion of wave, tide, and river processes; the salinity contrast between inflowing water and the standing body of water, the sediment discharge and sediment caliber, and the water depth into which the river flows (Bhattacharya 2006). Much of the sediment in a delta is derived directly from the river that feeds it, in contrast to other coastal depositional systems, in which sediment is derived both from the marine and the fluvial realm (Fig. 3.3, Boyd et al. 1992).

Deltas comprise three main geomorphic environments of deposition (Elliot 1986): the subaerial delta plain (where river processes dominate), the delta front (the coarser-grained area where river and basinal processes interact), and the prodelta (primarily muddy). These three environments roughly coincide with the topset, foreset, and bottomset strata of early workers (e.g., Gilbert 1885, Barrell 1912), although the boundaries overlap and specific definitions of the delta front are not widely agreed on. Galloway (1975) classified deltas by using a process-based scheme into river-dominated, wave-dominated and tide-dominated

(Galloway 1975). Deltas are fundamentally regressive in nature. During progradation they form upward-coarsening facies successions as delta plain deposits (distributary channels and their associated floodplains and bays) build over sandy mouth bars and delta-front sediments, which inturn build over muddy deeper-water prodelta facies (Elliot 1986). These facies successions display a distinct down-dip clinoform cross-sectional architecture. In a strike-oriented cross-section overlapping delta lobes typically result in lens-shaped stratigraphic units that exhibit a mounded appearance. As deltas are abandoned and transgressed they may be transformed into other depositional systems (e.g., transgressive barrier-lagoon system or estuary). The term 'braid delta' or 'braidplain delta' has been used to refer to a sandy or gravelly delta front fed by a braided river system and characterized by a fringe of active mouth bars (e.g., McPherson et al. 1987). As originally described by Gilbert (1890) and later by Postma (1990), the term Gilbert-type delta' refers to dominantly coarse-grained deltas that possess steeply dipping foresets. The formation of 'Gilbert-type' deltas requires coarse-grained sediment supply from possibly fault-bounded steep-sided canyons draining directly into a standing body of water (Gawthorpe & Colella 1990, Wescott & Ethridge 1990).

### 3.4. The Barrier-Lagoon System

According to Boyd et al. (1992), a barrier is defined as 'an elongate shore-parallel sand body which consists of a number of sandy units including longshore bars, beaches, dunes, tidal deltas, tidal inlets, washovers and spits, as well as an enclosed muddy facies consisting of salt marsh, lagoonal and bay fills. It may be connected to the mainland at either end and breached by tidal inlets, forming barrier islands. Barriers are most often generated during transgression and are commonly underlain by more landward facies, such as those deposited in estuaries, lagoons and marshes. Unlike deltaic and strandplain settings, barrier-lagoon systems develop in an embayed, wave-dominated coastal setting with mixed sediment supply (Fig. 3.3). They also require steady longshore sediment supply and low to moderate tidal range for their sustained development (Glaeser 1978).

According to Hoyt (1967), Swift (1975), Wilkinson (1975) and Davis (1994), the origin of barriers has been attributed to at least three mechanisms: (i) the vertical growth and emergence of offshore and/or longshore bars; (ii) the lateral migration of inlets or channel-spit sequences; and (iii) the detachment of beach ridges from the mainland by a rise in sea level. The later mechanism involves stepwise landward migration of barriers due to rapidly rising sea level, which is described by the 'stepwise coastal retreat' model of Rampino & Sanders (1980) and Elliot (1986). The formation of barrier-lagoon complex, in part, reflects of the tectonic setting of the basin. They preferentially develop on stable, relatively flat, low-gradient coastal plain to nearshore settings along passive continental margins or broad cratonic seaways (Davis 1994).

### 3.5. The Strandplain System

Strandplains are also shore-parallel sand bodies containing offshore transition zone, lower, middle, upper shoreface and foreshore sub-environments. They are characteristic of open shoreline settings that form in a non-embayed or linear, wave-dominated coasts with marine sediment supply (Boyd et al. 1992, Fig. 3.3). Strandplain sub-environments can be distinguished by a particular suite of textures, physical structures and biogenic features (Walker & Plint 1992, Galloway & Hobday 1996).

Offshore transition zone to lower shoreface deposits accumulate at the break in slope where the shoreface grades into the shelf. In a storm-dominated shoreface system, deposits of

this sub-environment are characterised by interbedded hummocky cross-stratified sandstones and bioturbated mudstones (Reading & Collinson 1996). In a wave-dominated shoreface system, wavy- and horizontal lamination are predominant than hummocky cross-stratification. Trace fossils such as *Terebellina*, *Chondrites*, *Teichichnus*, *Planolites*, *Phycosiphone*, *Rosselia*, *Thalassinoides*, *Asterosoma* and *Palaeophycus* are common (Pemberton et al. 1992).

Middle shoreface sub-environments are subject to more powerful waves and associated longshore and rip currents, leaving a complex depositional record. Sedimentary structures include horizontal to low-angle lamination, massive beds, as well as combined wave- and current-ripple laminations (Clifton et al. 1971). Amalgamated hummocky cross-stratified sandstones occur where storm effects predominate. Common trace fossils include *Skolithos*, *Ophiomorpha*, *Diplocraterion* and *Rosselia*.

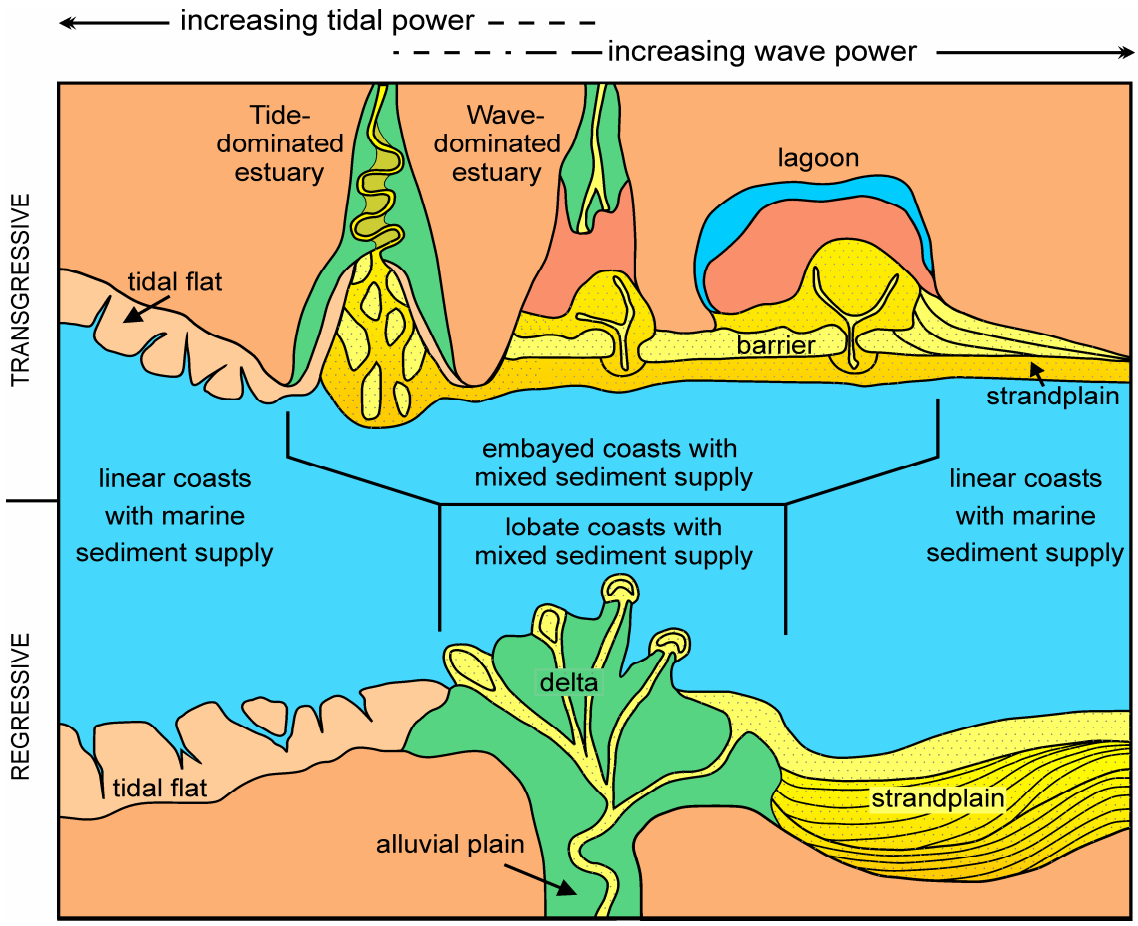


Fig. 3.3. Plan view of coastal depositional environments along transgressive and regressive shorelines, illustrating the relationships between river, wave and tidal processes, sediment supply and associated geomorphologies (modified after Boyd et al. 1992).

Upper shoreface sub-environments that correspond to the inner surfe zone are dominated by powerfull onshore, offshore and longshore currents. Deposits of the upper shoreface are characterised by alongshore or seaward-directed trough cross-beds and onshore-dipping planar cross-beds resulting from bar migration (Clifton et al. 1971). Foreshore sub-environments that correspond to the zone of wave swash usually comprise planar lamination dipping gently seaward, with low-angle discordances representing adjustment of the beach to

changes in wave regime or sediment supply (Clifton 1969). Trace fossils are usually rare in these envoronments and include scattered traces of long vertical burrows such as *Skolithos*.

The prograding strand-plain model, which was first proposed by Harms et al. (1975) and was expanded upon by Harms et al. (1982), has been applied successfully in many basins throughout the world. It predicts that prograding shoreline sandstones become progressively coarser and/or cleaner in an upsection direction, an attribute readily identifiable in well-logs in areas where rock data are sparse or absent.

### 3.6. The Tidal Flat System

Tidal flats are sheet-like sedimentary bodies that form in a non-embayed or linear, tide-dominated coasts with marine sediment supply (Boyd et al. 1992, Fig. 3.3). Tidal environments can be subdivided into three zones (from higher to lower elavated areas); namely, mud flats, mixed sand-mud flats and sand flats (Weimer et al. 1982). Suspended sediment concentration increases up the high-tidal flat as a result of decreasing tidal current velocities. Consequently, most progradational tidal flat successions show an upward-fining of grain size from lower sand flat and shallow subtidal channel deposits to mixed intertidal fine sandy and muddy facies capped by silty, bioturbated muds of the salt marsh (Klein 1971, Terwindt 1988). Deposits formed under tidal currents are generally more heterolithic than deposits formed during river floods because tidal currents fluctuate over shorter time scales (Nio & Yang 1991). The dominant internal structures include a variety of cross-bed types of simple or complex geometry. These include: (i) herringbone cross-bedding, (ii) flaser-, wavy- and lenticular bedding, (iii) reactivation surfaces within cross bed sets produced by the beveling of dune crests by sub-dominant reversing flows followed by the rebuilding of crests during subsequent dominant flows, (iv) mud drapes on cross-bed foresets, with distinctive patterns in the spacing of successive drapes, and (v) tidal rhythmites (Middleton 1991, Terwidt 1981).

Tidal flats display typical faunal associations which are adapted to the drastic changes in the environment from high to low tide (i.e.,, from water cover to emergence). Typical representatives are suspension feeders (e.g., bivalves and gastropods) living at or below the sediment surface and deposit feeders such as worms or crustaceans living behind U-shaped or irregular burrows (Reineck & Singh 1986).

As are all nearshore sediments, tidal deposits are strongly affected by relative sea level changes (Dalrymple & Makino 1989, Dalrymple et al. 1991). Sea level fall leads to a seaward migration of the tidal complex and usually causes partial or complete erosion of pre-existing tidal sediments. If such a situation persists for some time, the chances for preservation of tidal deposits, particularly of supratidal and intertidal mudflats, are very limited unless these have been early cemented. In contrast, intertidal and suprtidal sediments can easily follow a rising sea level and build up thick sequences because their sedimentation rate is sufficiently high. If the rise in sea level is slow tidal flats may enlarge their areal extent. Furthermore, specific tectonic settings such as long lasting, slowly subsiding shallow paltforms can maintain a tidal flat environment over long time periods.

## 4. Stratigraphic and Facies Analysis of the Adigrat Sandstone in the Mekelle Basin, Northern Ethiopia

In the Mekelle basin of northern Ethiopia, the Adigrat Sandstone succession is exposed in numerous localities around Mekelle (Fig. 2.1) and attains a total thickness of 430

m. In most of the studied areas (e.g., Wukro, Megab, Abiadi, Agwe and Samre), it unconformably overlies the Permo-Carboniferous Edaga Arbi Glacials. In the eastern outcrop areas (e.g., Berhale), it unconformably overlies the Neoproterozoic basement.

This section contains three parts. The first part deals with the analysis of facies, facies associations and depositional systems. The second part focuses on the stratigraphic stacking patterns of depositional systems in each of the studied localities, which is followed by the third part that deals with the intrabasinal correlation of stratigraphic units and the genetic interpretation of the sedimentary basin fill.

## 4.1. Depositional systems and facies associations

The nature of depositional systems and facies associations that fill a sedimentary basin is a reflection of the structural mechanisms controlling the formation of the basin. It is therefore imperative to constrain and acquire a good understanding of the geometry and internal architecture of the depositional systems involved before proceeding with stratigraphic correlations, construction of sedimentation models and making inferences about the evolution of the basin. Thus, the following section deals with the description and interpretation of the various depositional systems and facies associations enclosed within them.

Within the Adigrat Sandstone succession of the Mekelle basin, six broad classes of depositional systems are identified, namely (i) the fluvial system (ii) the fluvio-estuarine system, (iii) the deltaic system, (iv) the strandplain system, (v) the barrier island–lagoon system, and (v) the open-coast tidal flat system.

### 4.1.1. The Fluvial System (F)

#### Facies Association $F_1$

***Description*:** Facies association $F_1$ varies in thickness between 20–50 m and is characterized by sharp-based, predominantly trough cross-bedded, coarse- to fine-grained sandstones with abundant quartz pebbles and clay rip-up clasts at the base. Sorting is poor to moderate and small lenses of fine conglomerate are common. Grain size decreases upwards both on a forset and on a bedform scale. Although trough cross-bedding is predominant, horizontal bedding is also common. Planar-tabular cross-bedding is relatively rare. Very large-scale inclined strata with abundant rip-up clasts occur rarely (e.g., Fig. 4.1c). Thicknesses of individual cross-bed sets vary between 0.7 m and 2 m, but may occasionally reach 3 m. Forsets are 2–5 cm thick. In the lower part, sandstone bodies are usually amalgamated forming up to 8 m thick fining-upward cycles with sharp, erosive, irregular to concave-up lower boundaries (arrow in Fig. 4.1a). Towards the upper part of the succession isolated single storey sandstone bodies toped by laminated to massive mudstones become dominant.

Fine-grained facies (siltstones and mudstones) are proportionally minor in the amalgamated sandstone bodies but are more common in the isolated single storey bedforms. They are either massive or planar- to ripple-laminated. Thickness ranges from 10 to 30 cm and seldom reaches 60 cm. Desiccation cracks are common. Bioturbation and body fossils are absent.

***Interpretation*:** The predominance of coarse- to medium-grained sandstones with abundant scattered pebbles indicates a high-energy bed-load dominated depositional regime. The trough cross-bedded sandstones represent the migration of subaqueous sinuous-crested (3D) dunes along channel thalwegs (Collinson 1970, Harms et al. 1975). The non-bioturbated and uni-directional trough cross-bedded sandstones have usually been associated with in-channel

deposition in alluvial settings (Cant 1978, Walker & Cant 1984). The predominance of trough cross-bedding suggests the predominance of lower flow regime conditions within the channels (Leeder 1983). The large-scale inclined strata (e.g., Fig. 4.1c) may be interpreted as large-scale unit bars (Bridge 2006). Planar-bedded sandstones may represent the migration of low-relief bed waves (bed-load sheets) that have been formed due to reduced bed shear stress under lower stage plane bed conditions (Bennet & Bridge 1995). Their formation under upper stage plane bed conditions is less likely since these are usually associated with high bed-load transport rates of mainly sandy sediments with substantial suspended load (Bridge and Best 1997). Fine-grained facies (siltstones and mudstones) may represent either waning flood deposits settling on to temporarily abandoned areas within channels or they represent overbank deposits near channel banks during high flood stages. Their restricted lateral extension might be attributed to erosional truncation by actively cutting channels and frequent avulsions.

Unimodal palaeocurrent directions and the absence of marine indicators (e.g., tidal- or wave-generated structures) in $F_1$ suggest deposition in a nonmarine environment. Based on the geometry and the spatial/temporal distribution of channel fills, unit- and/or compound bars within channels (Fig. 4.1a), together with the absence of lateral accretion bedforms and the rarity of fine-grained deposits, the sandstone bodies in the facies association $F_1$ may be interpreted to have been deposited in braided river systems.

**Facies Association $F_2$**

***Description*:** Facies association $F_2$ is characterized by sharp-based medium- to fine-grained sandstones that grade upwards to thinly interbedded silt- and mudstones. Thicknesses of individual cross-bed sets vary between 0.2 m and 1 m. Bed sets are arranged in several fining-upward cycles that reach in thickness up to 5 m. Sandstone bodies are usually isolated single storey toped by laminated to massive mudstones. The scale of sedimentary structures decreases upwards from trough cross-bedding at the base to lateral accretion deposits (Fig. 4.1f) in the middle part and to planar- and ripple-lamination and massive beds at the top. Desiccation cracks (Fig. 4.1g) and rootlet mottling are common at the upper part of fining-upward cycles. Tidal or wave-generated sedimentary structures are absent. Bioturbation is rare and body fossils are absent.

***Interpretation*:** The medium- to fine-grained sandstones with interbedded silt- and mudstones indicate a mixed-load dominated relatively low-energy depositional regime, as compared to that of $F_2$. The upward transition from $F_1$ to $F_2$ probably indicates a reduction in the slope gradient of the fluvial graded profile and/or change in fluvial energy flux, fluvial style and sediment load (Shanley & McCabe 1994, Ye & Kerr 2000). The presence of lateral accretion bedforms in the sandstone intervals may at least suggest deposition meandering channels. The absence of tidal or wave-generated sedimentary structures indicates a nonmarine depositional environment. Thus, deposition in fluvial meandering river systems can be inferred for $F_2$. The mudstone intervals and the fine-grained sandstone and siltstone interbeds at the upper part of the fining-upward cycles are interpreted to represent overbank and crevasse splay deposits (Fig. 4.1e). In summary, the facies association is interpreted to reflect deposition in meandering fluvial channels and associated floodplains in a low-gradient alluvial plain.

### 4.1.2. The Fluvio-Estuarine System (FE)

The fluvio-estuarine system (FE) is composed of four facies associations: $FE_1$, $FE_2$, $FE_3$ & $FE_4$ (Table 1).

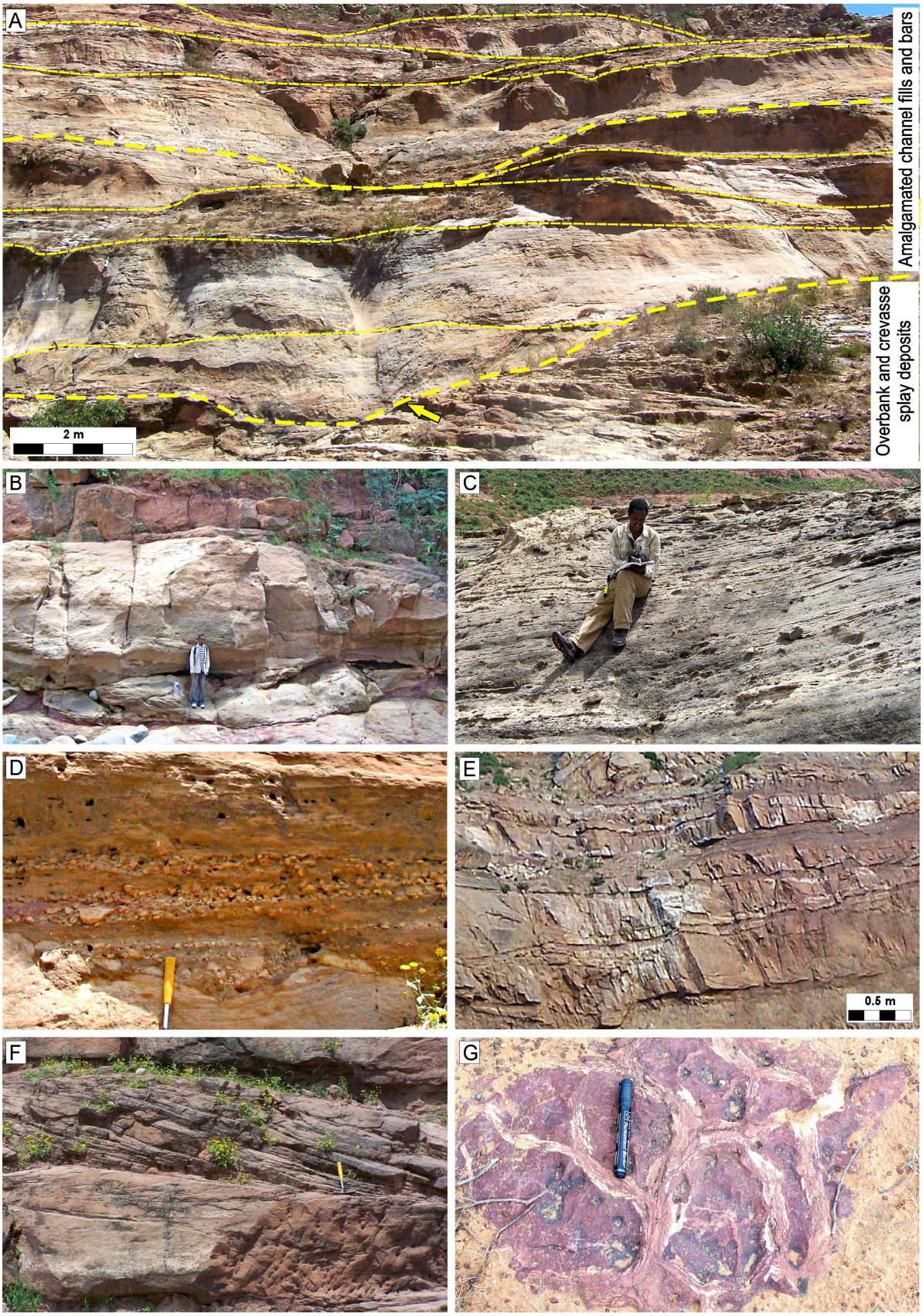


Fig. 4.1. Outcrop examples of the fluvial facies association (F). A & B. Amalgamated channel fills and bars, Megab section. C. Large-scale inclined strata sharply overlain by heterolithic floodplain facies, Abiadi section. D. Point bars of a meandering river system, Agwe section. E. Overbank and crevasse splay deposits. F. Channel lag deposits composed of qurtze pebbles and clay rip-up clasts, Agwe section. G. Desiccation cracks, Abiadi section.

Table 1. Summary of the main characteristics of the fluvial and the fluvio-estuarine depositional systems and facies associations

| Depositional systems and facies association | Lithology and sedimentary structures | Palaeocurrent patterns | Bioturbation | Fossils | Depositional environment |
|---|---|---|---|---|---|
| Fluvial System (F) | | | | | |
| Facies Associations | | | | | |
| F1 | upward-fining poorly to moderately sorted, trough cross-bedded, coarse- to fine-grained sandstones, abundant scattered quartz pebbles | unimodal | none | none | amalgamated braided fluvial channels, rare overbanks |
| F2 | isolated upward-fining moderately to well sorted, medium- to fine-grained sandstones, grading upwards into planar- to ripple-laminated silt- and mudstones; lateral accretion | unimodal to polymodal | rare | phytoclasts and cuticles | meandering fluvial channels, overbanks and crevasse splays |
| Fluvio-Estuarine System (FE) | | | | | |
| FE1 | upward-fining moderately to well sorted, coarse- to fine-grained sandstones, silty sandstones, lower part trough to planar-tabular cross-bedded, flaser- to wavy-laminated towards top, mud drapes on foresets | bi- to polymodal, abundant bipolar | sparse to moderate locally intense in the upper part | vertebrate bone fragments & teeth | tidally influenced upper estuarine channels |
| FE2 | massive to laminated silty mudstones with subordinate intercalations of thinnly bedded fine-grained sandstones and siltstones (heterolithic stratification), relict wavy- and ripple-lamination, minor small-scale trough cross-bedding | bi- to polymodal, abundant bipolar | moderate to intense | phytoclasts, rare pollen and spores | low-energy central estuary ('central basin '*sensu* Dalrymple et al. 1992) |
| FE3 | upward-coarsening from massive to laminated silty mudstones to planar and ripple-laminated sandstones, soft sediment deformation and convolute bedding | unimodal, occasionally bimodal | moderate to intense | rare phytoclasts | prograding estuarine bay head delta |
| FE4 | large-scale trough cross-bedded sandstones, mud draped foresets, reactivation surfaces, tidal rhythmites | bimodal with abundant bipolar | moderate | none | elongate tidal sand bars |
| FE5 | mainly planar-laminated sandstones with subordinate intercalations of flaser- to wavy-bedded silty sandstones and laminated to massive mudstones | bi- to polymodal | moderate to intense | phytoclasts, rare pollen and spores | upper-flow-regime sand flats with fringing tidal flate and marsh |

**Facies association $FE_1$**

***Description***: Facies association $FE_1$ ranges in thickness from 10–20 m and is composed of medium- to fine-grained sandstones that are capped by silt- and mudstones. Cross-bed sets are 0.3–0.7 m thick and rarely reach a meter. Foresets are 1–3 cm thick. Beds are commonly amalgamated into several bedsets forming up to 7 m thick, erosive based fining-upward units. Grains are moderately to well-sorted and well-rounded. The upward transition from sandy to muddy facies occurs at the uppermost part of sandstone bodies and is usually gradational and rarely sharp. Trough and planar-tabular cross-bedding are predominant in the lower sandy part, while horizontal and ripple lamination dominate the upper silty to muddy part. Mud-draped forsets (e.g., Fig. 4.2c) as well as lateral accretion (LA) surfaces are common. The geometry and spatial/temporal stacking patterns of sandstone bodies are variable from one studied locality to another. For example, in Megab and Wukro areas, sandstone bodies are sheet-like and are separated by reddish brown mudstones. In contrast, Agwe and Abiadi areas are characterized by narrow overlapping ribbons. The mudstones, which are 5–40 cm thick and commonly preserved on top of sandstone bodies, are either massive or horizontal laminated. Palaeocurrent directions in $FE_1$ are generally polymodal with frequent oppositely dipping ripple- and dune-scale cross strata (Fig. 4.2b). Burrowing is low to moderate in the lower part of sandstone bodies, although it increases in intensity upwards. Syneresis cracks occur in association with bioturbated horizons. Scattered vertebrate bone fragments and teeth occur at the base of sandstone bodies.

***Interpretation***: Erosive based fining-upward sandstone bodies and the upward decrease in the scale of sedimentary structures reflects deposition in an energy-declining environment (Walker & Cant 1984), which might in part be explained by channelized flow. Even though the rarity of distinct channel floor facies is not in favour of this interpretation, the presence of lateral accretion surfaces indicates deposition, at least in part, in sinuous channels (Allen 1964). Laterally extensive sheet-like geometry of the sandstone bodies may be related to lateral channel migration, suggesting slow contemporaneous subsidence (Ethridge 1985). The lateral variability in the geometry and spatial/temporal stacking patterns of sandstone bodies may be due to the variability in the rates of subsidence and sedimentation along depositional strike (cf. Catuneanu et al. 1998). The high degree of grain sorting and roundness may point to effective reworking prior to final deposition. Alternatively, the sediment source area might contain older shallow marine sandstones, which are predominantly composed of well-sorted and well-rounded grains. Mud drapes on foresets and oppositely dipping ripple- and dune-scale cross strata indicate tidal influence (Boersma & Terwindt 1981, Nio & Yang 1991, Dalrymple & Choi 2003).

The low to moderate bioturbation intensity may reflect the physicochemical stresses imposed upon trace-making organisms (Pemberton & Wightman 1994, MacEachern et al. 1999). Such stresses are usually attributed to either variable substrate consistency or episodic deposition or salinity fluctuation or a combination of all these three, which are typical of brackish water settings (Beynon et al. 1988, Gingras et al. 1999, MacEachern et al. 2005). The presence of syneresis cracks suggests the persistent mixing of fresh and marine waters, leading to salinity fluctuations (Gingras et al. 1998).

In summary, the sedimentological and ichnological attributes of the facies association $FE_1$ described above suggest deposition in tidally influenced estuarine channels. Similar tidally influenced estuarine channel deposits have been described by Rahmani (1988), Smith (1988) and Yang & Nio (1989). The formation of tidal estuarine system records the onset of transgression (Boyd et al. 2006, Catuneanu 2006). Hence, facies association $FE_1$ could be interpreted as having been deposited under transgressive conditions when the rate of sea level rise is in excess of sediment supply (cf. Allen & Posamentier 1994, Posamentier 2001).

**Facies association $FE_2$**

***Description***: Facies association $FE_2$ ranges in thickness from 3–10 m and consists of regular alternations of moderately to intensely burrowed, fine-grained sandstones and silty mudstones that are arranged in a small coarsening-up cycles (Fig. 4.3b). The sandstone beds are 10–50 cm thick. Although bioturbation obliterated internal stratification, a relict horizontal and/or gentle undulating stratification is visible. Sandstone bodies are lenticular with lateral extents in the range of a few tens of meters. Thickness of mudstone beds is commonly in the range of 5–60 cm, but may locally reach up to 1 m. The mudstones are predominantly massive and dark reddish brown in colour. Burrowing is moderately variable on a small scale but is relatively uniform throughout. The sandstone beds are less thoroughly burrowed than the mudstone beds. Identification of trace fossils at a generic level is difficult due to overprinting of burrows by pervasive red staining. Large *Rosselia rotatus* (Fig 4.4d), *Diplocraterion* and *Thalassinoides* are abundant. Syneresis cracks are common (Fig. 4.3c).

***Interpretation***: The predominance of suspended-load with subordinate mixed-load in the facies association $FE_2$ indicates deposition in a low energy environment. Small-scale fluctuations in energy are reflected by the small-scale interbedding of fine-grained sandy and muddy facies. Because there is no apparent evidence in $FE_2$ for either fluvial- or tidal- or wave-generated features, the structureless to horizontal laminated fine-grained sandstones might have probably been emplaced by density underflows generated at the bay head delta as it progrades into the protected estuary bay. Similar density underflows were described from the Congo River estuary (Heezen et al. 1964) and from the Cardium Formation (Walker 1995). The poor degree of sorting and roundness of framework grains may also suggest rapid emplacement of sand without effective reworking.

The mudstones are interpreted to have been deposited by settling out of suspension in a quiet water environment, possibly within the low-energy central part of the estuary (‘central basin’ *sensu* Dalrymple et al. (1992)). Syneresis cracks developed in the mudstone beds may suggest fluctuations in salinity, which is usually associated with the mixing of fresh and marine waters in the estuary (Plumer and Gostin 1981, MacEachern et al. 2005).

In summery, facies association $FE_2$ is interpreted to reflect deposition by suspension fall-out in the low-energy central part of the estuary. Quite water conditions were repeatedly interrupted by rapid and episodic deposition of sand beds resulting from increased seasonal river discharge and/or storm washover. $FE_2$ represents a part of transgressive deposits that form during sea level rise when the rates of rise outpace the sedimentation rates (Allen & Posamentier 1994).

**Facies association $FE_3$**

***Description***: Facies association $FE_3$ is 5–10 m thick and composed of fine- to medium-grained sandstones with interbedded dark reddish brown siltstones and mudstones (Fig. 4.3a). Bed thickness varies between 5 cm and 30 cm and occasionally reaches 60 cm. Sand grains are moderately to well-sorted and subrounded. Planar- and ripple-laminations are predominant, though locally massive beds are common, as well as flaser- and convolute bedding. Small-scale trough cross-bedded strata with foresets climbing up-dip on inclined bedding surfaces occur rarely. Beds are amalgamated into bedsets forming multiple, 2–3 m thick, prominent upward-coarsening successions (Fig. 4.3a) with sharp and scoured bases but no lags. The lower boundary is often low-angle inclined to flat and become wavy to irregular down-dip, where soft sediment deformation usually occurs. On a larger scale, sandstone

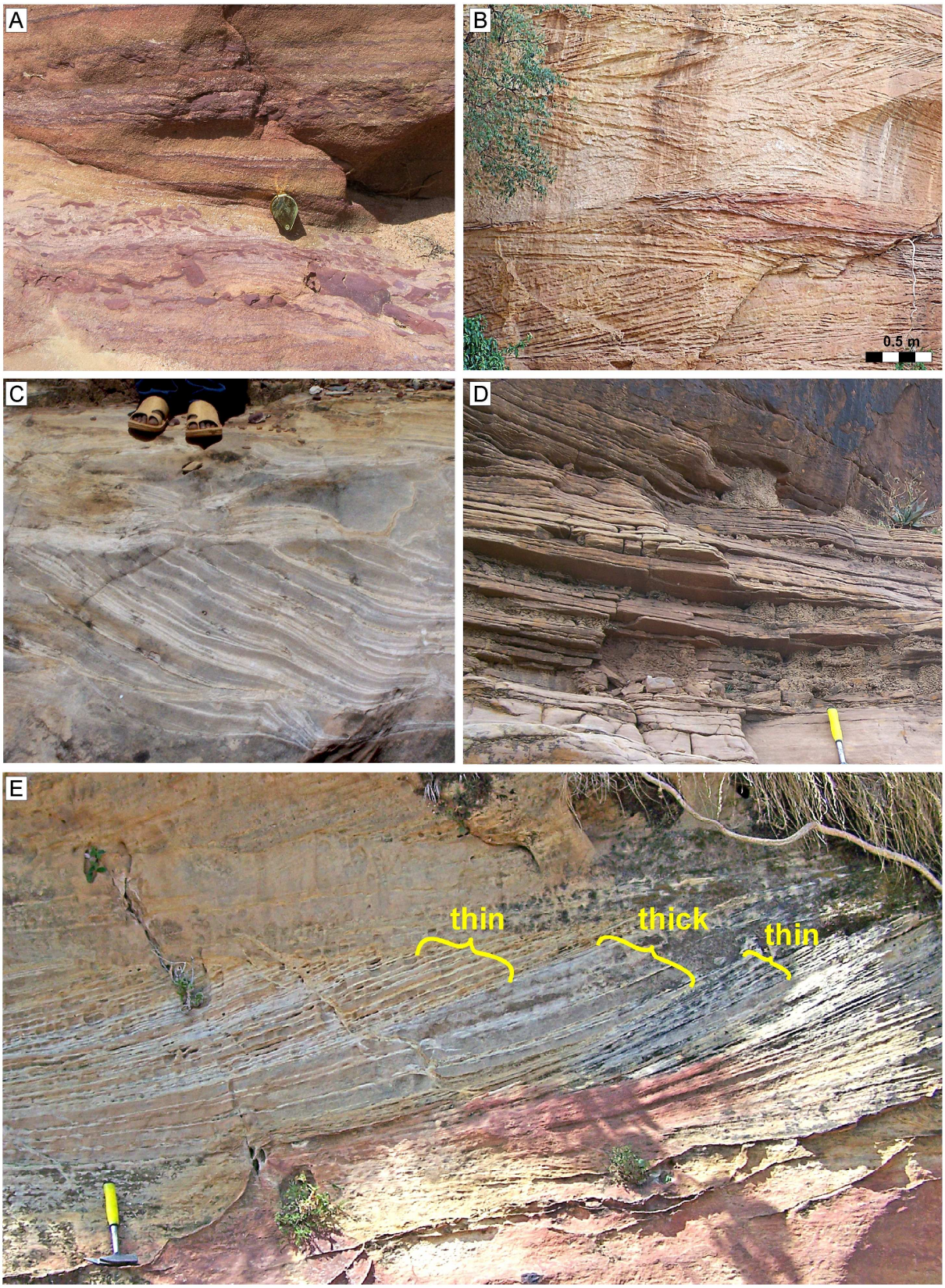


Fig. 4.2. Outcrop examples of the fluvio-estuarine system (FE). A. Tidal channels lag composed of mud rip-up clasts, Wukro section. B. Bi-directional (Herringbone-type) cross-bedding within tidal estuarine channel fill sandstones ($FE_1$), Abiadi section. C. Mud-draped foresets in tidal estuarine channel fill sandstones ($FE_2$), Megab section. D. Upper flow regime (UFR) plane beds ($FE_4$), Samre section. E. Tidal bundles from the trough cross-bedded elongate tidal bars ($FE_1$), Abiadi section.

bedsets form gently inclined strata that pass down dip into planar- laminated or massive siltstone and mudstone beds. The thickness of siltstone and mudstone beds ranges from a few centimeters up to 40 cm. These beds form laterally discontinuous wedge-shaped bodies. The degree of bioturbation is generally uniform, but slightly decreases upwards within each coarsening-up succession. The lower part is intensely burrowed whereas the upper part is moderately burrowed. Syneresis cracks and rooted horizons are occasionally encountered.

***Interpretation***: The coarsening-upward successions are interpreted to represent bay-head deltas that have probably prograded into shallow and quite waters of the central estuarine embayment. The gently inclined sandstone beds may represent delta front foresets whereas the flat-laying siltstone and mudstone beds represent bottomsets. The presence of wave ripples and flaser bedding suggests moderate wave and tidal influence. The high degree of bioturbation may reflect prolonged periods of fairweather conditions between episodic river floods (MacEachern & Pemberton 1994).

**Facies association $FE_4$**

***Description***: Facies association $FE_4$ is composed of two sandy facies with subordinate intercalations of silty and muddy facies. The first facies is predominantly made up of well-sorted, large-scale trough cross-bedded fine- to coarse-grained sandstones. Cross-bed sets are usually 0.5−1.5 m thick but may occasionally reach up to 2 m. Beds are amalgamated to form up to 5 m thick sandstone bodies. Mud drapes, reactivation surfaces, bimodal foreset orientation of cross-beds and bundles-wise upbuilding of foresets are common (Fig. 4.2e). Palaeocurrent directions are bi- to polymodal but NE- and SW-orientations are predominant. The second facies is composed of fine- to medium-grained planar- to very low-angle cross-bedded sandstones (Fig. 4.2d). Laminated to massive mudstones and flaser to wavy bedded fine-grained silty sandstones occur as intercalations. The degree of bioturbation is low to moderate in the sandstone beds but moderate to intense in the siltstone and mudstone beds.

***Interpretation***: The large-scale trough cross-bedded sandstones with mud-draped foresets are interpreted to represent elongate tidal sand bars deposited as terminal lobes at the mouth of a tide-dominated estuary (Dalrymple & Zaitlin 1989, Dalrymple et al. 1992). The predominance of NE- and SW-oriented palaeocurrent directions indicates deposition by evasive ebb and flood tidal currents. The bundles-wise upbuilding of foresets represents tidal rhythmites (Boersma & Terwindt 1981, Nio & Yang 1991). The planar- to very low-angle cross-bedded sandstones are interpreted to represent upper flow regime sand flat deposits (cf. 'UFR sand flats' of Dalrymple et al. (1992)). The intercalated flaser to wavy bedded fine-grained silty sandstones and laminated to massive mudstones represent tidal flat and fringing marsh deposits accumulated along the sides of the estuary.

### 4.1.3. The Deltaic System (D)

Deltas are well-developed in Megab, Abiadi, Agwe and Wukro areas. Deposits of the deltaic system in the Mekelle Basin may reach up to 60 m in thickness and are composed of a series of 8–10 m thick upward-coarsening and shallowing successions (e.g., Fig. 4.4a & b, 4.5a). Each of these successions contains up to three facies associations, $D_1$, $D_2$ and $D_3$ (Table 2).

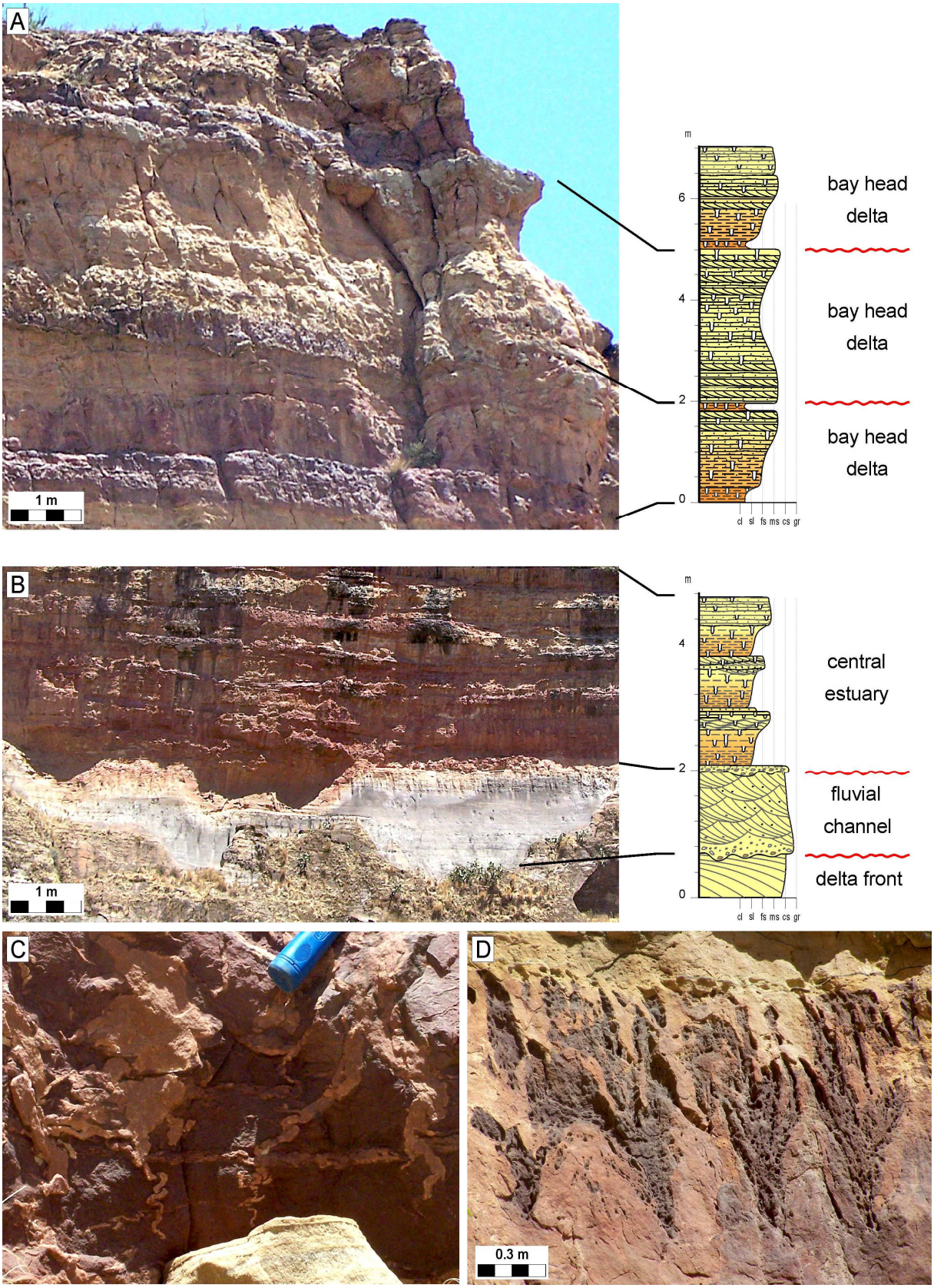


Fig. 4.3. Outcrop examples estuarine facies associations from the Megab section. A. The bay head delta facies association ($FE_3$). B. Heterolithic central estuarine facies association ($FE_2$) sharply overlying fluvial channel fill, which in turn is incised into the underlying deltaic deposits. C. Syneresis cracks. D. Cross-sectional view of large *Rosselia rotatus* reburrowed by *Diplocraterion* and *Thalassinoides*.

**Facies association $D_1$**

***Description***: Facies association $D_1$ is 1–4 m thick and is well-exposed in Megab, Wukro and Abiadi areas, while it is poorly exposed in other areas studied. It is composed of interbedded fine-grained sandstones, siltstones and mudstones (Fig. 4.4a). Thickness of sandstone beds varies between 0.3–2 m. Planar- and ripple-lamination is predominant, though low-angle cross-lamination and massive beds are also common. Hummocky cross-lamination occurs rarely. Soft sediment deformation in the form of small faults, folds and/or slumpes are frequent (arrows in Fig. 4.4d & e). Grains are poorly to moderately sorted and commonly show normal grading with abundant scattered coarse sand. Phytoclasts (up to 0.4 cm long) are common. Sandstone bodies have sheet-like geometry with flat to wavy bases.

Mudstone beds are 2–50 cm thick and form laterally discontinuous lenses and/or wedges of up to 2 m thick and 30 m wide. They are either massive or planar-laminated. Bioturbation is sporadic and usually concentrated along discrete horizons. Burrowing is sparse in the sandstone beds but moderate in the mudstone horizons.

***Interpretation***: The thinly bedded to laminated sandstones, their sheet-like geometry and their relatively poor degree of sorting suggest deposition by surge-type turbidity currents in a prodelta setting (Walker 1967). The graded beds reflect deposition from hyperpycnal density underflows generated at the river mouth during high-discharge floods (Wright et al. 1988, Mulder & Syvitski 1995). The soft sediment deformation features in the form of small faults and folds result from high sedimentation rates and are common in river-dominated deltas (Bhattacharya & Walker 1991, Leithold & Dean 1998). The occasional occurrence of hummocky cross-lamination suggests a moderate to weak storm influence. The bioturbated mudstone beds represent suspension fallout deposition in a relatively quite water environment. The alternate bedding of turbidite sheets and bioturbated mudstones may point to pronounced fluctuations in the rate of sedimentation, which is a common feature of prodelta settings (e.g., Kuehl et al. 1986, Alexander et al. 1991). The sporadic nature of burrowing and the low ichnodiversity may probably be associated with rapid sediment flux, which makes it difficult for permanent domiciles to be constructed and maintained (Leithold 1994, Leithold & Dean 1998). Rapid sediment flux may also lead to reduced concentration of food resources (Howard 1975).

**Facies association $D_2$**

***Description***: Facies association $D_2$ ranges in thickness from 3–8 m and is generally composed of coarse- to medium-grained sandstones with abundant clay rip-up clasts and extrabasinal pebbles. Because $D_2$ exhibits pronounced variation in grain size, palaeocurrent patterns and degree of bioturbation along depositional strike, it can be divided into two subfacies associations, namely $D_{2a}$ and $D_{2b}$.

Subfacies association $D_{2a}$ consists of moderately to well-sorted, orange brown, medium- to coarse-grained sandstones that are arranged in 3–5 m thick, steep-fronted clinoforms (Fig. 4.4c). These prograding clinoforms possess a broadly lobate geometry and downlap with gentle asymptotic contact either onto underlying finer-grained heterolithic bottomsets (facies association $D_1$) of the prodelta platform or onto underlying clinoforms. Dip angle decreases downwards along the axis of the lobate sandstone body from steeply dipping proximal beds to a more gently dipping distal beds. Clinoform foresets are 10–30 cm thick. Greyish white mudstones occur as clay rip-up clasts aligned on foresets. Burrowing is sparse to absent. Palaeocurrent directions are generally unimodal.

Subfacies association $D_{2b}$ is composed of poorly to moderately sorted, angular to sub-rounded (Plate I, Fig. D), medium- to coarse-grained sandstones with abundant quartz pebbles and clay rip-up clasts that are interbedded with fine-grained conglomerates. The varicoloured

appearance of $D_{2b}$ is one of its distinctive features (Fig. 4.4b, 4.5a), which enables its identification and tracking along depositional strike from Agwe up to Abiadi. It is marmoured with purple, light grey and orange colours. Thickness of individual sandstone beds varies between 0.3 m and 1.5 m, but may locally reach up to 3 m. Beds are amalgamated forming 3–8 m thick coarsening-upward successions. Conglomerates occur either as 10–30 cm thick interbeds and/or as lags on cross-bed foresets. Clasts are of 0.5–6 cm in diameter and are usually imbricated parallel to forset dip directions (Fig. 4.5b). This facies association consists of a wide variety of sedimentary structures. Large-scale planar-tabular cross-bedding and low-angle cross-stratification are predominant. Small-scale trough cross-bedding, wave and current ripple-lamination and massive beds are also common. The large-scale inclined strata are occasionally cut at the upper-middle slope by shallow, concave-up scoured surfaces that are up to 2 m deep and 20 m wide. These scoured surfaces have clay rip-up clasts on their bases and are filled with fining-upward facies consisting of medium- to fine-grained sandstones and capped by mudstones. Siltstone and mudstone layers are generally rare in $D_{2a}$ and occasionally occur as thin interbeds that may reach in thickness up to 40 cm. Palaeocurrent directions are generally unimodal with occasional reversals. Although bioturbated bedding surfaces are common burrowing is generally sparse to moderate. *Rosselia rotatus* (Fig. 4.5c) and *Thalassinoides* appear to be the dominant trace fossils.

***Interpretation***: This facies association is interpreted to reflect deposition in a high-energy environment where the interaction of fluvial, wave and tidal processes is at maximum. The prograding clinoforms of the subfacies association $D_{2a}$ with unimodal seaward-oriented palaeoflows reflect deposition from rapidly decelerating unidirectional flows in a river-dominated delta front environment (Hampson & Howell 2005). Despite their discontinuity and randomness, the greyish white mud drapes along foresets of clinoforms indicate a moderate tidal influence (Terwindt 1981, Middleton 1991). The low degree of bioturbation may be related to the high rate of delta front progradation, indicating increased sedimentation rates and heightened fluvial discharge. Rapid emplacement of sediments generally makes infaunal colonization of the substrate difficult (MacEachern et al. 2005). Other river-induced stresses might also have played a role, such as salinity changes and high water turbulance (Leithold & Dean 1998, Howard et al. 1975). Unburrowed to sparsely burrowed delta front deposits have been well-documented in ancient deltas, e.g., in the Pennsylvanian Palo Pinto Delta, Texas (Bhattacharya et al. 2003) and the Triassic Ivishak Formation, Prudhoy Bay, Alaska (Tye et al. 1999).

The poorly sorted, coarse-grained sandstones and interbedded fine-grained conglomerates of the subfacies association $D_{2b}$ are interpreted to represent deposition in a high-energy delta front. The shallow, concave-up scoured surfaces on the upper-middle slope are interpreted as chute or slope channels (Plink-Björklund & Steel 2005). These channels develop when stream mouth bars grow and start to restrict discharge from distributary channels, eventually leading to flow avulsion to a different area along the delta front (Willis 2005). The common occurrence of bioturbation on bedding surfaces, which are inferred to represent abandonment surfaces, suggests breaks or periods of nondeposition (MacEachern & Pemberton 1994). The predominance of vertical burrows reflects increased occurrences of sandy substrates available for opportunistic colonization (MacEachern et al. 2005).

Fig. 4.4. Facies associations of the deltaic system (D). A. An example of two prograding deltas (left) with the measured and interpreted vertical section (right), Megab section. B. Very coarse-grained and proximal delta front facies association ($D_{2b}$), Agwe section. C. Prograding clinoforms of the proximal delta front facies with abundant clay rip-up clasts, Megab section. D. & E. Soft-sediment deformation in the form of small faults (arrow in 'D') and slumps (arrow in 'E'), Megab section.

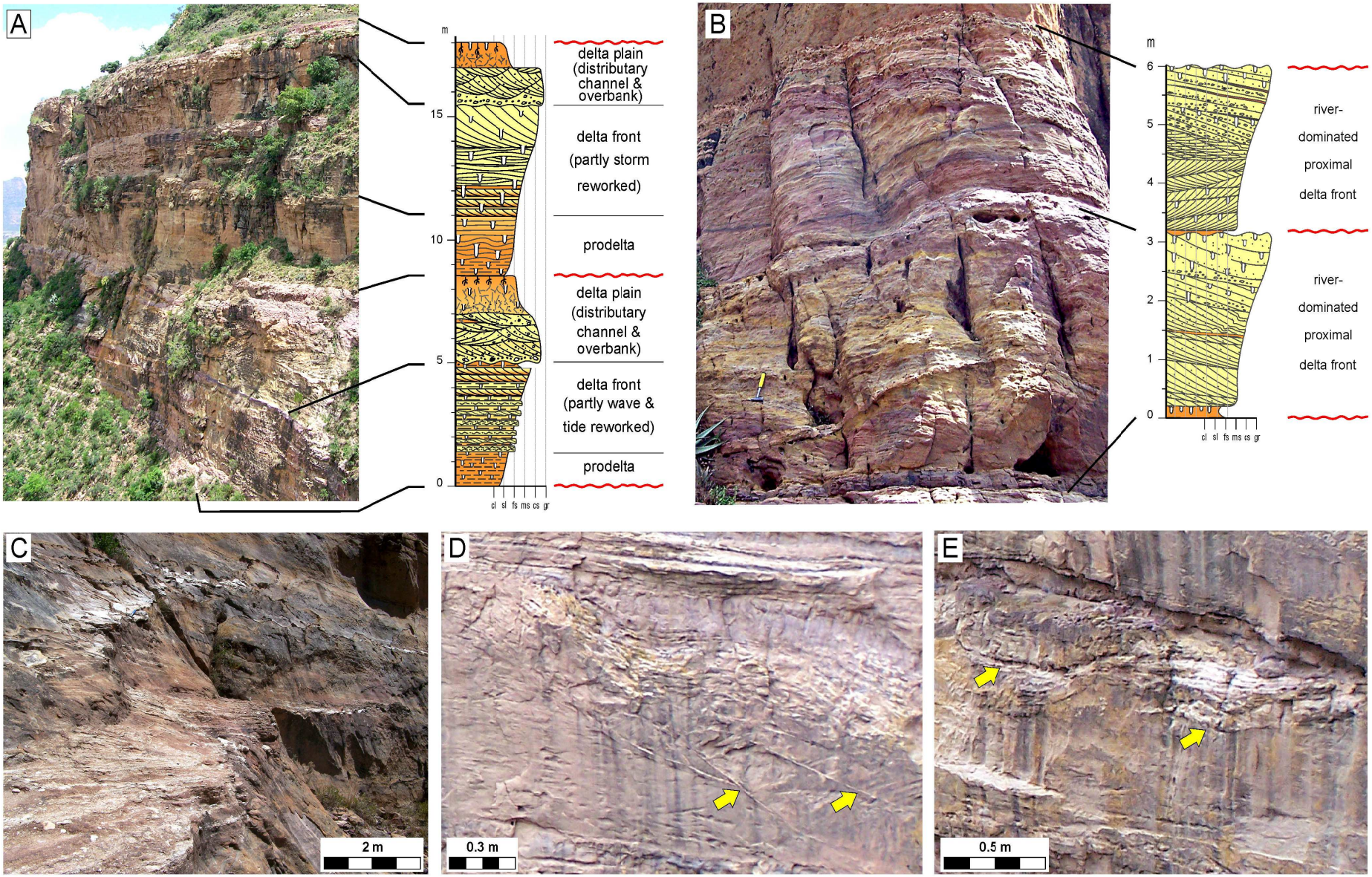
A
m
15
10
5
0
cl sl fs ms cs gr
delta plain (distributary channel & overbank)
delta front (partly storm reworked)
prodelta
delta plain (distributary channel & overbank)
delta front (partly wave & tide reworked)
prodelta
B
m
6
5
4
3
2
1
0
cl sl fs ms cs gr
river-dominated proximal delta front
river-dominated proximal delta front
C
2 m
D
0.3 m
E
0.5 m

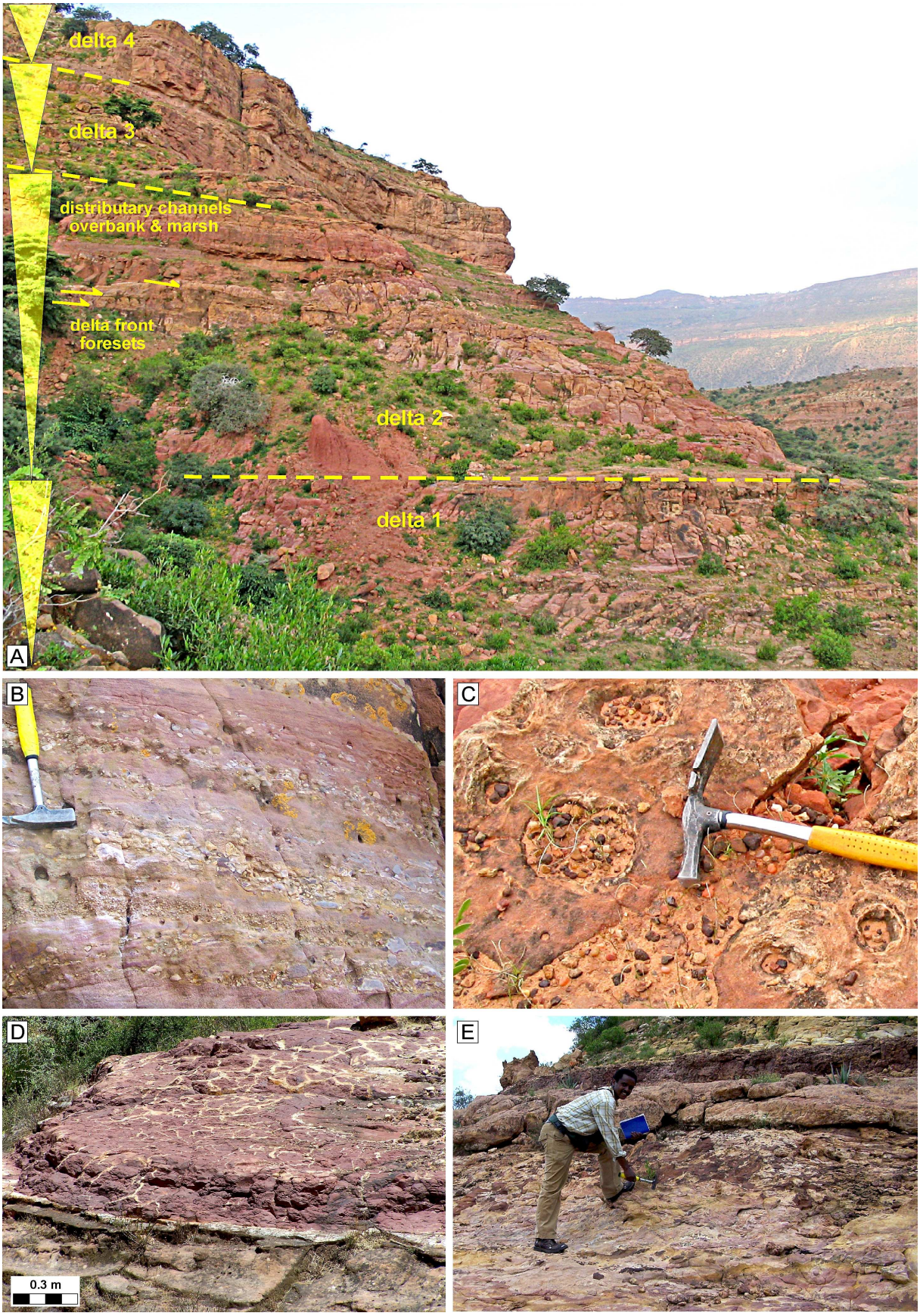


Fig. 4.5. Facies associations of the deltaic system (D). A. A cliff showing prograding delta lobes, Agwe section. B. Close-up view of coarse-grained to pebbly proximal delta front facies with abundant clay rip-up clasts ($D_{2b}$). C. Bedding plain view of large *Rosselia rotatus*. D. Mud cracks on a delta plain, Megab section E. Upper part of distrubutary channels of the delta plain facies association ($D_3$), Abiadi section.

The overall facies, geometry and textural appearance of $D_{2b}$ and the rarity of interbedded silty and muddy layers share some similarities to delta front deposits of 'Gilbert-type' deltas (Wescott & Ethridge 1990). Upwards in the succession, however, cross-bed sets with landward-directed palaeocurrent directions become abundant. This might indicate the gradual transition from an active delta progradation to a phase of abandonment, implying the inception of transgressive barrier-lagoon system. This transition produced a mixture of complex facies successions involving deposits of distributary mouth bars with flanking barrier islands, tidal inlets, restricted interdistributary bays and washover fans. A similar facies transition has been documented in the Holocene Mississippi Delta (Penland et al. 1988). Alternatively, the Pleistocene terrace deposits described by (Clifton 2006) or the migrating ridge-and-runnel system described by Davies et al. (1972) are other similar examples, both of which are characterised by pebbly sand deposited in a high-energy coastal setting.

**Facies association $D_3$**

***Description***: Facies association $D_3$ usually overlies delta front deposits ($D_2$) and ranges in thickness from 0.3–2 m. It is composed of fine- to coarse-grained sandstones that are capped by laminated to massive mudstones. Sandstone beds are 20–60 cm thick and erosionaly amalgamated forming a small fining-upward unit with erosive, concave-up to irregular bases (e.g., the uppermost part in Fig. 4.4a). The scale of sedimentary structures decreases upward from trough cross-bedding in the lower part to planar- and current ripple-lamination as well as mottled, massive beds in the upper part (Fig. 4.5e). Palaeocurrent directions are unimodal. The mudstones at the top are massive, 20–50 cm thick and dark reddish brown in colour. They usually cover the top flat surfaces of delta front deposits where the cross-bedded sandstones are absent. Desiccation cracks are common on upper bedding surfaces (Fig. 4.5d).

***Interpretation***: The erosive based fining-upward sandstone bodies, their unimodal palaeoflow directions and the upward decrease in the scale of sedimentary structures suggest deposition in fluvial distributary channels in a delta plain setting. In some studied localities (e.g., Megab, Fig. 4.5d), delta plain deposits are represented only by the massive rootlet mottled or mud cracked mudstone layers. Although other soil features, e.g., ped structures and soil horizons, are not discernible, the mudstones have a ferruginous paleosol appearance (Fig. 4.5e). Generally, the presence of rootlet mottling and/or mud cracks represents subaerial exposure.

In summary, the deltaic system (D) in the Mekelle Basin is composed of flat laying bottomsets of the prodelta platform ($D_1$), steeply inclined foresets (clinoforms) of the delta front slope ($D_2$), and distributary channel and/or floodplain deposits (topsets) of the delta plain ($D_3$). Palaeocurrent patterns and stratal terminations of the typically upward-coarsening units of the deltaic system indicate a general southeastward progradation. The deltaic deposits are interpreted to represent normal regression, which were formed when sedimentation rates outpace the low rates of sea level rise at the shoreline (cf. Posamentier & Vail 1988, Catuneanu 2006). Similar examples of regressive deltaic deposits have been documented from modern deltaic shorelines (e.g., Nile Delta (Sestini 1989) and Sao Francisco Delta (Dominguez 1996)), as well as from ancient deltaic shorelines (e.g., Blackhawk and Star Point Formations of the Book Cliffs, Central Utah (Hampson & Howell 2005, Posamentier & Morris 2000)).

Fig. 4.6. A. An outcrop example of the strandplain system (SP) (left) with the measured and interpreted vertical section (right), Megab section. B. Offshore transition to lower shoreface facies association ($SP_{1a}$), Megab section C. Heavily bioturbated lower to middle shoreface facies association ($SP_{1b}$), Megab section D. Hummocky cross-stratified sandstone ($SP_{1b}$), Samre section E. Gently dipping beach foreshore facies with low-angle discordances between sets, Samre section.

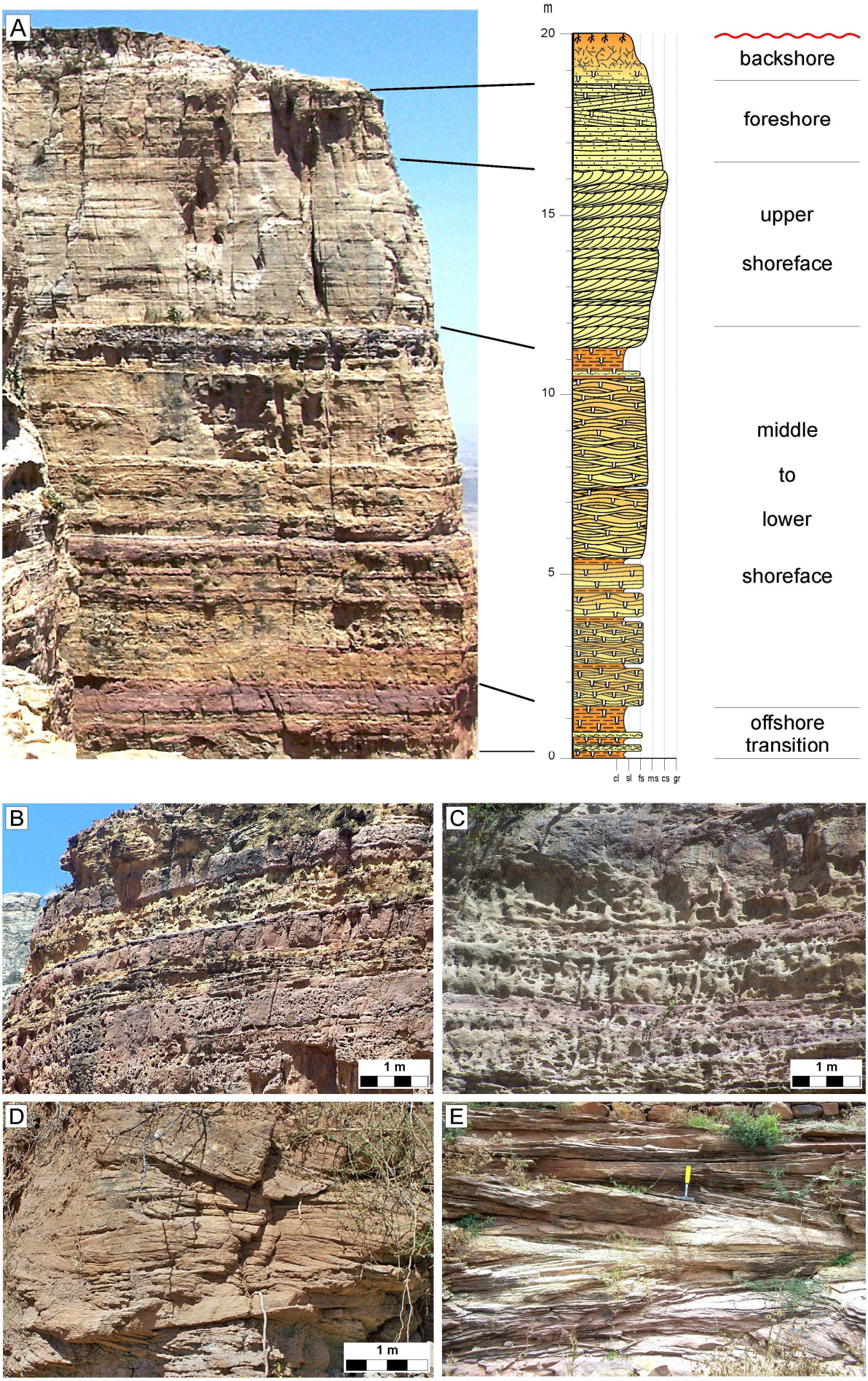
A
m
20
15
10
5
0
cl sl fs ms cs gr
backshore
foreshore
upper
shoreface
middle
to
lower
shoreface
offshore
transition
B
1 m
C
1 m
D
1 m
E

### 4.1.4. The Strandplain System (SP)

Two facies associations, $SP_1$ and $SP_2$ are identified in the strandplain deposits of the Mekelle Basin, (Table 2).

**Facies association $SP_1$**

***Description***: Facies association $SP_1$ consists of two facies, a lower facies $SP_{1a}$ and an upper facies $SP_{1b}$. The lower facies association $SP_{1a}$ is characterised by alternate bedding of hummocky cross-stratified (Plate I, Fig. E & F) medium- to very fine-grained sandstones and massive, heavily bioturbated silty mudstones (Fig. 4.6b). Mudstone beds, which predominate in the lower part and become proportionally minor upwards, are usually massive and less commonly planar- to wavy-laminated. They occur as regular interbeds, but occasionally show a random vertical distribution. Bed thickness ranges from 0.2 m to 1 m, but may rarely reach up to 2 m. The upper facies $SP_{1b}$ consists of hummocky cross-stratified (Fig. 4.6d) to planar-laminated sandstones with scattered fine pebbles. Heavily bioturbated massive beds are also common, as well as wave- and combined-flow ripple-laminations. Individual sandstone beds (0.3–1 m thick) are usually erosionaly amalgamated forming 4–8 m thick sandstone bodies. Grain size generally increases upwards and sorting is moderate. Burrowing is generally moderate to intense and may locally reach up to complete biogenic homogenisation (e.g., Fig. 4.6c).

***Interpretation***: There is substantial evidence to suggest that facies association $SP_1$ has been deposited in an open marine environment. The amalgamated, hummocky cross-stratified beds represent deposition by strong storm surges above but near storm wave base (Dott & Bourgeois 1982, Cheel & Leckie 1993, Dumas & Arnott 2006) in the lower to middle shoreface. Wave- and combined-flow ripple-laminated beds indicate fairweather deposition by lower-flow-regime oscillatory currents within the lower shoreface environment that experienced intermittent high-energy storms (Clifton 1982, Swift & Nummedal 1987). The heavily bioturbated massive beds may reflect either the involvement of large number of burrowing organisms or prolonged periods between storm events allowing total biogenic homogenisation (Ekdale et al. 1984, Frey & Pemberton 1984). Scattered fine pebbles represent post-storm lags. The mudstone beds reflect post-storm fairweather mud deposition by suspension fall-out of storm-derived sediments. In summary, the lower facies ($SP_{1a}$) is interpreted as having been deposited in a well-oxygenated offshore transition to lower shoreface environments. The upper facies ($SP_{1b}$) is interpreted to represent lower to middle shoreface deposits.

**Facies association $SP_2$**

***Description***: Facies association $SP_2$ appears to be characterised by three sandy facies, $SP_{2a}$ to $SP_{2c}$. The first facies ($SP_{2a}$) is 4–8 m thick and is composed of medium- to coarse-grained sandstones with few scattered fine pebbles. The geometry of sandstone bodies is variable but laterally extensive sheet-like tabular bodies are predominant. Individual sets are commonly 15–40 cm thick and rarely reach up to a meter. Sand grains are well-sorted and well-rounded. Grain size slightly increases upwards. The sandstone beds are predominantly small- to large-scale trough and planar-tabular cross-bedded (Fig. 4.6a) with subordinate planar- and ripple-lamination. Burrowing in $SP_2$ is sparse and characterized by few scattered traces of vertical dwelling infauna.

Table 2. Summary of the main characteristics of the deltaic and the strandplain depositional systems and facies associations

| Depositional systems and facies association | Lithology and sedimentary structures | Palaeocurrent patterns | Bioturbation | Fossils | Depositional environment |
|---|---|---|---|---|---|
| Deltaic System (D) | | | | | |
| Facies Associations | | | | | |
| D1 | alternation of poorly sorted fine-grained sandstones, silt- and mudstones, planar- to ripple-lamination, massive beds, soft sediment deformation | unimodal | sparse to moderate | phytoclasts | prodelta, suspension fall-out alternating with surge-type turbidity currents |
| D2a | moderately to poorly sorted medium- to coarse-grained sandstones, large-scale planar-tabular cross-bedding (steep fronted clinoforms), abundant clay rip-up clasts aligned on foresets | unimodal | sparse to absent | none | moderate to high-energy river-dominated delta front |
| D2b | upward-coarsening, poorly sorted coarse-grained sandstones and fine-grained conglomerates, large-scale planar-tabular and low-angle cross-bedding | unimodal, occasionally bimodal | sparse to moderate | none | high-energy river-dominated, wave-influenced delta front |
| D3 | upward-fining, trough cross-bedded coarse- to fine-grained sandstones, planar to ripple-laminated silt- and mudstones, massive rooted mudstones, desiccation cracks | unimodal | moderate, become intense upwards | phytoclasts, pollen and spores | delta plain distributary channels, overbanks and marsh |
| Strandplain System (SP) | | | | | |
| SP1a | alternating beds of hummocky cross-stratified to planar-laminated sandstones and massive silty mudstones | | intense, in part complete biogenic homogenisation | rare phytoclasts | offshore transition zone to lower shoreface |
| SP1b | amalgamated hummocky cross-stratified to planar-laminated sandstones, scattered fine pebbles | | moderate to intense | none | lower to middle shoreface |
| SP2a | small- to large-scale trough cross-bedded medium- to coarse-grained sandstones, abundant scattered pebbles | uni- to bimodal, | sparse to absent | none | upper shoreface |
| SP2b | well sorted, medium- to fine-grained sandstones, gently dipping planar-lamination with low-angle discordances between sets | unimodal | sparse | none | foreshore |
| SP2c | small- to large-scale trough cross-bedded, and/or planar-laminated fine- to coarse-grained sandstones, rootlet mottling | unimodal | moderate to intense | phytoclasts and cuticles | backshore dunes |

Facies $SP_{2b}$ is mainly composed of well-sorted and well-rounded, medium- to fine-grained sandstones (Plate I, Fig. C). Thin layers of coarse sand to fine pebble occur at some intervals. Individual beds are 0.8–2 m thick. They form 6–8 m thick and laterally extensive tabular sandstone bodies, but may locally reach up to 12 m in thickness. The dominant sedimentary structures are planar-lamination to gently dipping cross-lamination with low-angle discordances between sets (Fig. 4.6e). Well-developed, discrete heavy mineral concentrations occur in the form of laminae (Plate I, Fig. A). Burrowing is sparse. Facies $SP_{2c}$ contains both planar-lamination and trough cross-bedding but it differs from the other two facies in that it is usually disrupted by rootlet mottling and/or burrowing.

***Interpretation***: The internal sedimentary structures and the rarity of burrows, together with the absence of silty/muddy sediments in facies $SP_{2a}$ suggest deposition in a high-energy environment, probably in the upper shoreface. The trough and planar cross-bedded sandstones represent landward migrating 3D and 2D dunes deposited by high-energy onshore directed shoaling waves (Reading & Collinson 1996). The large-scale trough cross-bedded sets represent the migration of lunate megaripples in the breaker and surf zone of the upper shoreface (Clifton et al. 1971). Extensive reworking prior to final deposition is reflected by the high degree of grain sorting and rounding. The presence of predominantly vertical burrows may suggest that only deeply penetrating burrows are able to withstand the high-energy shoaling waves of the upper shoreface (MacEachern & Pemberton 1994, Bahn & Fielding 2004).

The planar-laminated and gently dipping cross-laminated sandstones of the second facies ($SP_{2b}$) with low-angle discordances between sets are interpreted to reflect deposition by the swash and backwash mechanism of waves in the beach foreshore environment (Reinson 1984). The low-angle discordances between sets represent the adjustment of the beach to changes in wave regime and sediment supply (Clifton 1969). The presence of heavy mineral layers suggests extensive reworking and concentration of grains by density. The presence of rootlet mottling in the facies $SP_{2c}$ might indicate deposition in a backshore environment. It has been well-documented that backshore deposits are commonly mottled and bioturbated than their foreshore counterparts (e.g., Howard 1972, Howard & Reineck 1981).

In summary, the strandplain system represents coarsening- and shallowing-upward progradational units containing, from bottom to top, offshore transition to lower shoreface, upper shoreface, foreshore and backshore deposits. They have been formed under regressive conditions in open shoreline settings when the rate of sedimentation was higher than the rate of sea level rise at the shoreline (cf. Posamentier & Vail 1988, Catuneanu 2006).

### 4.1.5. The Barrier Island - Lagoon System (BL)

Sedimentary successions belonging to the barrier-lagoon system are well-represented in all areas studied in the Mekelle Basin and consist of three facies associations, $BL_1$, $BL_2$ and $BL_3$ (Table 3).

#### Facies association $BL_1$

***Description***: Facies association $BL_1$ consists of two facies superimposed on each other. Both facies are composed of well-sorted and well-rounded, fine- to coarse-grained sandstones with scattered pebbles. The main difference between the two facies lies in the type and scale of sedimentary structures and the degree of bioturbation and rootlet mottling. The most distinctive facies is composed predominantly of planar- and wave ripple-laminated sandstones (Fig. 4.7b & d). Small-scale trough and planar cross-bedding occur subordinately and

hummocky cross-bedding occurs rarely. Individual beds vary in thickness from 0.3 m to 1.5 m. Beds are amalgamated forming up to 15 m thick sandstone bodies. Sandstone bodies have sharp erosive lower and upper boundaries. Amalgamation surfaces are usually horizontal or low-angle dipping, but occasionally wavy. Despite the high degree of grain sorting and rounding, local concentrations of pebble layers are common. No vertical grain size trends are discernible, though pebble layers become more frequent towards the top. Palaeocurrent directions are predominantly unimodal with locally common bimodal directions. Burrowing is sparse and very sporadic with few scattered *Ophiomorpha* and *Skolithos* traces.

The second facies is composed of small- to large-scale trough cross-bedded sandstones with curved bedding surfaces. Thickness varies between 2–6 m and individual set are 0.2–0.7 m thick. The sandstones are commonly extensively disturbed by burrowing and pervasive root penetration (Fig. 4.7a). In some rare circumstances, the primary structures are well-preserved and the cross-bedding resembles large-scale festoon cross-bedding (Fig. 4.7e). Burrowing is moderate to intense but is overprinted by rootlet mottling.

***Interpretation*:** The planar- to wave ripple-laminated sandstones are interpreted to represent spit beach and/or welded ridge deposits of the spit platform (Reinson 1984). Their vertical accretion is attributed to beach aggradation under fairweather conditions, while the wavy amalgamation surfaces (lower part in Fig. 4.7d) reflect erosional truncation during storms. This process of beach aggradation during fairweather conditions and erosion during storms is described by Sonu & Van Beek (1971) and later by Reading & Collinson (1996) as 'the beach cycle'. The small- to large-scale trough (festoon-like) cross-bedded sandstones with curved bedding surfaces (Fig. 4.7e) represent backshore dunes that are piled up by wind (Davis 1994). Backshore depositional environment is further supported by the higher degree of bioturbation and the pervasive rootlet mottling.

**Facies association $BL_2$**

***Description***: Facies association $BL_2$ consists of a complex intertonguing of the following two facies that can mainly be distinguished on the basis of variable combinations of small- and large-scale sedimentary structures, vertical stacking patterns and the dominant palaeocurrent direction.

The first facies is composed of well-sorted, megaripple cross-bedded, fine-grained sandstones (Fig. 4.8c). Thickness varies between 8–12 m and set thickness is within the range of 0.2–1 m. Megaripple foresets dip steeply at an angle of 20°–25° that become gentle down the lee face and tangentially join the set base. Thinner bottomsets with ripples migrating in the opposite direction to the main flow occur at the base of larger foresets. The upper part contains microdelta cross-bedding and beach stratification (Fig. 4.8a & b).

The second facies is composed of fine- to coarse-grained sandstones that are arranged in several erosive based fining-upward cycles. The main sedimentary structures are, from bottom to top, basal scour surface with coarse lags overlain by bidirectional medium- to large-scale planar-tabular cross-bedding (Fig. 4.8d), which in turn grades upwards into medium- to small-scale trough cross-bedding and ends up with either planar- and/or bidirectional ripple-lamination (Fig. 4.8f). Sandstone bodies are lenticular or wedge-shaped and top bioturbated. Reactivation surfaces are common. This facies is characterised by bi- to polymodal palaeocurrent directions.

Fig. 4.7. Outcrop examples of the barrier - lagoon system (BL) from the Agwe section, except 'E' which is from the Abiadi section. A. Pedogenically altered backshore facies. B. Spit beach facies. C. Washover channel and marsh facies. D. Spit beach cut at the top by washover channel. E. Locally preserved backshore eolian dunes. F. Lagoonal facies association. G. Dolomite layers intercalated with lagoonal mudstones.

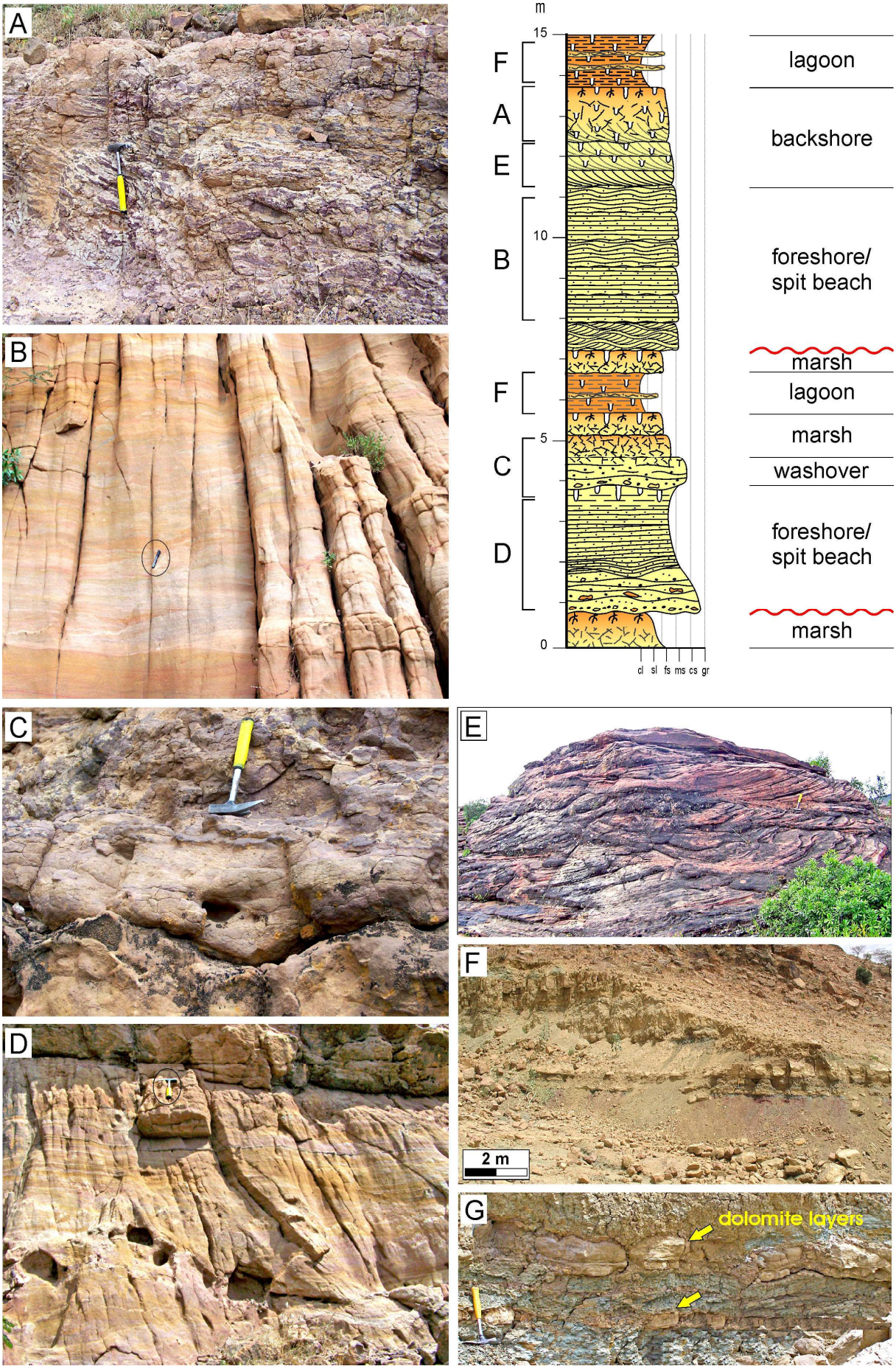
A
B
C
D
E
F
2 m
G
dolomite layers
m
15
10
5
0
F
A
E
B
F
C
D
cl sl fs ms cs gr
lagoon
backshore
foreshore/
spit beach
marsh
lagoon
marsh
washover
foreshore/
spit beach
marsh

Table 3. Summary of the main characteristics of the barrier-lagoon and the the open-coast tidal flat depositional systems and facies associations

| Depositional systems and facies association | Lithology and sedimentary structures | Palaeocurrent patterns | Bioturbation | Fossils | Depositional environment |
|---|---|---|---|---|---|
| Barrier - Lagoon System (D) | | | | | |
| Facies Associations | | | | | |
| Bl1 — Bl1a | well sorted and well rounded fine- to coarse-grained planar-laminated sandstones | unimodal | sparse, very sporadic | phytoclasts | barrier spit accretion in a spit platform |
| Bl1 — Bl1b | well sorted and well rounded, fine- to coarse-grained, trough cross-bedded sandstones | unimodal | moderate to intense | none | backshore dunes |
| Bl2 — BL2a | fine-grained sandstones, megaripple cross-bedding, microdelta cross-bedding, backflow ripples, beach stratification | unimodal | sparse | none | barrier formation through growth and emergence of offshore bars |
| Bl2 — BL2b | upward-fining, fine- to coarse-grained sandstones with abundant clay rip-up clasts as lags, bidirectional planar-tabular cross-bedding, flaser- and wavy bedding, washed-out ripples | bi- to polymodal, abundant bipolar | moderate | vertebrate bone fragments, phytoclasts | tidal inlet channels, flood tidal delta |
| Bl2 — BL2c | medium-grained sandstones, planar- and wave ripple-lamination, microdelta cross-bedding, bedding plane parting | unimodal | moderate to intense | tooth plates of lungfish, fragments of vertebrate bones, gastropods, bivalves, brachiopods | storm washover |
| BL3 | massive to laminated silty mudstones, rootlet mottling | | intense | aglutinated foraminifera rare scolecodonts, pollen and spores | subaqueous lagoon and fringing marsh |
| Open-Coast Tidal Flat System (OT) | | | | | |
| OT1 | coarse- to fine-grained trough and planar-tabular cross-bedded sandstones, grading upward into heterolithic silt- and mudstone, falser-, lenticular- and wavy bedding, rootlet mottling | bi- to polymodal | moderate, become intense to the top | phytoclasts, cuticles, pollen and spores | subtidal channels, intertidal to supratidal flats and marsh |

***Interpretation***: The megaripple cross-bedded sandstones with shoreward dipping foresets are interpreted to represent longshore bars (McKee & Sterrett 1961) formed by high-energy landward-directed shoaling waves in the wave build-up zone of the shoreface (Clifton et al. 1971). The vertical accretion of up to a meter thick cross-bed sets indicates strong wave agitation favouring the vertical growth of longshore bars (Walker & Plint 1992). Ripples in the smaller sets at the base of megaripple foresets that migrate in the opposite direction to the main flow are interpreted to represent backflow ripples (Boersma et al. 1968). The microdelta foresets have been formed when storm surges overtop and cut through the barrier and deposit a lobate-shaped detritus that protrude into the lagoon (Schwartz 1982). The upward change in the scale of sedimentary structures from megaripples to microdeltas and smaller-scale wave ripples may reflect the weakening of wave energy with decreasing water depth as the longshore bar emerges to form a barrier-lagoon system (Carter & Woodroffe 1994). This process is referred to, in terms of De Raaf et al. (1977), as bar maturation from an initial 'incipient and submerged' stage to final 'emergent' stage. The vertical growth and emergence of longshore bars is presumed to be one of the important mechanisms for the origin of barriers (Swift 1975).

The sharp, erosive based fining-upward bodies with coarse lags are interpreted to represent deposits of tidal inlet channels. The bidirectional large-scale planar-tabular cross-bedded sandstones suggest sand wave deposition by strong tidal currents and alternating flow reversals under lower flow regime conditions (Barwis & Macurath 1978, Hayes 1980). The overlying planar-laminae with interbedded bidirectional ripple-laminae reflect plane bed deposition under transitional or upper flow regime conditions (Hubard & Barwis 1976). The tidal inlet fills are usually overlain by the spit beach and backshore dune deposits of the facies association $BL_1$ to form channel-spit sequences. The lateral migration of tidal inlet deposits or channel-spit sequences is presumed to be another important mechanism for the origin of barriers (Swift 1975).

**Facies association $BL_3$**

***Description***: Facies association $BL_3$ ranges in thickness from 16–30 m and is characterised by an assemblage of heterolithic facies consisting of the regular interbedding of fine- to medium-grained silty sandstones and greenish grey to reddish brown mudstones. Individual sandstone beds range in thickness from 5 cm to 80 cm. Although alternate bedding is predominant, several sandstone beds are commonly amalgamated forming up to 2 m thick bedsets. Occasionally, up to 6 m thick planar-bedded sandstones with bedding-plane partings also occur. The geometry of sandstone bodies is mainly tabular or sheet-like with sharp, flat and/or wavy lower boundaries. Some massive sandstone bodies possess irregular scours at their base (Fig. 4.7c). Planar- and wave ripple-laminations are the predominant sedimentary structures. Heavily bioturbated massive beds are also common, as well as lenticular- and flaser bedded sandstones. Small-scale planar-tabular and trough cross-bedding are also present but less common.

Fig. 4.8. Outcrop examples of the barrier island and lagoon system (BL). A. Sandstones showing beach stratification, Samre section. B. Microdelta cross-bedded sandstones, Samre section. C. Megaripple cross-bedded sandstones with well-developed backflow ripples at the base of foreset laminae, Samre section. D. Large-scale bidirectional planar-tabular cross-bedded sandstones of the lower part of tidal channel facies, Agwe section. E. Flood-tidal delta facies scoured by washover channel, which in turn is overlain by marsh deposits, Abiadi section. F. 'Washed-out' ripples migrating in opposite directions, from the upper part of tidal channel facies, Agwe section. G. Flaser-bedded sandstones with mud drapes (upper part of tidal channel facies, Abiadi section).

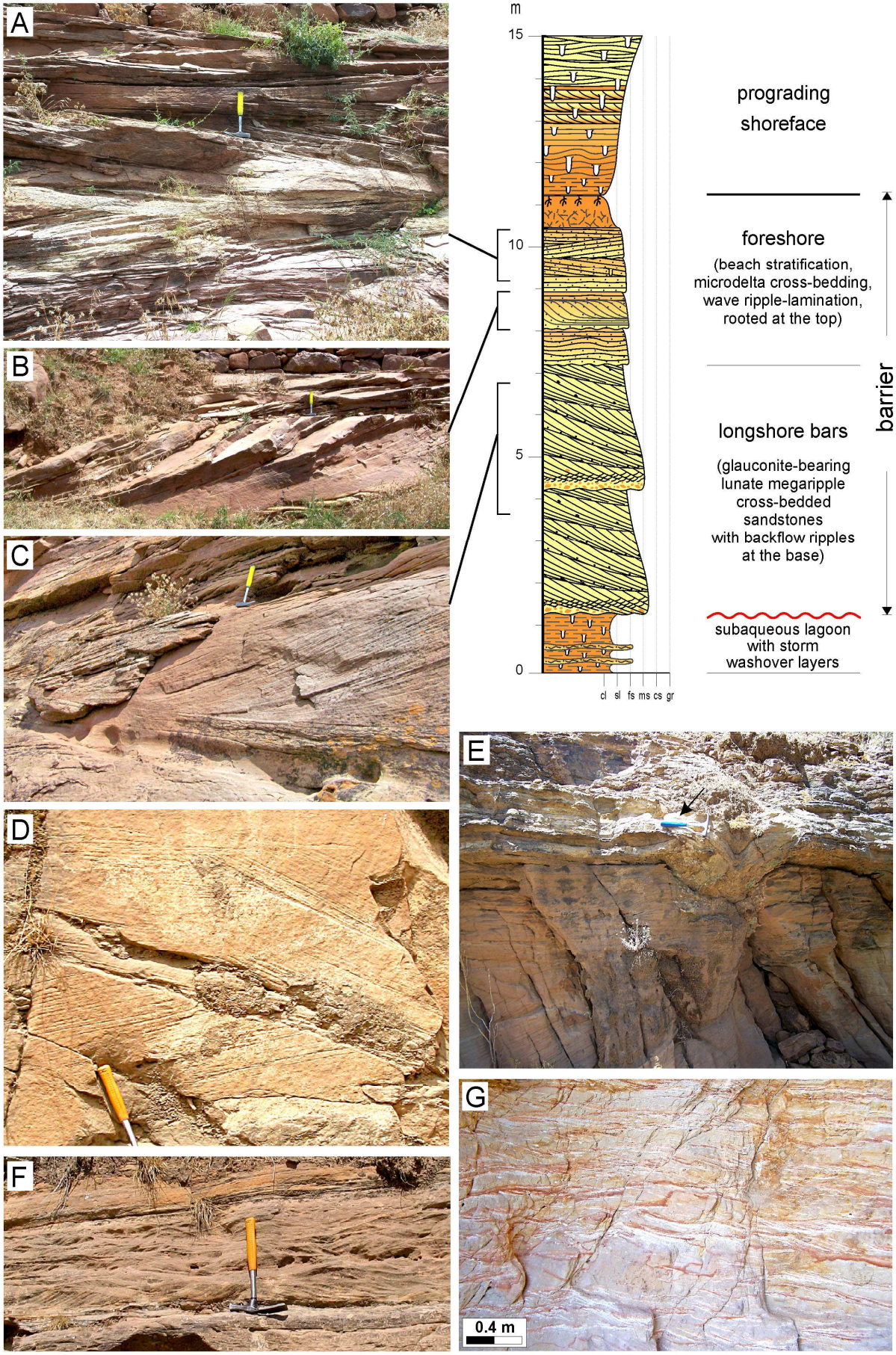
A
B
C
D
E
F
G
m
15
10
5
0
cl sl fs ms cs gr
prograding shoreface
foreshore
(beach stratification, microdelta cross-bedding, wave ripple-lamination, rooted at the top)
longshore bars
(glauconite-bearing lunate megaripple cross-bedded sandstones with backflow ripples at the base)
subaqueous lagoon with storm washover layers
barrier
0.4 m

Sandstone bedding surfaces exhibit different types of physical and biogenic sedimentary structures, including various forms of wave and current ripple marks, abundant trace fossils (e.g., *Skolithos*, *Diplocraterion* and *Thlassinoides*, Fig. 4.9a–c), plant imprints and halite pseudomorphs (Fig. 4.9d). Wood fragments (up to 15 cm long) occur frequently. Body fossils are also present within the sandstone beds including brackish water bivalves (Fig. 4.9e & f) and vertebrate fossils of various faunal compositions (Fig. 4.10c-f). Apart from various types of coprolites, the vertebrate fauna includes tooth plates of lungfish, teeth of actinopterygian fish (cf. *Lepidotes*) and hybodontid sharks, along with abundant remains of marine crocodiles (*thalattosuchian*).

The muddy facies consists mainly of greenish grey mudstones with subordinate reddish brown mudstones. Individual beds vary in thickness between 20 cm and 1.5 m. Most of the greenish grey mudstone beds are planar-laminated and display primary fissility, though massive bioturbated beds are also present. Intercalations of dolomite layers and lenses (5–20 cm thick) are common, but not abundant (Fig. 4.7g). The mudstones contain brackish water to fully marine body fossils, including brachiopods, gastropods, scolecodonts and agglutinated foraminifera (e.g., *Ammodiscus*) (Fig. 4.10a & b). In addition, some of the greenish grey mudstones are rich in phytoclasts, cuticles and well-preserved palynomorphs (see Sec. 6). The reddish brown mudstones are massive and blocky with scattered greenish grey spots. Rootlet traces and desiccation cracks are common.

***Interpretation***: Based on its proximity to barriers and the presence of brackish water bivalves, dolomite horizons and halite pseudomorphs, this facies association is interpreted to reflect deposition in a back-barrier lagoonal setting. The planar- and wave ripple-laminated sheet-like sandstone bodies with bedding-plane partings are interpreted to represent washover fans. The presence of fully marine fossils along with diverse remains of marine vertebrates indicates a shallow marine sediment source and deposition by storm surges (Leatherman & Williams 1977). The irregular scours at the base of massive sandstones (e.g., Fig. 4.7c) have been carved by storm surges, and interpreted to represent washover channels (Andrews 1970). The small-scale planar-tabular and trough cross-bedded sandstones, as well as the lenticular- and flaser beds are interpreted to represent deposits of back-barrier tidal channels and tidal flats (Carter 1978, Terwindt 1988).

The mudstone beds are interpreted to reflect suspension fall-out deposition in quiet water environments, probably in lagoons and tidal flats. The massive reddish brown mudstones with desiccation cracks and root traces represent marsh and swamp deposits formed on sand and mud flats of the lagoonal margin, and on emergent washover flats (Boothroyd 1985, Nichols 1989). The presence of abundant phytodetrital material and humidity-loving palynomorphs points to the existence of humid climatic conditions. Nonetheless, the presence of dolomite horizons and halite pseudomorphs indicates periodic desiccation.

Summarising, the barrier island and lagoon system in the Mekelle Basin consists of three facies associations $BL_1$ to $BL_3$, which are interpreted to represent spit platform (with spit beaches and backshore dunes), longshore bars and/or tidal inlet fills and enclosed subaqueous lagoons with associated storm washover, flood tidal delta, restricted tidal flat and fringing marsh deposits.

### 4.1.6. The Open-Coast Tidal Flat System (OT)

***Description***: The open-coast tidal flat system (OT) is composed of a single facies association, namely $OT_1$, which is characterised by fine- to coarse-grained sandstones that are arranged in several erosive based fining-upward cycles. These cycles consist, from bottom to top, of basal

scour surfaces with coarse lags overlain by bidirectional large-scale planar-tabular cross-bedded, medium- to coarse-grained sandstones, which grade upward into medium- to small-scale trough cross-bedded, fine- to medium-grained sandstones. The upper part of the succession is characterised by flaser to wavy bedded sandstones and lenticular bedded siltstones with intercalated laminated to massive silty mudstones. Sandstone bodies are usually isolated single storey and rarely amalgamated. Mud drapes on forsets and reactivation surfaces are common. Bioturbation is moderate to intense, especially in the upper fine-grained parts of the cycles.

***Interpretation***: Based on the presence of bidirectional cross-bedding, mud-draped foresets and reactivation surfaces, the sandstone bodies are interpreted to represent subtidal channel fills and tidal bars. The sandstones are basically similar to the tidal inlet channels described in the barrier-lagoon system in Sec. 4.1.5. The main difference is that the planar laminated spit beach deposits are absent. The flaser, lenticular and wavy bedded sandstones with interbedded silt- and mudstones represent mixed intertidal flat deposits. The massive and rooted mudstones at the top are deposited in mud flats and marshes in a supratidal environment. The upward-fining cycles from subtidal channel fills at the base to supratidal flat deposits at the top suggest progradation that occurs as the rate of sediment supply is in excess of the rate of relative sea level rise at the shoreline (cf. Posamentier & Vail 1988, Catuneanu 2006). Similar examples of modern prograding tidal flat deposits are described from the German Bight (Davis & Clifton 1987) whereas ancient counterparts are well-described by Klein (1971) and Reinson (1992).

## 4.2. Stratigraphic Stacking Patterns

Cyclic changes in the processes that form individual depositional systems are the main causes for the variation in the large-scale spatial and temporal stratigraphic stacking patterns within a sedimentary basin fill. Thus, this section deals with the manner in which depositional systems are stacked using the data from six vertical sedimentologic sections logged in Wukro, Megab, Abiadi, Agwe, Samre, and Berhale areas (see Fig. 1b for locations). These sections are described and interpreted below.

### 4.2.1. Samre area

***Description***: The studied section (N 13°11′09″/E 39°12′08″) in Samre area is located 2 km southeast of the town Samre. The Adigrat Sandstone succession is about 190 m thick and unconformably overlies the Edaga Arbi Glacials. The lower boundary is marked by a visible and irregular or uneven erosion surface that truncates the underlying Permo-Carboniferous glacial deposits. The upper boundary to the overlying Antalo Limestone is marked by poorly developed noncalcareous paleosols and no erosion surface is discernable. The succession can be divided into two stratigraphic units, which are referred to as *Unit I* and *Unit III*. This nomenclature (i.e., *Unit III* instead of *Unit II*) is adopted to avoid confusion during intrabasinal correlation (see Sec. 4.3). These units are separated from each other by a subaerial exposure surface of either fluvial incision or lateritic paleosol (Plate I, Fig. H). The lateritic paleosol horizon can be traced outside the incised valley for several tens of kilometers along the outcrop belt.

Fig. 4.9. Outcrop examples of trace- and body fossils of the facies association $BL_3$. A. Bedding plane view *Thalassinoides* (*Th*), Agwe section. B. Cross-sectional view of *Skolithos* (*Sk*), Agwe section. C. Bedding plane view of *Diplocraterion habichi* (*Dh*) and poorly preserved *Thalassinoides*, Abiadi section. D. Halite pseudomorphs, Agwe section. E & F. Brackish water bivalves, Agwe section. G. Brachiopod, and H. Gastropod shells from washover sandstone layers, Samre section.

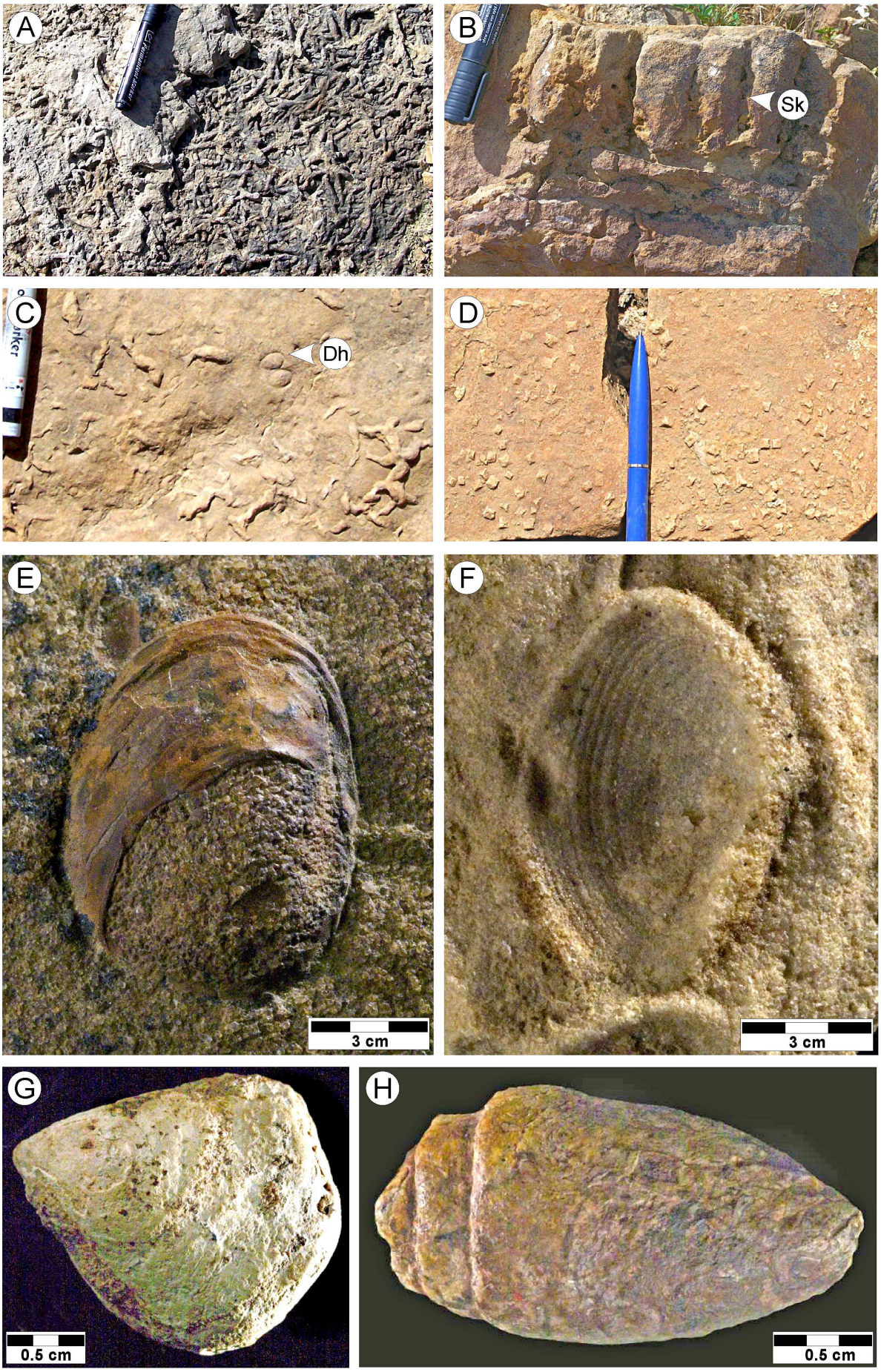
A
B
Sk
C
Dh
D
E
3 cm
F
3 cm
G
0.5 cm
H
0.5 cm

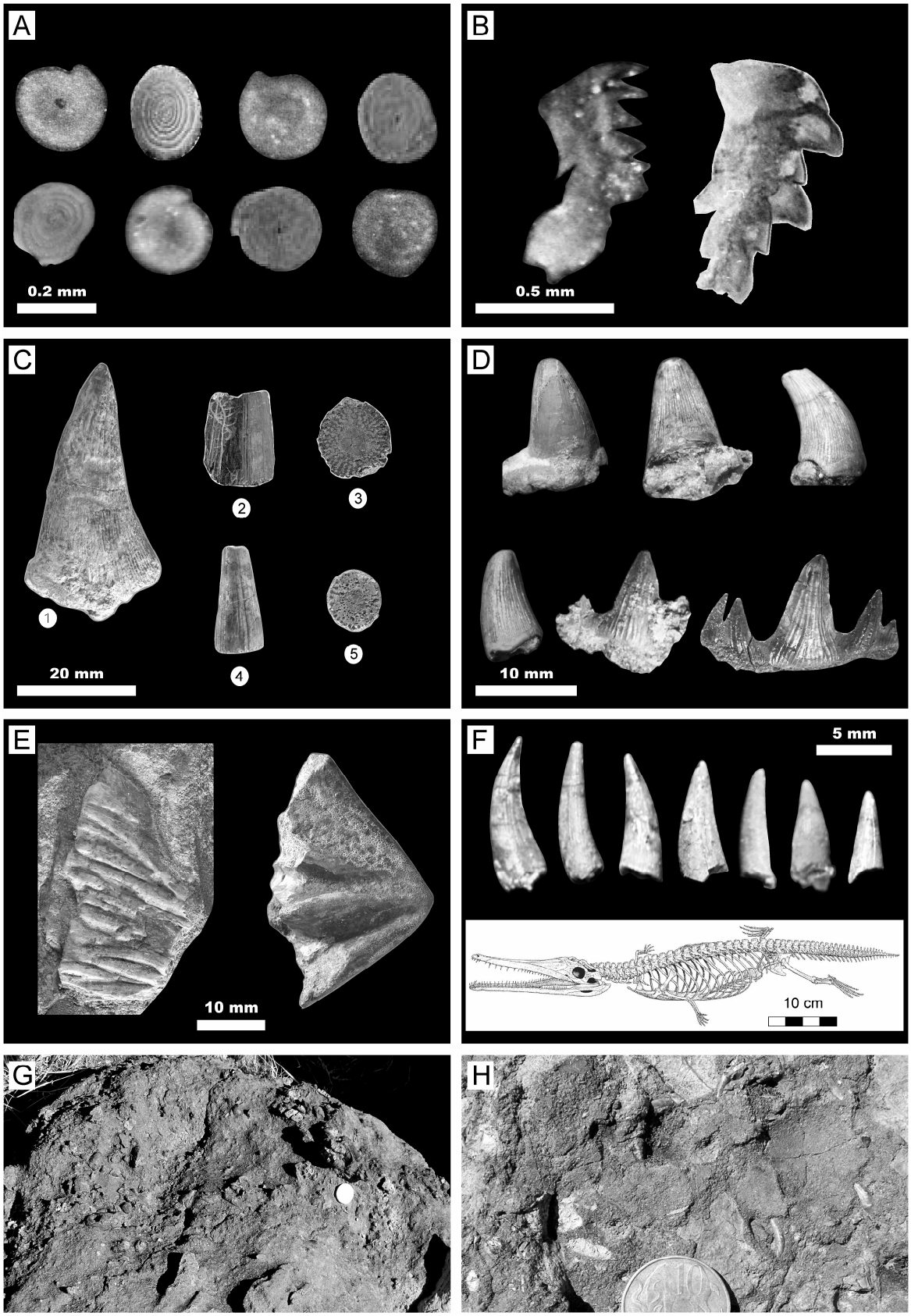


Fig. 4.10. A. Agglutinated foraminifera (*Ammodiscus* sp.). B. Scolecodonts, Samre section. C. Teeth of a capitosaurid temnospodyl, '3' & '5' are horizontal cross-sections of '2' & '4' respectively, Samre section. D. Teeth of hybodontid shark, Wukro section. E. Tooth plates of lungfish, Samre section. F. Piercing teeth of a marine crocodile (*thalattosuchian*), Wukro section. The lower picture shows the skeleton reconstruction after Pierce & Benton (2006). G. & H. Host sandstones out of which the fossils in 'D' and 'F' were extracted.

The lower unit (*Unit I*) is about 95 m thick and consists of three depositional systems; namely, a fluvio-estuarine system at the base, a barrier-lagoon system in the middle and a shoreface system at the top (Fig. 4.12). The fluvio-estuarine deposits are laterally discontinuous with variations in thickness between 4–12 m. They are only preserved in shallow valleys that are up to 12 m deep and metres to tens of metres wide. They are made up of basal estuarine channel-fill sandstones grading upward into upper-flow-regime plane beds (i.e., UFR sand flats of Dalrymple et al. (1992)) and tidal sand bars with intercalated tidal flat and fringing marsh deposits. The channel-fill sandstones contain coarse lag deposits at their base that are rich in vertebrate remains (Fig. 4.10c-e), including large fang teeth of a capitosaurid temnospondyl, teeth of hybodontid sharks, tooth plates of lungfish, as well as various types of coprolites. Mud drapes along cross-bed foresets are common. The tidal sand bars exhibit bioturbation along reactivation surfaces. Marsh deposits contain desiccation and syneresis cracks as well as subvertical burrows.

The barrier-lagoon system in the middle part of *Unit I* is composed of a 25 m thick barrier-spit and subaqueous lagoon complex. The lower part of the barrier is dominated by steeply dipping magaripple cross-bedding that grade upward to microdelta cross-bedding, planar lamination and beach stratification. The sandstones contain scattered glauconite grains (Plate I, Fig. B). The lagoonal deposits are dominated by greenish grey mudstones that embody agglutinated foraminifera and rare scolecodonts, whereas the intercalated washover sandstone beds contain scattered shells of brachiopods, gastropods, vertebrate bone fragments and abundant coprolites. Massive, dark reddish brown mudstone beds are intercalated within the greenish grey mudstones.

The shoreface deposits in the upper part of *Unit I* consist of two upward-coarsening progradational sets. Each of them is about 28–32 m thick and characterised by a wave ravinement surface with basal coarse lag overlain by offshore transition to lower shoreface deposits comprising interbedding of heavily bioturbated muddy siltstones and hummocky cross-stratified to planar-laminated fine-grained sandstones. Trough cross-bedded medium- to coarse-grained sandstones of the upper shoreface that are capped by planar-laminated fine-grained sandstones of the foreshore characterise the upper parts of the sets. The foreshore deposits are partly silicified and are usually covered by lateritised paleosol.

The upper stratigraphic unit (*Unit III*) is about 100 m thick and is basically similar to the lower one with respect to vertical stacking pattern of depositional systems except that it contains a fluvial complex at the top. Alike that of the lower unit the fluvio-estuarine system at the base of the upper unit is also laterally discontinuous. It is about 50–55 m thick. The succession is composed of channel-fill and bay head delta sandstones and siltstones grading upward into 7 m thick massive siltstones and mudstones of the central estuary ('central basin' of Dalrymple et al. (1992)) and overlain by a 20 m thick estuarine mouth-barrier complex, in which storm washover and flood tidal delta sandstones are the predominant facies with subordinate intercalations of marsh and tidal flat deposits. The shoreface system is composed of a single upward-coarsening progradational set of about 25 m thick. Although it has a general similarity in vertical facies succession to the progradational sets of the lower unit, it differs in the fact that upper shoreface sandstones are not trough cross-bedded but planar- to low-angle laminated. Amalgamated fluvial channel fills and pedogenically altered overbank deposits characterise the top of the succession.

***Interpretation***: The unconformity at the base of the Samre section that erosionaly truncates the underlying Permo-Carboniferous glacial deposits represents a disconformity surface (*sensu* Bates & Jackson 1987). The lateral discontinuity and thickness variation in the basal fluvio-estuarine deposits might be attributed to the irregular or asymmetric pre-transgression

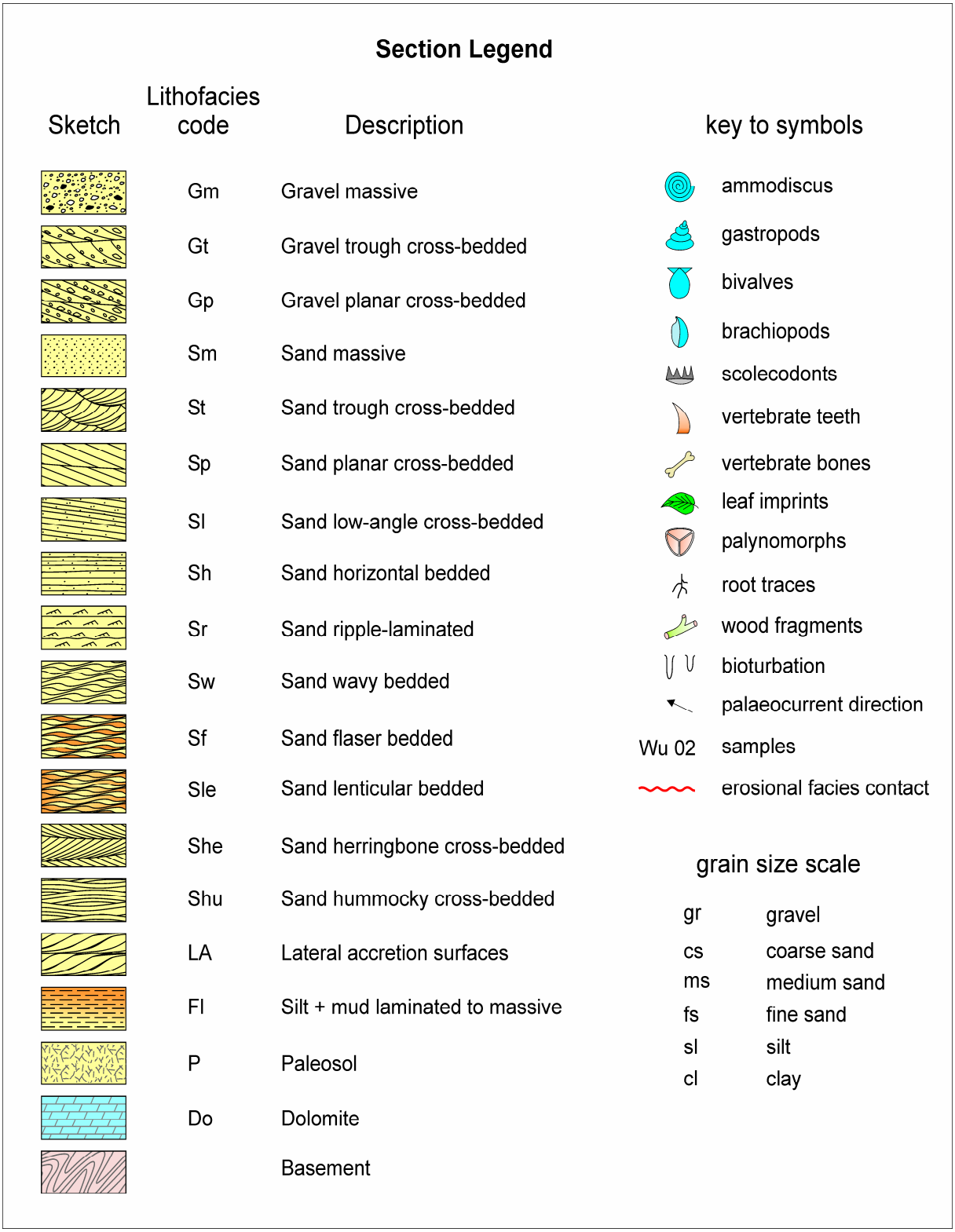


Fig. 4.11. Legend for sedimentary sections including sketches employed in lithologs, lithofacies codes, key to symbols and grain size scale.

topography of the palaeovalley they fill, which might have been created by differential erosion of the bedrock by fluvial and/or tidal currents (Ashley & Sheridan 1994). Fluvial erosion during falling sea level and tidal inundation during rising sea level, both of them erode channels into the substrate and create incised valleys (Demarest & Kraft 1987,

Nummedal & Swift 1987, Swift et al. 1980). Although fluvial incision is created during sea level lowstand, infilling occurs during rising sea level (Suter et al. 1987, Colman & Mixon 1988). The presence of marine vertebrate remains (e.g., teeth of hybodontid sharks and tooth plates of lungfish) in the channel lag deposits along with scattered glauconite grains in the sandstones suggest the predominance of marine sediment supply. Furthermore, the high degree of sorting and roundness of sand grains points to effective marine reworking. The vertical facies succession containing estuarine channel-fills, UFR sand flats and tidal sand bars with fringing marsh and tidal flat deposits suggest a tide-dominated estuary (Dalrymple et al. 1992, Boyd et al. 2006). Indicators of tidal influence include mud drapes along cross-bed foresets of the basal channel-fill sandstones (Terwindt 1981) and reactivation surfaces within tidal sand bars (Nio & Yang 1991). The presence of vertical dwelling structures formed by opportunistic suspension feeders and syneresis cracks may indicate a brackish-water setting (Pemberton & Whiteman, 1992, Plummer & Gostin 1981). The presence of desiccation cracks in close association with syneresis cracks and subvertical burrows suggest that the emergence was ephemeral, i.e., incipient desiccation cracks.

In the middle part of *Unit I*, the vertical facies succession containing steeply dipping megaripple cross-bedding, microdelta cross-bedding, planar lamination and beach stratification may suggest the formation of a barrier-lagoon system through vertical growth and emergence of longshore/offshore bars (Swift 1975). The presence of glauconite grains, shells of brachiopods and gastropods in the sandstones, along with wave-generated sedimentary structures points to intense sediment reworking and considerable wave action, but moderate tidal range (Hayes 1975, de Raaf et al. 1977, Nummedal & Swift 1987). The presence of agglutinated foraminifera (predominantly *Ammodiscus*) in the greenish grey mudstones suggests the presence of brackish-water lagoons associated with the barrier system.

The two upward-coarsening and shallowing progradational sets of the shoreface system in *Unit I* containing massive heavily bioturbated and hummocky cross-stratified fine-grained sandstones of the lower shoreface grading upward into trough cross-bedded sandstones of the upper shoreface are interpreted to indicate a storm-dominated non-barred nearshore system (Clifton 2006). The subordinate intercalations of oppositely dipping low-angle cross-bedded sets may suggest a moderate tidal modulation of the storm beds (Yang et al. 2008). Trough cross-bedded medium- to coarse-grained sandstones of the upper shoreface represent 3D dunes that migrate landward under the asymmetric flow of shoaling waves during fairweather conditions on a high-energy coast with abundant sand supply (Clifton et al. 1971).

In the fluvio-estuarine deposits of the upper stratigraphic unit (*Unit III*), the vertical facies succession from a river-dominated channel/overbank and bay head delta facies through a mixed-energy muddy 'central basin' to a wave-dominated barrier/spit is interpreted to represent a wave-dominated estuary (Dalrymple et al. 1992, Boyd et al. 2006). The channel and overbank deposits are poorly sorted and lack any indicators of marine influence, such as tidal structures, bioturbation and marine fossils suggesting a purely fluvial origin. Evidence for estuarine environment comes from the overlying bay head deltas that exhibit an upward-coarsening succession resulting from progradation during estuary filling (Reinson et al. 1988, Allen and Posamentier 1993, Broger et al. 1997). The massive, heavily bioturbated siltstones and mudstones of the central estuary may act as a prodelta region of the bay head delta. The predominance of headward (240°–320°) prograding storm washover and flood tidal delta sandstones within the estuary mouth/barrier complex indicates the fact that the mouth frequently experienced relatively high to moderate storm wave and tidal energy.

Fig. 4.12. Samre section.

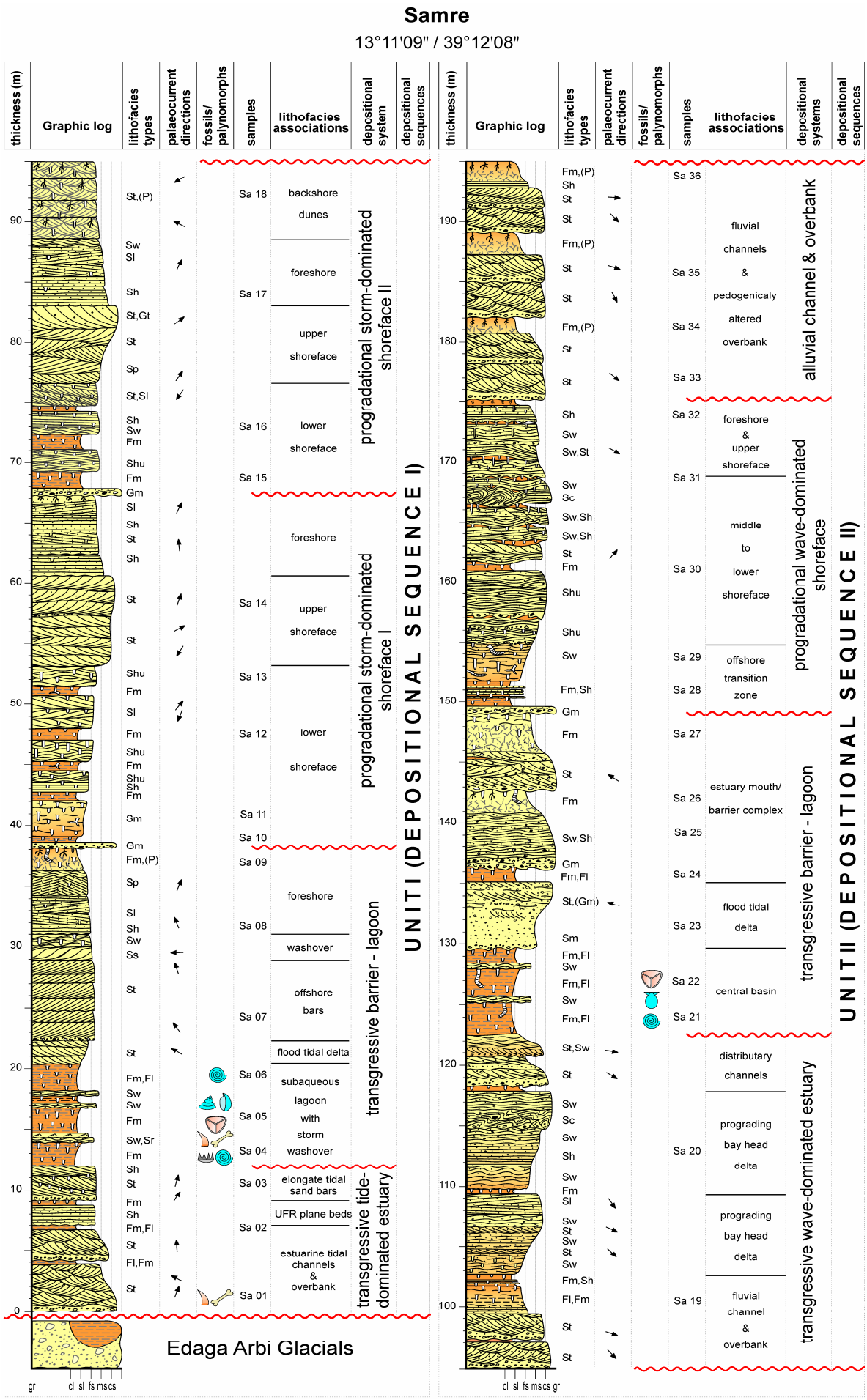
Samre
13°11'09" / 39°12'08"
thickness (m)
Graphic log
lithofacies types
palaeocurrent directions
fossils/ palynomorphs
samples
lithofacies associations
depositional system
depositional sequences
backshore dunes
foreshore
upper shoreface
lower shoreface
progradational storm-dominated shoreface II
foreshore
upper shoreface
lower shoreface
progradational storm-dominated shoreface I
foreshore
washover
offshore bars
flood tidal delta
subaqueous lagoon with storm washover
transgressive barrier - lagoon
elongate tidal sand bars
UFR plane beds
estuarine tidal channels & overbank
transgressive tide-dominated estuary
UNITI (DEPOSITIONAL SEQUENCE I)
Edaga Arbi Glacials
fluvial channels & pedogenicaly altered overbank
alluvial channel & overbank
foreshore & upper shoreface
middle to lower shoreface
offshore transition zone
progradational wave-dominated shoreface
estuary mouth/ barrier complex
flood tidal delta
central basin
transgressive barrier - lagoon
distributary channels
prograding bay head delta
prograding bay head delta
fluvial channel & overbank
transgressive wave-dominated estuary
UNITII (DEPOSITIONAL SEQUENCE II)
gr cl sl fs ms cs

In contrast to *Unit I*, the shoreface system of *Unit III* is made up of relatively finer-grained sandstones, in which planar- to wavy-lamination is predominant than hummocky and swaley cross-stratification. This indicates a fine sandy non-barred nearshore system characterised by flatter beach–nearshore profile on a high-energy coast where fairweather conditions predominate, rather than storms (Clifton 2006). The succession lacks medium- to large-scale trough cross-bedding that typifies the upper shoreface of coarser shorelines. The amalgamation of fluvial channel fills at the top of the succession indicates the culmination of shoreface progradation due to increased continental sediment supply than can be redistributed by coastal and/or nearshore marine processes.

### 4.2.2. Agwe area

***Description***: In Agwe area, the location of the studied section is 3 km east of the town Agwe at N 13°33′07″/E 39°03′33″ (Fig. 2.1). The Adigrat Sandstone succession is about 400 m thick and unconformably overlies the Edaga Arbi Glacials (Fig. 4.13). The succession can be divided into three stratigraphic units: a lower unit (*Unit I*) composed of a tidal-estuarine and a shoreface system; a middle unit (*Unit II*) composed of a fluvial and a deltaic system; and an upper unit (*Unit III*) consisting of a barrier-lagoon, an open coast tidal flat and a fluvial system. The boundary between *Unit I* and *Unit II* is marked by a erosional truncation surface and/or interfluve paleosol horizon whereas the boundary between *Unit II* and *Unit III* is characterised by a widespread lateritic paleosol developed on top of an abandoned delta plain (Plate I, Fig. G).

The fluvio-estuarine deposits at the base of the Agwe section are 35–40 m thick. The succession consists, from bottom to top, of basal estuarine channel-fill sandstones, elongate tidal sand bars and tidal point bars with intercalated tidal flat and marsh deposits. Cross-bed sets of the channel deposits possess bimodal to polymodal palaeocurrent directions. Elongate tidal sand bars are well-developed and contain mud drapes and tidal rhythmites. Successive tidal bundles display a thick/thin relationship. The tidal point bars at the upper part of the succession intertongue with bioturbated tidal flat and salt marsh deposits. The tidal estuarine deposits are overlain by a 22 m thick, upward-coarsening shoreface deposits.

The succession is irregularly truncated by renewed valley incision and deposition of a 25 m thick major multistorey fluvial complex (lower part of *Unit II*). The channel-fill deposits are composed of erosive based, dominantly trough cross-bedded and poorly sorted coarse-grained sandstones and fine-grained conglomerates with abundant rip-up clasts of up to 30 cm in diameter. Palaeocurrent directions are unimodal, i.e., to the SE. Fine-grained overbank deposits are rare. No tidal sedimentary structures are observed. Individual channel sand bodies are 3–5 m thick and fine upwards. The top of the fluvial succession is covered by a paleosol horizon.

The deltaic deposits in upper part of *Unit II* are up to 70 m thick and are composed of a series of 7–10 m thick upward-coarsening and shallowing progradational sets (Fig. 4.13). The sandstones are poorly to moderately sorted, medium- to coarse-grained and are interbedded with fine-grained conglomerates. Scattered pebbles and pebble pockets consisting mainly of basement gneiss and quartzite are abundant. Bioturbated and rooted siltstone and mudstone facies are subordinate and they usually occur on delta plains, in interdistributary bays and marshes. Large-scale planar-tabular cross-bedding and low-angle cross-stratification are predominant in delta front slopes and mouth bars. Small-scale trough cross-bedding and current ripple-lamination are common in distributary channels and overbank areas. Palaeocurrent directions are generally to the southeast. The geometry of sandstone bodies is generally lobate that thicken towards the southeast. Bioturbated bedding surfaces are abundant. The top of the deltaic succession is highly affected by lateritisation.

Deposits of the barrier-lagoon system (lower part of *Unit III*) that erosionaly truncates the underlying deltaic deposits reach up to 170 m in thickness, making up nearly one third of the total thickness of the Agwe section. In its lower part, the succession consists of vertically stacked barrier spits with interstratified backbarrier deposits. The barrier spits are composed of well-sorted and well-rounded, predominantly planar- and wave ripple-laminated fine- to coarse-grained sandstones with scattered pebbles. The backbarrier deposits contain heterolithic marsh, tidal flat and lagoonal facies that are commonly extensively disturbed by burrowing and pervasive root penetration. The succession changes its character towards the top, in which tidal inlet channel fills, flood tidal delta and washover deposits predominate. Spit accretion become less prominent, although it occurs on top of tidal inlet fills. Washover deposits contain brackish-water bivalves, lungfish fragments, wood fragments, halite pseudomorphs and abundant traces of benthic organisms. The lagoonal deposits are dominated by greenish grey mudstones with frequent intercalations of dolomite layers and thin sandstone sheets. The mudstones contain agglutinated foraminifera, phytoclasts, cuticles and well-preserved palynomorphs (see Sec. 6).

The transition from a barrier-lagoon complex to an open coast tidal flat system (~40 m thick) occurs in the upper part of *Unit III*, whereby the succession is dominated by erosionaly based tidal channel fills and elongate tidal sand bars. Muddy and silty facies are rare. The channel fill sandstones are composed of well-sorted, fine- to medium-grained sandstones that are arranged in several erosive based fining-upward cycles. Medium- to small-scale, bimodal to polymodal trough cross-bed sets are predominant. Sets containing SW-dipping foresets are frequent. Bidirectional (NW- and SE-dipping) planar-tabular cross-bed sets are also common. Overturned cross-bed sets occur rarely. Flaser-bedded, planar- and/or bidirectional ripple-laminated silty sandstones occur towards the top of channel fill deposits along with massive bioturbated beds. The elongate tidal bars are usually 4–7 m thick and are characterised by upward-coarsening facies successions, which pass from massive bioturbated fine-grained sandstone into trough cross-bedded medium-grained sandstones.

The uppermost part of *Unit III* is characterised by a 35 m thick fluvial succession. The lower part of the fluvial succession contains 2–5 m thick, multi-storey, internally scoured, dominantly trough cross-bedded and poorly sorted coarse-grained to pebbly sandstones that grade upwards to heterolithic deposits consisting of isolated single-storey channel-fill sandstones, point bars and interbedded massive to laminated silty mudstones. Rootlet mottling and desiccation cracks are common in the silty mudstones.

***Interpretation***: In the fluvio-estuarine deposits at the base of the Agwe section, the presence of bimodal to polymodal palaeocurrent directions, mud drapes and tidal rhythmites indicate a tide-dominated estuary (Dalrymple 1992, Nio & Yang 1991). This interpretation is further supported by the absence of bay head delta facies association, which is characteristic of wave-dominated estuaries (Honig & Boyd 1992, Boyd et al. 2006). Successive tidal bundles within the elongate tidal bars that display thin-thick-thin relationship are interpreted to represent semi-monthly (neap-spring-neap) cycles (Dalrymple et al. 1991, Tessier 1993, Archer 1994). The occurrence and preservation of tidal rhythmites suggests that tidal sedimentation overwhelmingly dominates the depositional regime (Archer 1998, Archer et al. 1994). Furthermore, the development of cyclic rhythmites implies elevated tidal range (i.e., macrotidal setting) and usually the presence of coastal embayments (Dalrymple et al. 1991, Tessier et al. 1995). The widespread occurrence of tidal rhythmites within the basal estuarine deposits in most of the studied stratigraphic sections of the Mekelle Basin has significant implications on the structural aspects of the depositional setting; this topic will be discussed further under ‘basin evolution’ in Sec. 8.

Fig. 4.13. Agwe section.

## Agwe

13°33'07" / 39°03'33"

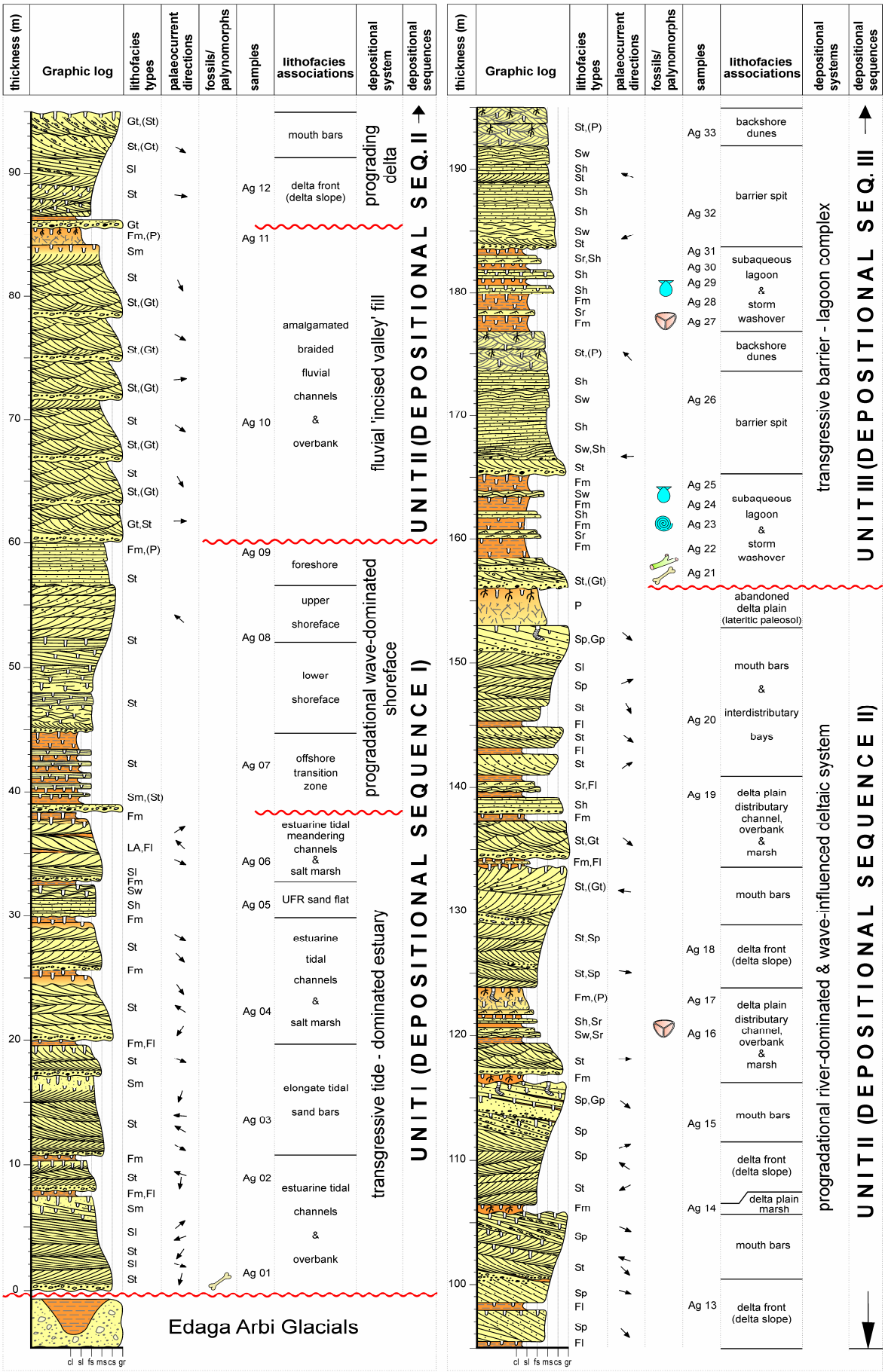

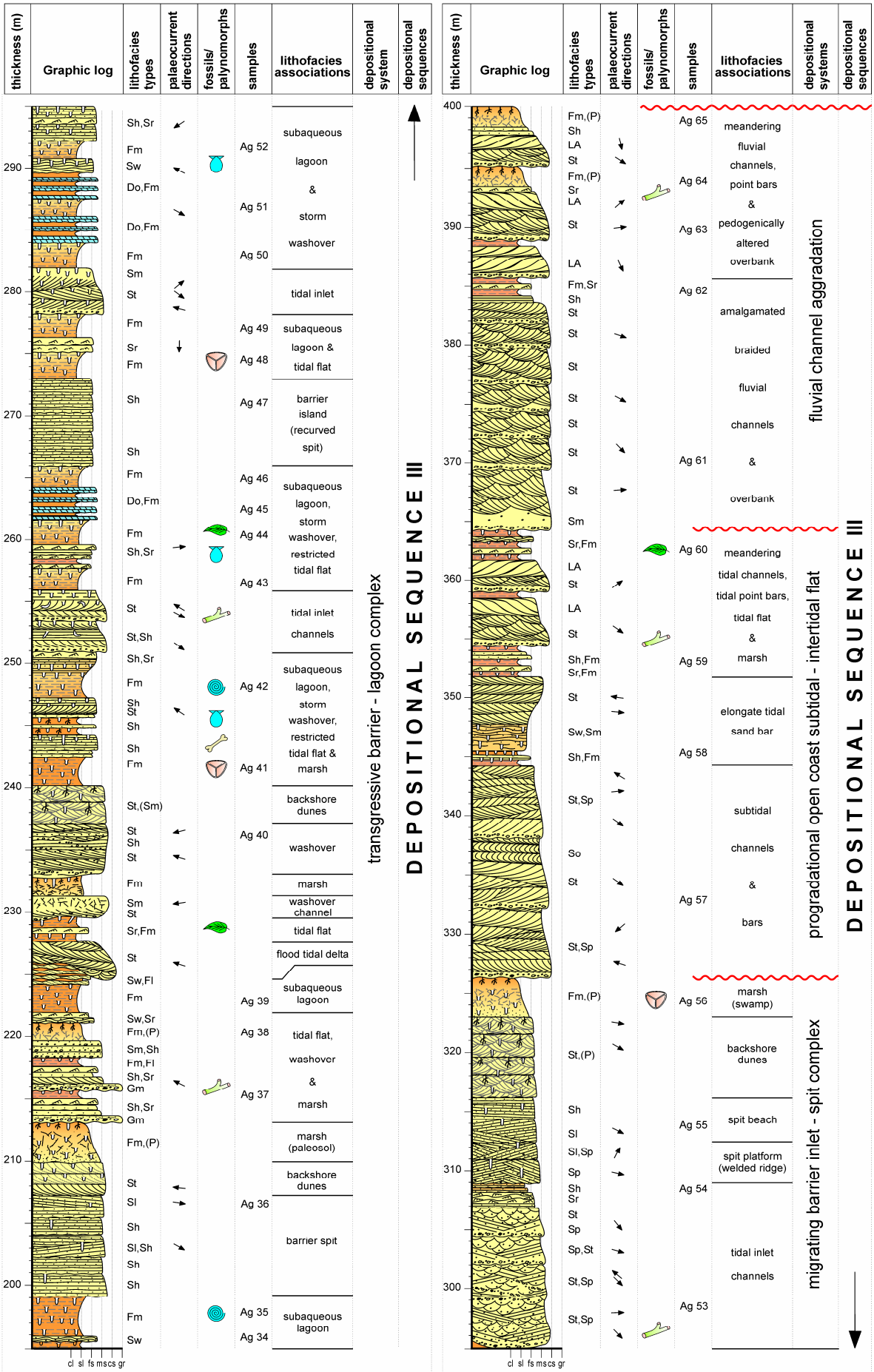


Fig. 4.13. Agwe section (continued).

The greater thickness of the basal Agwe estuary fill (~40 m) as compared to that of Samre (~12 m) is attributed to larger estuary volume, a parameter closely related to coastal plain gradient. According to Boyd et al. (1992), a rise in sea level on a flat coastal plain generates a relatively longer estuary with larger volume than on a steeper coastal plain. Consequently, the basal Agwe estuary may be interpreted to have formed on a relatively gentler coastal plain than that of Samre estuary.

The nature of the facies succession developed in an estuary provides a clue to the morphology (shape and geometry) of the valley system being flooded (Salomon & Allen 1983). Tidal amplification is unlikely to occur in irregularly shaped valleys (Nichols & Biggs 1985). Hence, the predominance of tidal sedimentary structures in the basal Agwe estuary might imply that it either has or subsequently developed a funnel-shaped geometry, like that of the Gironde estuary (Salomon & Allen 1983). Since high tidal range occurs in deep coastal embayments (e.g., drowned river valleys) that possess sufficient length (at least several hundred kilometers) to reach tidal resonance (Open University Team 1989), the Agwe estuary must have had a comparable length for cyclic tidal rhythmites to be formed and preserved.

Renewed valley incision and deposition of a major multistorey fluvial complex at the base of *Unit II* is attributed to changes in the fluvial energy flux in response to corresponding changes in the slope gradient of the fluvial graded profile, which is in turn a function of tectonism (e.g., source area uplift) and/or differential subsidence or fluctuations in environmental energy imposed by climatic shifts (Holbrook 1996, Miller & Erikson 2000). Continued rise in fluvial sediment supply resulted in the establishment of a deltaic system as recorded by several dominantly coarse-grained upward-coarsening progradational sets in the upper part of the middle stratigraphic unit. The predominance of SE-oriented palaeocurrent directions and the abundance of riverborne pebble pockets and layers mainly composed of basement gneiss and quartzite is interpreted to indicate a river-dominated deltaic system. The subordinate occurrence of NW-oriented paleocurrent directions suggests a moderate wave influence. No tidal influence can be inferred since tidal structures are absent. The frequent occurrence of bioturbated and rooted horizons on top of upward-coarsening progradational sets may point to repeated abandonment and delta lobe switching that might possibly be related to autogenic processes, such as localised tectonic rejuvenation of the source area or local climatic fluctuations (Bhattacharya & Giosan 2003, Hampson & Howell 2005). The succession has basic similarities with 'Gilbert-type' deltas of Wescot & Ethridge (1990), such as the Pliocene Abrioja delta (Postma 1984) and the Eocene La Trona delta (Marzo & Anadón 1988). The widespread lateritisation on top of the deltaic succession is interpreted to record the transition from an active delta progradation to a phase of abandonment.

Following delta abandonment and lateritisation, the inception of transgressive barrier-lagoon system is recorded by the three vertically stacked barrier spits with interstratified backbarrier deposits. These deposits are interpreted to represent stepwise landward migration of barriers due to rising sea level, as proposed by the 'in-place drowning' model of Rampino & Sanders (1980) and Elliot (1986) or the 'stepwise coastal retreat' model of Clifton (2006). The partial to nearly complete preservation of these transgressive coastal successions implies that the rise in sea level must have been rapid (Davis & Clifton 1987). The accumulation of a significant proportion of lagoonal facies with associated storm washover, restricted tidal flat and fringing marsh deposits towards the middle part of the barrier-lagoon complex might probably indicate a relatively stillstand sea level (Kendall & Harwood 1996). However, the presence of intercalated dolomite layers and halite pseudomorphs record smaller fluctuations in relative sea level and periodic desiccation of the lagoon (Kendall 1988). The lagoonal facies is characterised by low diversity brackish water fauna (e.g., brackish water bivalves and agglutinated foraminifera), suggesting that the tidal range must have been low with few narrow and ephemeral inlets (Glaeser 1978). Generally, the presence of evidences for both high and low salinity conditions indicates extreme salinity fluctuation within the lagoon.

The vertical change in facies succession from a spit-dominated microtidal barrier system in the lower part of *Unit III* to a mesotidal inlet-dominated system in the middle part is interpreted to record a falling sea level (Tye & Moslow 1993, Cheel & Leckie 1990). Migrating channel-spit successions are typical of prograding mesotidal coasts (Galloway & Hobday 2006). Wave-generated structures, primarily low-angle swash lamination of the spit platform and spit beach are interpreted to reflect reestablishment of the beach profile onto the inlet-fill succession (Hobday & Horne 1977). Barrier destruction and formation of an open coast macrotidal flat is recorded by the prograding subtidal channels and bars that overlay the inlet-spit complex. The preservation of such widely extended subtidal deposits might have been favoured by slower rate of relative sea level fall (Davis & Clifton 1987). Continued fall in relative sea level is recorded by fluvial aggradation over tidal deposits at the uppermost part of the Agwe section.

### 4.2.3. Abiadi area

***Description***: The studied section in Abiadi area is located on the eastern boarder of the town (N 13°37′12″/E 39°01′02″) where several rockhewn churches are carved in. The Adigrat Sandstone succession unconformably overlies the Edaga Arbi Glacials and is unconformably overlain by Tertiary flood basalts. The thickness reaches up to 430 m (Fig. 4.14). The lower boundary is marked by uneven erosion surface that truncates the underlying Permo-carboniferous glacial deposits. The top of the succession is lateritised up to a depth of about 30 m. A threefold subdivision of the succession into stratigraphic units (*Unit I*, *Unit II* and *Unit III*) is possible because the three units are separated from each other by a prominent subaerial exposure surface of fluvial incision and/or lateritic paleosol. *Unit I* is about 120 m thick and consists of a lower tidal-estuarine system and an upper nearshore marine (shoreface to inner shelf) system. *Unit II* is about 110 m thick and is composed of a basal fluvial incised valley fill and a deltaic system, whereas *Unit III* is made up of a lower barrier-lagoon complex, an upper open coast tidal flat system and an uppermost fluvial system.

The tidal-estuarine deposits at the base of the Abiadi section (*Unit I*) are 50–55 m in thickness. They are predominantly made up of well-sorted, medium- to fine-grained and cross-bedded quartz sandstones filling up to 3.5 m deep estuarine tidal channels. The top of the channels are bioturbated with *Ophiomorpha* and *Thalassinoides*. Horizontal to very low-angle cross-bedded sandstones of the UFR sand flat facies, lateral accretion deposits of the tidal point bars and silty mudstones belonging to marsh facies occur subordinately. Elongate tidal sand bars that characterise the uppermost 10 m of the succession contain large scale trough cross-bedded sets with foresets dipping mainly to the northeast. Although marine fossils are absent, evidence of tidal current processes are abundant, including flaser and wavy bedding, mud drapes, bimodal foreset orientation of cross-beds and bundle-wise upbuilding of foresets.

The nearshore marine (shoreface to inner shelf) system at the upper part of *Unit I* is about 65 m thick and is composed of three upward-coarsening progradational sets. The lower set consists of intercalations of current ripple-laminated very fine-grained sandstones and massive to laminated silty mudstones that are bioturbated by *Chondrites* and *Terebellina*. These grade upwards to less bioturbated, small- to large-scale trough and planar-tabular cross-bedded fine- to coarse-grained sandstones of the upper shoreface and covered at the top by planar-laminated and rooted foreshore deposits. Mud-draped and bipolar-oriented foresets are common. The middle and upper sets are composed of hummocky cross-stratified fine-grained sandstones with interbedded heavily bioturbated silty mudstones of the lower shoreface that grade upwards to trough cross-bedded sandstones of the upper shoreface.

Fig. 4.14. Abiadi section.

## Abi Adi

13°37'12" / 39°01'02"

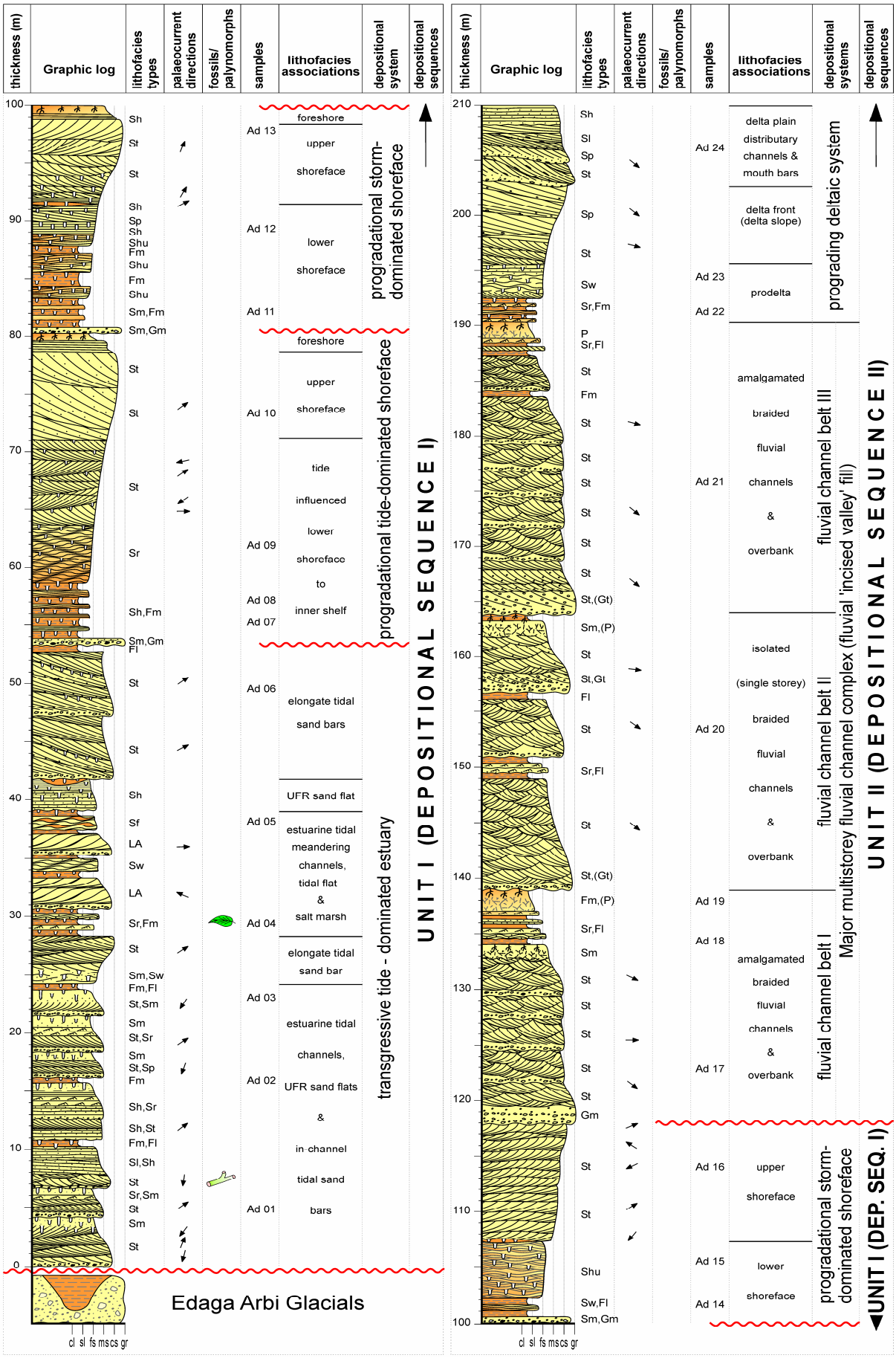

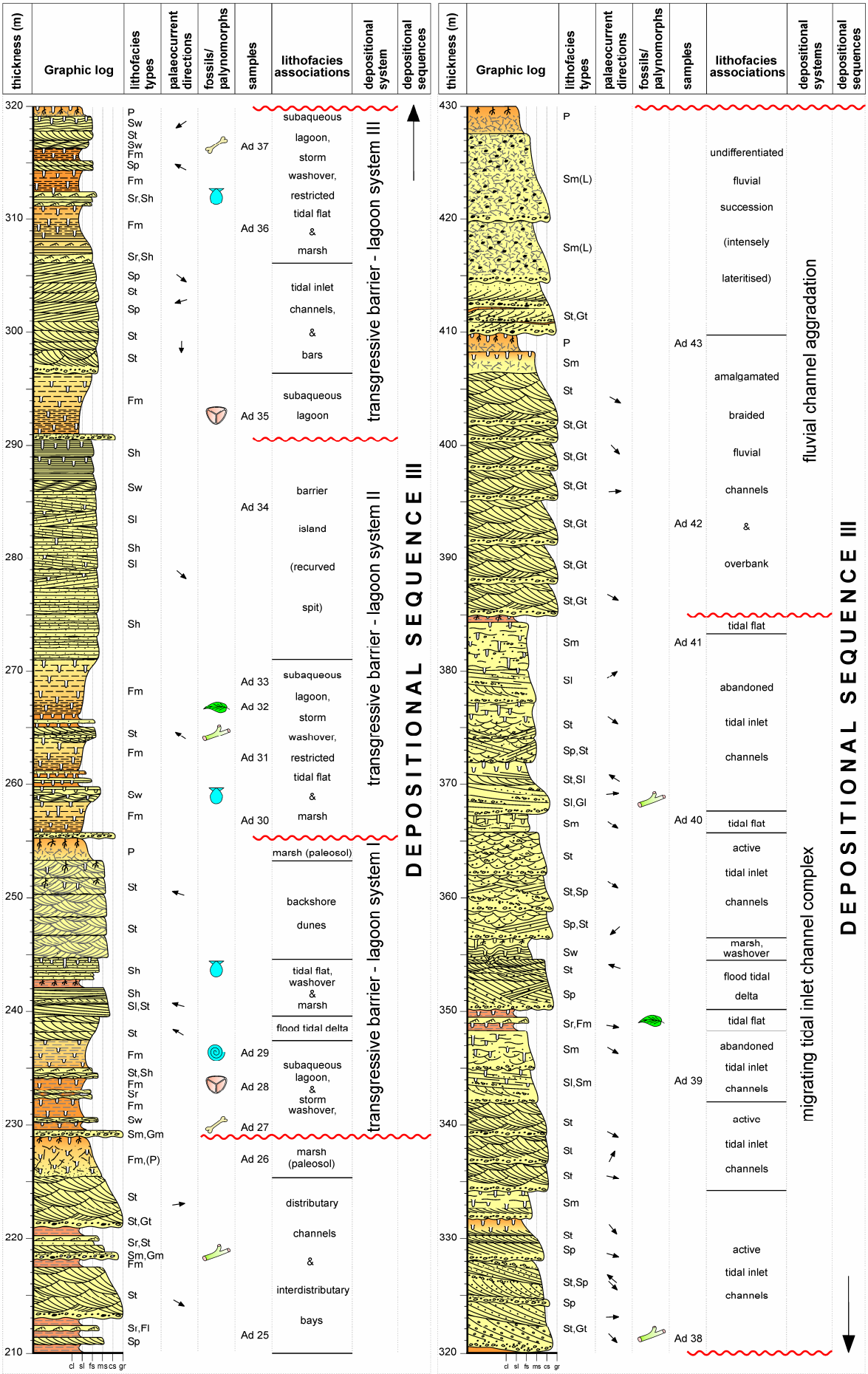


Fig. 4.14. Abiadi section (continued).

The shoreface deposits are erosionaly truncated and overlain by a major multistorey fluvial channel complex. The succession is 72 m thick in the measured section and is composed of three channel belts separated from each other by overbank fines and paleosols. The lower and upper channel belts (channel belts I and III) predominantly consist of 3–5 m thick, amalgamated braided fluvial channel fills and minor overbank deposits whereas the middle channel belt is made up of isolated single storey but deeper (5–10 m thick) channels. The channels in all the three channel belts are filled mainly with poorly sorted, trough cross-bedded, pebbly coarse-grained sandstones. Palaeocurrent directions are unimodal within each channel belt and are oriented towards the east-southeast. Desiccation cracks and rootlet mottling is common in the overbank deposits. Bioturbation is absent.

The deltaic deposits that overlay the fluvial channel complex are up to 40 m thick and are composed of wave ripple-laminated to massive silty mudstones and fine-grained sandstones of the prodelta that grades upward to large-scale low-angle stratified sandstones of the delta front slope, and then, to planar-tabular and trough cross-bedded pebbly sandstones filling distributary channels and mouth bars of the delta plain. Fine-grained sediments are relatively minor and are restricted to interdistributary bays, overbank and marsh areas. Palaeocurrent directions are unimodal to the east-southeast. The top of the delta plain succession is covered by a lateritised paleosol.

The barrier-lagoon complex of *Unit III* is up to 90 m thick and is composed of three barrier spits each of them underlain by a backbarrier lagoonal facies. The lower barrier consists of flood tidal delta, washover and backshore dune sandstones whereas the middle barrier is dominated by spit accretion. Tidal inlet channel fills and in-channel bars characterise the upper barrier. The lagoonal facies is dominated by greenish grey mudstones with subordinate reddish brown, mottled marsh mudstones and washover sheet sandstones. The greenish grey mudstones are rich in agglutinated foraminifera, mainly *Ammodiscus*. Few of these mudstone layers contain well-preserved palynomorphs. Brackish water bivalves, lungfish fragments and trace fossils, mainly *Diplocraterion habichi*, are common on bedding surfaces of washover sheet sandstones. The succession is similar to the barrier-lagoon deposits of the Agwe area except that the thickness of the preserved deposits is significantly lower.

Towards the upper part of *Unit III*, a barrier system dominated by spit accretion is replaced by a tidal inlet channel fill succession of up to 65 m thick. It contains four 15–18 m thick fining-upward successions; the lower three of these successions are characterised by top bioturbated, bi- to polydirectional trough and planar-tabular cross-bedded medium- to coarse-grained sandstones, whereas the fourth one contains intensely bioturbated fine- to medium-grained sandstones with hardly discernible primary structures. The tidal channel fill succession is erosionaly truncated and overlain by amalgamated braided fluvial channel fill succession (the uppermost part of *Unit III*), which is composed of two fining-upward units containing poorly sorted pebbly coarse-grained sandstones. The lower unit is dominated by trough cross-bedding whereas the upper unit is extensively lateritised.

***Interpretation***: In the basal estuarine deposits of *Unit I*, the vertical facies succession containing top bioturbated tidal channels, UFR sand flats, tidal point bars and elongate tidal bars suggests deposition in an exclusively tide-dominated estuary (Dalrymple 1992, Boyd et al. 2006). The presence of bipolar palaeocurrent directions, mud-draped foresets, reactivation surfaces and tidal rhythmites are unequivocal evidences of tidal influence (Middleton 1991, Nio & Yang 1991, Dalrymple 1992). The predominance of SW-oriented palaeocurrent directions within the channel fills indicates a flood-dominated tidal current regime. Upwards in the succession, however, the dominance of NE-oriented palaeocurrent directions in the large-scale foresets of the linear tidal bars suggests an ebb-dominated tidal current regime. The mega-foresets were probably formed by northeastward progradation of terminal lobes at

the mouth of the estuary (Nio & Yang 1991). Generally, frequent and periodic tide-induced changes in current speed and direction within the estuary are indicated by the presence of oppositely migrating dune- and bar-scale cross-strata. The occurrence and preservation of tidal rhythmites with abundant thick-thin alternations of sand-mud couplets indicating semi-monthly (neap-spring-neap) tidal cycles (Allen 1981) is additional evidence that tidal sedimentation totally dominates the depositional regime (cf. Archer 1998).

The estuarine deposits are basically similar to that of Agwe with respect to facies architecture. As deduced from the elongation direction of linear tidal sand bars a generally NE-opening estuary funnel seems to have existed in the Abiadi area. These bars are largely deposited by ebb tidal current processes in contrast to that in the Agwe estuary, which are dominated by flood tidal current deposits. Such differences in tide-dominated deposits may arise, however, due to the fact that ebb and flood tidal currents may follow different flow paths on and off the coastline (Dalrymple et al. 2003). The absence of estuarine deposits in between the two studied areas might suggest the presence of a local topographic high.

In the nearshore marine deposits of *Unit I*, the presence of mud drapes and bipolar palaeocurrents in the lower progradational set may indicate a tide-influenced shoreface depositional environment (Swift 1975, Smith 1988, Berné et al. 1993). In the lower fine-grained part of the set, the presence of *Chondrites* and *Terebellina* belonging to the Cruziana ichnofacies (MacEachern & Pemberton 1992, MacEachern et al. 2005, MacEachern & Bann 2008) suggests a distal lower shoreface to inner shelf setting. The coarsening-upward facies succession may be interpreted as tidal sand ridge, similar to those described by Bridges (1982), Mutti et al. (1985), Simpson & Eriksson (1991). The deposit is typical of a barred high- to moderate-energy prograding shoreline system under fairweather conditions with significant tidal influence (Clifton 2006). The presence of wave- and storm-generated structures such as hummocky cross-stratification, together with intensive bioturbation in the middle and upper progradational sets points to a nonbarred storm-dominated shoreface system (Swift & Nummedal 1987, Clifton 2006).

The major multistorey fluvial channel complex that erosionaly truncates the underlying shoreface deposits is interpreted to represent a fluvial incised valley fill. They can be interpreted as compound fills (Zaitlin et al. 1994) since they represent multiple cycles of incision and deposition. The unimodal cross-bed distribution, together with the absence of bioturbation and the lack of any evidence of tidal current processes, suggest that these sandstones were deposited in a purely fluvial environment. The cross-bedded sandstones were deposited from fields of subaqueous linear and sinuous dunes migrating along the valley thalwegs. The stacked channel units in the *channel belts I* and *II* may indicate flow segregation into multiple channels within the valley, whereas the thicker channel fills of the *channel belt III* may suggest that a single flow occupied the full width of the valley. The overall uniform and monotonous nature of the palaeovalley fill may be interpreted to record very rapid or possibly catastrophic vertical aggradation caused by a repeated oversupply of sediments, which might be related to repeated tectonic rejuvenation of the source area and/or high frequency climatic fluctuations (Shanley & McCabe 1994, Posamentier 2001, Catuneanu et al. 2003).

In the deltaic system of *Unit II*, the unimodal palaeocurrent directions and the poorly sorted nature of the sandstones of the delta front, distributary channels and mouth bars suggest a river-dominated delta. The presence of wave ripple-lamination in the prodelta sediments indicates a minor wave influence. The lateritised palaeosol horizon on top of the deltaic succession represents a phase of abandonment and subaerial exposure. The transition from a braided fluvial channel complex to a prograding river-dominated deltaic system records a continued oversupply of sediments in excess of the relative rise in sea level (cf. Bhattacharya & Giosan 2003, Kulp et al. 2005, Willis 2005). The deltaic deposits in Abiadi have many similarities in facies succession with that of Agwe and they possess equivalent stratigraphic

positions. The reduced thickness and the insignificant wave influence in the Abiadi delta may suggest that they were deposited in a more proximal area (over kilometers landward) relative to their equivalent counterparts in Agwe.

The superposition of the three transgressive barrier-lagoon systems in *Unit III* suggests a rapid rate of transgression, but stepwise landward barrier migration due to rising sea level (Rampino & Sanders 1980, Elliot 1986, Clifton 2006). A brackish water lagoonal setting is indicated by the presence of low diversity brackish water fauna. Alike that of Agwe section, the observed vertical change in facies succession from a spit-dominated microtidal barrier system to a mesotidal inlet-dominated system in the Abiadi section is interpreted to record a falling sea level (Cheel & Leckie 1990, Tye & Moslow 1993). The overlying inlet channel fill deposits are interpreted to result from lateral barrier-inlet migration (Kumar & Sanders 1974, Moslow & Tye 1985). The lower three inlet fill successions containing bimodal to polymodal cross-bedded sandstones represent active inlet fills located on active barrier-island whereas the intensely bioturbated upper one may represent an abandoned inlet fill probably located in backbarrier areas (cf. Moslow & Tye 1985). The presence of an abandoned inlet fill in backbarrier areas may suggest that inlet channels did not only migrate laterally towards the net longshore drift direction but also onshore and offshore due to changes in relative sea level and sediment supply. The change in facies succession from the mesotidal inlet-dominated system to the amalgamated braided fluvial channel system is interpreted to record the seaward shift of facies belts (progradation) due to a falling sea level (Cheel & Leckie 1990, Tye & Moslow 1993, Galloway & Hobday 2006).

### 4.2.4. Megab area

***Description***: The studied section in the Megab area is located at the upstream end of the Werii River (N 13°54′50″/E 39°21′10″), about 10 km southwest of the town Hawzen. The Adigrat Sandstone unconformably overlies the Edaga Arbi Glacials. The lower boundary is characterised by an irregular surface of fluvial incision that truncates the underlying glacial deposits. The top of the succession is exposed and part of the Jurassic deposits is removed by recent erosion. The thickness reaches up to 350 m (Fig. 4.15). Similar to Abiadi and Agwe areas, the succession can be subdivided into three stratigraphic units (*Unit I*, *Unit II* and *Unit III*) that are separated from each other by prominent subaerial exposure surfaces of erosion and/or lateritic paleosols.

*Unit I* is about 100 m thick and consists of a fluvio-estuarine and a shoreface system. The fluvio-estuarine deposits are composed of predominantly trough cross-bedded fine- to coarse-grained sandstones filling irregularly cut valleys that are several tens of meters deep and kilometers wide. The lower 25 m are characterised by amalgamated fluvial channel fills with fairly unimodal paleocurrent directions that are oriented towards the northeast. The succession changes its character in the overlying 30 m, where mud-draped foresets, bioturbation, flaser- and wavy bedding, and bimodal palaeocurrent directions become abundant. These deposits are overlain by up to 12 m thick superimposed elongate tidal sand bars. Cross-bed sets within these bars contain large-scale mud-draped foresets dipping mainly to the southwest and northeast. The shoreface deposits, which characterise the upper part of *Unit I*, contain three up to 10 m thick upward-coarsening progradational sets. Each of them consists of planar-laminated to hummocky cross-stratified, bioturbated silty mudstones with interbedded fine-grained sandstones of the lower shoreface grading upwards to trough cross-bedded sandstones of the upper shoreface.

*Unit II* is about 140 m thick and is composed of a lower fluvial channel complex, which is overlain by a deltaic succession. The fluvial deposits range in thickness from 60–65 m. The lower part is characterised by 6–8 m thick amalgamated braided channel fills that change upwards, in the middle part, to erosionaly stacked channel units where the thickness of

individual sandstone bodies is reduced by nearly a half. The upper part of the succession contains isolated channel fills that are capped by overbank fines. The fluvial channel complex grades upward into a deltaic succession that may reach up to 70 m in thickness. The deltaic system comprises several upward-coarsening progradational units. These units consist of laminated to massive, usually bioturbated fine-grained sandstones, siltstones and mudstones of the prodelta platform that grade upwards into medium- to coarse-grained sandstones that are arranged in 3–5 m thick, steep-fronted (10°–25°) clinoforms. The prograding clinoforms possess a broadly lobate geometry and downlap with gentle asymptotic contact onto underlying finer-grained heterolithic bottomsets of the prodelta platform. The upper parts of these progradational units are characterised by distributary channel and crevasse splay sandstones with intercalated marsh and overbank fines.

*Unit III* is about 140 m thick and consists, in its lower part, of a tide-dominated estuarine and, in its upper part, a nearshore marine (shoreface to inner shelf) depositional system. Tidal estuarine deposits are predominantly composed of heterolithic intertidal to supratidal facies with subordinate subtidal channel deposits filling shallow valleys cut most commonly into the underlying paleosols developed on the abandoned delta plain and rarely into delta front sandstones. The nearshore marine system of *Unit III* is basically similar to that of *Unit I* since it also contains offshore transition zone, lower and upper shoreface deposits. Nonetheless, it differs from *Unit I* because: (i) it contains a single progradational set, (ii) the offshore transition zone to lower shoreface deposits are significantly thicker and intensely bioturbated, and (iii) low-angle planar-laminated foreshore deposits are well-preserved. Deposits of the offshore transition zone are characterised by a heavily bioturbated intercalation of hummocky cross-stratified sandstones and laminated to massive silty mudstones. These deposits are sharply overlain by less intensely bioturbated, hummocky cross-stratified lower shoreface sandstones. The upper shoreface to foreshore deposits at the top of the nearshore marine succession are composed of planar-laminated, well-sorted and well-rounded fine- to medium-grained sandstones. Small-scale trough cross-bedding and ripple-lamination occurs subordinately but large-scale trough cross-bedding is absent.

***Interpretation***: The three stratigraphic units in the Megab section, alike those sections described above, are interpreted to represent three well-defined and unconformity bounded transgressive-regressive depositional cycles. The basal fluvial deposits of *Unit I* containing two superimposed channel belts are interpreted as 'incised valley' fills accumulated during a lowstand sea level (cf. Zaitlin et al. 1994, Dalrymple 2006). They were deposited in a purely fluvial environment or in a river-dominated innermost part of an estuary as indicated by unimodal paleocurrent directions and the absence of tidal influence. The vertical transition from fluvial to tidal-estuarine facies succession suggests a reduction in the rate of supply of fluvial sediments relative to the rate of creation of accommodation space (cf. Allen & Posamentier 1994, Boyd et al. 2006). The presence of tidal channel fills and linear tidal sand bars suggests deposition in a tide-dominated estuary (Dalrymple et al. 1992). Northeast- and southwest-dipping foresets of the elongate tidal sand bars generally indicate a northeast-opening estuary funnel in the Megab area. The three upward-coarsening progradational sets at the upper part of *Unit I* represent deposition in a storm-dominated shoreface to inner shelf environment in a high-energy, nonbarred, coarse sandy nearshore, in which storm effects predominate (Clifton 2006).

The fluvial complex at the base of *Unit II* represents renewed valley incision and subsequent infilling as the rate of sediment supply exceeds the rate of sea level rise (Shanley & McCabe 1994). The valley was incised on the underlying shoreface deposits as the sediment transport capacity of rivers exceeded the load that they actually carried, in

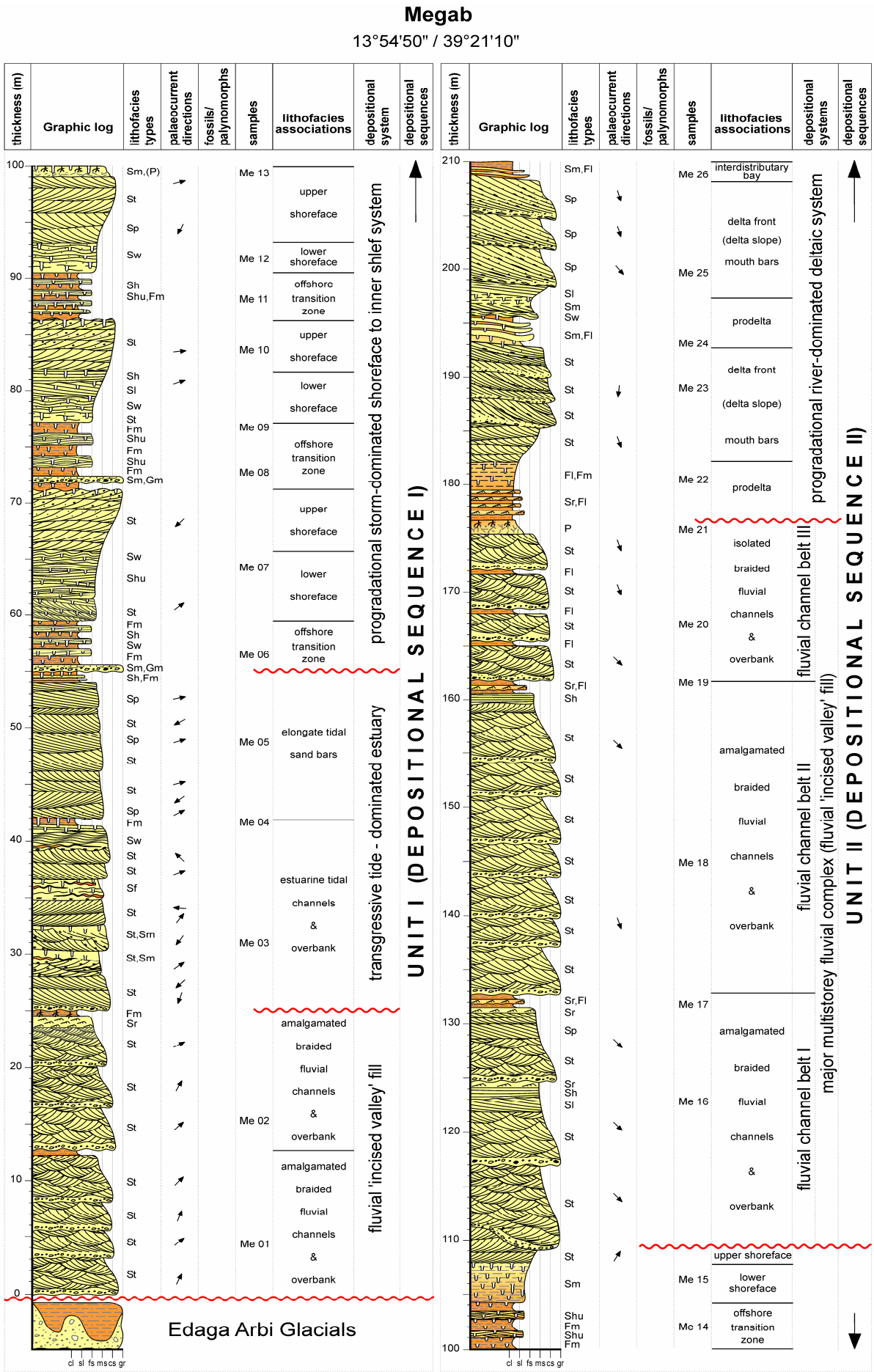


Fig. 4.15. Megab section.

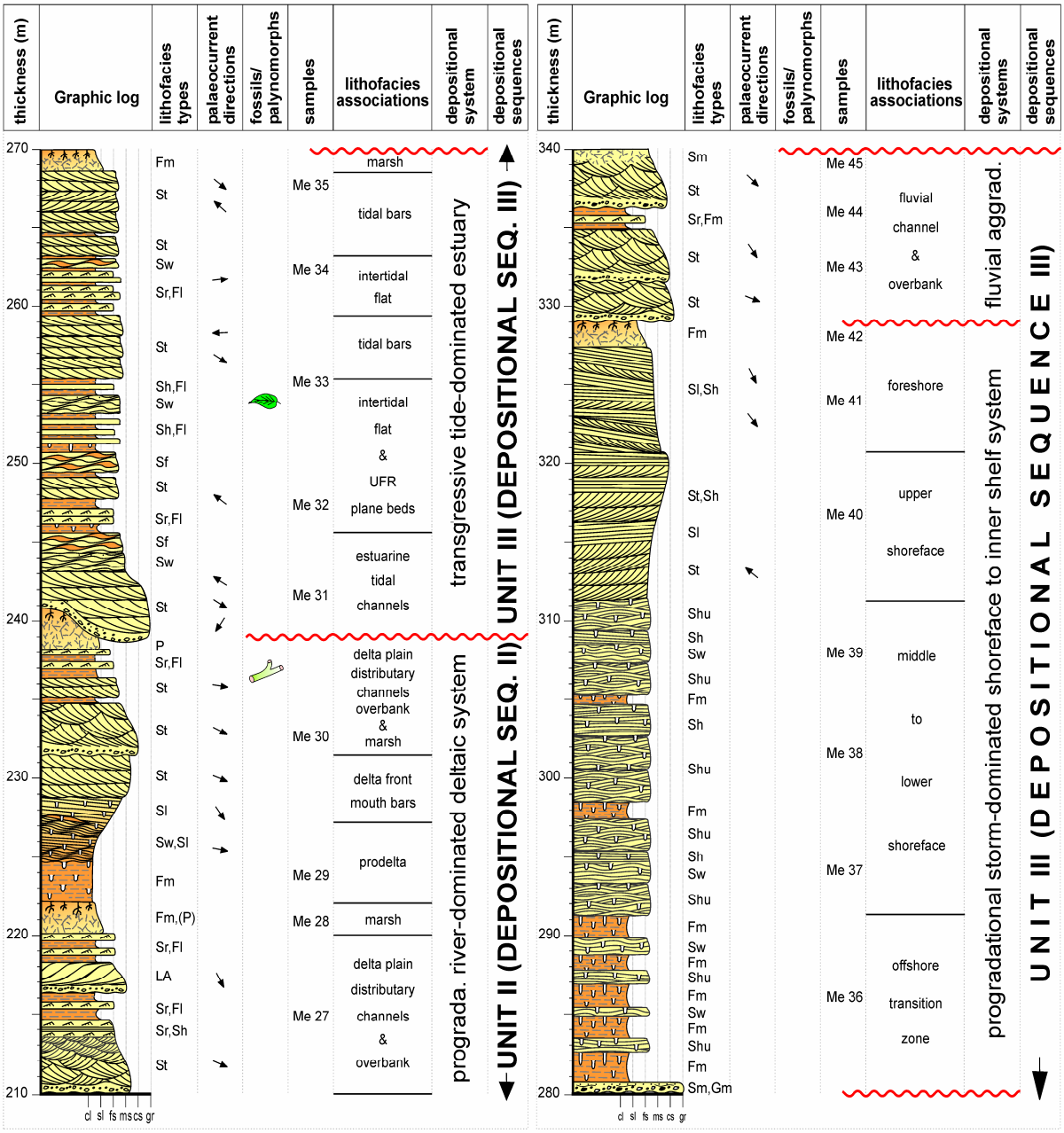


Fig. 4.15. Megab section (continued).

which case the excess energy of the rivers led to erosion of its substrate (Dalrymple 2006). The overall upward-fining of the fluvial complex from amalgamated to isolated channel fills (from high-energy lowstand rivers to the sluggish transgressive river systems) is mainly a consequence of continuous coastal aggradation and the associated shallowing of the fluvial graded profile during sea level rise, coupled with the denudation of the source area (cf. Posamentier et al. 1988, Shanley & McCabe 1993, 1994). The transition from fluvial aggradation to deltaic progradation in the upper part of *Unit II* may suggest the onset of regression, as the rate of sea level rise is unable to cope with the excess sediment supply. The prograding clinoforms with unimodal palaeoflow directions and their lobate geometry may suggest deposition in a river-dominated delta front environment (Hampson & Howell 2005). The deltaic progradation is most probably the result of high fluvial input combined with rapid subsidence of the delta front sands into the underlying muddy prodelta. The low degree of

bioturbation may be related to the high rate of delta front progradation, indicating increased sedimentation rates and heightened fluvial discharge. Rapid emplacement of sediments generally makes infaunal colonization of the substrate difficult (MacEachern et al. 2005). Widespread paleosol formation on the delta plain suggests delta abandonment and a lowstand sea level.

In the lower part of *Unit III*, the establishment of a tide-dominated estuary on top of the abandoned delta plain records renewed rise in sea level. The tidal channel deposits at the base of the succession fill irregular, shallow and laterally discontinuous depressions that are tens of metres wide and several meters deep. These channels were most probably incised by tidal erosion during transgression. The upward-coarsening nearshore marine (shoreface to inner shelf) deposits of *Unit III* represent a progradational (regressive) system deposited during a falling sea level. The presence of heavily bioturbated, laminated to massive silty mudstones with intercalated hummocky cross-stratified sandstones at the base of the succession may suggest a dominance of fairweather conditions, although storm effects exist. Such conditions are characteristic of a barred, low-energy inner shelf setting (Clifton 2006). However, the presence of less intensely bioturbated, hummocky cross-stratified lower shoreface sandstones at the middle part of the succession indicates a nonbarred, high-energy storm-dominated nearshore marine setting. Furthermore, the fine-grained and planar-laminated surf and swash zone deposits of the upper shoreface and the absence of large-scale bedforms suggests a flatter beach–nearshore profile, which is characteristic of a non-barred high- to moderate-energy nearshore (upper shoreface) in a fine sandy coast under fairweather conditions (Clifton 2006).

### 4.2.5. Wukro area

***Description***: The location of the studied section in the Wukro area is at about 2 km north of the town Wukro, on the escarpment located west of the main road connecting the towns Wukro and Adigrat (N 13°48′42″/E 39°35′59″). The stratigraphic position of the Adigrat Sandstone succession is similar to Agwe and Samre areas in that it unconformably overlies and is overlain by the Edaga Arbi Glacials and the Antalo Limestone respectively. The succession is 360 m thick and can be divided into three stratigraphic units: *Unit I*, *Unit II* and *Unit III* (Fig. 4.16).

*Unit I* is about 90 m thick and consists of fluvio-estuarine deposits that grade upwards to shoreface deposits. The fluvio-estuarine deposits are up to 55 m thick and are predominantly composed of tidal channels and elongate tidal sand bars with interbedded UFR sand flats. Basal fluvial channel fill sandstones are only up to 5 m thick and play a proportionally minor role in the overall facies succession. UFR sand flat deposits are predominantly composed of planar-laminated sandstones with subordinate low-angle cross-bedded sandstones. Flaser and lenticular bedding occur rarely, as well as partially preserved tidal rhythmites. Elongate tidal sand bars that dominate the upper part of the estuarine succession are mainly composed of trough cross-bedded sandstones with or without mud drapes. Palaeocurrent directions are generally bimodal but SW-oriented foresets dominate over the NE ones.

The shoreface deposits that characterise the upper part of *Unit I* are up to 35 m thick and consist of two upward-coarsening units. These include, from bottom to top, bioturbated mudstone with intercalated wavy- to horizontal laminated siltstones of the offshore transition zone grading upwards to hummocky cross-stratified silty sandstones of the lower shoreface, and then to trough cross-bedded sandstones of the upper shoreface. These progradational units are capped by planar-laminated sandstones and paleosol horizons.

Fig. 4.16. Wukro section.

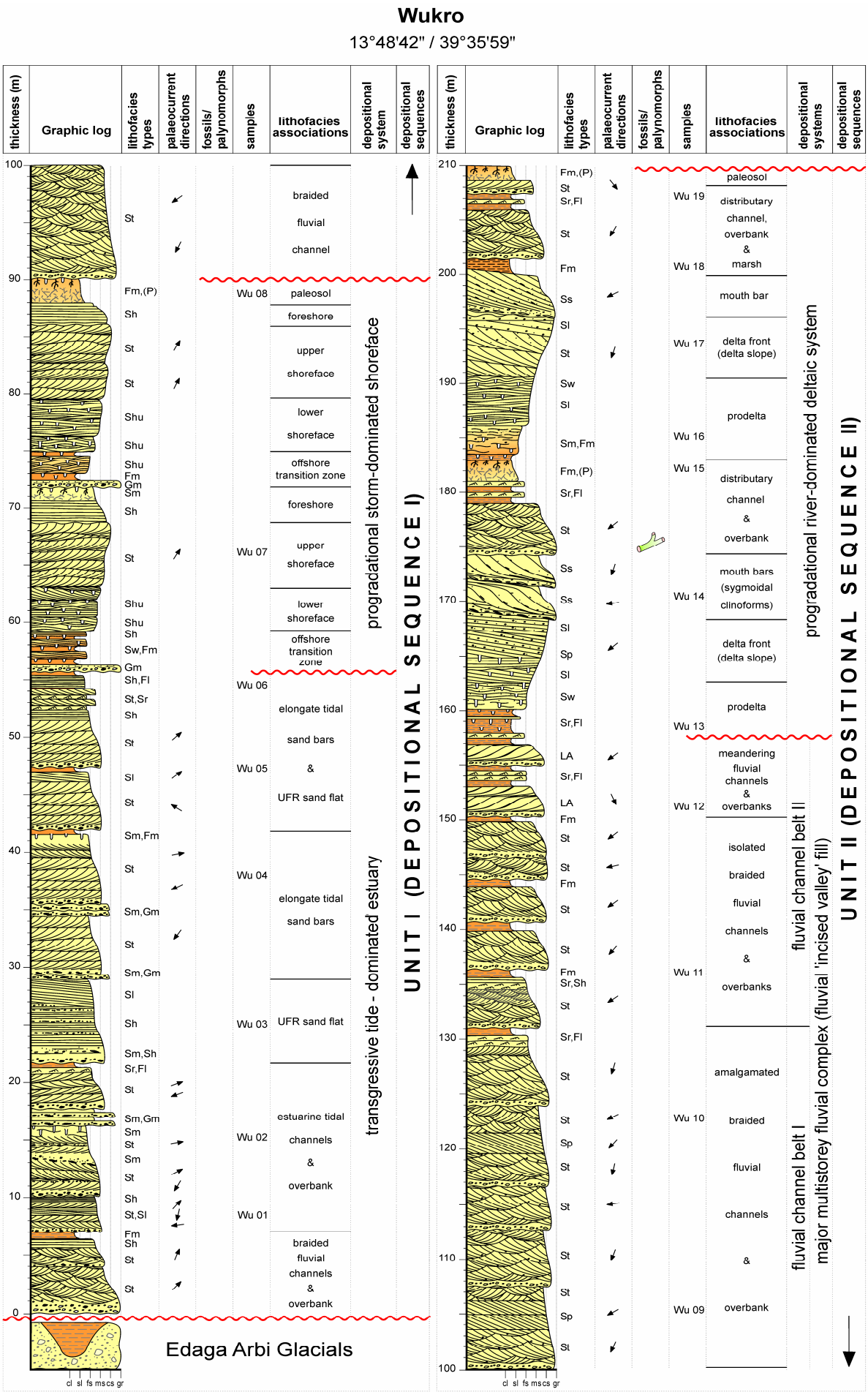
Wukro
13°48'42" / 39°35'59"
thickness (m)
Graphic log
lithofacies types
palaeocurrent directions
fossils/ palynomorphs
samples
lithofacies associations
depositional system
depositional sequences
braided fluvial channel
paleosol
foreshore
upper shoreface
lower shoreface
offshore transition zone
foreshore
upper shoreface
lower shoreface
offshore transition zone
elongate tidal sand bars & UFR sand flat
elongate tidal sand bars
UFR sand flat
estuarine tidal channels & overbank
braided fluvial channels & overbank
progradational storm-dominated shoreface
transgressive tide - dominated estuary
UNIT I (DEPOSITIONAL SEQUENCE I)
Edaga Arbi Glacials
cl sl fs ms cs gr
paleosol
distributary channel, overbank & marsh
mouth bar
delta front (delta slope)
prodelta
distributary channel & overbank
mouth bars (sygmoidal clinoforms)
delta front (delta slope)
prodelta
meandering fluvial channels & overbanks
isolated braided fluvial channels & overbanks
amalgamated braided fluvial channels & overbank
progradational river-dominated deltaic system
fluvial channel belt II
fluvial channel belt I
major multistorey fluvial complex (fluvial 'incised valley' fill)
UNIT II (DEPOSITIONAL SEQUENCE II)

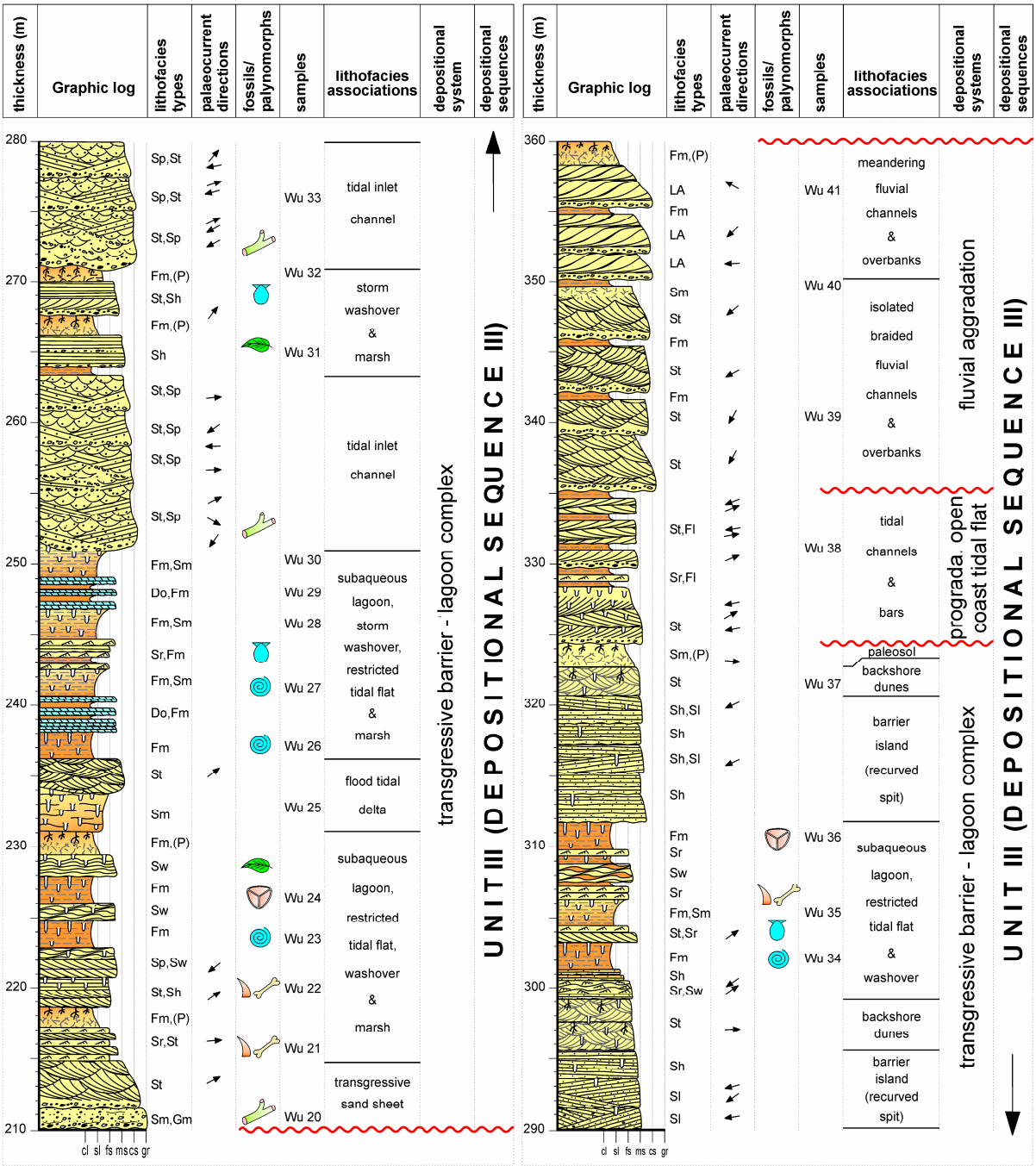


Fig. 4.16. Wukro section (continued).

*Unit II* is about 120 m thick and comprises, in its lower part, a fluvial channel complex that grades upwards into deltaic deposits. The fluvial complex is about 70 m thick and is composed of a lower amalgamated braided channel fills that change upwards to isolated meandering channel fills that are capped by overbank fines. The deltaic system ranges in thickness from 50–55 m and comprises two upward-coarsening progradational units. These units consist of planar- and wavy-laminated to massive, usually bioturbated fine-grained sandstones, siltstones and mudstones of the prodelta platform that grade upwards into large-scale planar-tabular and sigmoidal trough cross-bedded medium- to coarse-grained sandstones of the delta front slope and distributary mouth bars. The uppermost parts of the deltaic

succession are characterised by trough cross-bedded sandstones filling distributary channels and silty mudstones deposited in overbank and marsh environments of the delta plain.

*Unit III* is about 140 m thick and consists of a barrier-lagoon complex that changes upwards to an open coast tidal flat system and ends up with isolated fluvial channel fills and pedogenically altered overbank deposits. The barrier-lagoon complex is composed of three barrier islands, each of them are underlain by a backbarrier lagoonal succession. The lower barrier contains exclusively tidal inlet channel fills whereas the middle barrier contains a mixture of tidal inlet, spit platform/spit beach and backshore eolian dunes. The upper barrier is predominantly characterised by spit accretion. Mud rip-up clasts and wood fragments are common in the basal lag deposits of tidal inlet channels. The backbarrier deposits comprise bioturbated subaqueous lagoonal mudstones with intercalated storm washover, restricted tidal flat and fringing marsh deposits. They contain brackish-water bivalves, agglutinated foraminifera (e.g., *Ammodiscus*), teeth of actinopterygian fish (cf. *Lepidotes*) and hybodontid sharks, ribs and isolated teeth of marine crocodiles (*thalattosuchian*) along with myriad types of coprolites. Intercalations of dolomite layers are common. Vertical burrows, mainly *Diplocraterion*, are abundant on bedding surfaces of washover sheet sandstone layers. The upper part of *Unit III* is made up of subtidal channel fills and tidal sand bars with intercalated heterolithic tidal flat deposits. The succession ends up with isolated single-storey braided fluvial channel-fill sandstones and point bars with interbedded massive to laminated overbank mudstones. Palaeocurrent directions are unimodal and oriented to the southwest.

***Interpretation***: The stratigraphic development of the Wukro section is basically similar to that of Agwe, Abiadi and Megab sections. In the fluvio-estuarine deposits of *Unit I*, the vertical facies succession containing basal fluvial channel fills, top bioturbated tidal channels, UFR sand flats and elongate tidal bars suggests deposition in a transgressive tide-dominated estuary (Dalrymple 1992, Boyd et al. 2006). The presence of SW- and NE-oriented palaeocurrent directions points to the presence of evasive flood- and ebb tidal currents. This tidal flow path suggests a northeast opening estuary funnel in the Wukro area.

At the base of *Unit II*, renewed valley incision and deposition of a major amalgamated braided fluvial channel complex (channel belt I in Fig. 4.16) records a change in the fluvial energy flux and a corresponding rapid vertical aggradation caused by an oversupply of sediments, which might be related to source area uplift and/or a change in climate (Shanley & McCabe 1994). The overall upward change in fluvial style from amalgamated to isolated braided and meandering stream deposits (channel belt II) is interpreted to record continuous denudation of the source area and the associated lowering of the slope gradient of the fluvial graded profile (Shanley & McCabe 1994, Blum & Tornqvist 2000). The system goes, beyond filling a narrow fluvial incised valley, to progradation of a river-dominated deltaic system (upper part of *Unit II*) suggesting continued supply of larger sediment loads and deposition rates, which might have inhibited sediments reworking by basinal currents.

The barrier-lagoon system in the lower part of *Unit III* is interpreted to record a renewed rise in sea level. The succession contains three superimposed barrier-lagoon systems suggesting a relatively rapid sea level rise with accompanied low rate of sediment supply (Rampino & Sanders 1980, Clifton 2006). The vertical change in facies succession from a mesotidal inlet-dominated system in the lower part of *Unit III* to a spit-dominated microtidal barrier system in the middle part indicates a continued rise in sea level (Tye & Moslow 1993, Cheel & Leckie 1990). The high degree of similarity in the fossil content of the lagoonal deposits in the Wukro area with that of Agwe and Abiadi areas as well as their occurrence at similar stratigraphic levels might suggest that they were deposited at the same time. The prograding subtidal channels and bars that overlay the barrier-lagoon complex records the establishment of an open coast macrotidal flat due to a falling sea level (Hobday & Horne 1977). As proposed by Davis & Clifton (1987), slower rate of relative sea level fall might

have favoured the preservation of prograding tidal flat deposits. Fluvial aggradation over tidal deposits at the uppermost part of the Wukro section records continued fall in relative sea level.

### 4.2.6. Berhale area

***Description***: Berhale area is located at the easternmost periphery of the Mekelle Basin (Fig. 2.1). The studied section (N 13°39′17″/E 39°51′00″) is located about 25 km southeast of the town Berhale. Unlike the other studied sections, the Adigrat Sandstone succession unconformably overlies the Neoproterozoic Basement and is 'disconformably' overlain by the Antalo Limestone. The 230 m thick succession can be divided into two stratigraphic units: *Unit I* and *Unit III*.

*Unit I* is about 110 m thick and consists of basal estuarine deposits that grade upwards to a barrier-lagoon succession and ends up with a storm-dominated shoreface (Fig. 4.17). The estuarine deposits are composed of fluvial channel fills passing upwards to tidal channel fills, tidal flat and marsh deposits. These deposits are overlain by a barrier-lagoon complex, which contains two superimposed barriers and/or tidal inlets with interstratified backbarrier lagoonal deposits. *Unit III* is about 120 m thick and consists of a barrier-lagoon complex, which is composed of two tidal inlet systems, and changes upwards to open-coast tidal flat deposits. The uppermost part of the unit is characterised by fluvial channel and overbank deposits.

***Interpretation***: The vertical stacking pattern in the Berhale section is basically similar to that of other areas studied. The only exception is the absence of the fluvio-deltaic middle unit (*Unit II*) in this area. The change from a tide-dominated estuary to a barrier-lagoon complex indicates a change in the coastal morphology during continued rise in sea level (Hayes 1979). Subsequent fall in relative sea level, addition of fluvial sediments and the combination of wave and/or storm reworking of previous sediments led to shoreface progradation at the upper part of *Unit I*. The cyclic development of the third unit (*Unit III*) from a transgressive barrier-lagoon system to a prograding open-coast tidal flat, and then to fluvial aggradation is a similar situation, which is well-described and interpreted in other areas studied (e.g., in Wukro, Agwe). Therefore, the interpretation therein also applies for *Unit III* in the Berhale area.

## 4.3. Intrabasinal Correlation

The large-scale spatial and temporal stratigraphic stacking patterns within a sedimentary basin fill are believed to be results of the interaction between regional to global causal factors and modifying local environmental processes (allogenic and autogenic factors, *sensu* Beerbower (1964)). An important requirement for distinguishing the relative roles of these factors is to link the appropriate process with an observation and correlate similar observations from different regions that occurred within equivalent time periods. Consequently, this section deals with intrabasinal correlation of the three stratigraphic units and the enclosed depositional systems that build the various portions of the basin fill as they were recognised from the six vertical profiles described and discussed in the previous section. The basin wide stratigraphic correlation is illustrated in three cross-sections (Fig. 4.18-20), in which the first two will be referred to as the southwestern- and the northeastern segment. The SW-segment extends from the Abiadi area in the west passing through Agwe to the Samre area in the south (Fig. 4.18). The NE-segment connects the Megab area in the north, by crossing through Wukro, to the Berhale area in the east (Fig. 4.19). The third one incorporates all vertical profiles studied and represents a composite cross-section for the whole basin (Fig. 4.20). All cross-sections are constructed by taking the base of the Antalo Limestone as a reference datum.

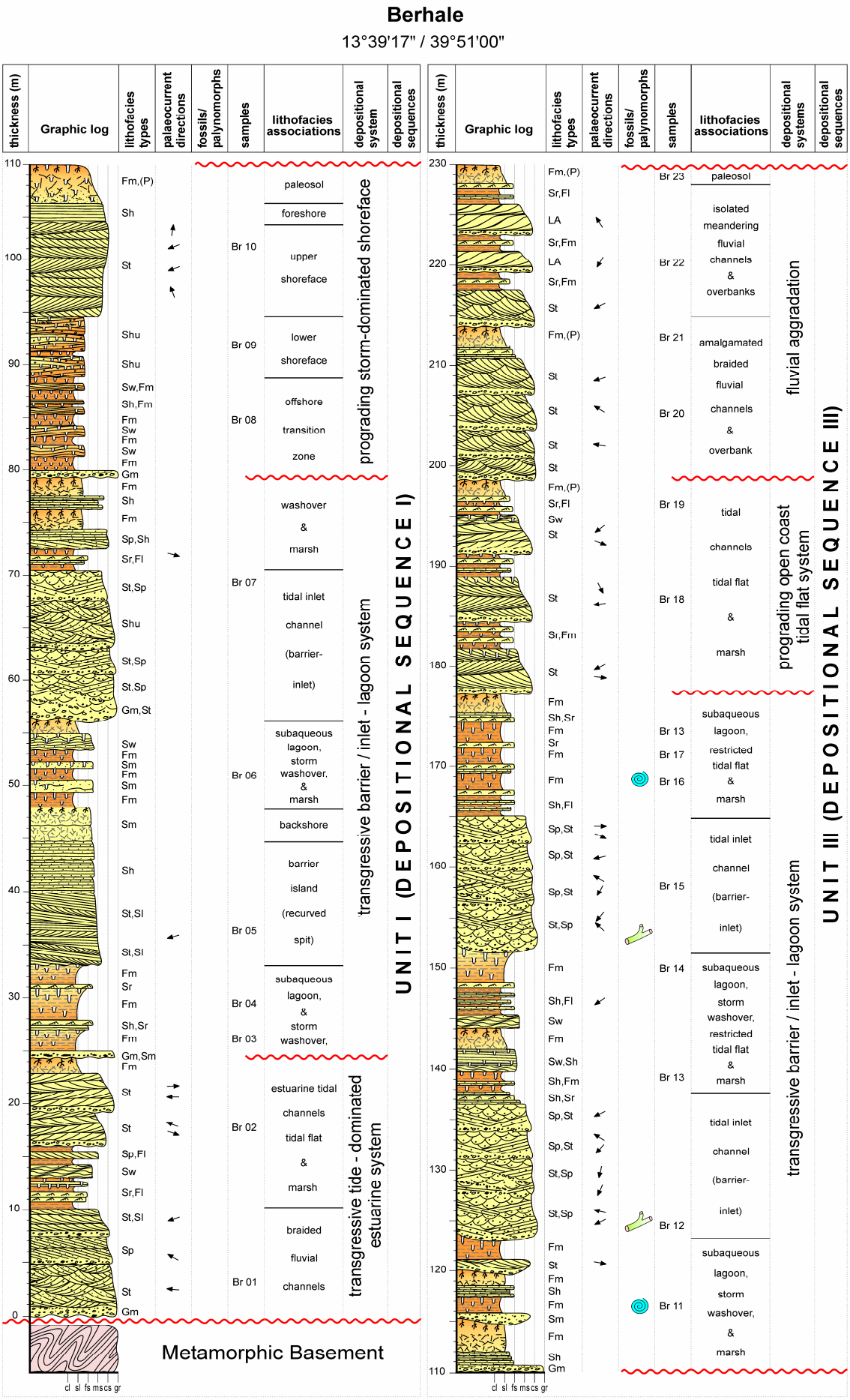


Fig. 4.17. Berhale section.

***Description***: The thickness of the Adigrat Sandstone succession decreases along strike as it is portrayed in the two segments. In the SW-segment, it decreases from the west (i.e., Abiadi-Agwe area) towards the south (Samre area). In the NE-segment, it decreases from the north (Megab-Wukro area) towards the east (Berhale area). The number of recognisable stratigraphic units as well as the thickness of each individual unit varies along these directions. Whilst all the three stratigraphic units are well-represented in the west and in the north, only two units could be recognised in the south and in the east with the absence of *Unit II*. Higher variation in thickness can be observed in *Unit I* and *II*, whereas the thickness variation in *Unit III* is fairly moderate.

In the SW-segment (Fig. 4.18), the fluvial and deltaic systems that characterise *Unit II* assume a wedge-shaped cross-sectional geometry that pinches out between Agwe and Samre areas. The barrier-lagoon system of *Unit III* is persistent throughout the cross-section but the overlying open-coast tidal flat system in the west interfingers laterally with the shoreface system towards the south. Moreover, the amalgamated braided fluvial channel complex changes partly to isolated braided and/or meandering system towards the south. In the NE-segment (Fig. 4.19), as *Unit II* pinches out between Wukro and Berhale areas, the barrier-lagoon deposits of *Unit III* intertongue laterally with the incised valley estuarine deposits towards the Megab area. Likewise, the open-coast tidal flat system represents a lateral equivalent of the shoreface system.

***Interpretation***: The variation in the number of recognisable stratigraphic units as well as the variation in thickness of the whole succession from the north and the west to the south and the east is interpreted to reflect marked differences in sedimentation and subsidence rates. Based on characteristic combinations of sedimentation and subsidence rates, it is clearly apparent from the cross-sections that two different areas can be recognised in the basin. These variables have been assigned relative values (e.g., low, moderate and high) on the basis of the preserved thicknesses of stratigraphic units (reflecting subsidence rates) and composition of facies and depositional environments (reflecting sedimentation rates). The two areas and their characteristic variables are: (i) northern and western areas that are generally characterised by relatively high sedimentation and subsidence rates, and (ii) southern and eastern areas with relatively low sedimentation and subsidence rates. This pronounced contrast would have not been apparent if the course clastic wedge of *Unit II* would have been absent.

In the lower unit (*Unit I*), the rapid lateral thickness variation within relatively short distances is attributed to the irregular antecedent topography of the pre-transgressive ancestral drainage system, which might have been created by differential erosion of the bedrock by fluvial and/or tidal currents (e.g., Ashley & Sheridan 1994). Both fluvial and tidal currents erode channels into the substrate and create incised valleys (Demarest & Kraft 1987, Swift et al. 1980). The dominantly coarse-grained fluvio-deltaic succession that characterises *Unit II* is the result of relatively high and rapid rate of sedimentation, which might most probably be related to a tectonic activity (rifting and/or source area uplift). The deltaic deposits possess steeply dipping foresets that resemble the dominantly coarse-grained 'classic Gilbert-type delta' originally described by Gilbert (1890) and later by Postma (1990). The formation of 'Gilbert-type' deltas requires coarse-grained sediment supply from possibly fault-bounded steep-sided canyons draining directly into a standing body of water (Gawthorpe & Colella 1990, Wescott & Ethridge 1990). Palaeocurrent directions suggest that the coarse clastic wedge was shaded in a half-centripetal manner from the north and the west towards a common central point. This implies the existence of an uplifted source area further to the north and west of the towns Abiadi and Megab. The absence of this unit in the east and the south (e.g., Berhale and Samre) together with the widespread occurrence of paleosol(s) on top of the underlying unit may suggest that these areas were sites of nondeposition and pedogenesis.

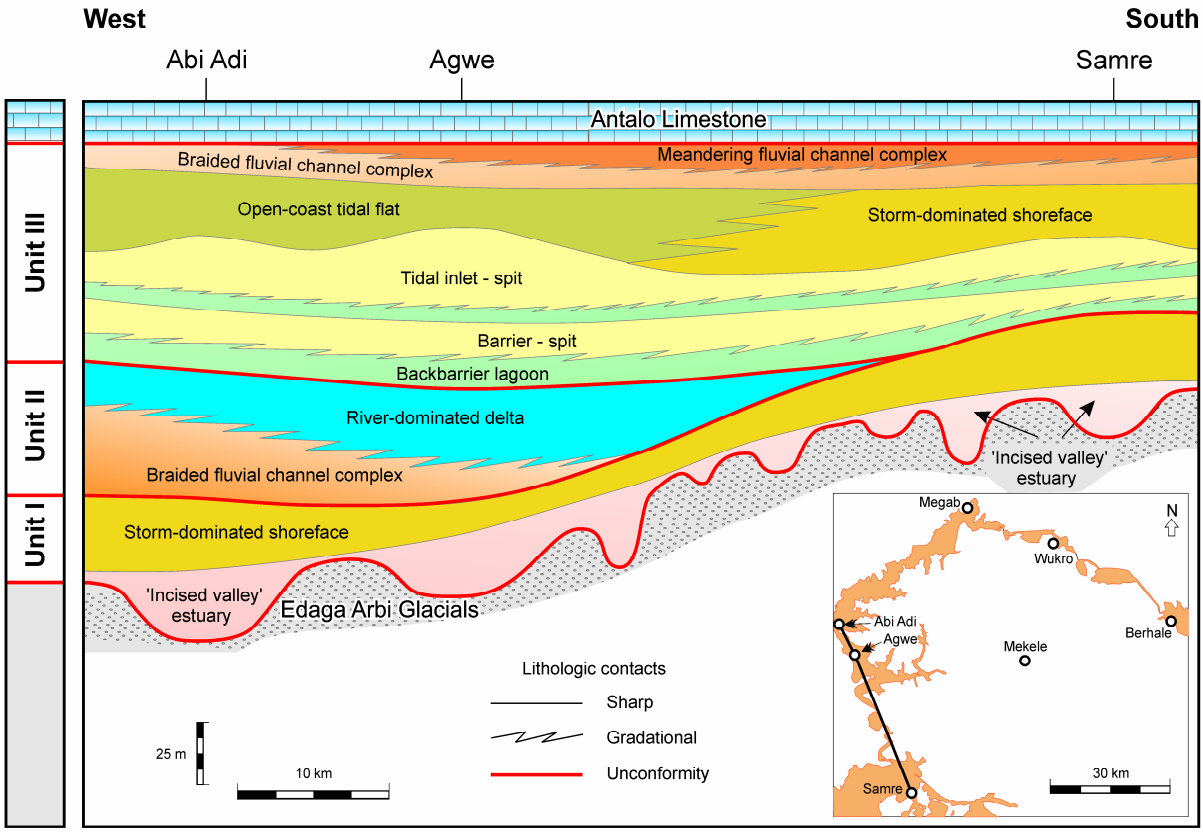


Fig. 4.18. A cross-section, referred to as the SW-segment, illustrating correlation between Abiadi, Agwe and Samre areas in the southwestern part of the Mekelle Basin. The base of the Antalo Limestone is taken as a reference datum.

The lateral thickness variation in the barrier-lagoon system of *Unit III* may result from a number of factors. Relatively thicker barrier-lagoon deposits are recorded in Agwe and Wukro areas than elsewhere. The most common explanations why the deposits are thicker in some areas and thinner in the other areas along the coast are: (i) the variation in the preservation potential of the barrier-spit lithosomes due to variable rates of shoreface erosion (Kraft et al. 1987, Demarest & Kraft 1987); (ii) the distribution and abundance of washover and backbarrier sand flats which creates environments favourable for barrier-spit stabilisation by marsh growth (Reinson 1884); and (iii) the variation in sediment transport pathways along the coast (onshore-offshore, landward and coast-parallel) (Kraft et al. 1987). Anyone of the above three factors or a combination of them might have caused the observed lateral thickness variation in the system.

The origin of barrier islands has been much debated and the problem has been discussed in more detail in Davis (1994). According to Hoyt (1967), Swift (1975) and Wilkinson (1975), the origin of barriers has been attributed to at least three mechanisms: (i) the vertical growth and emergence of offshore and/or longshore bars; (ii) the lateral migration of inlets or channel-spit sequences; and (iii) the detachment of beach ridges from the mainland by a rise in sea level. All of these three mechanisms have been documented in the Mekelle Basin at different stratigraphic levels and localities studied. It is not uncomplicated to distinguish between these various modes of origin, particularly as many barriers show evidence of composite development and modification. Barrier formation through vertical growth and emergence of offshore and/or longshore bars is documented in Samre area (Fig

4.11). In contrast, the lateral (coast-parallel) migration of channel-spit sequences has been noticed in Agwe and Abiadi areas. The third mechanism involves stepwise landward migration of barriers due to rapidly rising sea level, which is described by the 'stepwise coastal retreat' model of Rampino & Sanders (1980), Elliot (1986) and Clifton (2006). This mechanism is well-documented in Agwe, Abiadi and Wukro areas.

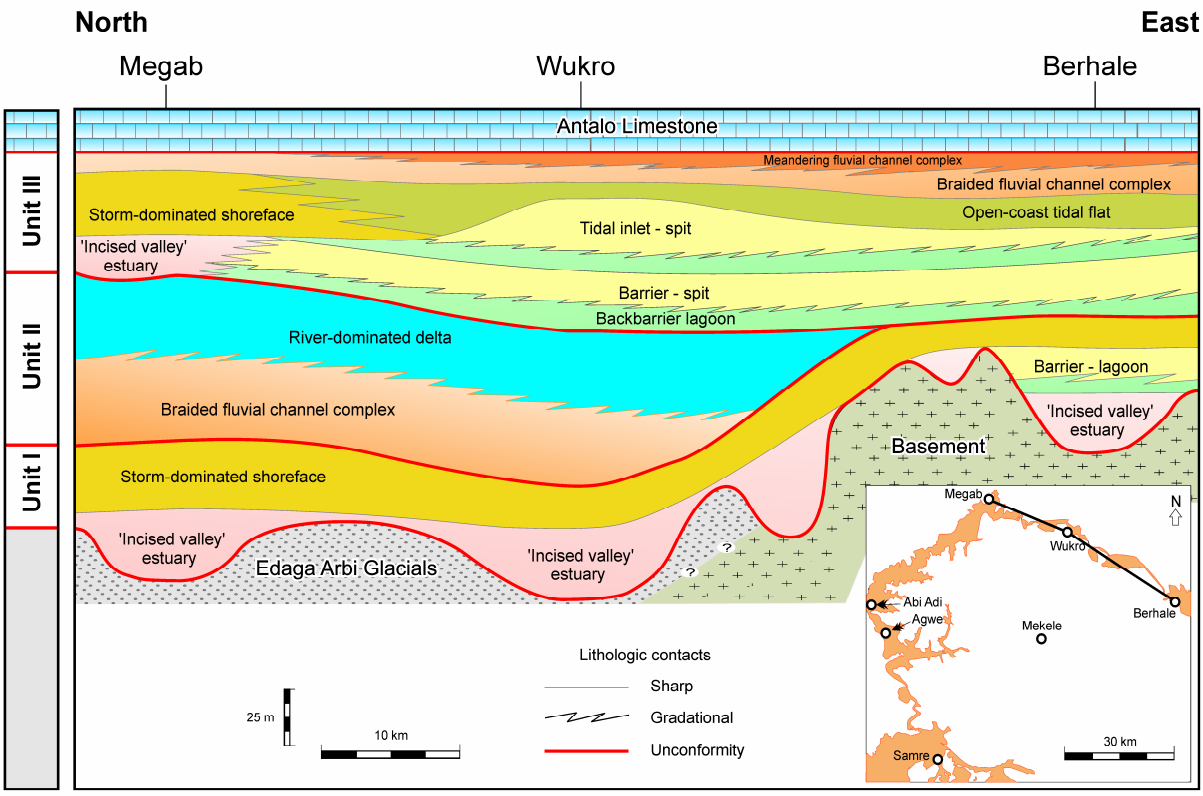


Fig. 4.19. A cross-section, referred to as the NE-segment, illustrating correlation between Megab, Wukro and Berhale areas in the northeastern part of the Mekelle Basin. The base of the Antalo Limestone is taken as a reference datum.

Many, if not most, studies on the evolution of coastal systems reveal that barrier islands (or barrier spits) and lagoons are generated during transgression (Kraft et al. 1973, Boyd et al. 1992, Davis 1994). However, there are also few studies that acknowledge barrier formation during regression (Morton 1979, Scholle & Spearing 1982). In the Mekelle Basin, barriers and lagoons have been formed by landward migration and upward accretion during transgression when the rates of sea level rise outpaced the rates of sedimentation at the shoreline (cf. Posamentier & Vail 1988, Clifton 2006, Catuneanu 2006). The partial to nearly complete preservation of these transgressive coastal sequences (e.g., in the Agwe section) implies that the rise in sea level must have been rapid (Davis & Clifton 1987).

The lateral facies intertonguing of the shoreface system with the open-coast tidal flat system in the upper part of *Unit III* may reflect the variation in the relative effectiveness of tidal or wave/storm processes along the coast. The areas with open-coast tidal flat system (i.e., Abiadi, Agwe, Wukro and Berhale) are characterised by high tidal range and low wave power. In contrast, the areas with storm-dominated shoreface system (i.e., Megab and Samre areas) are characterised by low tidal range and high wave/storm activity. The along-coast variation in the relative power of tides or waves is attributed to the variation in coastal morphology, nearshore bathymetry and the orientation of the coast with respect to dominant

wave approach (Hayes 1775, 1979). When tidal currents are stronger and abundant sediment supply is available, a low-gradient wedge of tidal flat sediments builds out seaward. The low-gradient flat greatly reduces the incoming swell wave power and waves cannot break on any part of the tidal flat. The opposite explanation applies to microtidal coastal segments dominated by high wave power.

In the uppermost part of *Unit III*, the overall upward change in fluvial style from an initial higher energy braided to a final lower energy meandering system is most probably related to the gradual decrease in topographic slope which might be caused by the pattern of differential subsidence, with increasing rates from proximal to distal direction for rifts or divergent continental margin basins (Leeder & Gawthorpe 1987). Generally, as far as the Adigrat Sandstone succession is concerned, lack of subsurface as well as outcrop data in the central part of the Mekelle Basin do not allow making genuine inferences of proximal-distal trends. This is because large areas of the central part of the basin are covered by the Late Jurassic Antalo Limestone.

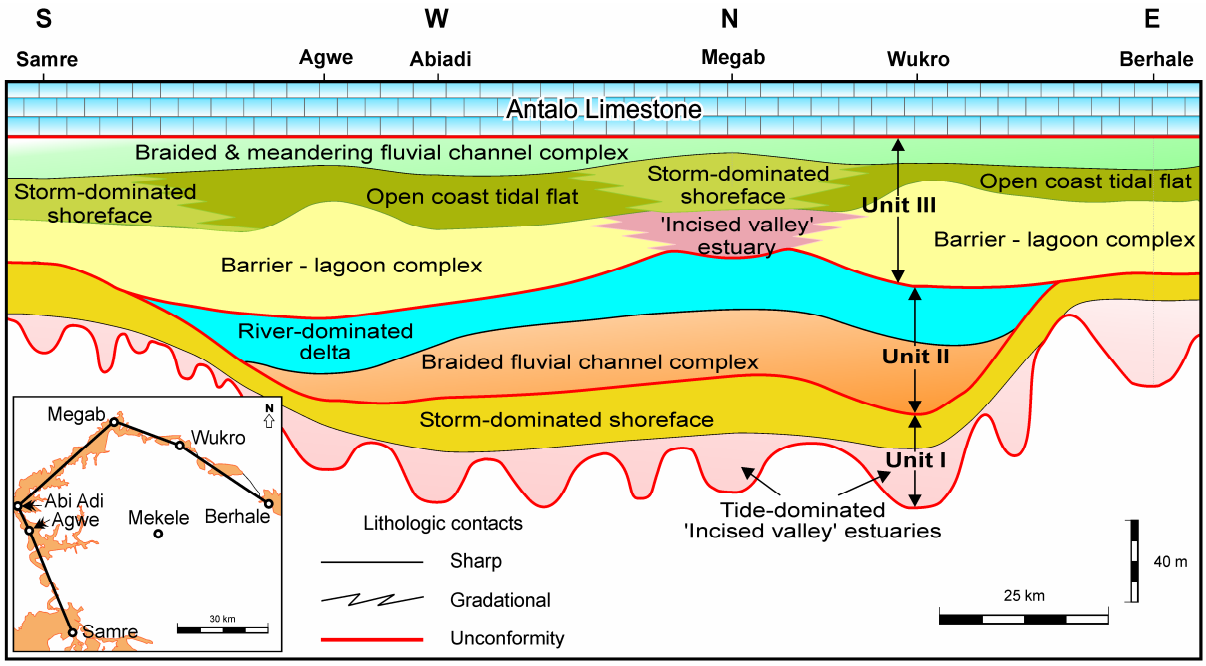


Fig. 4.20. A composite cross-section for the whole basin. The base of the Antalo Limestone is taken as a reference datum.

## 5. Stratigraphic and Facies Analysis of the Adigrat Sandstone in the Blue Nile Basin, Central Ethiopia

In the Blue Nile Basin, the Adigrat Sandstone succession is exposed predominantly in vertical cliffs on both sides of the Blue Nile River canyon (locally called Abay River canyon), whose numerous tributaries also carve smaller canyons that add an important three-dimensional quality to the exposures. The succession attains a total thickness of up to 195 m and unconformably overlies latest Carboniferous(?) to Middle Triassic siliciclastic successions, here referred to as the 'Pre-Adigrat III'. In the eastern outcrop areas (e.g., in the Dejen area), it is unconformably overlain by the Middle Jurassic evaporite deposits of the Gohatsion Formation. In the western outcrop areas (e.g., in Yejube, Fincha, Dedu, Amuru and Bokotabo), it is unconformably overlain by Tertiary flood basalts (Fig. 2.2).

The description and classification procedures adopted in this section are the same as those used for the Mekelle Basin in Sec. 4. The analysis of facies, facies associations and depositional systems will be dealt with in the first part. The second part focuses on the stratigraphic stacking patterns of depositional systems in each of the studied localities, which is followed by the third part that deals with the intrabasinal correlation of stratigraphic units.

### 5.1. Depositional Systems and Facies Associations

The Adigrat Sandstone succession in the Blue Nile Basin consists of three depositional systems: namely, (i) fluvio-estuarine, (ii) barrier-lagoon and (iii) strandplain systems.

#### 5.1.1. The Fluvio-Estuarine system

The fluvio-estuarine system grades lateraly into the barrier-lagoon system in a seaward direction and is composed of four facies associations, $FA_1$ to $FA_4$.

**Facies association $FA_1$**

***Description*:** Having a laterally restricted geographic distribution in the Blue Nile Basin, facies association $FA_1$ is only well-represented in the southwestern outcrop areas (e.g., in Fincha and east of Amuru areas, while it is absent in other studied areas. The thickness reaches a maximum of 50 m. It is composed of lenticular, single storey, trough- and low-angle cross-bedded, medium- to coarse-grained sandstones and massive to laminated siltstones and mudstones (Fig. 5.1a). Individual sandstone beds are 0.5–3 m thick and have shallow concave-up erosion surfaces at their base. Sorting is poor to moderate and a fining-upward grain-size trend is discernible from coarse-grained sandstone with scattered pebbles at the base to fine-grained sandstones, siltstones and mudstones at the top. Lateral accretion (LA) surfaces are observed in some sandstone bodies. Trough cross-bed foresets dip to the northeast.

The mudstone intervals range in thickness from 0.3–1 m, but may occasionally reach up to 2 m. Their contact with the underlying sandstone beds is usually gradational but they are erosionaly truncated at the top. Although they are moderately to intensely bioturbated and rooted, relict planar lamination is clearly visible. Intervals of planar to current ripple-laminated, very fine-grained sandstone and siltstone with mud drapes are commonly intercalated as interlaminae or thin interbeds. Current ripples occasionally show opposite oriented migration directions. Intense colour mottling gives the mudstone intervals a varicoloured appearance. Purple to greyish blue colour predominates with orange and light pale grey mottles that taper and branch downwards (arrow in Fig. 5.1b). Angular blocky ped structures and soil horizons (Fig. 5.1b & c) are also observed but are not widespread. Borrowing is generally rare.

***Interpretation*:** The lenticular geometry, the shallow concave-up erosive bases, and fining- and thinning-upward trends observed in the sandstone bodies indicate deposition within channels. The trough cross-bedded sandstone bodies represent the migration of subaqueous 3D dunes along channel thalweg(s) (Harms et al. 1982). The upward transition from trough to low-angle cross-bedding may reflect the abandonment and scouring of 3D dunes by rapidly falling water, which in turn indicates that the bedforms were not in equilibrium with flow conditions throughout their generation (Allen 1984). The presence of lateral accretion (LA) surfaces observed indicate that deposition took place, at least in part, in point bars of meandering channels. Palaeocurrent data measured from cross-bed foresets suggest a unimodal northeast-directed palaeoflow.

The mudstone intervals and the fine-grained sandstone and siltstone interbeds are interpreted to represent overbank and crevasse splay deposits. The downward tapering and branching, orange to light greenish grey mottles are interpreted as traces of roots and rootlets (e.g., Retalleck 1990). The development of angular blocky peds is related to the shrinking and swelling of clays during repeated wetting and drying episodes (Retalleck 2001), pointing to incipient pedogenesis. The pale gray to purple colour of the mudstones indicates moderate to poor drainage conditions during pedogenesis (Kraus & Hasiotis 2006). Features recording subaerial emergence (root traces, ped structures, etc) suggest deposition in a floodplain environment.

In summary, the facies association is interpreted to reflect deposition in fluvial channels and associated floodplains in a low-gradient fluvial-dominated upper estuary.

**Facies association $FA_2$**

***Description*:** Facies association $FA_2$ is well-represented in Dejen area and, to a lesser extent, in Yejube and Dedu areas. The thickness ranges from 20 m to 60 m. It consists of massive silty mudstones ($FA_{2a}$) and inclined heterolithic sandstones and mudstones ($FA_{2b}$).

The sandstone intervals are dominated by inclined heterolithic sandstone/mudstone stratification (IHS) (Fig. 5.1d). The thickness of individual IHS bodies ranges from 0.5 to a maximum of 3 m. They usually possess sharp, undulating erosive bases with pebble lags. Trough and planar-tabular cross-beds, if present, are restricted to the base while low-angle (<10°) inclined, 5–30 cm thick, internally ripple-laminated, moderately- to well-sorted, fine- to medium grained sandstone beds with a few centimeters thick mudstone interlaminae dominate towards the top. Planar stratified sandstone bodies are also present but are less abundant. The geometry of IHS bodies is mainly sheet-like, although smaller, wedge- and ribbon-shaped bodies are also common. Desiccation cracks are abundant on bedding surfaces. Burrowing in the IHS beds is sparse to moderate but increases in intensity towards the top. Palaeocurrent directions measured from trough and planar-tabular cross-bed foresets are highly variable, though a slight dominance can be seen towards the NE. Dip directions of LA surfaces show a more or less bimodal NW and SE orientations.

The IHS beds grade upward into massive and faintly laminated mudstones. The transition from sand- to mud-dominated heterolithic facies is in most cases gradational. The mudstone intervals range in thickness from a few decimeters up to 7 m and are usually punctuated by thin (<30 cm), discrete sandstone layers and lenses. Scattered quartz pebbles, organic detritus, wood fragments and desiccation cracks are abundant. Intensive bioturbation totally disrupted primary sedimentary structures, with relict bedding features visible only in the bottom parts of the intervals.

Burrowing is variable on a small scale but generally increases in intensity upwards throughout the succession. The recorded ichnogenera are diverse but variably distributed, with local dominance of particular trace fossils (e.g., *Thalassinoides* and *Psilonichnus* in Fig. 5.2b). Syneresis cracks commonly occur in association with bioturbated horizons (Fig. 5.2d).

The appearance of the mudstone intervals is not uniform throughout the succession. Intervals dominated by grey-yellow-orange horizons randomly alternate with intervals of purple and red horizons without discernible cyclicity. In addition to the varicolouration of this facies, rootlet mottling is obviously pervasive and ped structures are abundant. Slickensides and pseudoanticlines are also common.

Fig. 5.1. A. Fluvial channel and overbank deposits of $FA_1$, Fincha section. B. Blocky ped structure and root traces (arrow), Dejen section. C. Slickensides in pedogenically altered overbank deposits, Dejen section. D. Inclined heterolithic stratification (IHC) in $FA_2$ interpreted as estuarione point bars, Dejen section. E. Close-up view of 'D' showing mud drapes along lateral accretion surfaces. F. Lenticular to wavy bedding, Yejube section. G. Flaser bedding in estuarine deposits of $FA_2$, Yejube section.

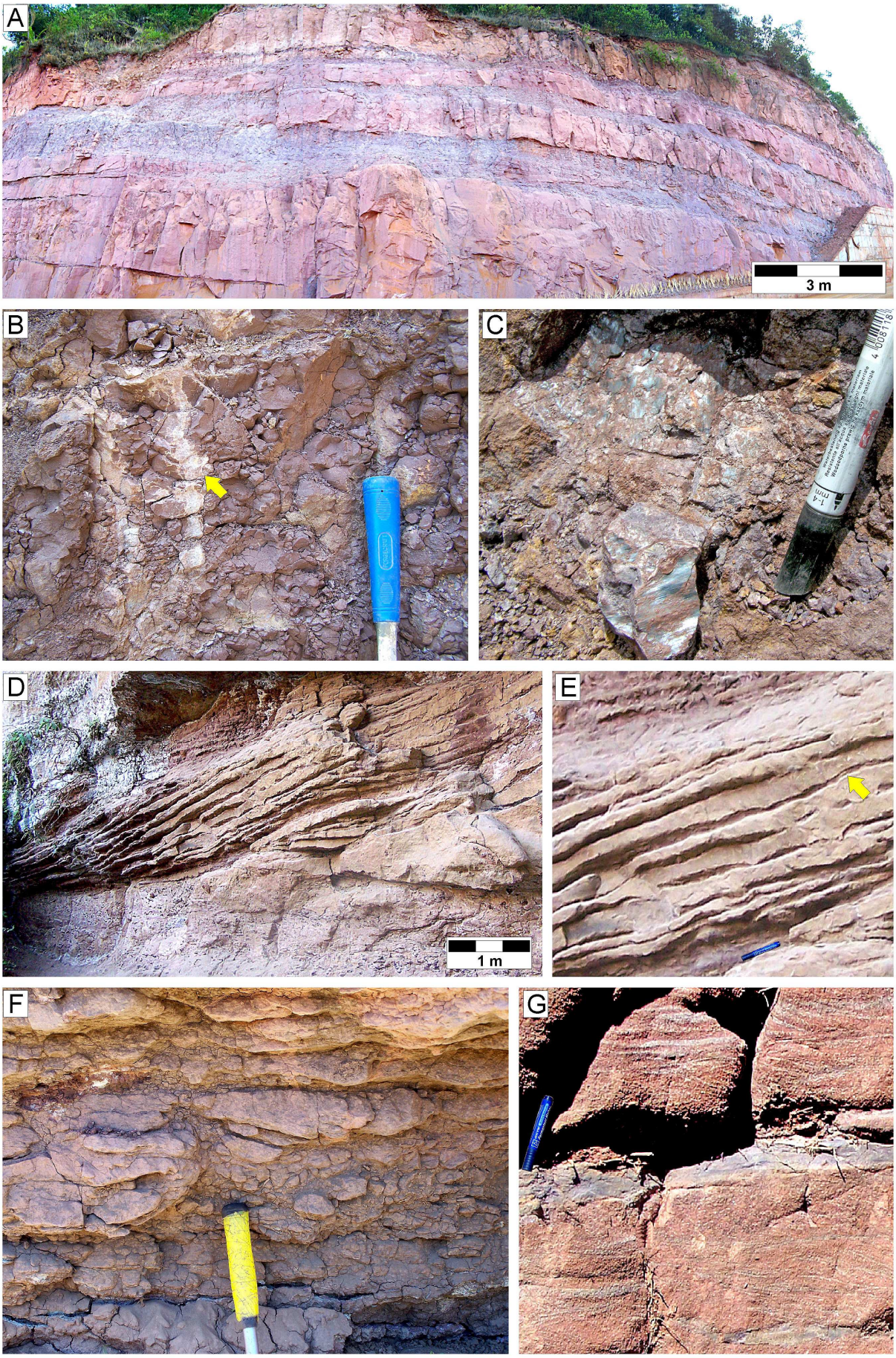
A
3 m
B
C
D
1 m
E
F
G

***Interpretation*:** The upward fining and the decrease in scale of sedimentary structures within individual cycles can be best explained by a channel environment (Tyler & Ethridge 1983), which may reflect an upward decrease in flow velocity and channel depth (Allen 1970). Sharp, erosive-based sandstone bodies with pebble lags likely suggest channelized flow as well. However, deeply incised, concave-up channel bases are rare, inferring that the depositional surface is relatively flat and readily susceptible to small changes in depositional processes. The IHS deposits are interpreted to represent laterally accreting bars (Thomas et al. 1987) within shallow estuarine channels. Mud drapes (Plate II, Fig. F) that are superimposed on LA surfaces indicate rapid fluctuations in flow velocity. Hence, the IHS deposits in this facies can be interpreted as tidally influenced estuarine point bars. The high degree of roundness and the dominance of quartz arenites indicate textural and mineralogical maturity, which points to a more intensive phase of reworking prior to final deposition. The dominance of NE-dipping cross-bed foresets, together with LA surfaces dipping orthogonal to them (i.e., to the NW and SE) indicates that the main sediment dispersal system is NE-oriented.

Massive mudstone intervals make up the bulk of the total succession, indicating that deposition took place predominantly from suspension in a low-energy, central estuarine environment (Dalrymple et al. 1992). The intercalated, thin sandstone layers and lenses may represent storm washover deposits. The intensive bioturbation, the widespread pedogenic alteration and desiccation cracks might suggest that sedimentation took place during seasonal storm and/or flood events with longer-term drying-out periods. The pervasive rootlet mottling and abundant ped structures in many, but not all, of the mudstone intervals may be attributed to pedogenesis in floodplains within the incised-valley estuary. Hence, these mudstones can be referred to as paleosols (Retallak 1988). Slickensides and pseudoanticlines that result from differential shear forces within the soil are additional evidences for pedogenesis (Retallak 1990). Alternation of grey-, purple- and red paleosols reflect that soil drainage or the soil moisture regime also alternated from poorly-drained to moderately- and to well-drained conditions and vice versa (Kraus and Hasiotis 2006). Such paleosols usually form within or near the zone of water-table fluctuation and register the availability of moisture through time, which may suggest the seasonality of the paleoclimate (Kraus and Aslan 1993). Traditionally, the almost complete lack of marine body fossils and the widespread occurrence of rooted intervals would have meant that much of these facies association would have been interpreted as purely non-marine (e.g., fluvial floodplain or fluvio-lacustrine).

However the facies succession exhibites an overall upward increase in the degree of bioturbation. The thoroughly burrowed silty mudstones, containing abundant *Thalassinoides* and *Psilonichnus* (e.g., Fig. 5.2b & c) reflect brackish water conditions in the central basin (MacEachern & Pemberton 1994). This interpretation is further supported by the presence of syneresis cracks, which represent salinity-induced subaqueous shrinkage cracks formed by the contraction of clay minerals (Plumer & Gostin 1981).

Generally, the facies association shows an upward transition from tidal estuarine point bars and tidal sand bars composed of muddy sand with inclined heterolithic stratification to massive estuarine mud, suggesting deposition within the central low-energy part of an estuary.

**Facies association $FA_3$**

***Description*:** Facies association $FA_3$ is well-represented in Dedu, Yejube and Fincha areas, but is not present in other studied areas. It is characterized by a coarsening-upward succession composed of massive mudstones at the base, grading upward into lenticular-, wavy- and flaser bedded, fine-grained silty sandstones and ends up with planar-tabular cross-bedded fine- to medium-grained sandstone.

The massive mudstones are 1–2 m thick and dark red in colour. They are overlain by 0.3–0.5 m thick, lenticular bedded, fine-grained silty sandstone with mudstone interlaminae. The sandstone lenticles are commonly disconnected and exhibit soft-sediment deformation (Fig. 5.1f). The lenticular beds grade upward to well-sorted, wavy and flaser bedded fine-grained sandstones that range in thickness from 2.5 m to 4 m. Wave ripples are more or less symmetric and small with an average length/height ratio (ripple index) of about 5 or less. The flaser bedded sandstones possess up to 5 cm thick, continuous, pale grey mud flasers, although smaller, discontinuous and bifurcated flasers filling ripple troughs are also common (Fig. 5.1g). These beds are overlain by up to 2 m thick, planar-tabular cross-bedded, fine- to medium-grained sandstones. Mud drapes are very abundant on ripple and cross-bed foresets. Burrowing is moderate to sparse overall. Vertically accreted tidal rhythmites showing cyclic thick/thin pairings of individual bundles occur occasionally (Fig. 5.2e).

Palaeocurrent directions are variable. The orientation of symmetric ripple crests indicates a NE-SW oscillation direction. Current ripples and planar cross-bed foresets exhibit a bipolar, NE- and SW-oriented palaeoflow (arrows in Fig. 5.2f).

***Interpretation*:** The upward coarsening and thickening of beds and bed sets together with the change in bedding from lenticular and wavy through flaser, and finally to planar and trough cross-stratification reflects a change from a low energy, suspension-dominated to a high energy, bed-load-dominated depositional regime ( Allen 1970, Allen & Posamentier 1994). The vertical stacking of lenticular-, wavy- and flaser-bedded sandstones might correspond to the classic tripartite zones of tidal flats, namely supra-, inter- and subtidal flats (Klein 1971 Weimer et al. 1982). Wavy- and flaser-bedding are characteristic of tidal settings (Reineck & Wunderlich 1968, Clifton 1982). Mud drapes along foresets are additional diagnostic features of tidal environments (Visser 1980, Boersma & Terwindt 1981, Smith 1988). Planar and trough cross-bed sets represent migration of 2D and 3D dunes during periods of high-energy tidal currents (Dalrymple et al. 1992). The alternating sand/mud laminae that display cyclic thick/thin pairing of individual bundles represent tidal rhythmites (Archer & Feldman 1994, Tessier et al. 1995), probably reflecting semi-monthly (neap-spring.neap) tidal cycles (Kvale et al. 1995). Small-scale symmetric ripples with ripple index of < 5, which fall under the category of combined flow ripples (Reineck & Singh 1986), suggest moderate wave influence. The soft-sediment deformation observed in the sandstone lenticles are common features of estuarine bay head deltas (e.g., Garrison & van den Bergh 2006), and also of tidal bars (e.g., Clifton 1982, Mutti et al. 1985, Reineck & Singh 1986). Bimodal-bipolar palaeocurrent patterns indicate the presence of ebb and flood tidal currents. The dominance of the NE mode with a subordinate SW mode may suggest the dominance of ebb over flood tidal currents. The paucity of burrows, their sporadic distribution and the low ichnodiversity might reflect stressful conditions under strong fluctuations of salinity (Buatois et al. 1997), which likely suggests a brackish-water setting (i.e., an estuary or a lagoon) (Pemberton & Whitemann 1992, MacEachern & Pemberton 1994, Gingras et al. 1999).

Two possible depositional scenarios that can be drawn out from these sedimentological attributes would be either prograding tidal bars in a tide-dominated estuary (e.g., Mutti et al. 1985) or bay head deltas in a mixed tide- and wave-dominated estuary (e.g., Biggs 1967, Garrison & van den Bergh 2006). Most of the observed features are similar to the estuarine "tidal bar" facies of Mutti et al. 1985, which has been widely adapted in facies models of tidal systems (e.g., Dalrymple et al. 1992, Johnson & Baldwin 1996). Such successions could only be preserved if they are formed within coastal embayments, such as estuaries or lagoons (Davis & Clifton 1987). Deposition in coastal embayments might also have favoured the preservation of tidal rhythmites (Archer 1998).

**Facies association $FA_4$**

***Description*:** Facies association $FA_4$ ranges in thickness from 20–30 m and is well-represented in Yejube and Dedu areas. It is composed of a complex mixture of massive to crudely cross-bedded, very coarse-grained sandstone and fine-grained conglomerate (Fig. 5.2g & h).

The sandstone-conglomerate intervals vary in thickness between 2–5 m. They possess sharp bases with prominent, very irregular to concave-up erosional scours. Because of the coarseness of the sediments, bedding is rarely sharp, often indistinct in the lower part. Sorting is poor and grain-size slightly decreases upwards, and cross-bedding and set bounding surfaces become more distinct. Clasts commonly display either a sub-horizontal alignment or a slightly down-dip orientation parallel to foresets or (Fig. 5.2g). They are composed predominantly of quartz with subordinate mudstone intraclasts. Lenticular mudstone wedges sandwiched between cross-bed sets are common. The main types of bedding that characterise FA4 sandstone-conglomerate package is crude planar-tabular and trough cross-bedding with subordinate sub-horizontal to low-angle cross-bedding and occasional wavy lamination (Fig. 5.2h). Palaeocurrent measurements from cross-bed foresets show generally bimodal distribution, with dominant SW and NE modes. Burrowing is sparse to absent.

***Interpretation*:** The concave-up erosional scours at the base of the sandstone-conglomerate packages, with up to 5 m thalweg depth, indicate that deposition occurred in an environment in which active cutting of channels prevailed. The irregular and deeply incised erosional surfaces at the base of these deposits result from tidal scouring within the constricted estuary-mouth tidal channels and can be referred to as tidal ravinement surfaces (Allen 1991, Allen & Posamentier 1994). The coarse grain-size, the lack of burrows and mud drapes suggest deposition in a high-energy environment. The dominant SW- and NE-directed palaeocurrent modes indicate landward and seaward sediment transport by flood- and ebb-tidal currents respectively. The involvement of beachface depositional processes, although subordinate, is indicated by the crude, landward-dipping, low-angle gravel stratification and clast imbrication. Such structures, for instance, may apparently result from berm accretion (Maejima 1982, Forbes & Taylor 1987). The horizontal alignment of gravels and the occasional presence of wavy lamination may also point to some sort of swash and backwash movements or onshore/offshore motions in a beach foreshore environment (Hiroki & Terasaka 2005).

In summary, the facies association may represent high-energy, flood- and ebb-dominated estuary mouth (tidal inlet and tidal delta) deposits in the marine-dominated outer estuarine environment. Similar estuary mouth deposits have been described by Kraft et al. (1987), Zaitlin & Schultz (1990), Pattison (1992), Roy (1994) and Johnson & Levell (1995). Moreover, the succession is truncated at the top by a wave ravinement surface, and is overlain by proper shallow marine facies in which hummocky cross-stratification predominates. Such a stratigraphic position implies that the two facies units are genetically related, which also supports an estuary mouth interpretation.

Fig. 5.2. A. Heavily bioturbated central estuarine mudstones with intercalated estuarine point bars and storm washover layers, Dejen section. B. Close-up view of 'A' showing T-shaped (*Thalassinoides*) and Y-shaped (*Psilonichnus*) boxworks. C. Bedding plane view of *Thalassinoides* (*Th*), and D. Syneresis cracks (*sy*) in $FA_2$, Dejen section. E. Tidal rhythmites showing cyclic thick/thin pairings of individual bundles interpreted to indicate neap-spring.neap (n-s-n) tidal cycles, Yejube section. F. Bidirectional planar-tabular cross-bedding in $FA_4$, Dejen section. G. Fine-grained conglomerates with nearly sub-horizontal clast imbrication ($FA_4$), Yejube section. H. Low-angle to wavy laminated pebbly coarse-grained sandstones ($FA_4$), Yejube section.

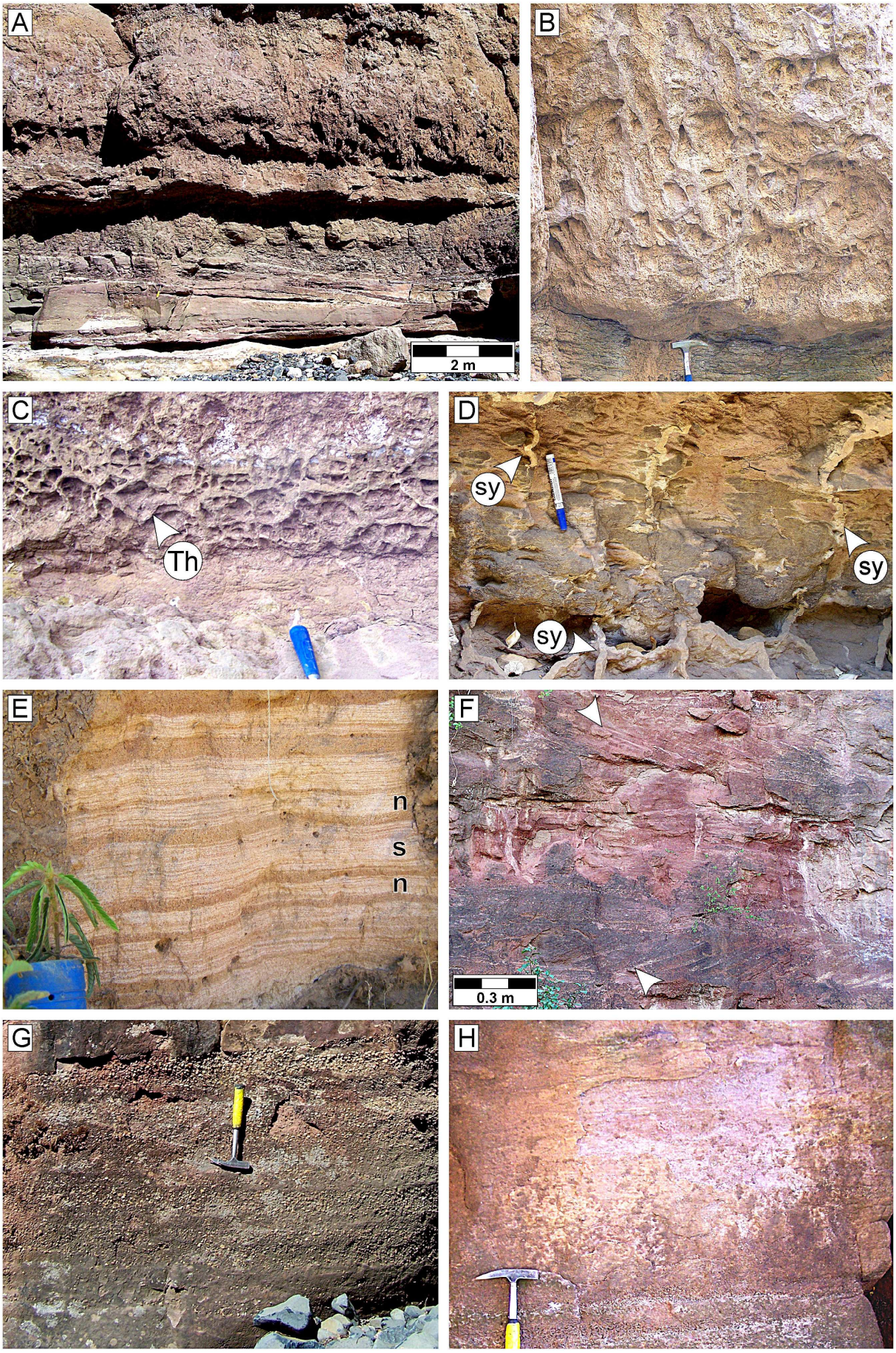
A
2 m
B
C
Th
D
sy
sy
sy
E
n
s
n
F
0.3 m
G
H

### 5.1.2. The Barrier - Lagoon System

The barrier - lagoon system is well-represented only in Dejen, Yejube and Dedu areas and laterally intertongues with the fluvio-estuarine system in the landward direction between Fincha and Dedu areas. It is composed of two facies associations, i.e., $FA_5$ and $FA_6$.

**Facies association $FA_5$**

***Description*:** Facies association $FA_5$ consists of three facies, $FA_{5a}$ to $FA_{5c}$. The first facies ($FA_{5a}$) is composed of dominantly medium to coarse-grained, oppositely dipping planar and trough cross-bedded sandstones (Fig. 5.3a & b). Beds are 0.5–2 m thick and form wedge-shaped sand bodies that are bounded by subhorizontal to low-angle dipping erosion surfaces (e.g., arrows in Fig. 5.3c.). The base of these amalgamated sandstone bodies is characterized by a major concave-up erosional scour surface often marked by pebble lag. Occasionally, these erosional scours are filled with up to a meter thick, planar- to ripple-laminated heterolithic facies (lower part in Fig. 5.3d), which contain escape structures (fugichnia) (Fig. 5.3f). The overall thickness ranges from 4–6 m and grain size fines upwards from coarse- to medium-grained sand. Palaeocurrent directions are bi- to polymodal. Apart from escape traces observed in the heterolithic deposits, scattered *Ophiomorpha* burrows occur throughout.

The second facies ($FA_{5b}$) is characterised by low-angle planar-tabular cross-bedded, pebbly coarse-grained sandstones. The most characteristic feature of these sandstones is low-angle dipping planar-stratification with discordant sets of laminae (Fig. 5.3e). Thickness may reach up to 5 m. These facies is usually overlain by well-sorted and well-rounded (Plate II, Fig. C), mainly planar-tabular cross-bedded, medium- to coarse-grained sandstones of the third facies ($FA_{5c}$) (Fig. 5.3g). Small-scale trough cross-beds are also present. Set thickness is highly variable, often varying between 0.1–0.3 m, but may reach up to 2 m. Total thickness ranges from 3 to 5 m. Burrows are rare to absent.

***Interpretation*:** Deeply scoured surfaces with pebble lags overlain by oppositely dipping cross-bed sets of the first facies ($FA_{5a}$) are interpreted as tidal inlet channels (De Raaf & Boersma 1971, Nio & Yang 1991). Subhorizontal to low-angle dipping secondary erosion surfaces (arrowed in Fig. 5.3c) are interpreted as accretionary flanks of in-channel bars (Yang & Nio 1989). The thickness of the inlet lithosome (in this case 6 m) approximates the scour depth of the inlet channel (Reinson 1984). The fine-grained heterolithic facies at the base of some channel scours are interpreted to represent restricted abandoned channel-fills (Carter 1978). The presence of fugichnia in these facies records the burial of organisms or their entrainment during high energy flow conditions related to the migration of subaqueous dunes (MacEachern & Pemberton 1994). The presence of *Ophiomorpha* indicates that only deeply penetrating burrows are ideally suited to such a dynamic environment (MacEachern & Pemberton 1994, MacEachern et al. 2005). The lack of mud drapes, which normally are common features of tidal bedding, indicate a more or less constantly active water column.

The low-angle planar cross-beds of the second facies ($FA_{5b}$) represent beach-stratification that are formed by the swash-backwash mechanism in the swash zone. They are interpreted to represent spit beach and/or welded ridge deposits of the spit platform (Reinson 1984). The slight discordances between sets of laminae reflect adjustment of the beach to changes in wave regime or sediment supply (Clifton 1969). Some spit beach deposits preserve sedimentary structures related to fairweather beach aggradation and erosional truncation during storms. The overlying well-sorted, dominantly planar-tabular cross-bedded sandstones of the third facies ($FA_{5c}$) are interpreted to represent backshore eolian dunes. In summary, the

facies association $FA_5$ is interpreted to represent the lateral migration of tidal inlet-spit sequence.

**Facies association $FA_6$**

Facies association $FA_6$ is characterised by the regular interbedding of fine- to coarse-grained sandstones and reddish brown mudstones. It is similar in facies composition to the 'central basin' facies association $FA_2$, which is well-described in the fluvio-estuarine system in Sec. 5.1.1. The only basic difference is that it lacks beds characterised by inclined heterolithic stratification. $FA_6$ is dominated by massive heavily bioturbated mudstones with abundant intercalations of washover sheet sandstones. This facies association is interpreted to have deposited in backbarrier lagoonal setting.

### 5.1.3. The Strandplain System

The strandplain system is well-represented in Dejen, Yejube and Dedu areas and comprises three facies associations, i.e., $FA_7$ to $FA_9$ which are vertically stacked to form an upward-coarsening and shallowing progradation sets.

**Facies association $FA_7$:**

***Description*:** Facies association $FA_7$ consists of interbedded fine-grained sandstones and massive to laminated mudstones. Individual sandstone and mudstone beds range in thickness from 0.1–0.6 m. The main sedimentary structures in the sandstone intervals are hummocky cross-stratification, planar- and wave ripple-lamination with rare small-scale planar-tabular cross-bedding. Burrowing is moderate in the sandstone intervals and very intense in the mudstone intervals. *Chondrites* and *Phycosiphon* dominate the background ichnofabric, but are overprinted by a relatively large *Rosselia* (Fig. 5.4b). Escape structures (fugichnia) and equilibrium-adjustment structures are common (Fig. 5.4c).

***Interpretation*:** The alternation of hummocky cross-stratified, parallel- and wave ripple-laminated sandstones and bioturbated mudstones records the regular interplay of episodic storm deposition and quiet-water sediment fallout (Buatois & Mangano 2003; Buatois et al. 2005, MacEachern et al. 2005). The presence of hummocky cross-stratification clearly points to a storm origin for the sandstone beds (Arnott & Southard 1990, Dumas & Arnott 2006). The dominance of middle-to-deep-tier deposit-feeders, like *Chondrites* and *Phycosiphon* in the mudstone intervals reveals post-storm, fairweather deposition (Bromley & Ekdale 1984, Seilacher & Aigner 1991, Pemberton & MacEachern 1997, MacEachern 2005). Escape traces (fugichnia) and equilibrium-readjustment indicate the ability of trace-maker(s), particularly *Rosselia*, to repeatedly shift their structures to the new sediment-water interface to keep pace with episodic storm deposition (MacEachern et al. 2005). Relying on all these sedimentologic and ichnologic attributes, this facies association is interpreted to reflect deposition in the offshore transition zone.

Fig. 5.3. A & B. Bidirectional trough and planar-tabular cross-bedded sandstones of the tidal inlet channel-fill ($FA_{5a}$), Amuru section. C. Accretionary flanks (arrows) of in-channel bars within tidal inlet fill, Dejen section. D. Silt- and mudstones filling restricted abandoned inlet channel scours, Dejen section. E. Spit beach sandstones showing low-angle cross-stratification with discordant sets of laminae, Amuru section. F. Escape traces (fugichnia) in abandoned inlet fill, Dejen section. G. High-angle planar-tabualr cross-bedding in coastal eolian dune sandstones, Dejen section.

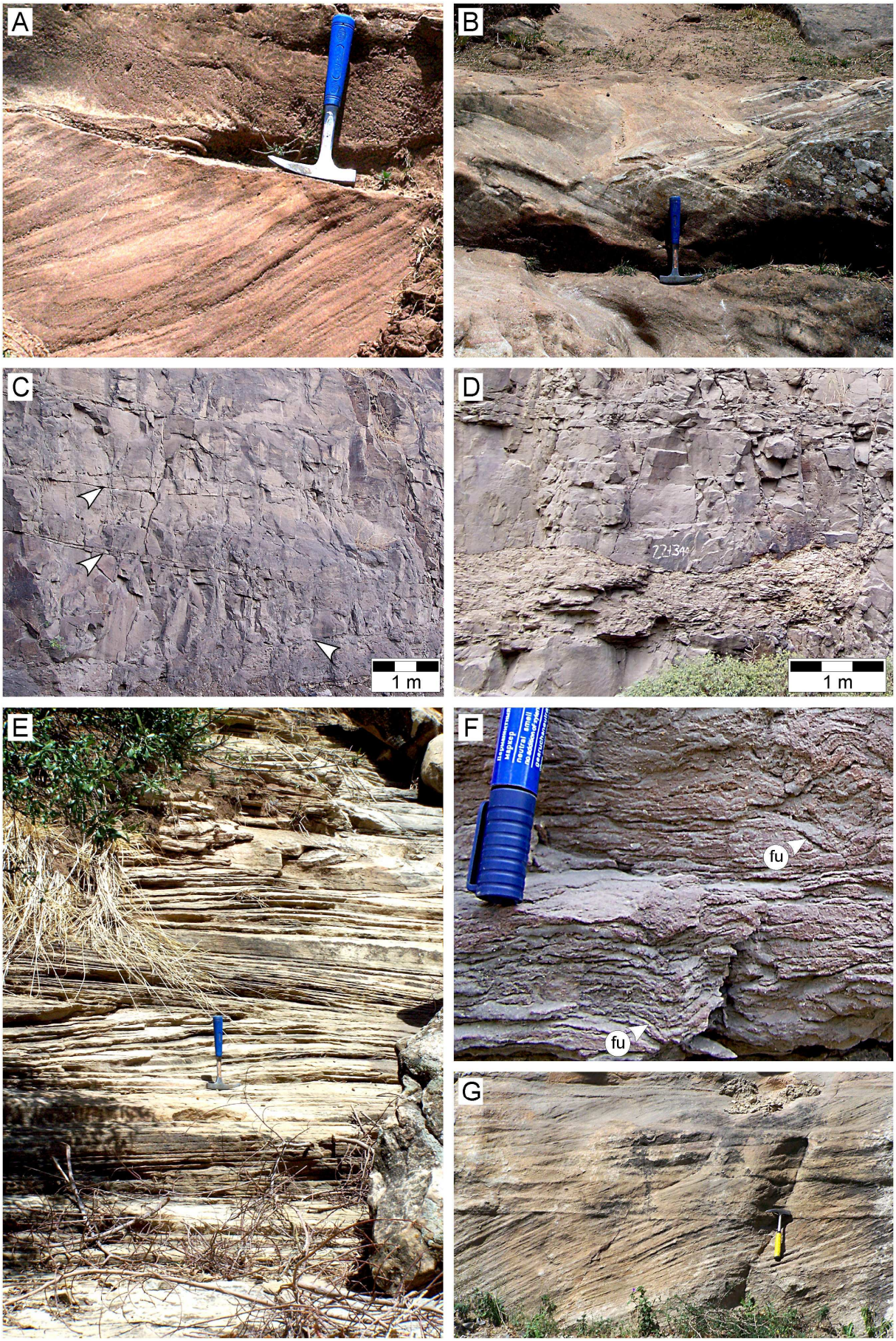
A
B
C
1 m
D
1 m
E
F
fu
fu
G

**Facies association $FA_8$**

***Description*:** Facies association $FA_8$ is mainly composed of hummocky and swaley cross-stratified, fine- to medium-grained sandstones (Fig. 5.4d). Small-scale planar-tabular cross-bedding occur locally. Individual sandstone beds are generally 2–5 m thick, but may locally reach up to 8 m. They are commonly erosionaly amalgamated and form laterally persistent tabular sandstone bodies that can be traced for several kilometers. Internal erosion surfaces separating hummocky cross-stratified bedsets are usually overlain by discrete, 15–50 cm thick, bioturbated mudstones. Scattered quartz pebbles are abundant, although they also locally concentrate along truncation surfaces and may form layers and lenses up to 50 cm thick. Hummock and swale amplitudes range from 15–50 cm, while wavelength ranges from 3–5 m.

The intensity of burrowing in this facies is highly variable. In some intervals, it is so intense that bedding is indistinct (e.g., Fig. 5.4e), whereas in others, bioturbation is low to moderate so that the stratification is clearly visible. The thin mudstone layers and lenses in-between HCS beds are however thoroughly burrowed. The ichnological suite includes *Thalassinoides*, *Chondrites*, *Phycosiphon*, *Rosselia* and *Paleophycus* besides other indeterminate ichnospecies.

***Interpretation*:** Hummocky cross-stratification is produced by episodic storm wave activity and wave-generated surges above but near storm wave base (Dott & Bourgeois, 1982; Hunter & Clifton, 1982; Walker & Plint, 1992; Dumas & Arnott, 2006). The thick, amalgamated, hummocky cross-stratified beds in $FA_8$ represent proximal storm beds. They record high-energy, long-period oscillatory-dominant combined flows during storms, where aggradation rates are high enough to preserve hummocks but unidirectional current speeds are sufficiently low (Dott & Bourgeois 1982, Cheel & Leckie 1993, Dumas et al. 2005). Swaley cross-stratified beds are presumed to be formed in a similar manner but above HCS beds (Dumas & Arnott 2006). They may represent the highest energy equivalents in a continuum from the underlying HCS beds (Leckie & Walker 1982). The occasional presence of planar-tabular cross-bedding may indicate the local rise in unidirectional flow component (above 10 m/s, *sensu* Dumas et al. 2005), which destabilizes the development of hummocks. The scattered fine pebbles in the HCS and SCS beds are interpreted as remnants of post-storm lags. The thin, bioturbated mudstone layers and lenses may represent fairweather suspension fall-out deposits between storm events. The presence of suspension-feeding structures, such as *Rosselia*, may suggest the local accumulation of organic detritus that was kept in suspension by high energy combined flows (Nara 1995). *Thalassinoides*, *Chondrites*, *Phycosiphon* and *Paleophycus* are usually restricted to the thin, mudstone intervals and represent the resident, post-storm fairweather assemblage. This facies is interpreted to represent deposition in a storm-dominated lower to middle shoreface environment.

**Facies association $FA_9$**

***Description*:** The facies association $FA_9$ is characterised by coarse-grained, planar-tabular and trough cross-bedded sandstones with sharp or slightly erosive bases (Fig. 5.4f). Trough cross-bedding with asymptotic, sigmoidal bottomsets are common. Low-angle cross-bedding occurs occasionally. Cross-bed sets are 20–30 cm thick. Cosets are 0.6–1 m thick and are bounded by sharp, horizontal erosive surfaces. Amalgamated cosets form up to 4 m thick, laterally extensive tabular sandstone bodies. However, they are frequently incised by up to 6 m deep tidal inlet channels. Palaeocurrent directions are extremely variable. In Dejen they show bimodal orientation (W and SE) with slight dominance of the SE mode. In Amuru and

Bekotabo areas NW mode is predominant, while in Yejube and Dedu areas the NE mode is more significant. Trace fossils are rare to absent, except very few, simple vertical burrows, belonging to *Skolithos*, *Cylindrichnus* and *Ophiomorpha*. This facies association is well-represented in most of the studied areas.

***Interpretation*:** The presence of predominantly coarse-grained sandstones and the lack of mud drapes and burrows in second facies suggest deposition in high-energy, current-dominated environment, where there was less time for the settling of suspended clay. Multidirectional trough and planar cross-beds indicate the complex hydraulic environment of the breaker and surf zone, with shore-normal currents generated by plunging waves superimposed on shore-parallel wave-driven currents (Clifton et al. 1971, Carter 1978). NE-SW oriented bidirectional cross-beds are interpreted to represent the migration of 2D and 3D dunes formed by the onshore/offshore wave motion, whereas the NW-SE oriented bidirectional cross-beds may be attributed to deposition by strong longshore current. The presence of vertical burrows, most commonly dwelling structures (e.g., *Skolithos* and *Ophiomorpha*) represent the opportunistic colonisation by suspension-feeding infauna, which are often associated with high-energy environments (Frey et al. 1990). This facies is interpreted to represent upper shoreface deposits.

## 5.2. Stratigraphic stacking patterns

In the Blue Nile Basin detailed vertical sedimentologic sections were taken in the following six localities, namely Dejen, Yejube, Dedu, Fincha, Amuru and Bekotabo areas (Fig. 2.2 for locations). These sections are used to study the vertical and lateral stacking patterns of depositional systems and for the identification of key stratigraphic surfaces, which provide the basis for a basin wide correlation. The measured sections are described and interpreted below.

### 5.2.1. Dejen area

***Description***: In Dejen area the studied section (N 10°04′54″/E 38°11′26″) is located 25 km south of the town Dejen near the Abay River bridge. In this area, the Adigrat Sandstone succession ranges in thickness from 60 m to 195 m. It unconformably overlies the 'Karoo-equivalent' Pre-Adigrat III succession and is unconformably overlain by the evaporite deposits (the Gohatsion Formation of Assefa (1991)).

The measured section in Dejen area reaches up to 195 m in thickness and consists of two stratigraphic units, namely the lower red unit (*Unit I*) and the upper white unit (*Unit II*) (Fig. 5.5). The main lithologic difference between the two is that the red unit contains significant amount of silty and muddy facies whereas the white unit is strongly dominated by coarse sandy facies with very minor amounts of fine-grained facies. Furthermore, the red unit was pervasively affected by oxidation whilst the overlying white unit was not. These units are bounded by subaerial exposure surfaces of nondeposition and pedogenesis that are marked by paleosols (Plate II, Fig. G & H).

Fig. 5.4. A. General view of prograding shoreface deposits (left) with the measured and interpreted section (right). The arrow shows hummocky cross-stratification, Dejen section. B. Heavily bioturbated offshore transition zone deposits ($FA_7$), Yejube section. C. Line-drawing of 'B' that shows large *Rosselia* (*Ro*), escape traces (fu) and equilibrum-adjustment structures (ea). D. Hummocky cross-stratified lower shoreface deposits ($FA_8$), Dejen section. E. Bioturbated lower shoreface sandstones with cross-sectional view of *Thalassinoides* (*Th*), Dejen section. E. Trough to planar-tabular cross-bedded upper shoreface sandstones ($FA_9$), Dejen section. F. Horezontal laminated foreshore sandstones ($FA_9$), Fincha section.

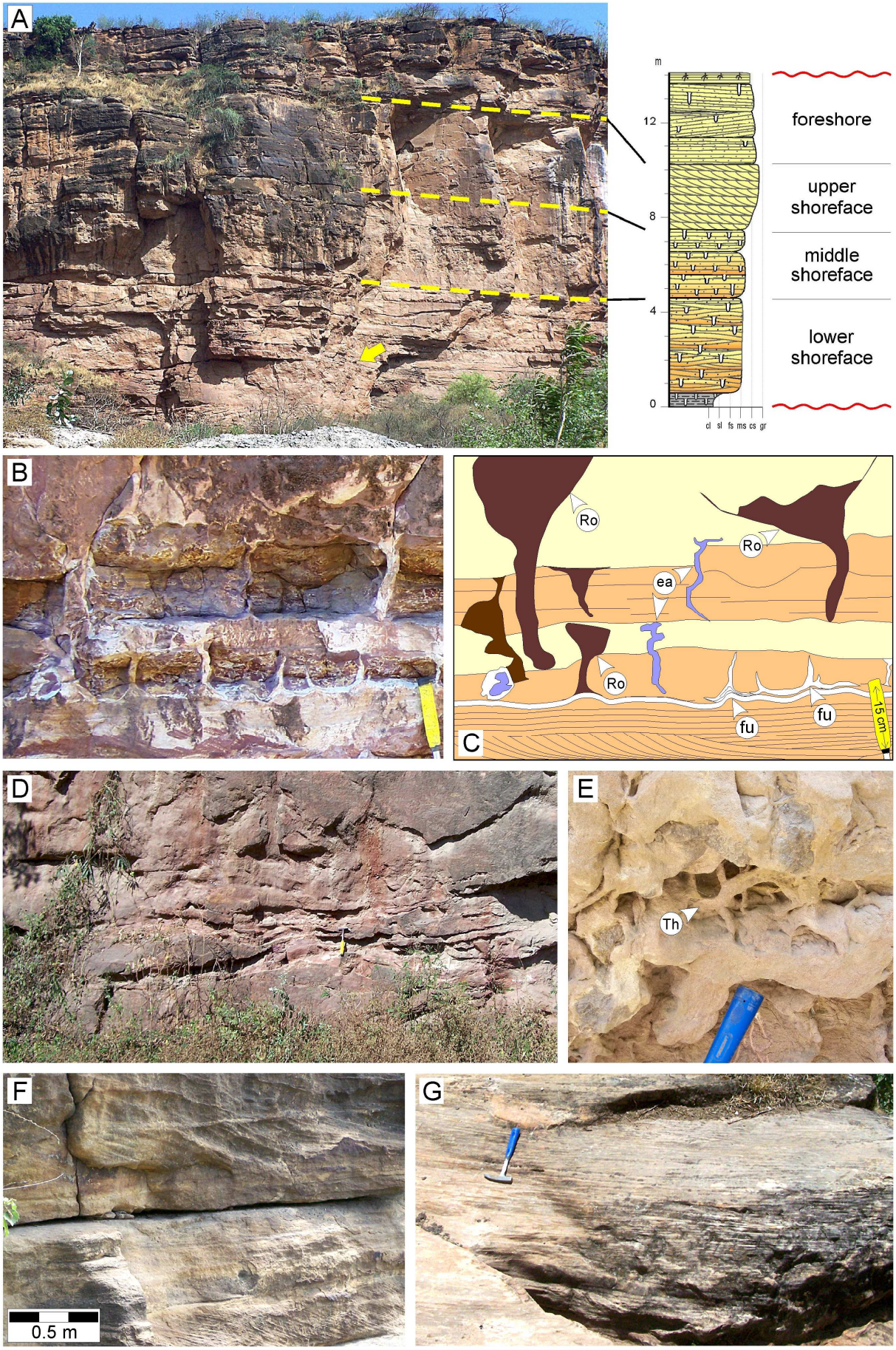
A
m
12
8
4
0
cl sl fs ms cs gr
foreshore
upper shoreface
middle shoreface
lower shoreface
B
C
Ro
Ro
ea
Ro
fu
fu
15 cm
D
E
Th
F
0.5 m
G

The red unit (*Unit I*) is 155 m thick at the location of the measured section, but laterally diminishes to less than 60 m west- and southward within a short distance. The basal unconformity is marked by a thick and strongly developed paleosol profile with well-developed calcic ($E_k$) horizon and a thick red to purple clayey subsurface ($B_t$) horizon (see Fig. 5.9d, Plate II, Fig. H). The unit is composed of fluvio-estuarine deposits at its lower part, barrier-lagoon deposits in the middle part and a nearshore marine (shoreface) deposits in the upper part.

The fluvio-estuarine deposits that characterise the basal part of the red unit are up to 60 m thick and consist, from bottom to top, of tidal flat and marsh deposits that grade upwards to upper estuarine channel-fill sandstones (Plate II, Fig. D) and pedogenically altered overbank deposits, bay-head delta sandstones, massive estuarine mudstones with subordinate estuarine point bars and elongate tidal bars. These are overlain by a 40 m thick barrier-lagoon complex consisting of heavily bioturbated lagoonal mudstones with intercalated washover, marsh, flood tidal delta/tidal inlet and backshore dune deposits. The barrier-lagoon deposits are top truncated by a wave ravinement surface and overlain by 60 m thick nearshore marine (shoreface) deposits, which consist of two upward-coarsening progradational sets.

The white unit is about 40 m thick and is separated from the underling red unit by a thin paleosol horizon that can be traced everywhere in the Dejen area (Fig. 5.9e & f). The thickness is fairly constant with little lateral variation as compared to the underlying red unit. It is composed of a lower barrier-inlet complex and an upper nearshore marine (shoreface) succession. As mentioned above, course to very coarse sandy facies is predominant with minor fine-grained sandstones and bioturbated muddy siltstones that are restricted to the offshore transition zone and filling local abandoned tidal inlet channels. The white sandstones contain scattered glauconite grains.

***Interpretation***: The paleosol horizons at the base of the two stratigraphic units represent periods of nondeposition and/or erosion created generally during sea level fall by subaerial processes. Hence, they are interpreted to indicate subaerial unconformities (sensu Sloss et al. 1949). Since they are unconformity-bounded, the two stratigraphic units can be interpreted to represent depositional sequences (*sensu* Mitchum 1977). The high degree of paleosol maturity is presumed to be characteristic of those paleosols formed at major geological unconformities (Retallack 1984). According to Kraus (1999), such strongly matured paleosols reflect prolonged periods of landscape stability.

The lateral thickness variation of the red unit within short distances may suggest the sedimentary infilling of antecedent topographic depressions that were cut by the ancestral drainage system during sea level fall. The fluvio-estuarine deposits that characterise the lowermost part of the red unit are generally tidally influenced; therefore, they are interpreted as transgressive estuarine deposits formed as the rate of sea level rise outpaces the rate of sedimentation (cf. Allen & Posamentier 1993). The stratigraphically lowest facies association contains tidal sedimentary structures (e.g., wavy, lenticular and flaser bedding) and brackish water trace fossils, providing the evidence for the onset of a marine transgression. Basal coarse fluvial channel fills that may represent sea level lowstand have not been observed. Their absence may be attributed to removal by transgressive erosion and/or tidal reworking following the onset of sea level rise (Reinson 1984, Catuneanu 2006). The heavily bioturbated mudstones of the low-energy central estuary with low diversity trace fossil suite and syneresis cracks provide evidence for a brackish water estuarine setting (Plumer & Gostin 1981, MacEachern et al. 2005). The upward facies transition from tidally influenced upper estuarine channels to backstepping bay head deltas and then to massive central estuarine mudstones is interpreted to indicate a change from a tide-dominated to a wave-dominated estuarine setting (Dalrymple et al. 1992). This change may be attributed to a transition in the type of coastal setting from a river-mouth-dominated to an open shoreline setting (Davis & Clifton 1987).

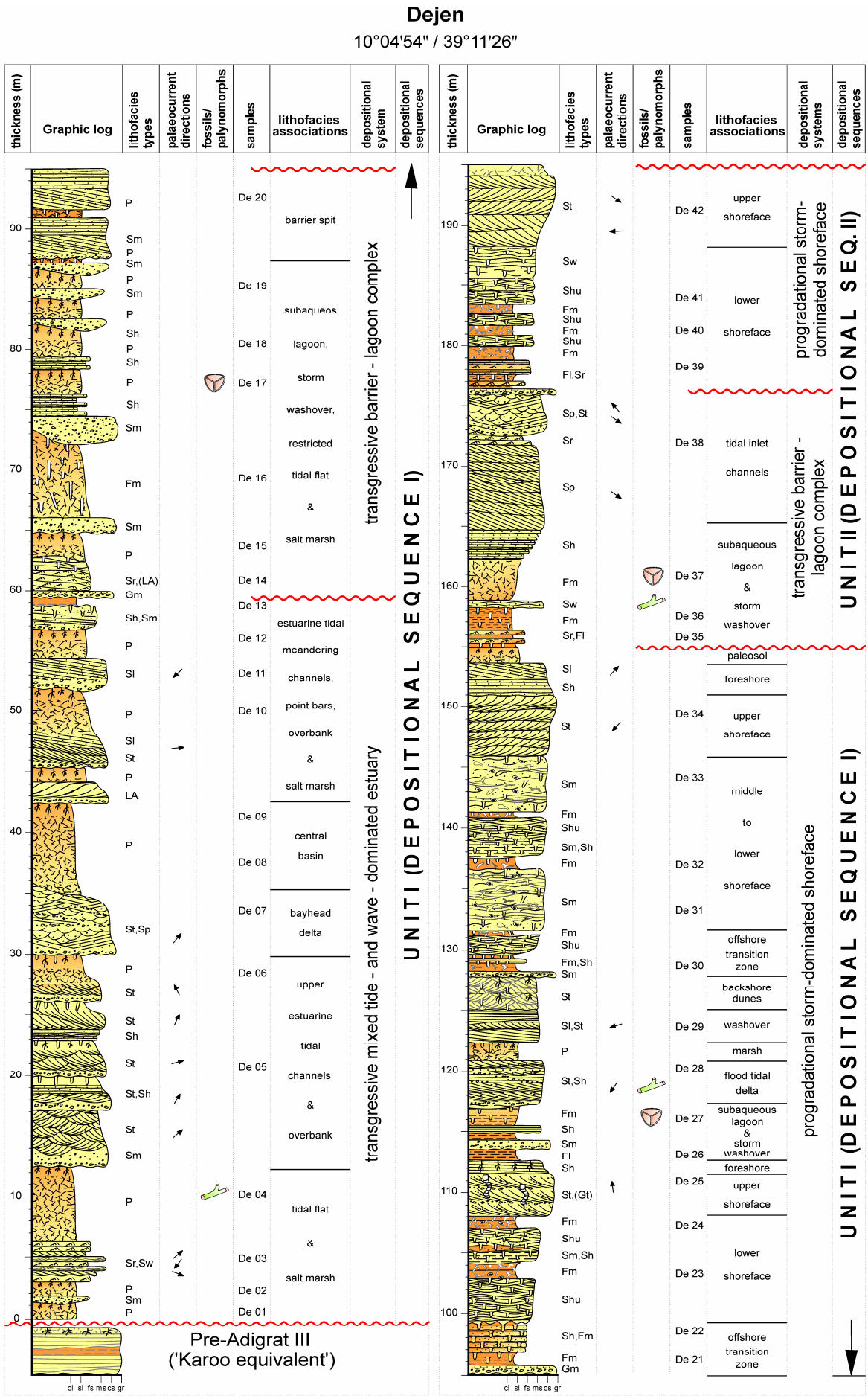


Fig. 5.5. Dejen section.

The barrier-lagoon and inlet-spit successions that characterise the middle part of the red unit are interpreted to represent transgressive deposits formed during the retrogradational (landward) shift of depositional systems as the rate of sea level rise continued to exceed the sedimentation rate. The preservation of the barrier-lagoon complex suggests that the rise in relative sea level must have been rapid (Swift 1975, Davis & Clifton 1987). Slow rise in sea level would have resulted in the destruction of the barrier system by transgressive erosion, similar to that predicted by the 'erosional shoreface retreat' model of Nummedal & Swift (1987). Deposits of the barrier complex are top truncated by an erosion surface, which is interpreted as a wave-ravinement surface (*sensu* Swift 1975). The overlying coarsening- and shallowing-upward nearshore marine deposits are interpreted to indicate shoreface progradation (regression) in a strandplain setting. They record the end of the transgression and the onset of progradation as the rate of sediment supply starts to outpace the rate of sea level rise (Posamentier et al. 1988, Galloway 1989). The predominance of amalgamated hummocky cross-stratified sandstones in the prograding nearshore marine deposits suggests deposition in a storm-dominated shoreface setting (Cheel & Leckie 1993, Dumas & Arnott 2006).

The barrier-inlet and the upward-shallowing shoreface deposits of the white unit are also interpreted to record transgressive and regressive phases. The absence of estuarine deposits in the lower part of the unit may suggest significant shoreface erosion during transgression. This mechanism of erosional shoreface retreat is usually favoured by slow rate of sea level rise (Nummedal & Swift 1987).

In summary, both units have been developed on a high-energy, nonbarred, coarse sandy open coast, in which storm effects predominate and sand supply is abundant. The preservation of significant amount of fine-grained facies in the red unit is attributed to the rapid rate of transgression. The pervasive red staining of the red unit suggests uplift and oxidation prior to the deposition of the overlying white unit.

### 5.2.2. Yejube area

***Description***: The location of the studied section (N 10°08′59″/ E 37°40′32″) in the Yejube area is along a small tributary of the Chemoga River, 10 km west of the town Yejube. The Adigrat Sandstone succession unconformably overlies the 'Karoo-equivalent' Pre-Adigrat III succession and unconformably overlain by Tertiary flood basalts. The thickness ranges from 130 m to 165 m. The measured section is quite similar to that of Dejen, which lies 56 km east of it, as it also contains two stratigraphic units that are separated by a paleosol horizon.

The subaerial unconformity at the base of the red unit is underlain by a 4 m thick paleosol that shows strong macro- and micromorphological similarities with that observed in the basal Dejen section. The unit starts with a 25 m thick upward-coarsening facies succession containing tidal flat, marsh and estuarine channel deposits that grade upwards into estuarine bay-head delta (Fig. 5.6). Tidal influence becomes more evident in these deposits and tidal rhythmites are occasionally preserved. The deposits are overlain by heterolithic deposits of the low-energy central estuary, which are in turn irregularly and deeply scoured by erosion surfaces and overlain by estuary mouth sandstones. The barrier-inlet complex is up to 50 m thick and is characterised by subaqueous lagoon, washover and fringing marsh deposits that grade upwards into interbedded flood tidal delta and tidal inlet channel-fill sandstones. These are erosionaly truncated by a flat to wavy ravinement surface and overlain by 36 m thick nearshore marine deposits, which are in turn exposed and covered by a thin paleosol horizon.

In contrast to the red unit, the white unit is only represented by the barrier-inlet complexes. The fluvio-estuarine and nearshore marine deposits, which are observed in the white unit in the Dejen section, are absent in the Yejube area. The barrier-inlet complexes are

about 25 m in thickness and are characterised by lagoonal and/or generally backbarrier facies that are incised by tidal inlet channels.

***Interpretation***: The strong similarity of paleosol horizons that bound the two units of the Yejube section with that of the Dejen section indicates that they might have been formed at the same time under similar conditions. The vertical juxtaposition of the barrier-inlet complex over the fluvio-estuarine deposits of the red unit records transgression. The erosion surfaces at the base of the tidal inlet deposits are interpreted to have been cut by tidal processes during transgression (tidal ravinement surfaces, *sensu* Swift 1968). The flat to wavy erosion surfaces that truncate the underlying barrier-inlet complexes are commonly associated with the overlying storm-dominated deposits, suggesting that erosion at these surfaces is the result of storm wave processes (wave ravinement surfaces, *sensu* Swift 1968). The occurrence of wave ravinement surface above tidal inlet sandstones records continued deepening during transgression. The prograding nearshore marine deposits with coarsening-shallowing-upward trends are interpreted to record regression. The absence of estuarine deposits at the base the white unit may be attributed to the absence of lowstand valley incision associated with the reduced sediment supply by rivers. The absence of nearshore marine deposits at the top of the white unit may be due to either the rate of sea level fall highly exceeding the rate of tectonic subsidence or the rate of sea level rise being significantly less than the rate of tectonic uplift. This scenario is well-described by Plint (1988) and Posamentier et al. (1992) as 'forced regression', which is supposed to occur independent of the variations in sediment supply.

### 5.2.3. Dedu area

***Description***: The studied section in Dedu area is taken along a steep footway (N 09°40′55″/E 37°33′57″) down the western cliff of the Guder River canyon, 3 km east of the town Dedu. The Adigrat Sandstone succession unconformably overlies the 'Karoo-equivalent' Pre-Adigrat III succession and is overlain by Tertiary flood basalts. The measured section reaches up to 100 m in thickness. The red unit (*Unit I*) is about 75 m thick, which is almost half of the recorded thickness in Yejube and Dejen, whereas the thickness of the white unit (*Unit II*) is fairly unchanged (Fig. 5.7). The succession starts with 25 m thick fluvio-estuarine deposits containing tidal flat, marsh, tidal bar and isolated shallow tidal creek channel facies. These are overlain by 30 m thick barrier-lagoon deposits that consist of tidal inlet and flood tidal delta facies associations, which in turn are truncated and overlain by nearshore marine deposits. Palaeocurrent directions are bimodal and oriented towards the NE and SW directions.

The white unit consists of 5 m thick heterolithic deposits that are cut by a flat to slightly wavy ravinement surface and are overlain by up to 20 m thick inlet-spit succession, the top of which exhibits features of subaerial exposure. Palaeocurrent directions are bi- to polymodal but SE mode is predominant.

***Interpretation***: The reduction in the thickness of the red unit from Yejube to Dedu may suggest up-dip thinning of the unit towards the southwest. Although the unit is characterised by similar facies associations and depositional systems in both study areas, thickness reduction due to uplift and erosion is, at least in part, also very likely. The succession is interpreted, like that of the Yejube section, to record two transgressive-regressive episodes. Palaeocurrent patterns in the two units indicate a southwesterly transgression for the red unit and a northwesterly transgression for the white unit. This change in palaeocurrent patterns has significant implication to the evolution of the basin and discussed in detail in Sec. 8.

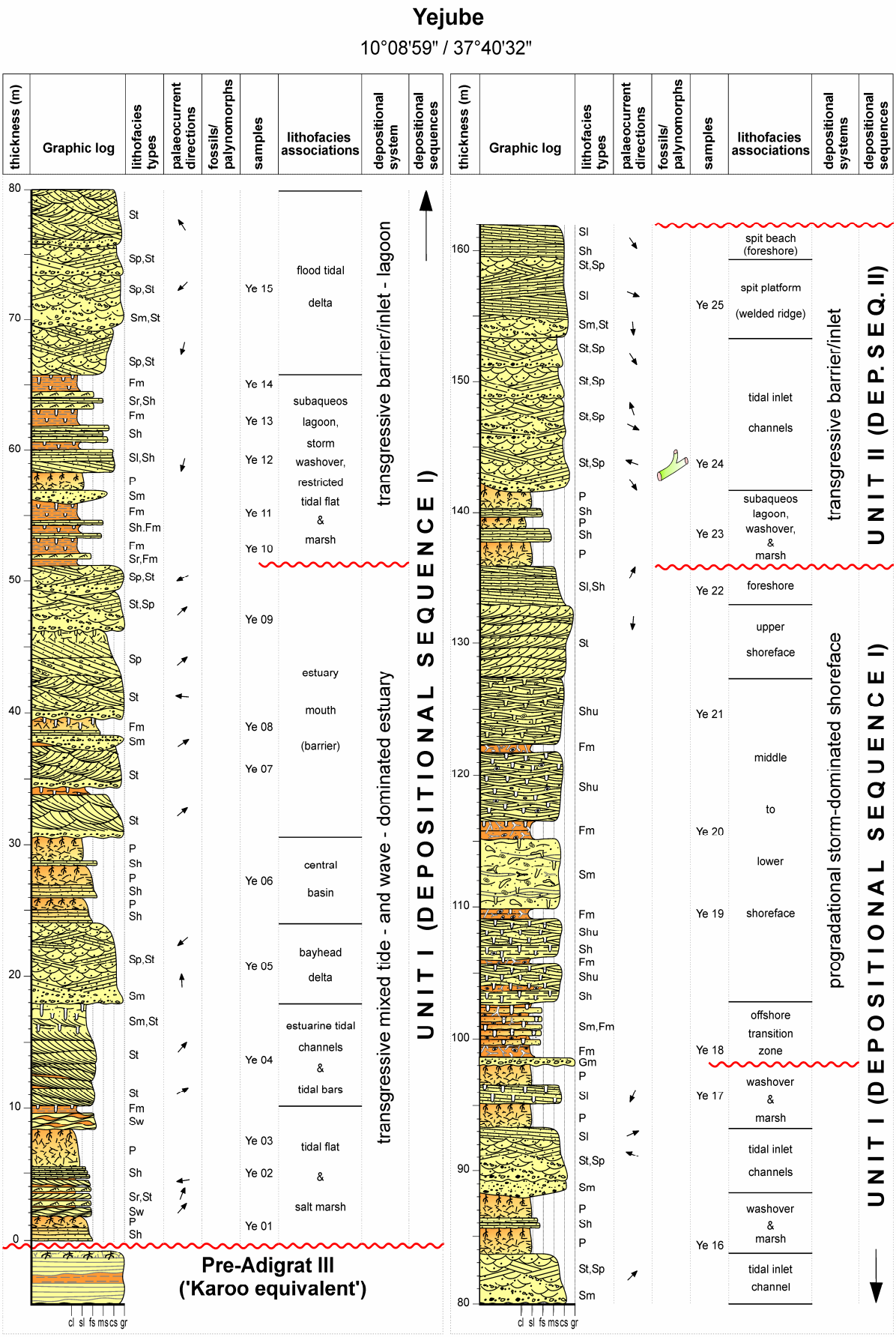


Fig. 5.6. Yejube section.

### 5.2.4. Fincha area

***Description***: In Fincha area, the location of the studied section (N 09°42′22″/E 37°20′05″) is 16 km north of the town Fincha. Alike in Dedu and Yejube areas, the sedimentary succession in the Fincha area is sandwiched between the 'Karoo-equivalent' Pre-Adigrat III succession and the Tertiary flood basalts. The thickness of the measured section reaches up to 80 m. The red unit (*Unit I*) is 55 m thick and is composed of amalgamated braided fluvial channel sandstones that grade upwards to isolated braided and meandering channel fills with associated crevasse splays and overbank deposits (Fig. 5.7). Palaeocurrent directions are unimodal and oriented to the northeast. The white unit is 25 m thick and possesses a similar facies composition like that in the Dedu area. It is composed of bi- to polymodal cross-bedded tidal inlet channel fills grading upwards into planar- to low-angle stratified spit platform and spit beach deposits.

***Interpretation***: The unimodal cross-bed distribution and the absence of any evidence of tidal current processes suggest that the red unit is deposited in a purely fluvial environment or in the fluvial-dominated uppermost part of an estuary. The predominance of NE-oriented palaeocurrents points to the main direction of the sediment dispersal system. The coarse-grained and unsorted nature of the channel-fill sandstones may suggest the source area lay not far to the southwest and/or south. Up-dip thinning of the unit towards the southwest is indicated by a further reduction in thickness from the Dedu to the Fincha area. The transition from the fluvial uppermost part of the estuary to the mixed-energy middle part lies most probably between these two areas. The similarity in thickness and facies composition of the white unit in Fincha and Dedu areas may indicate that the rate of transgression might have been similar in these two areas.

### 5.2.5. Amuru and Bekotabo areas

***Description***: The studied section in the Amuru area is located 10 km north of the town Amuru (N 10°02′53″/E 37°01′28″). The sedimentary succession ranges in thickness from 50 m to 70 m. It unconformably overlies the 'Karoo-equivalent' Pre-Adigrat III succession and is unconformably overlain by recent soil and alluvium deposits. The measured section in Amuru is 55 m thick and consists of only the upper white unit (*Unit II*) whilst the lower red unit (*Unit I*) is absent (Fig. 5.8). The succession is composed of three vertically stacked tidal inlet-spit systems. Palaeocurrent directions are bi- to polymodal with slight predominance of northwest mode. The tidal inlet channel fills are mainly made up of medium- to large-scale trough and planar-tabular cross-bedded sandstones. Herringbone-type cross-bedding is common as well as large-scale flute casts with their tapered ends pointing in opposite directions (Fig. 5.9a-c). The spit platform and the spit beach deposits that characterise the upper parts of the inlet-spit systems are composed of well-sorted and well-rounded low-angle to planar-laminated sandstones.

In the Bekotabo area, the studied section (N 10°23′18″/E 37°00′52″) is located 2 km northeast of the village Bekotabo. The sedimentary succession, which also contains only the white unit (*Unit II*), reaches up to 70 m in thickness (Fig. 5.8). It unconformably overlies the 'Pre-Adigrat II' sediments and is unconformably overlain by Tertiary flood basalts. The vertical facies succession is basically similar to that of the Amuru section but it differs in the fact that wavy lamination is common in the spit beach deposits.

***Interpretation***: The absence of the red unit in these two areas suggests that the unit pinches out laterally in a short distance northwest of the Fincha area. Its absence may be due to uplift and erosion prior to the deposition of the white unit or the area is not affected by the first

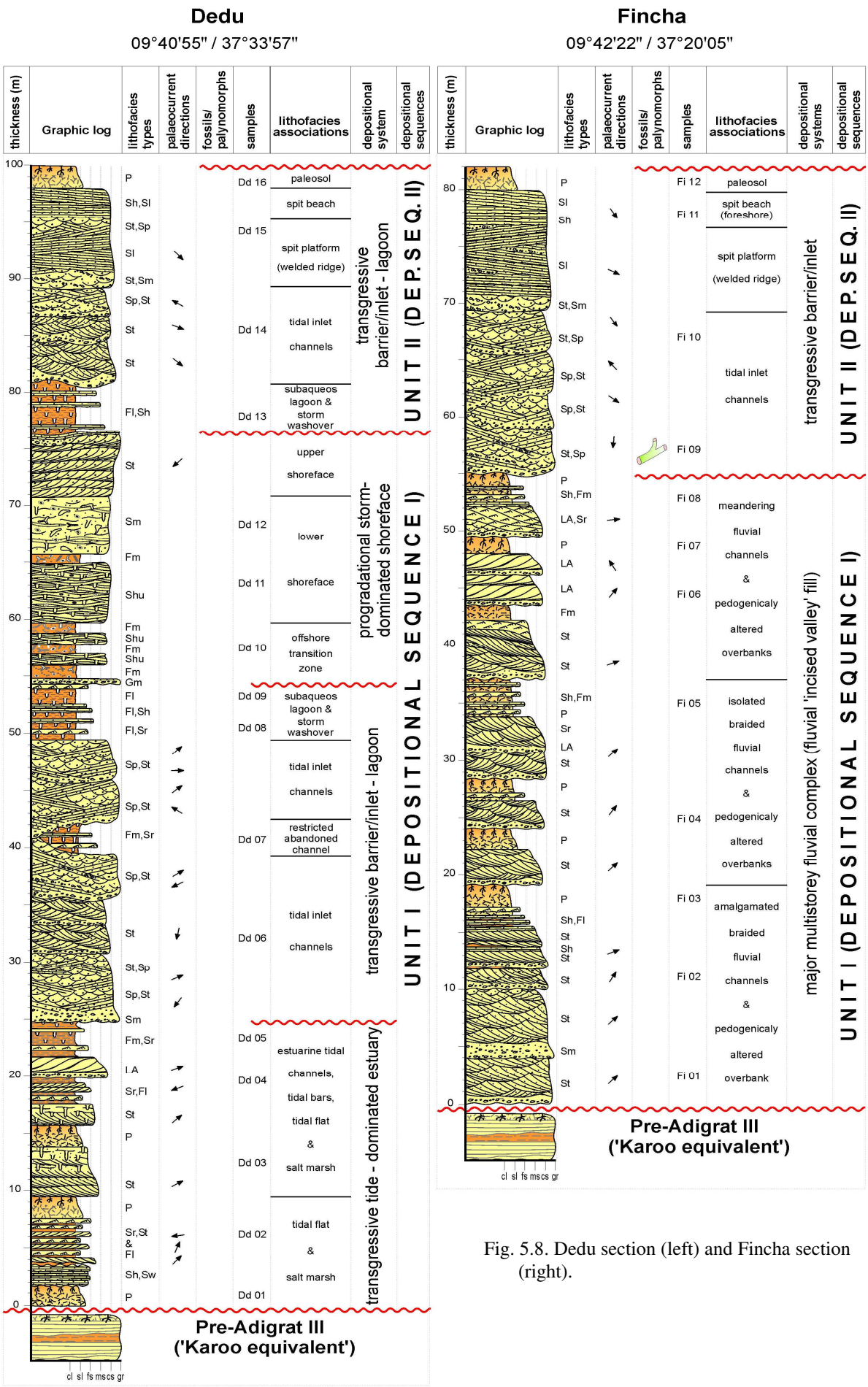


Fig. 5.8. Dedu section (left) and Fincha section (right).

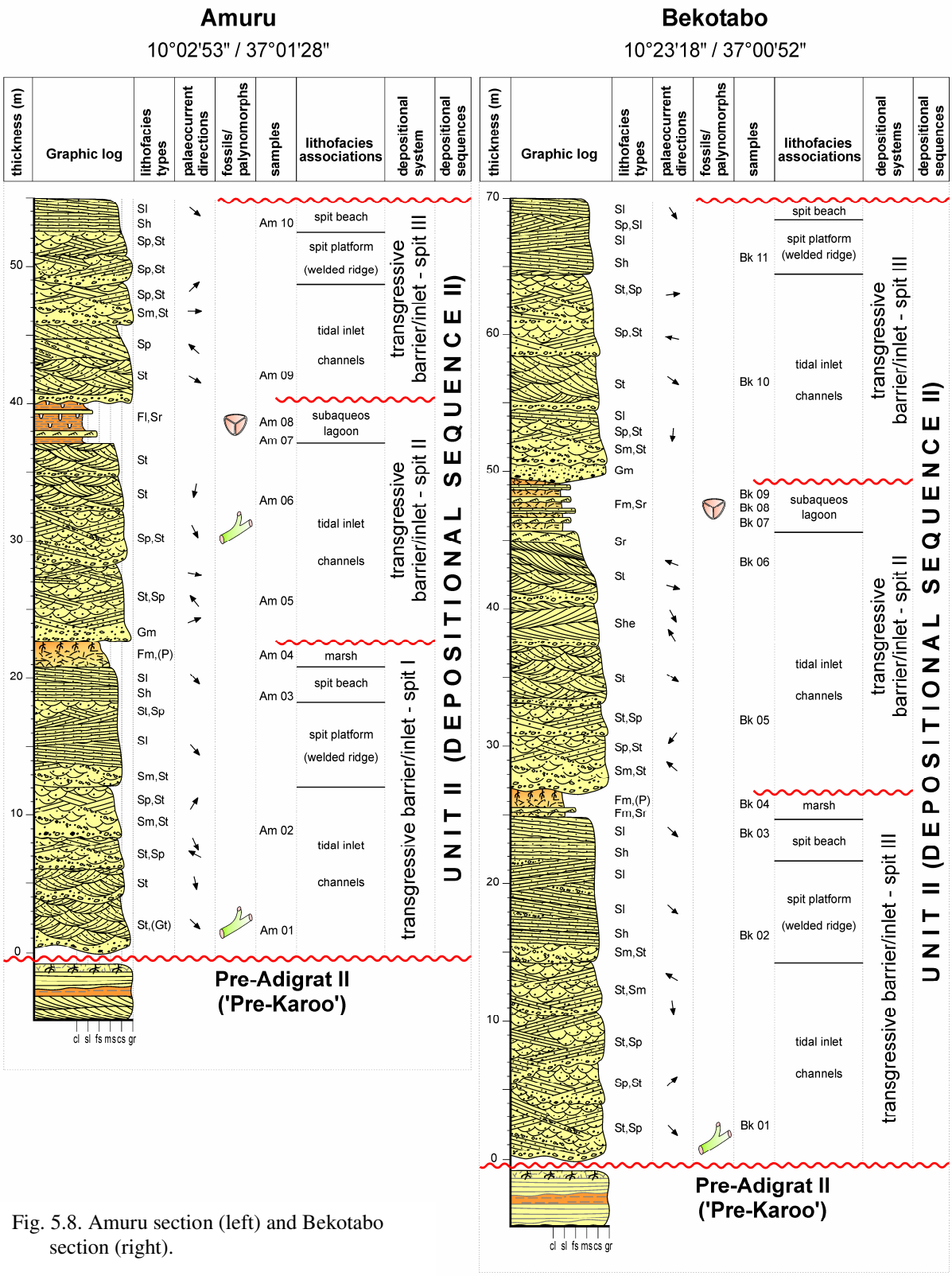


Fig. 5.8. Amuru section (left) and Bekotabo section (right).

transgressive-regressive episode. Depositional pinch out is more likely than erosional pinch out because the estuarine system with its landward limit of fluvial and tidal facies at its head to the seaward limit of coastal to nearshore marine facies at its mouth is well-preserved. The increased thickness of the white unit in this area as well the vertical stacking of three barrier-inlet systems may be related to a relative still stand sea level which might have favoured the

vertical aggradation. Herringbone-type cross-bedding as well as large-scale flute casts with their tapered ends pointing in opposite directions are characteristic features of tidal deposits.

### 5.3. Intrabasinal Correlation

Based on the six vertical sections, which are described and interpreted in Sec 5.2, an east-west section-to-section correlation of stratigraphic units and intra-unit depositional systems is performed and illustrated in a dip-oriented cross-section in Fig. 5.10. The paleosol profile (Fig. 5.9d), which developed on top of the 'Karoo-equivalent' Pre-Adigrat III succession, can be traced throughout the basin. It can therefore be regarded as a significant time-stratigraphic marker and forms a principal basis for correlating the basal unconformity of the Adigrat Sandstone succession in the Blue Nile Basin. Such paleosol profiles are presumed to form at major geological unconformities (Retallack 1984) and they reflect prolonged periods of landscape stability (Kraus 1999). Additional time-stratigraphic marker for the basal unconformity comes from Anisian–Carnian palynologic assemblage recovered from the top of the underlying succession (see Sec. 6). The second important marker horizon is the paleosol profile that separates the two stratigraphic units (Fig. 5.9d & e). This horizon can also be traced throughout the basin and is used as a reference datum for the construction of the cross-section in Fig. 5.10.

***Description***: In the red unit (*Unit I*), the thickness of the succession increases from the southwest (i.e., Fincha) towards the northeast (i.e., Yejube and Dejen). The facies composition and the nature of depositional systems also vary in this direction. Continental to coastal plain facies dominates in the southwest whereas the northeastern areas are dominated by shallow marine facies. The geometry of the sedimentary body as a whole can be described as a landward-tapering wedge that progressively pinches out onto the pre-Adigrat deposits towards the southwest. In the lower part of the red unit, the mixed-energy estuarine deposits intertongue in the up-dip direction with the fluvial system around the Dedu area. Likewise, the barrier-lagoon deposits interfinger with the meandering fluvial deposits between Fincha and Dedu areas. The shoreface deposits in the upper part of the red unit pinch out in a short distance southwest and west of Dedu. Palaeocurrent measurements in the fluvial deposits suggest a general northeast-directed sediment dispersal system. Palaeocurrent directions from estuarine tidal channels and bars indicate a NE-SW tidal flow path. Moreover, flood tidal delta and washover deposits in the barrier-lagoon system are characterised by broadly SW-oriented palaeoflow.

In regard to the white unit (*Unit II*), thickness increases from the east towards the west. However, the variation in thickness is moderate as compared to that of the red unit. The sandstone unit possesses a tabular or sheet-like geometry that covers wide areas in the basin. It is relatively uniform internally and lateral variation in facies composition appears to be minor. The transition from the red to the white unit is accompanied by a major change in palaeocurrent patterns. Bimodal palaeocurrents in the tidal inlet channels suggest a SE-NW tidal flow path. Gently dipping foreset laminae of the spit beach indicate a SE-dipping coastal gradient in most of the areas studied.

***Interpretation***: The increase in thickness of the red unit from southwest to the northeast is attributed to the increasing rate of subsidence from proximal to distal direction along the depositional dip. The landward-tapering wedge-shaped geometry of the sedimentary body can be best explained by a southwestward transgression. Palaeocurrent patterns in the fluvio-estuarine deposits and the basinward transition from continental to shallow marine facies may point to a northeastward-opening funnel-shaped coastal embayment. The up-dip superposition

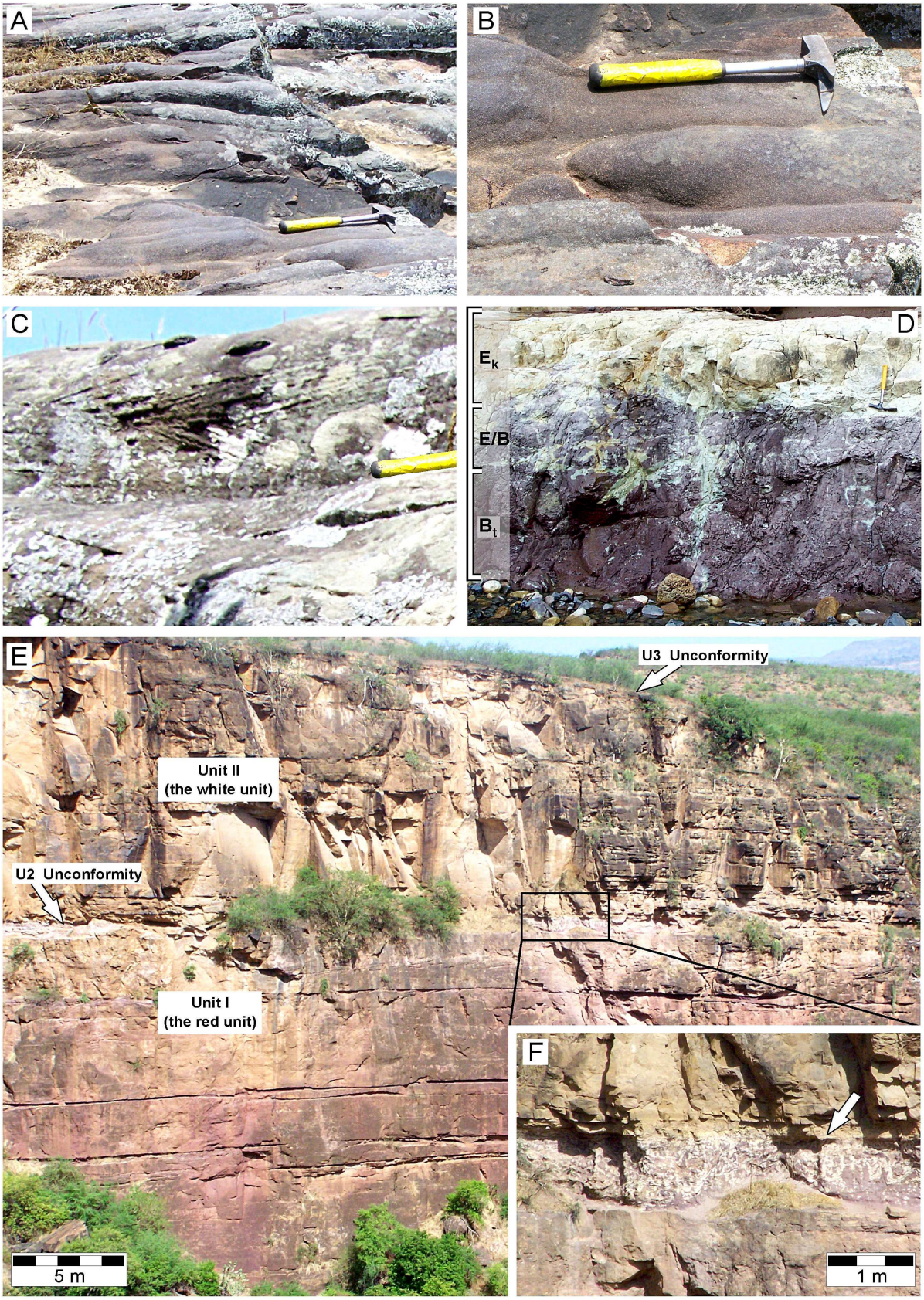


Fig. 5.9. A. Flute casts with their tapered ends pointing in opposite direction, Amuru section. B. Close-up view of flut casts. C. Herringbone cross-bedding from tidal inlet fill sandstones, Amuru section. D. A paleosol profile that marks the basal unconformity at the base of the red unit, an example from the Dejen area. The profile is characterised by a well-developed calcic ($E_k$) horizon, a gradational E/B and a thick red to purple clayey subsurface ($B_t$) horizon. E. The unconformity (U2) separating the red and the white units, which is also marked by a paleosol horizon, Dejen area. F. Close-up view of the paleosol horizon in 'E'.

of barrier-lagoon deposits over the fluvio-estuarine deposits indicates transgression. SW-oriented palaeoflow direction of the flood tidal delta and washover deposits also supports transgression towards the southwest.

The sheet-like geometry and the wide aerial extent of the white unit suggests a rapid lateral inlet migration but a continuous slow transgression (Demarest & Kraft 1987). As described in the previous section, the unit is characterised by sand-dominated inlet/spit facies with minor underlying backbarrier lagoonal facies. The lack of backbarrier facies is largely due to their erosional removal during the lateral migration of the inlet/spit system along the barrier. The enhanced thickness of the unit in Amuru and Bekotabo may be explained by a temporary balance between sediment supply and relative rise in sea level, in which situation shore-zone facies occupy a relatively fixed geographic position while aggrading vertically. Similar examples of vertically stacked barrier-inlet successions are known in the geologic record; for example, the Tertiary Frio Formation of the Texas Gulf Coast (Galloway et al. 1982), which attains an exceptional thickness of over 1000 m.

The shift in the palaeocurrent patterns from the northeast in red unit to the southeast in the white unit suggests a significant change in the basin configuration, which is most probably related to uplift, and basin inversion. Tectonic uplift might also be supported by the fact that the red unit was affected by pervasive oxidation while the overlying white unit was not. This change in the basin configuration has a major implication to the geodynamic evolution of the basin and thus will be dealt in a more detail in Sec. 8. SE-NW-oriented tidal flow path and SE-dipping beach foreset laminae in the white unit points to transgression from the southeast.

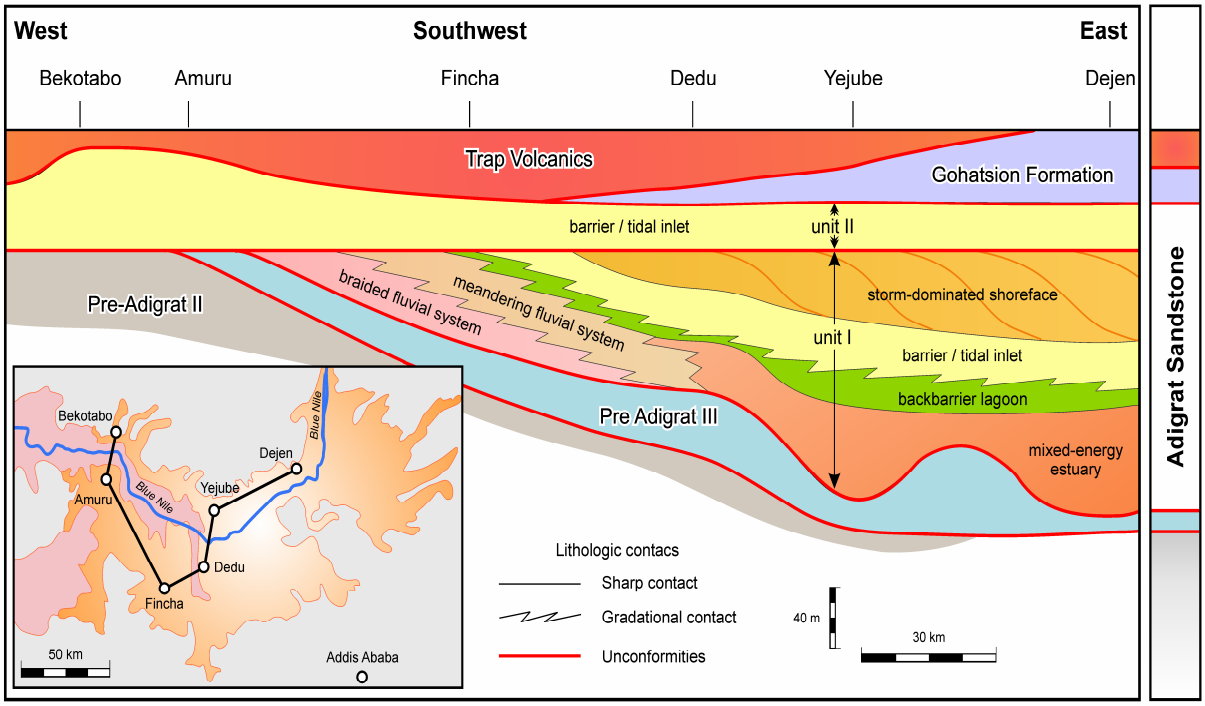


Fig. 5.10. A cross-section illustrating section-to-section correlation of stratigraphic units and intra-unit depositional systems in the Blue Nile Basin. The unconformity separating *Units I* and *II* is used as a reference datum.

## 6. Palynology

Palynology has generally been regarded as an important tool for biostratigraphic correlation and age determination of otherwise unfossiliferous continental and marginal marine strata.

However, little has been published on the palynology of Ethiopia with up until now only five articles, most of them from the Ogaden Basin (e.g., Worku 1988, Geletu 1998, Geletu & Wille 1998). The first record of palynological data in this country was made by Davidson & McGregor (1976) from western Kefa and Ilubabor provinces of southwestern Ethiopia, which reports the occurence of Permian strata in these areas. Bussert & Schrank (2007) gave an account of latest Carboniferous–Early Permian pollen and spores from the glacigenic sediments in Northern Ethiopia. Apart from a single report about the presence of Middle Triassic playnomorphs in the Fincha valley of central Ethiopia (Geletu & Wille 1998), no palynological study has ever been conducted on the Mesozoic sediments that crop out over wide areas in the central and northern part of the country.

This section deals with the analysis of palynological data recovered from the Adigrat Sandstone succession in the Mekelle and Blue Nile basins with the aim of: (i) assessing the composition and temporal (up-section) distribution of palynomorphs; (ii) erecting informal assemblage zones; (ii) assisting the established lithostratigraphic subdivision with biostratigraphic data; and (iii) assisting interbasinal correlation of the sandstone succession as well as regional correlation.

### 6.1. Composition of Palynomorphs

Based on the 16 productive samples collected at different stratigraphic levels from the Adigrat Sandstone succession in the Mekelle and Blue Nile basins, the composition and up-section distribution of palynomorphs indicate a major sequential break separating two distinct and major microfloras. These include a lower *Falcisporites*-dominated microflora belonging to corystosperms (de Jersey 1975, Dolby & Balme 1976) and an upper *Callialasporites*-dominated microflora (Balme 1957, de Jersey 1975) that apparently belong to araucariacean and cheirolepidiacean conifers (Filatoff 1975).

In the lower part of the succession (*Unit I*), the microfloral assemblage is dominated by non-taeniate disaccate gymnospermous pollen, mainly belonging to *Falcisporites*. Pteridophyte spores are generally subordinate elements. Ephedrales- and Cycadales-type pollen occur very rarely, as well as small (20–25 µm Ø), spherical, inaperturate pollen (Fig. 6.3e–h) that are referred to as *Spheripollenites* (Couper 1958). Most of the specimens assigned to *Spheripollenites* do not possess characteristic features of *Classopollis* and/or *Exesipollenites*, which were originally described by Balme (1957). Taeniate disaccate and Araucariaceae-type pollen are absent.

In the middle part of the succession (*Unit II*), however, inaperturate gymnospermous pollen (*Classopollis*, *Araucariacites* and *Callialasporites*) appear to be predominant with fairly high abundance. Similarly, pteridophyte spores (mainly laevigate trilete spores, e.g., *Dictyophyllidites* sp.), which occur as accessory components in *Unit I*, become predominant in the middle part of the section (*Unit II*). Disaccate pollen grains, which dominated the microfloral assemblage in *Unit I*, become extremely rare and represented by few specimens of *Alisporites*.

In the upper part of the succession (*Unit III*), the assemblage is dominated by trilete spores that possess extremely diverse sculptural types, amongst which *Ischyosporites*, *Klukisporites*, *Converrucosisporites* and *Neoraistrikia* are the prominent forms. Laevigate

Fig. 6.1. Magnifications: x400 (Fig. A-C), and x650 (Fig. D-Q). A-B. *Falcisporites australis*. C. *Alisporites similis*. D-F. *Minutosaccus crenulatus*. G-H. *Enzonalasporites* sp. I-J. *Samaropollenites speciosus*. K. *Staurosaccites quadrifidu*. L-M. *Cyacadopites stonei*. O. *Ephedripites macistriatus*. P. *Playfordiaspora velata*. Q. *Platysaccus Queenslandi*.


A
B
C
D
E
F
G
J
I
H
K
L
M
N
O
P

trilete spores are also well-represented in the uppermost part, but in a rather moderate abundance. Bryophytic spores are rare throughout and represented by few specimens of *Staplinisporites*. Trilete spores with striate sculpture (e.g., *Cicatricosisporites*) and disaccate pollen are entirely absent. A list of identified spore-pollen species together with their stratigraphic ranges is given in Fig. 6.5. Photomicrographs of most of the listed species are presented in Fig. 6.1–4. Morphotypes which could not be identified to existing species have been assigned a generic affinity only. The percentage composition of each spore and/or pollen genus given in parenthesis below is based on 200 grains counts per sample.

## 6.2. Assemblage zones

On the basis of the above described distribution patterns and group compositions of palynotaxa, three informal assemblage zones have been identified within the Adigrat Sandstone succession. The lower two zones are common for both the Mekelle and Blue Nile basins since they are essentially similar with regard to the qualitative and quantitative composition of palynomorphs, whereas the third assemblage zone has not been recognised in the Blue Nile Basin (Fig. 6.6). The other significant difference between palynomorph assemblages of the two basins lies on the mode of preservation. Samples from the Mekelle Basin provided better preserved palynomorphs than those from the Blue Nile Basin. The age assignments for the assemblage zones are based on correlations with palynofloras documented in adjacent regions of Gondwana. A comparison with the assemblages of the Australian Mesozoic (Dolby & Balme 1976, Helby et al. 1987, 2004) was of great biostratigraphic importance since these microfloras have been dated precisely by marine fauna.

The proposed assemblage zones, in ascending order, are: AZ I, Late Triassic (Late Carnian–Early Rhaetian); AZ II, latest Early Jurassic (Early Toarcian); and AZ III, latest Early–Middle Jurassic (Late Toarcian–Early Callovian). The upper age limit of the siliciclastic succession in both basins is independently constrained by marine fauna recovered from the base of the overlying Antalo Limestone. Based on a fairly rich foraminifera fauna (e.g., *Nauitiloculina oolithica*, *Praekurnubia crusei*, *Valvulina* gr. *negeoni*, *Kurnubia palestiniensis*, *Trochamina* sp. and *Cylindroporella* sp.), a Late Callovian–Early Oxfordian age has been assigned by Bosellini et al. (1997) for the base of the limestone unit in the Mekelle Basin. Additional evidence comes from the Oxfordian ammonites (i.e., *Gregoryceras* cf. *fouquei* and *Dichotomosphinctes* cf. *rotoides*) recovered from few metres upwards (Matire et al. 2000). In the Blue Nile Basin, the presence of *Pfenderina* sp. and *Nautiloculina oolithica* at the base of the limestone unit points to a Callovian age (Russo et al. 1994). Age constraints for the lower boundary of the Adigrat Sandstone relied entirely on spore-pollen data since independent age control by marine fauna is lacking.

### Assemblage Zone I (AZ I)

The principal characteristics of the assemblage are the dominance of non-taeniate disaccate gymnospermous pollen (68-70%) and the low proportion of pteridophyte spores (10-15%). Ephedrales- and Cycadales-type pollen, as well as other small indeterminate inaperturate pollen (i.e., *Spheripollenites*) represent less than 2% of the assemblage.

**Dominant**: *Falcisporites australis*, *Falcisporites stabilis*, *Falcisporites* sp. *Minutosaccus crenulatus*, *Samaropollenites speciosus*, *Staurosaccites quadrifidus, Alisporites similis*, *Alisporites thomasii*, *Alisporites* sp., *Playfordiaspora velata*, *Platysaccus queenslandi*, *Platysaccus* sp.

**Subordinate**: *Dictyophyllidites mortoni*, *Dictyophyllidites* sp., *Uvaesporites* sp. *Calamospora* sp., *Enzonalasporites* sp.

**Rare**: *Ashmoripollis reducta*, *Cyacadopites stonei*, *Cyacadopites* sp. *Ephedripites macistriatus*, *Spheripollenites* sp.

**Associated fossils**: Vertebrate fossils assigned to temnospondyl amphibian (capitosaurid), including a partial mandible (cf. *Abiadisaurus witteni*, Warren et al. 1998) and large fang teeth (Müller et al. 2007), along with tooth plates of lungfish and various types of coprolites. Invertebrate fosslis include poorly preserved shells of brachiopods and gastropods (Fig. 4.9g-h), agglutinated foraminifera (mainly *Ammodiscus*) and scolecodonts (Fig. 4.10a & b).

**Suggested age**: Late Triassic (Late Carnian–Early Rhaetian).

**Correlation and remarks**: Assemblage Zone I can be compared with Late Triassic Gondwana palynofloras that have been well-described from East Africa, Madagascar, India and Australia. Since the Triassic palynology of Gondwana is best documented from the Australian continent, the palynozonation of the Traissic of Australia is treated as the standard to which reference can be made regarding the age of AZ I. The predominance of non-taeniate disaccate pollen and the absence of taeniate ones, which dominated the Early Triassic microfloras of the region, imparts a clear affinity of AZ I to the upper part of the *Falcisporites* Superzone described by (de Jersey 1975, Playford et al. 1982, Helby et al. 1987). In terms of diversity a closer correspondence can be demonstrated with the *Minutosaccus crenulatus* Oppel Zone of western Australia (Dolby & Balme 1976, Helby et al. 1987). *Staurosaccites quadrifidus* has not been encountered in the AZ I of the Mekelle Basin but is abundant in the Blue Nile basin. However, the species is prominent together with *Ovalipollis ovalis* in the uppermost part of the underlying 'Karoo-equivalent' Pre-Adigrat III succession. Moreover, key species belonging to the *Staurosaccites quadrifidus* Oppel Zone of Dolby & Balme (1976) and Helby et al. (1987) are missing (e.g., *Camerosporites secatus* and *Infernopollenites claustratus*), suggesting that AZ I might be younger than Ladinian (Fig. 6.6). The presence of *Samaropollenites speciosus* points to the fact that the whole Carnian interval could not be ruled out. Similarly, the presence of *Ashmoripollis reducta* as a rare element indicates that the assemblage might be as young as Early Rhaetian. The absence of forms that can genuinely be assigned to *Classopollis* and/or *Exesipollenites*, as well as the absence of key Hettangian species (e.g., *Perinopollenite elatoides*), impedes correlation with *Corollina torosa* Oppel Zone of western Australia (Helby et al. 1987). AZ I can also be compared with those of Zone III B, but may extend down into the upper part of Zone III A of Madagascar (Goubin 1965). Late Triassic microfloral assemblages dominated by non-taeniate disaccate pollen has also been described from Tanzania (Hankel 1987), India (Maheshwari & Kumaran 1979) and Antarctica (Farabee et al. 1989).

---

Fig. 6.2. Magnifications: x650 (Fig. A-I, K, M), x800 (Fig. J, L, O, R) and x1000 (Fig. N, P, Q). A-D. *Callialasporites turbatus*. E-F. *Callialasporites* cf. *dampieri*. G-H. *Araucariacites australis*. I. *Concavisporites* sp. J. *Matonisporites* sp. K. *Triplanosporites* sp. L. *Todisporites* sp. M. *Cyathidites* sp. N. *Matonisporites equiexinus*. O-P. *Dictyophyllidites mortonii*. Q. *Dictyophyllidites harrisii*. R. *Deltoidospora* sp.

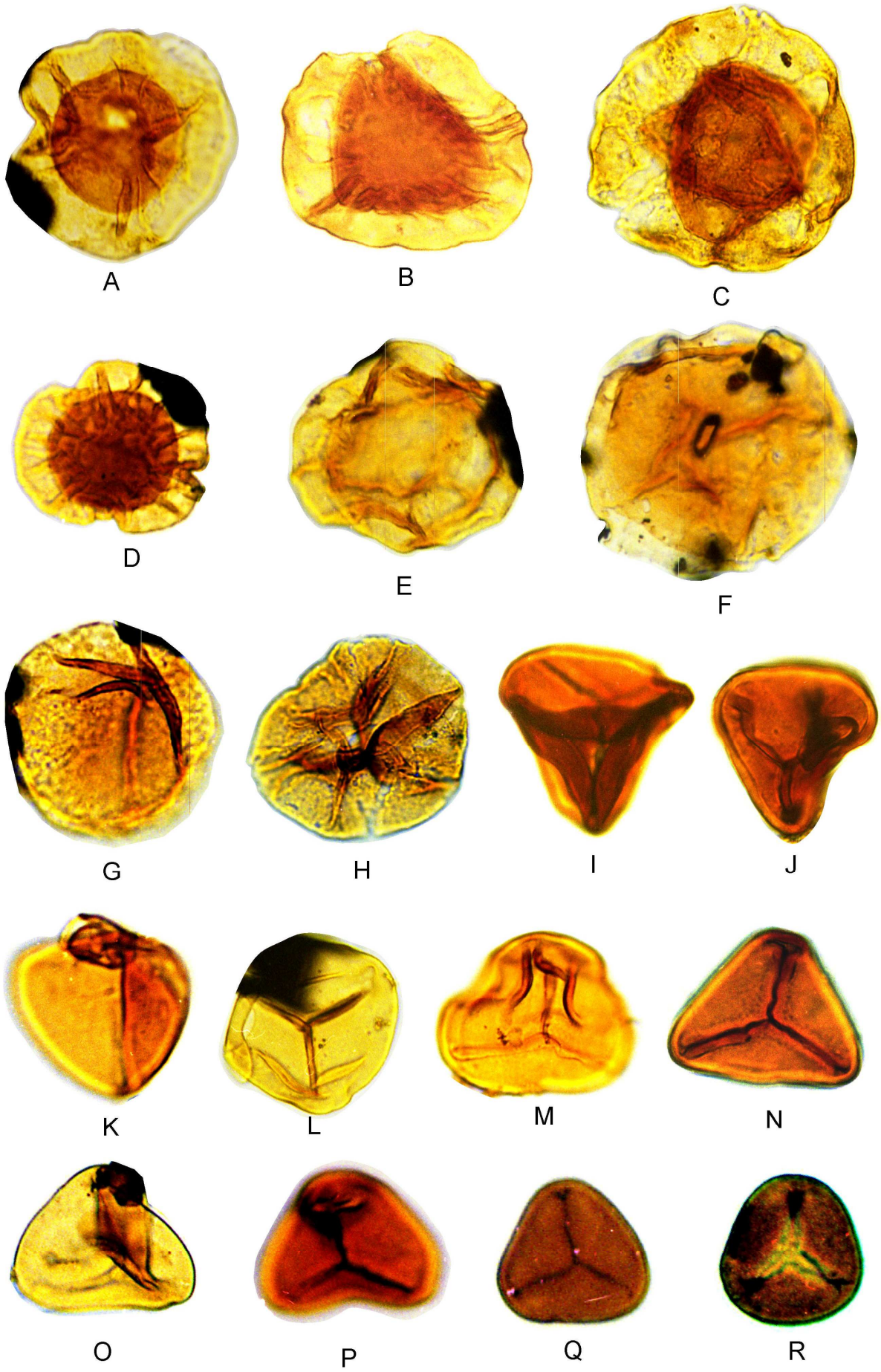
A
B
C
D
E
F
G
H
I
J
K
L
M
N
O
P
Q
R

**Assemblage Zone II (AZ II)**

The assemblage contains high frequencies of *Araucariacites* and *Callialasporites*, which together constitute about 37–40%. Highly diverse and predominantly laevigate trilete spores compose about 35% of the assemblage and *Classopollis* form about 25–30%. Other highly sculptured triletes represent less than 5%. Bryophytic and Lycophytic spores are of minor importance, and together with rare disaccate pollen (mainly *Alisporites* sp.) make up less than 1% of the assemblage.

**Dominant**: *Araucariacites australis*, *Araucariacites* sp., *Callialasporites turbatus*, *Callialasporites dampieri*, *Classopollis torosus*, *Classopollis meyeriana*, *Classopollis simplex*, *Spheripollenites* sp., *Triplanosporites* sp., *Dictyophyllidites* sp., *Concavisporites* sp., *Cyathidites* sp., *Deltoidospora* sp., *Matonisporites equiexinus, Matonisporites* sp., *Gleicheniidites senonicus, Gleicheniidites* sp., *Cibotiumspora sinuata*, *Cibotiumspora jurienensis*, *Obtusisporites canadensis*, *Undulatisporites* sp. and *Todisporites* sp.

**Subordinate**: *Ischyosporites crateris*, *Klukisporites scaberis*, *Converrucosisporites* sp., *Verrucosisporites* sp. and *Uvaesporites argentaeformis*.

**Rare**: *Alisporites* sp., *Cycadopites* sp. and *Staplinisporites caminus*.

**Associated fossils**: nonsilicified wood fragments.

**Suggested age**: latest Early Jurassic (Early Toarcian).

**Correlation and remarks**: In AZ II, the predominace of palynoflora with araucariacean and cheirolepidiacean affinities allows a broad comparison with the *Callialasporites dampieri* Superzone of Australia (Balme 1957, de Jersey 1975, Filatoff 1975, Price et al. 1985). One of the most significant observations with regard to the transition from AZ I to AZ II is that the *Falcisporites*-dominated microflora had become rare or were extinct and replaced by araucarians and podocarps. According to Helby et al. (1987), the boundary between the two microfloras is usually distinct, representing a substantial extinction horizon. The present assemblage can be correlated with the lower *Callialasporites turbatus* Oppel Zone of western Australia (Helby et al. 1987, 2004). The first appearance of *Callialasporites turbatus* in the Toarcian is the most reliable chronostratigraphic marker in the region (Filatoff 1975). Although *Classopollis* is abundant in AZ II the species *Corollina torosa* has not been documented in the order of 50%+. Therefore, a correlation with the *Corellina torosa* Oppel Zone (Helby et al. 1987, 2004, Reiser & Williams 1969) is unlikely. This may be taken as an evidence for a Late Rhaetian to Pliensbachian hiatus, which separates *Unit I* and *II* within the Adigrat Sandstone succession in the Mekelle and Blue Nile basins. The hiatus has also been recognised throughout the East African margin and the Arabian platform (see reginal correlation in Sec. 9, Al-Husseini 2008, Hankel 1994, Sharland et al. 2001). Similar *Araucariacites* and *Callialasporites*-dominated assemblage zones have been described from the latest Early–early Middle Jurassic successions of Kenya (Hankel 1994), Tanzania (Balduzzi et al. 1992, Hankel 1994), Madagascar (Hankel 1994), India (Tripathi 2001) and Antarctica (Truswell et al. 1999).

Fig. 6.3. All Magnifications are x1000. A. *Cibotiumspora sinuata*. B. *Cibotiumspora jurienensis*. C. *Undulatisporites* sp. D. *Obtusisporites canadensis*. E-H. *Spheripollenites* sp. I. *Classopollis torosus*. J. *Classopollis meyeriana*. K. *Classopollis anasillos*. L-N. *Classopollis simplex*. O-Q. *Classopollis cf. torosus*. R-S. *Uvaesporites argentaeformis*. T-U. *Gleicheniidites senonicus*. V. *Calamospora* sp. W. *Cyacadopites minimus*.

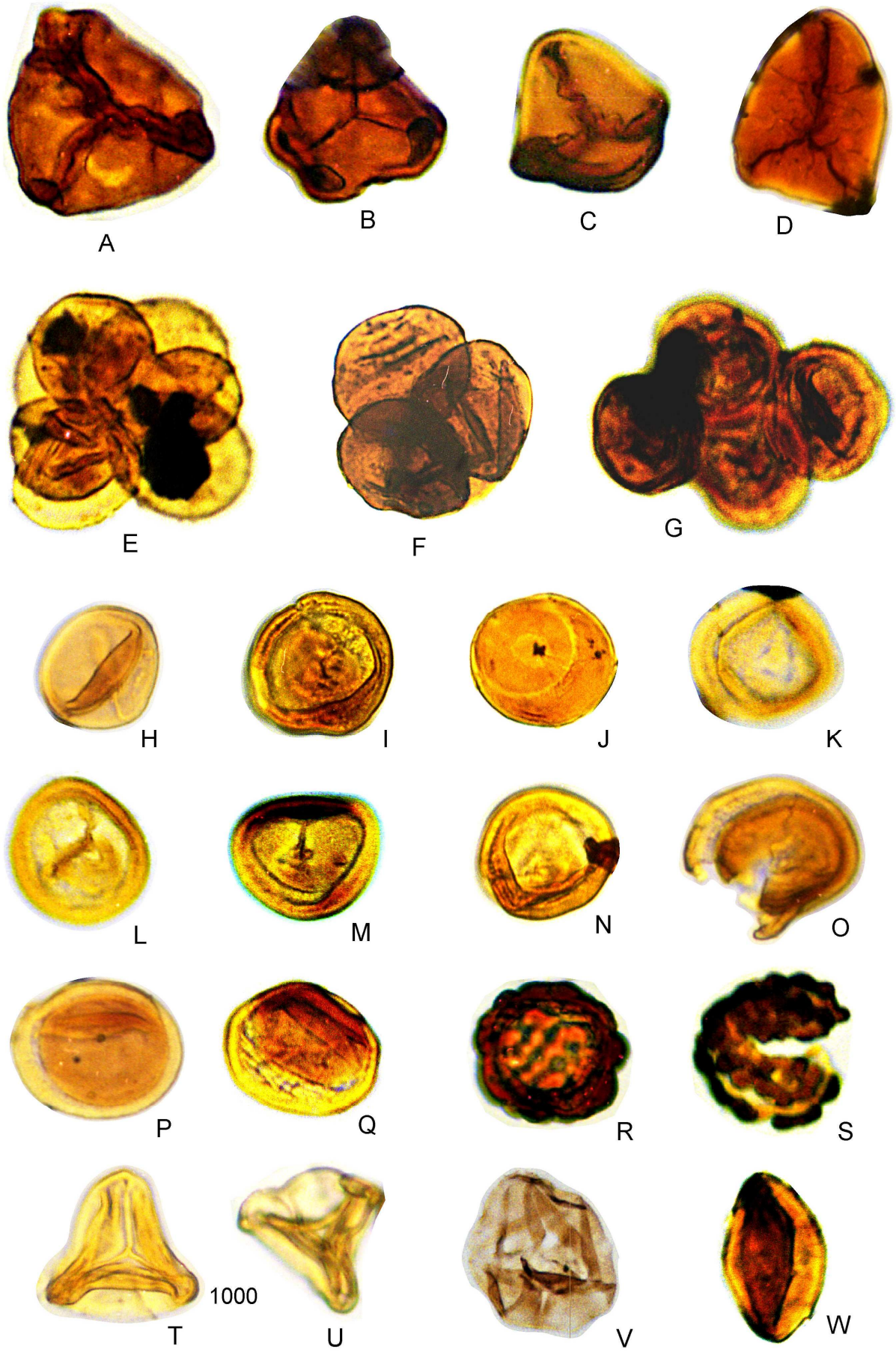
A
B
C
D
E
F
G
H
I
J
K
L
M
N
O
P
Q
R
S
T
1000
U
V
W

**Assemblage Zone III (AZ III)**

The assemblage is characterised by the predominance of highly sculptured trilete spores (35–38%) and Araucariaceae-type pollen (25–28%). While *Classopollis* remained prominent with its 22–27 %, the relative proportion of smooth trilete spores declines to 10–15%. Other indeterminate miospores represent less than 1% of the assemblage. Schizaeaceae-type spores that possess characteristic straite sculptures (ribbed triletes of Couper 1958) (e.g., *Cicatricosisporites*) are absent, as well as disaccate pollen.

**Dominant**: *Concavissimisporites variverrucatus, Concavissimisporites* sp., *Concavissimisporites* sp., *Impardecispora* ap., *Ischyosporites crateris*, *Ischyosporites volkheimeri*, *Ischyosporites* sp., *Klukisporites lacunus*, *Klukisporites scaberis*, *Klukisporites variegatus*, *Trilobosporites* sp., *Neoraistrickia* sp., *Verrucosisporites* sp., *Converrucosisporites* sp., *Rotverrusporites equatibossus*, *Baculatisporites comaumensis*, *Uvaesporites argentaeformis*,

**Subordinate**: *Araucariacites australis*, *Araucariacites* sp., *Callialasporites dampieri* and *Callialasporites* sp., *Dictyophyllidites* sp., *Concavisporites* sp., *Cyathidites* sp., *Deltoidospora* sp., *Gleicheniidites senonicus*, *Matonisporites* sp., *Cibotiumspora sinuata*, *Obtusisporites canadensis*, *Undulatisporites* sp., *Callialasporites turbatus*, *Classopollis meyeriana*, *Classopollis simplex* and *Spheripollenites* sp.

**Rare**: *Staplinisporites* sp., *Cycadopites minimus* and indeterminate miospores.

**Associated fossils**: Agglutinated foraminifera (*Ammodiscus*), brackish water bivalves, vertebrate remains (skull material, osteoderms, vertebrae, ribs, limb elements and piercing teeth of a marine crocodile (*thalattosuchian*, Müller et al. 2007), fragments of actinopterygian fish (cf. *Lepidotes*) and teeth of hybodontid sharks), diverse coprolites and trace fossils (*Skolithos*, *Thalassinoides*, *Diplocraterion*).

**Suggested age**: latest Early–Middle Jurassic (Late Toarcian–Early Callovian).

**Correlation and remarks**: Palynomorphs of the AZ III have been recovered from the barrier-lagoon succession (*Unit III*) of the Mekelle Basin and they were not recognised in the Blue Nile Basin. The continued abundance of *Araucariacites* and *Callialasporites* through the transition from AZ II to AZ III, together with diverse vertebrate remains of Toarcian *thalattosuchian* crocodyliform (Müller at al. 2007. Pierce & Benton 2006), suggests that the hiatus between Unit II and III may be of a short duration (i.e., in the order of several Ma or less). Therefore, a Late Toarcian age has been assigned for the base of the present assembladge. The dominance of highly sculptured triletes (e.g., *Concavissimisporites*, *Converrucosisporites*, *Ischyosporites* and *Klukisporites*) and the absence of *Cicatricosisporites* might enable a correlation with Reyre's (1973) Saharan palynosubzone 5a (Middle Dogger–Callovian). The predominance of key species including *Ischyosporites volkheimeri*, *Klukisporites scaberis*, *Concavissimisporites variverrucatus* and *Neoraistrickia* sp. in the upper part of AZ III allows a close correspondence with the *Contignisporites cooksoniae* Oppel Zone (Filatoff 1975, Helby et al. 1987), which is Bathonian to Middle Callovian in age. The upper age limit of the assemblage is well-constrained by the Late Callovian to Early Oxfordian foraminifra recovered from the overlying Antalo Limestone (cf. op. cite).

Fig. 6.4. All magnifications are x1000. A-B. *Concavissimisporites variverrucatus*. C. *Impardecispora* sp. D. *Klukisporites scaberis*. E. *Ischyosporites crateris*. F. *Klukisporites lacunus*. G. *Staplinisporites caminus*. H. *Trilobosporites* sp. I. *Baculatisporites comaumensis*. J. *Apiculatisporis* cf. *carnarvonensis*. K-N. *Neoraistrickia* sp. O-P. *Converrucosisporites* sp.

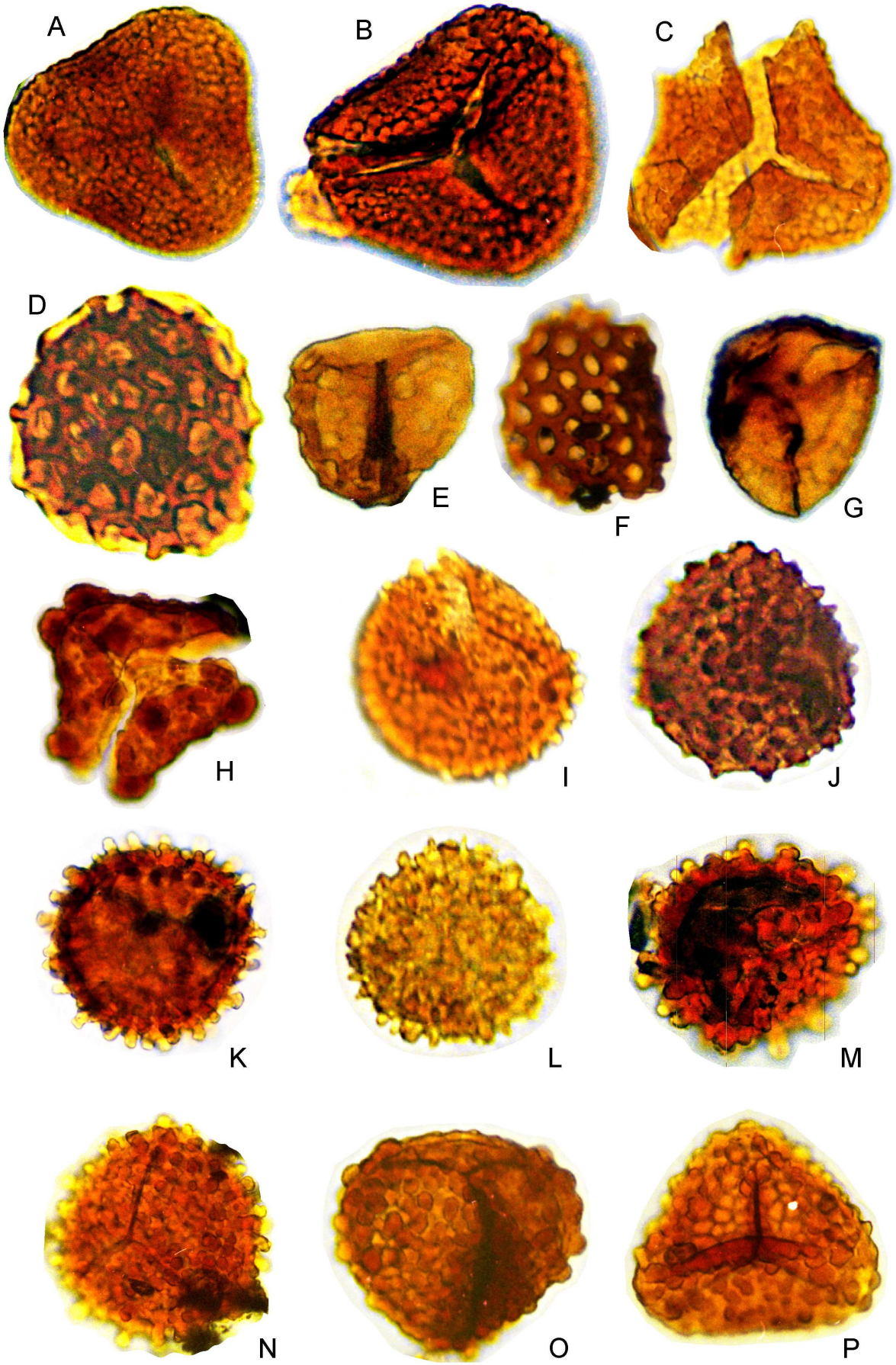
A
B
C
D
E
F
G
H
I
J
K
L
M
N
O
P

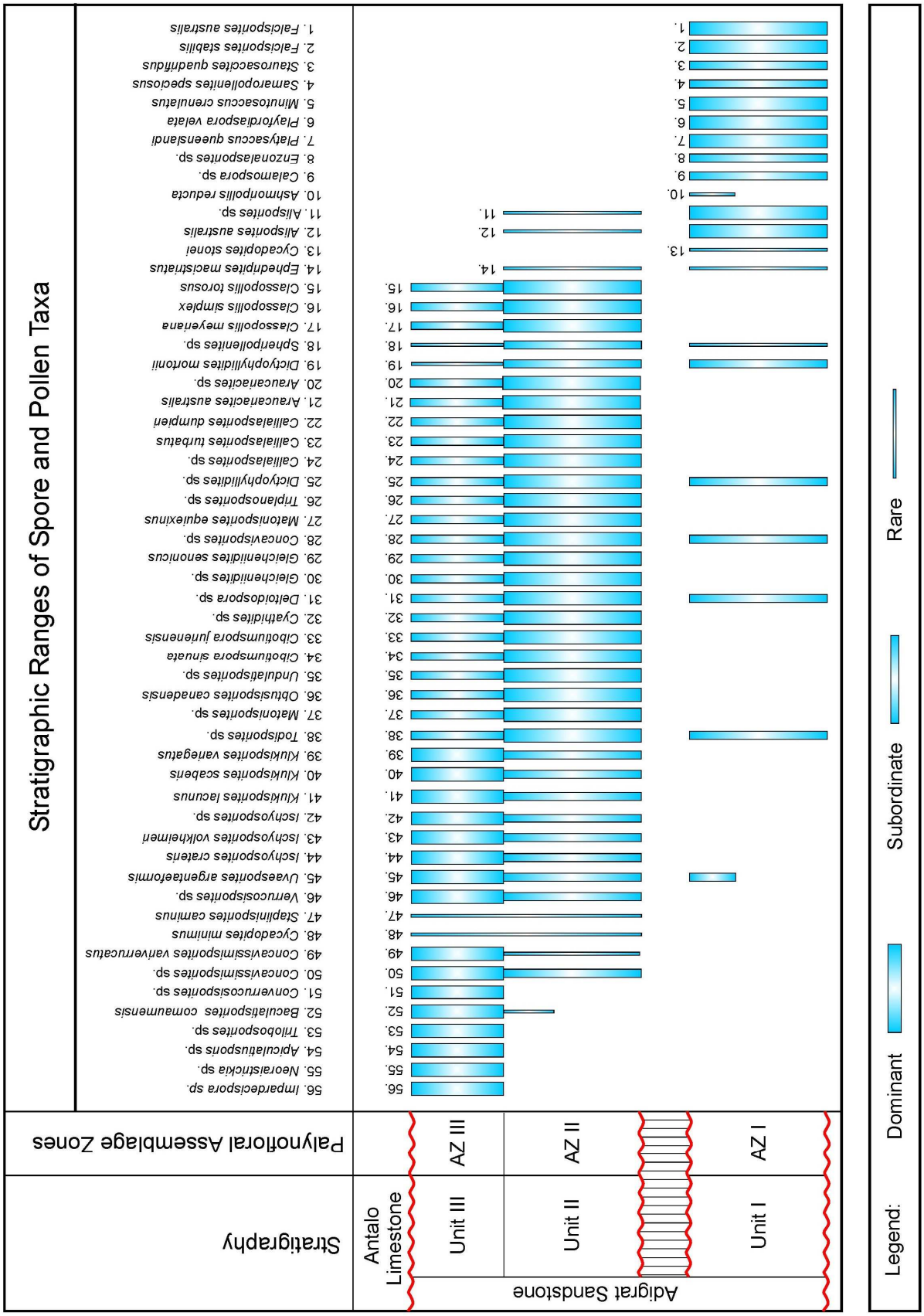


Fig. 6.5. Stratigraphic range chart of selected spore and pollen taxa and their relative abundances expressed as domonant, subordinate and rare.

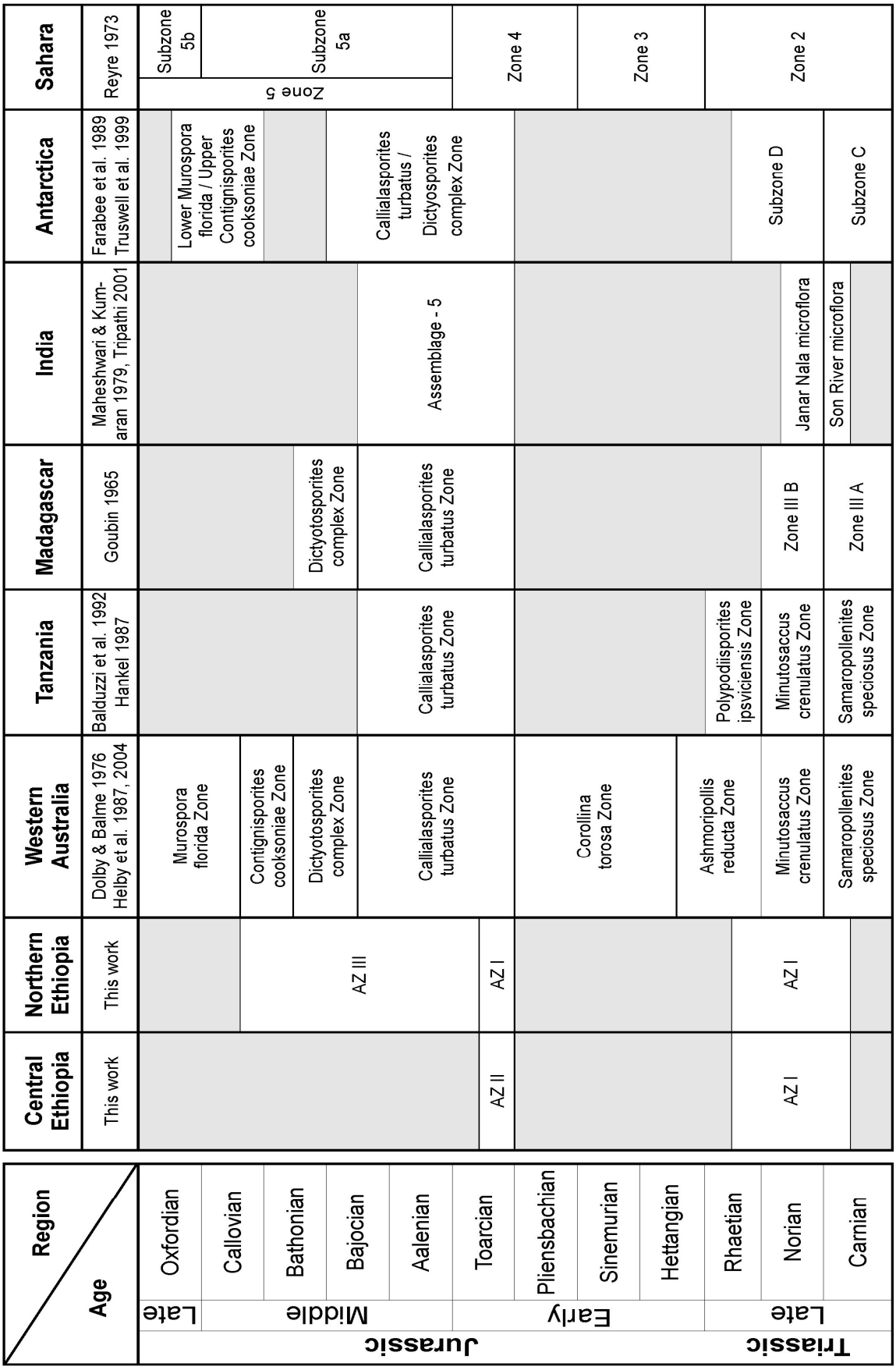


Fig. 6.6. Comparison between the Late Triassic to Middle Jurassic palynofloral zones of central and northern Ethiopia with the spore-pollen zonation schemes of western Australia, Tanzania, Madagascar, India, Antarctica and Sahara.

## 7. Interbasinal correlation between Mekelle and Blue Nile basins

Numerous unconformity-bounded stratigraphic units have been identified in the Mekelle and Blue Nile basins. Analysis of facies and depositional systems in each unit, as well as the intrabasinal correlation in their respective basins, was given in the previous sections. The main purpose of this section is to correlate these stratigraphic units between the two basins and to demonstrate the overall similarities and differences in facies associations and depositional systems of age equivalent units. The correlation is based on detailed lithostratigraphic and biostratigraphic information obtained in this study in combination with previously published data. In some cases where age diagnostic fossils are lacking biostratigraphic data from immediately adjacent basins (e.g., Ogaden or Berbera basins) will be considered.

### Unit I

*Unit I* that represents the first stratigraphic unit in both basins is Late Triassic (Late Carnian–Early Rhaetian) in age. Microflora indicative of Late Triassic age have been recovered from argillaceous intercalations of the fluvio-estuarine deposits that characterise the lowermost part of the unit. The assemblage is dominated by non-taeniate disaccate pollen predominantly belonging to *Falcisporites* with subordinate pteridophite spores and rare *Ephedripites* and *Cycadopites* (Fig. 6.1). As shown by the comparisons with Gondwana palynofloras, the absence of taeniate disaccate pollen and the occurrence of key species such as *Minutosaccus crenulatus* and *Samaropollenites speciosus* impart a strong correspondence with Late Triassic assemblages (Fig. 6.6). Vertebrate remains discovered at the base of the unit in the Abiadi area (cf. *Abiadisaurus*, Warren et al. 1998) were also supposed to indicate the same age.

The basal unconformity (U1) in both basins is marked by a subaerial exposure surface of erosion and/or nondeposition (pedogenesis), and exhibits a pronounced physical expression in the field. It is interpreted to be tectonic in origin, and is possibly related to crustal uplift in southwestern and western Ethiopia. Further to the west, in central Sudan, emplacement of alkaline magmatic complexes provides additional evidence to crustal uplift in the region (see Sec. 10, Fig. 10.1, Cutis & Lenz 1985, Müller-Sohnius & Horn 1994). According to Schandelmeier et al. (1997) and Geiger et al. (2004), faulting seems to have ceased during the Late Triassic, and the East African margin and the Arabian platform were characterised by post-rift thermal subsidence. Thus, the basal Late Triassic unconformity and the subsequent transgression represent major correlatable events across the study area. The transgression is interpreted to result from the post-rift thermal subsidence enhanced by eustasy.

The strata within *Unit I* in both basins consist of transgressive tide-dominated estuarine and prograding storm-dominated shoreface deposits. Palaeocurrent patterns in both basins are also similar (i.e., to the NE) suggesting that the sediments might have been accumulated on a vast shallow gulf, which was funnelled northeast into the Neotethys. This implies that the two areas were tectonically linked throughout the Late Triassic, and were joined by a seaway throughout much of this time. Thus, based on the above-discussed similarities, mainly depositional systems, palaeocurrent patterns and age, *Unit I* can be well-correlated across the two basins with fairly low uncertainty.

### Unit II

The second stratigraphic unit (*Unit II*) is Late Liassic (Early Toarcian) in age. In the Mekelle Basin, microfloras indicating a Late Liassic age have been recovered from silty mudstones interpreted to represent delta plain marshes and overbanks. The assemblage is characterised by high frequencies of *Callialasporites* and *Araucariacites*, as well as laevigate trilete spores

(e.g., *Dictyophillidites*, *Concavisporites* and *Deltoidospora*) and *Classopollis*. This assemlage seems to correspond with the lower *Callialasporites turbatus* Oppel Zone, indicating a Early Toarcian age (Reiser & Williams 1969, Helby et al. 1987, 2004). In the Blue Nile Basin, however, microfloral evidence is rather poor and restricted to poorly preserved *Callialasporites*, *Araucariacites* and *Classopollis*. Nonetheless, the unconformity separating the *Units I & II* is well-documented by physical field evidence as it is marked by a paleosol horizon that can be traced throughout the basin. Moreover, the sediments of *Unit I* were entirely red stained whilst *Unit II* was almost unaffected (see Plate II, Fig. A & B). This suggests uplift and extensive oxidation of *Unit I* before the deposition of *Unit II*. The U2 unconformity in the Mekelle Basin also exhibits similar features, even though the paleosol horizon is discontinuous and is interrupted in many places by fluvial incision.

The U2 unconformity may also be interpreted to be tectonic in origin, and is most probably related to active rifting associated with the developing rift between East and West Gondwana. Thermal uplift and widespread erosion during the Early Liassic have been well-documented in many areas in East Africa and Arabia (Fig. 9.1). In some areas (e.g., in Yemen, Somalia, Tanzania and Madagascar), the crustal uplift was accompanied by volcanic activity (see Fig. 10.2).

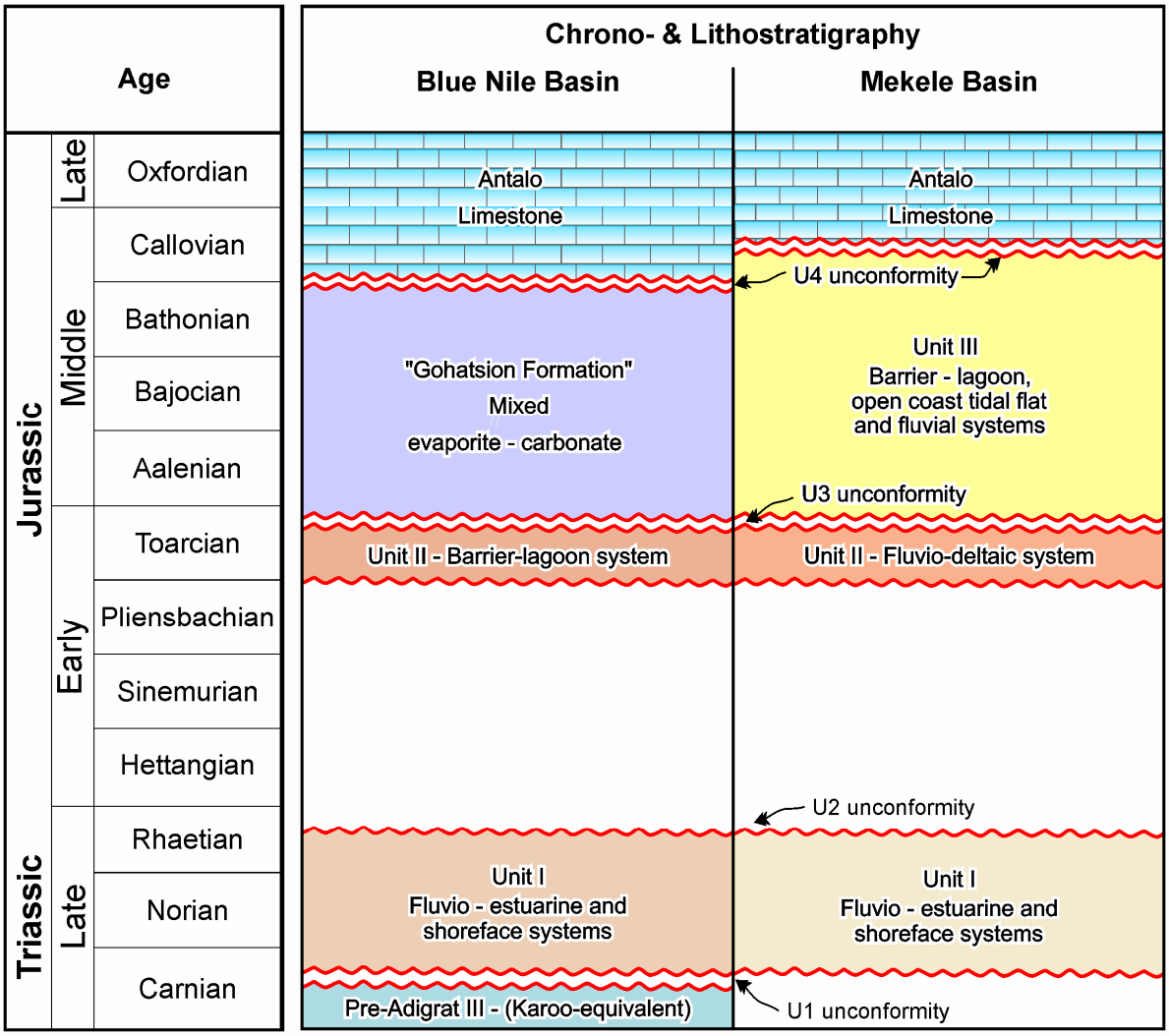


Fig. 7.1. Chrono- and lithostratigraphic correlation of the Late Triassic to Middle Jurassic sedimentary successions of the Blue Nile and Mekelle basins.

No direct similarity can be inferred regarding facies successions and depositional systems within *Unit II* in the two basins. In the Mekelle Basin, the unit is composed of coarse-grained sandstones and conglomerates of fluvial and deltaic origin whereas in the Blue Nile Basin the unit is of barrier/inlet-spit origin. The most important factors that brought about these differences are the source and supply of sediments, the variation in coastal morphology, and the role of waves, tidal- and river currents. The fluvio-deltaic deposits appear to have been accumulated in a rift basin in which faulting and uplift of rift shoulders were active (Fig. 8.3b). The key similarity in the strata of *Unit II* in both basins is that they possess the same palaeocurrent patterns, indicating deposition on a SE-dipping cratonic margin. This indicates the abandonment of the previously existing NE-dipping depositional gradient and its replacement by a SE-dipping one. Such significant avulsive switch in palaeocurrent pattern across the U2 unconformity can be best explained by rifting and basin inversion. This phase is most probably related to active rifting associated with the developing rift between East and West Gondwana that commenced during the Toarcian. Widespread intracontinental rifting was documented all over the East African margin and the Arabian platform during the Late Liassic, heralding this time the full separation of East and West Gondwana (Hughes 1988, Grabowsky & Norten 1995, Reynolds et al. 1997, Geiger et al. 2004). Despite the differences in facies associations and depositional systems in the two basins, *Unit II* can be correlated across these basins with low to moderate uncertainty on the basis of similarities in stratigraphic position, palaeocurrent patterns and the common U2 unconformity.

**Unit III**

The uppermost stratigraphic unit, which is recognised only in the Mekelle Basin, is Middle Jurassic (Late Toarcian to Early Callovian) in age. Rich microflora has been recovered from the lagoonal deposits in the lower part of the unit in the Agwe, Abiadi and Wukro areas. The assemblage is dominated by *Callialasporites* and *Araucariacites* with concomittent decline in the abundace of *Classopollis* and *Spheropollenites*, which may correspond to the *Callialasporites turbatus* Oppel Zone of Helby et al. (1989). This assemblage is indicative of a Late Toarcian to Bajocian age for the barrier-lagoon deposits. Vertebrate remains, especially piercing teeth of a marine crocodile (*thalattosuchian*) recovered from the basal transgressive lag deposits in the Wukro area also suggest a Toarcian age (cf. Westphal 1962, Pierce & Benton 2006). In the upper part of the succession, the predominance of highly sculptured triletes, such as *Concavissimisporites variverrucatus*, *Impardecispora* sp. *Ischyosporites crateris*, *Klukisporites volkheimeri* and *Converrucosisporites* sp., points to a Bathonian to Callovian age (e.g., Reyre 1973). However, the upper boundary of *Unit III* is further constrained by fairly rich foraminifera fauna (e.g., *Nauitiloculina oolithica*, *Praekurnubia crusei*, *Valvulina* gr. *negeoni*, *Kurnubia palestiniensis*, *Trochamina* sp. and *Cylindroporella* sp.) recovered at the base of the overlying Antalo Limestone, indicating Late Callovian to Early Oxfordian age (Bosellini et al. 1997).

In the Blue Nile basin, there is no siliciclastic unit that can be correlated with *Unit III* of the Mekelle Basin. Instead, a 450 m thick evaporite-dominated succession (Gohatsion Formation of Assefa (1981)) that crops out in the eastern part of the basin is considered the equivalent of *Unit III*. The U3 unconformity that separates the *Units II* and *III* in the Mekelle basin is marked by widespread pedogenesis and subsequent lateritisation that was developed on abandoned delta plain sediments. In the western and southwestern part of the Blue Nile Basin, U3 is overlain by the Tertiary trap basalts. Towards the east (e.g., in the Dejen area), however, the nature of U3 is very ambiguous. An abrupt change in facies succession can readily be discernible across U3 from coarse sandy upper shoreface facies of *Unit II* to the overlying evaporite-dominated Gohatsion Formation. Nonetheless, the lack of age diagnostic fossils in the Gohatsion Formation impedes to constrain the upper age limit. The base of the

equivalent Hamanlei Formation in the Ogaden Basin contains *Vidalina martana*, *Lingulina tenera* and *Orbitopsella praecursor*, indicating a Pliensbachian age (ELF-Somalia, unpubl. rep. 1977, in Bosellini 1989, Geletu 1998). If the reported diachronity from the southeast (i.e., the Ogaden Basin) towards the northwest (i.e., the Blue Nile Basin) holds true, the Toarcian age assignment to *Unit II* in the Blue Nile Basin appears to be reliable.

The nature of U4 unconformity at the top of *Unit III* in the Mekelle Basin remains to be the most controversial. According to Bosellini et al. (1997), the contact to the overlying Antalo Limestone (his "Antalo Supersequence") is gradational. The author considered the lowermost 20-30 m mixed carbonate and clastic succession as "Transitional Beds". Nonetheless, field observation indicates that the succession is composed of marls and shales with intercalated oolitic/bioclastic calcarenites and bioturbated sandstones with abundant brachiopods, bivalves and crinoids. This facies association suggests a transgressive barrier-lagoon depositional environment. The fossiliferous calcarenites and sandstones represent storm washover deposits. The few intercalated massive reddish brown mudstone layers, upon which the interpretation of Bosellini et al. (1997) is based, are bioturbated and rooted but do not show well-developed soil texture and soil horizons. These layers are rather interpreted to represent fringing marsh deposits associated with the backbarrier lagoons. Therefore, the subaerial exposure surface U4 should be placed at the base of the so-called 'Transitional Beds'.

## 8. Geodynamic stages of basin evolution and depositional models

A common feature of all types of sedimentary basins is that they owe their origin to crustal subsidence relative to surrounding, often uplifted, areas. In any stratigraphic study, the type of basin that hosts the sedimentary succession under analysis is the fundamental variable that needs to be constrained in regard to depositional strike and dip directions within the basin, the general structural style of the basin and the location and type of faults or folds. This task can easily be achieved by conducting a regional seismic survey. However, in the absence of any kind of regional subsurface data, outcrop-based stratigraphic analysis, i.e., the spatial and temporal stacking patterns of depositional systems that fill the basin, remains to be the only means of deciphering the structural mechanisms that control the formation of the basin. In this context, the various geodynamic stages in the evolution of the Mekelle and Blue Nile basins could apparently be understood by comparing the stratigraphic architecture as well as the nature and position of unconformities in the Late Triassic–Middle Jurassic sedimentary succession with the principal tectonic events that affected Gondwana during that time. Hence, this section attempts to outline the geodynamic stages of basin evolution and proposes depositional models for the various stratigraphic units recognised and discussed in the previous sections.

### Phase 1. Post-rift thermal subsidence: a stable passive margin-type basin (Late Triassic)

The term 'post-rift' refers to the period subsequent to the Karoo rift system that was inferred to have terminated at the end of the Middle Triassic (Geiger et al. 2004). If the Toarcian rifting is taken into account, this phase can also be referred to as "pre-rift" phase. This evolutionary phase summarises how the accommodation space was developed for the deposition of the lower stratigraphic unit (*Unit I*), which is inferred to contain transgressive tide-dominated estuarine and prograding (regressive) storm-dominated shoreface deposits.

The widespread occurrence of tide-dominated estuarine deposits at the lower part of the unit suggests the existence of a coastal embayment(s). The overall northeastward-

thickening wedge-shaped geometry of the depositional body and palaeocurrent directions derived from tidal channel fills and elongate tidal bars point to the fact that the embayment was open towards the northeast, where it ultimately opened to the Neotethys. The general similarity in the stratigraphic position, facies and depositional trends of *Unit I* in the Mekelle and Blue Nile basins suggests that the two basins might have been structurally linked during the Late Triassic. This indicates that the Late Triassic shallow gulf, which encroached into the Arabian platform from the northeast (Le Nindre et al. 1990a, b), had most probably reached the northern and central parts of Ethiopia (see Fig. 10.1). The connection of Saudi Arabia with Ethiopia through a Neotethyan seaway has an important bearing on the palaeotectonic and palaeogeographic scenario of the region; a topic which will be addressed in more detail in Sec. 10.

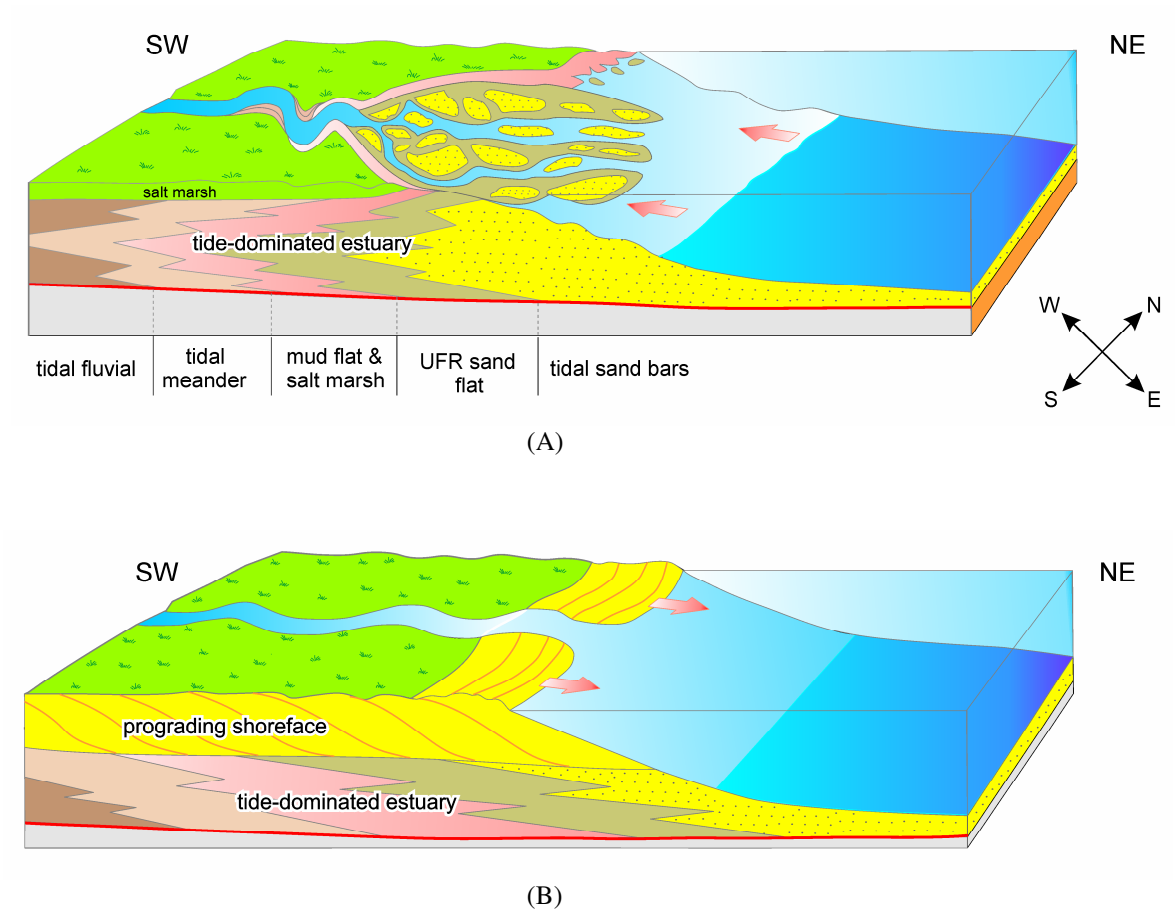


Fig. 8.1. A common depositional model for *Unit I* in both the Mekelle and Blue Nile basins. A. Relative sea level rise causing flooding of the coastal area and resulting in the formation of trasgrassive tide-dominated estuarine system. B. Relative sea level fall causing basinward progradation of the shoreface. Arrows mark the migration directions of facies belts.

The question is whether this coastal embayment initially originated as a lowstand incised valley or as a broad structurally defined embayment. In contrast to flooded river valleys, which scale generally to the size of the associated river system, significantly wider coastal embayments can be formed by broad tectonic variation in subsidence rate or localised structural faults or folds (Willis 2005). The development and preservation of tidal rhythmites within the basal estuarine deposits in most of the studied areas have significant implications on the structural aspects of the depositional setting, primarily in regard to basin geometry and

water depth. Cyclic rhythmites develop in settings with elevated tidal range, i.e., in macrotidal settings (Dalrymple & Makino 1989, Tessier et al. 1995). Although tidal range and strength of tidal currents along particular segments of coastlines are controlled by a complex set of variables, the following four are inferred to be the most important ones: (i) the orientation of the shorelines relative to progression of tidal wave, (ii) the geometry of bathymetric shoaling, (iii) the presence or absence of shallow seaways connecting larger bodies of water, and (iv) tidal resonance where basin dimension match a harmonic of the tidal wave (Archer & Hubbard 2003, Dalrymple 1992, Open University Team 1989). High tidal range and faster tidal current speeds require a strong degree of tidal resonance (broadly a function of basin length) and progression of the tidal wave around the basin (a function of bathymetric irregularities in the basin) (Dalrymple 1992). Therefore, the presence of tidal bundles suggests that the basin have possessed sufficient length, which is in the order of several hundred kilometers (cf. Open University Team 1989), to reach resonance and to allow a progressive wave to oscillate and resonate with the open oceanic tides. Moreover, the basin floor must have had significant bathymetric irregularities that have restricted the progression of the tidal wave around the basin so that rising tides could be funnelled into the estuaries to raise the tidal range. Consequently, an initial origin as flooded river valley(s) is less likely for the whole basin, since these are too narrow to significantly restrict the patterns of ocean circulation. In summary, the basin must have initially evolved as an intracratonic embayment (a semi-enclosed gulf) and represents a part of a significantly wider and deeply embayed coastline along the southwestern margin of the Neotethys. The depositional model for *Unit I* is presented in Fig. 8.1a & b.

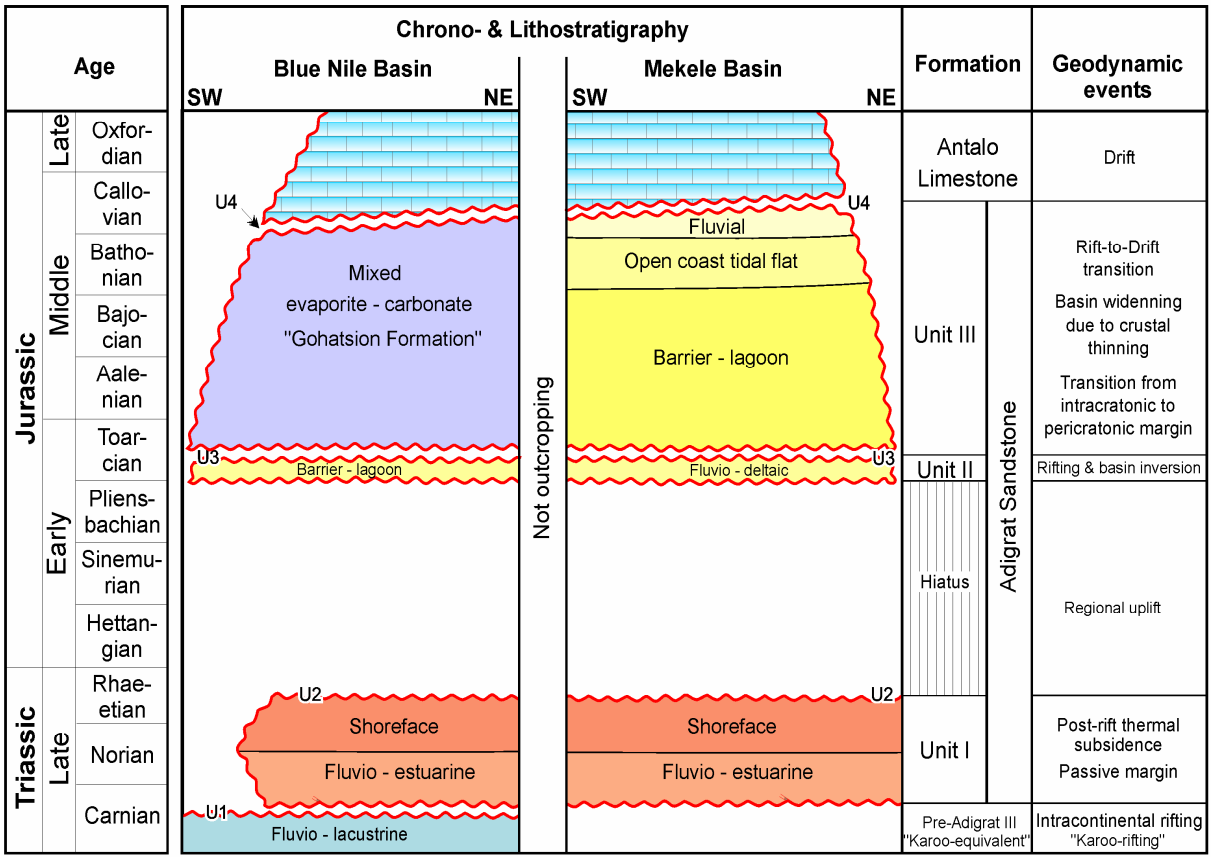


Fig. 8.2. A summary of the stratigraphy of northern and central Ethiopia with the corresponding geodynamic events.

**Phase 2. Regional Uplift (Early Liassic)**

This phase corresponds to a period of nondeposition and/or erosion in northern and central Ethiopia as it was manifested by emergence and widespread oxidation, as well as partial erosional unroofing of the Late Triassic and older successions. In western Ethiopia, along the border to Sudan, exposure of basement rocks over wide areas and the absence of pre-Late Triassic successions might be related to Early Liassic erosion. The Late Triassic succession survived this erosion, owing most likely to the fact that it was deposited in a coastal embayment. Crustal uplift during the Early Liassic affected not only northern and central Ethiopia but also the whole East African margin and the Arabian platform, resulting in an extensive depositional hiatus in the sedimentary record of the region (see Sec. 9, Fig. 9.1). Widespread erosion related to the Early Liassic thermal uplift in the East African margin is well-documented by Hankel (1994) and Geiger et al. (2004), and in the Arabian platform by Murris (1980), Sharland et al. (2001) and Al-Husseini (2008).

Moreover, volcanic activity most probably associated with the Early Liassic regional uplift was recorded in various localities. The most important ones are: (i) up to 25 m thick basaltic seals in several places of northwestern Somalia (Beydoun 1970, Abbate et al. 1987), (ii) up to 200 m thick volcanic succession containing alternating lava flows and pyroclastics, which was penetrated by an oil-well drilled in northeastern Somalia (Elf Somalia unpubl. rep. 1972, in Bosellini 1989), (iii) WSW-ENE striking basaltic dikes in Yemen (Kainz 1990), (iv) in southern Somalia, Tanzania and Madagascar (Hankel 1994). Further to the north, intensive volcanic activity of Early Liassic age was recorded by the Asher volcanics in the Levant (Gvirtzman et al. 1992).

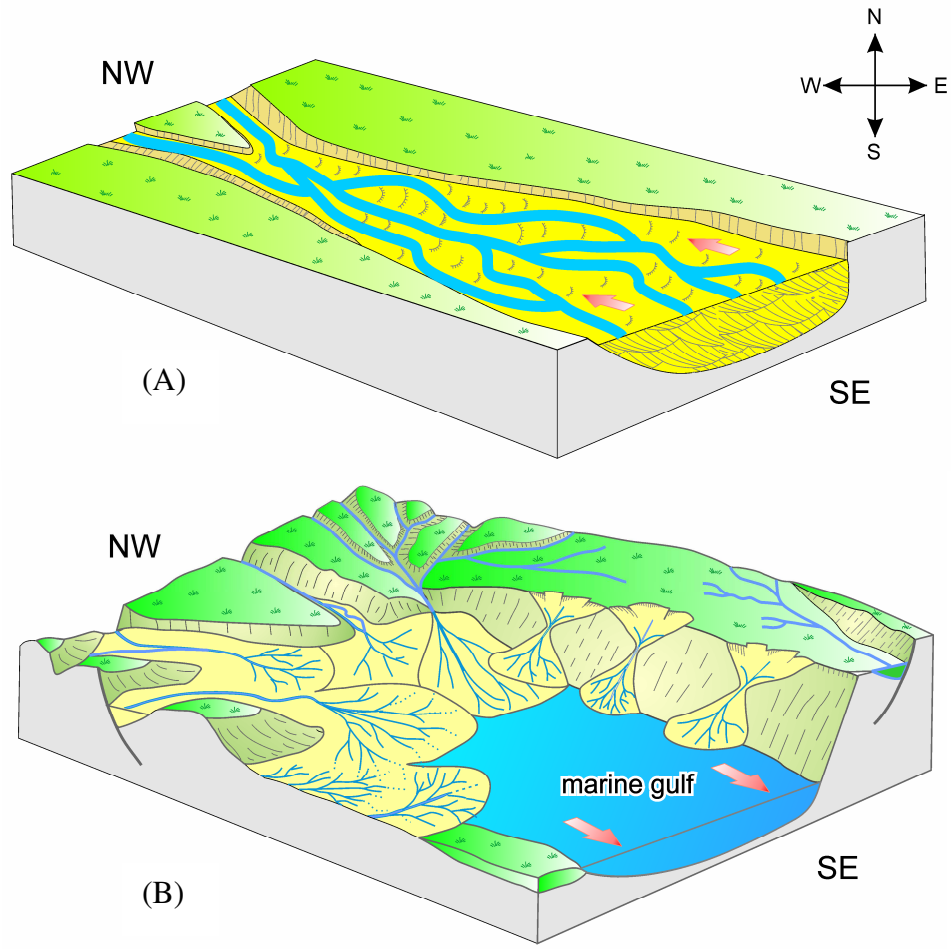

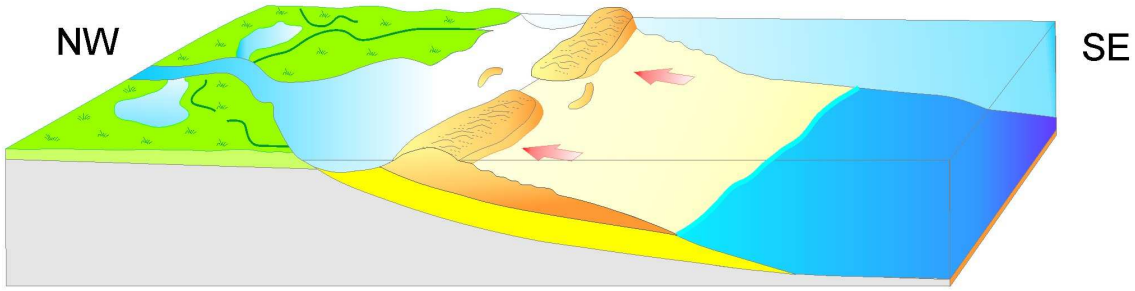


(C)

Fig. 8.3. Depositional models for *Unit II*. A. fluvial 'incised valley' fill deposits, and B. prograding deltaic deposits ('Gilbert-type' fan delta) in the Mekelle Basin. C. Transgressive barrier-lagoon deposits in the Blue Nile Basin. The most important factors that brought about these differences in depositional systems within *Unit II* in the two basins are the source and supply of sediments, the variation in coastal morphology, and the role of waves, tidal- and river currents. Arrows mark the migration directions of facies belts.

**Phase 3. Syn-rift phase: a phase of basin inversion (Late Liassic)**

This phase corresponds to a major change in the structural configuration of the basin from a stable, northeast-facing passive margin to an active southeast-facing pericratonic downwarp that opens to an evolving divergent margin between East and West Gondwana. During this time, the NE-directed drainage system was abandoned and a southeast-oriented drainage system was established. In other words, the depositional dip was inverted from the northeast to the southeast, suggesting basin inversion.

In the Mekelle Basin of northern Ethiopia, an extensive valley system was incised into the underlying shoreface deposits during a major relative sea level fall in the Late Liassic. The valleys were filled with amalgamated braided channel sandstones during the subsequent relative sea level rise (Fig. 8.3a). The valley fill deposits are dominantly coarse-grained to pebbly and suspended-load deposits are rare. Sets and cosets are often vertically stacked, suggesting broadly vertical accretion prevailed. This monotonous palaeovalley fill is therefore inferred to record high rate of sedimentation caused by enhanced sediment supply. Palaeocurrent directions from basal fluvial deposits suggest that the basin has started to experience a half-centripetal drainage system opened to the southeast. Continued oversupply of sediments resulted in the progradation of 'Gilbert-type' deltas (Fig. 8.3b). The formation of 'Gilbert-type' deltas requires coarse-grained sediment supply from possibly fault-bounded steep-sided canyons draining directly into a standing body of water (Gawthorpe & Colella 1990, Wescott & Ethridge 1990). Palaeocurrent directions suggest that the coarse clastic wedge was also shaded in a half-centripetal manner from the north and the west towards a common central point, which may have been situated in the vicinity of the town Mekelle. This implies the existence of an uplifted source area further to the west and north of the towns Abiadi and Megab. Thus, the fluvio-deltaic deposits indicate that the basin has evolved from a northeast-deepening passive margin to a southeast-facing, possibly fault-controlled, broadly downwarping basin with margins characterised by a relatively steep coastal to nearshore profile.

In the Blue Nile Basin of central Ethiopia, the syn-rift phase corresponds to the deposition of an extensive inlet/spit-dominated barrier sand carpet (*Unit II*, Fig. 8.3c). The sheet-like geometry and the wide areal extent of the unit is attributed to the lateral growth of the barrier complex through coast-parallel inlet channel migration and spit elongation (Hoyt

1967, Swift 1975). Such barrier development is more common along steeper, higher relief coastal zones of tectonically active margins (Hayes 1975, Nummedal & Swift 1987). Palaeocurrent patterns from tidal inlet channel and flood tidal delta deposits indicate SE- and NW-directed ebb- and flood tidal flows respectively, suggesting transgression generally from the southeast. This transgression is most likely associated with the encroachment of a shallow gulf to the central and northern Ethiopia from the southeast.

Thus, the newly developed gulf represents a part of the northwestward-branching epicontinental seaway that penetrated between the Arabian and Indian Shields. This long and branching seaway is supposed to widen towards the Tethyan ocean to the northeast (cf. Scotese 1991, Riccardi 1991, Reynolds et al 1997). Most workers (e.g., Besairie & Collignon 1972, Bosellini 1989, Mette 1993, Luger et al. 1994, Plummer 1994, Reynolds et al. 1997) proposed that this transgression was the result, in part, of the rifting stage heralding the Gondwana break-up and in part of a global rise in eustatic sea level (Haq et al. 1987, Hallam 1988). The Toarcian was a period of widespread extensional deformation of both continental and oceanic crust (Bassoullet et al. 1993). Early Toarcian age transgressive-regressive depositional episode in the region (e.g., in Ogaden, Mandera-Lugh and Ahl-Mado basins) have been unequivocally confirmed by Foraminifera and Ammonite findings (cf. Bosellini 1989, Mette 1993), which appears to correlate well with the third order depositional cycle 'UAB-4-4.3' of Haq et al. (1987).

**Phase 4. Post-rift thermal subsidence (early Middle Jurassic)**

In the Mekelle basin, this phase corresponds to delta abandonment and the inception of transgressive barrier-lagoon system, which is most probably related to the continuous crustal thinning and subsidence along the evolving rift between East and West Gondwana. Following delta abandonment, which is marked by widespread lateritisation of the delta plain deposits, a process of transgressive submergence took place in which several cycles of barrier-lagoon complexes migrated northeastward (i.e., inferred landward direction during deposition of *Unit III*, Fig. 8.4a). The formation of barrier-lagoon complex, in part, reflects the tectonic setting of the basin. They preferentially develop on stable, relatively flat, low-gradient coastal plain to nearshore settings along passive continental margins or broad cratonic seaways (Davis 1994). They also require steady longshore sediment supply and low to moderate tidal range for their sustained development (Glaeser 1978). In this context, the presence of laterally continuous barrier-lagoon deposits in the Mekelle basin may suggest that the basin have evolved from a possibly fault-controlled, broadly downwarping basin to a southeast-facing cratonic seaway characterised by low-gradient coastal to nearshore profile and micro- to mesotidal range. The landward migration of the barrier-lagoon complex over the abandoned delta plain is attributed to the marine transgression progressing from the southeast as the rate of sea level rise exceeds the rate of sediment supply (cf. Boyd et al. 1992). The preservation and vertical accretion of several barrier-lagoon cycles records a very rapid rate of sea level rise (Davis & Clifton 1987). Slower rate of sea level rise would have facilitated shoreface erosion.

**Phase 5. Rift-to-drift transition (late Middle Jurassic)**

This phase is characterised by barrier destruction and establishment of an open-coast tidal flat system. As relative sea level starts to fall, the elongate shoestring sand bodies of the uppermost barrier were destructed and cannibalised by a number of tidal inlet channels which cut through them. The destruction of barriers was concomitantly accompanied by the establishment of prograding open-coast tidal flats and strandplains as the rate of sediment

supply exceeded the rate of sea level rise. Continued fall in sea level resulted in placing the new fluvial graded profile above the topography (termed as 'positive fluvial accommodation' by Shanley & McCabe (1994)) by enhancing the sediment load relative to the transport capacity of the rivers. This process triggered fluvial aggradation at the top of the stratigraphic succession.

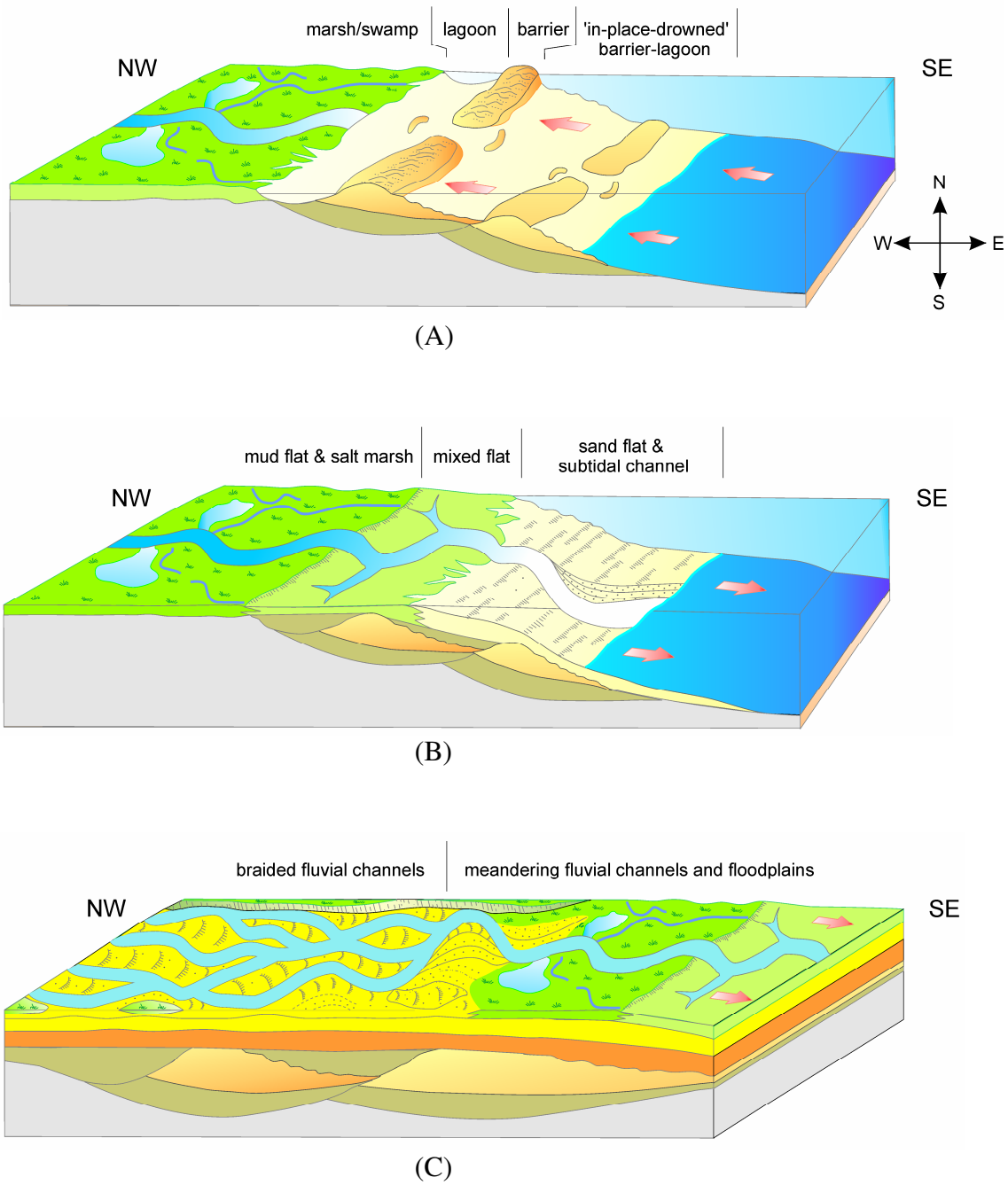


Fig. 8.4. Depositional models for *Unit III* in the Mekelle Basin. A. Renewed rise in the relative sea level resulting in the landward migration of transgressive barrier-lagoon deposits (rapid rise in relative sea level resulted in 'in-place drowning' of previously deposited barrier and the formation of a new one on the landward side). B. Falling relative sea level resulting in the progradation of open coast tidal flat over the barrier-lagoon. C. Continued fall in the relative sea level led to fluvial aggradation over tidal flat deposits. Note that the equivalent of *Unit III* in the Blue Nile Basin are the evaporite deposits of the Gohatsion Formation.

## 9. Regional correlation

The Late Triassic-Middle Jurassic depositional epoch throughout the East African margin and the Arabian platform is characterised by the development of numerous mixed clastic-evaporite, evaporite-carbonate and clastic-carbonate units with boundaries reflecting regional shifts in tectonic and hydrographic regimes. Many of these stratigraphic units are known only in general terms and have not been studied in sufficient detail to permit detailed correlation. In the Mekelle Basin of northern Ethiopia, the units are entirely composed of siliciclastic sediments, whereas in the Blue Nile Basin of central Ethiopia they are made up of mixed clastic-evaporite sediments. The basal clastic succession which is widespread in the region is collectively known in Ethiopia and Somalia as the "Adigrat Sandstone". In the following section, this sandstone succession and the embedded stratigraphic units identified in the Blue Nile and Mekelle basins will be correlated with other contemporaneous stratigraphic units in the southeastern Ethiopia, Eritrea, southern Arabian Peninsula (Saudi Arabia and Yemen), Somalia, Kenya, Tanzania, Madagascar and western India.

In the ***Ogaden Basin*** of southeastern Ethiopia, up to 250 m thick siliciclastic succession of continental origin, also referred to as "Adigrat Sandstone", was penetrated by a number of wells and was reported to contain microflora of Rhaeto-Liassic age (Worku & Astin 1992, Geletu 1998). In contrast, a Hettangian to earliest Toarcian age has been assigned to microflora recovered from the same wells (O. Hankel, pers. comm., in Mette 1993). Relying on the core description of Worku & Astin (1992), the succession exhibits more similarity with *Unit II* than *Unit I*. Thus, the succession could not certainty be correlated with *Unit I* of the Mekelle and Blue Nile basins. Generally, the existence of Late Triassic deposits in the Ogaden Basin that are equivalent to *Unit I* of the Mekelle and Blue Nile basins is highly questionable. Upwards in the succession, the presence of *Orbitopsella praecursor* in the lower Hamanlei Formation indicates a Pliensbachian to Early Toarcian age (Geletu 1998), which appears to be partly the equivalent of *Unit II* (Fig. 9.1). The middle and upper Hamanlei Formations of the Ogaden Basin are correlative to *Unit III* of the Mekelle Basin and the Gohatsion Formation in the Blue Nile Basin.

In the ***Red Sea Hills*** of southeastern Eritrea, the Adigrat Sandstone succession is reported to reach up to 1,775 m in thickness (Hutchinson & Engels 1970). Although biostratigraphic evidence is poor the succession is supposed to be the equivalent of the Adigrat Sandstone of the Mekelle and Blue Nile basins (Bosellini et al. 1997). In south-central Eritrea, Kumpulainen et al. (2006) have identified a siliciclastic succession, which they referred to as "Another Sandstone". Based on palaeocurrent patterns the succession might be correlative to *Unit I* of the Mekelle and Blue Nile basins. No correlative equivalent units are known in Eritrea for *Units II* and *III*.

In ***northern Somalia*** outcrops of Late Triassic deposits are unknown in most localities. However, straite bisaccates indicative of Permian to Early Triassic age are reported from a 127 m thick 'Karoo-equivalent' siliciclastic succession in a well drilled in the Hafun area of northeastern Somalia (ELF Somalia, unpubl. rep. 1972, in Bosellini 1989). In northern Somalia, basins developed during the Toarcian rifting include the Berbera, Bihendula-Borema and Ahl Mado basins. In the Berbera and Borema basins, a 130 m thick fluvial to coastal plain succession, referred to as "Adigrat Formation", is underlain by Early Liassic basalt flows and passes upwards into Bihen Limestone of Late Bathonian–Callovian age (Bruni & Fazzuoli 1977). These two formations can broadly be correlated to *Units II* and *III* of the Mekelle Basin, whereas only the lower part of the so called "Adigrat Formation" is correlative to *Unit II* of the Blue Nile basin. Similarly, the Adigrat and the Dhadhabo formations of the Ahl Mado Basin are considered equivalent to *Unit II* of the Mekelle and Blue Nile basins. *Unit III* in the Mekelle Basin is correlative to the Qarariye, Dahab and Garura formations of the Ahl Mado Basin.

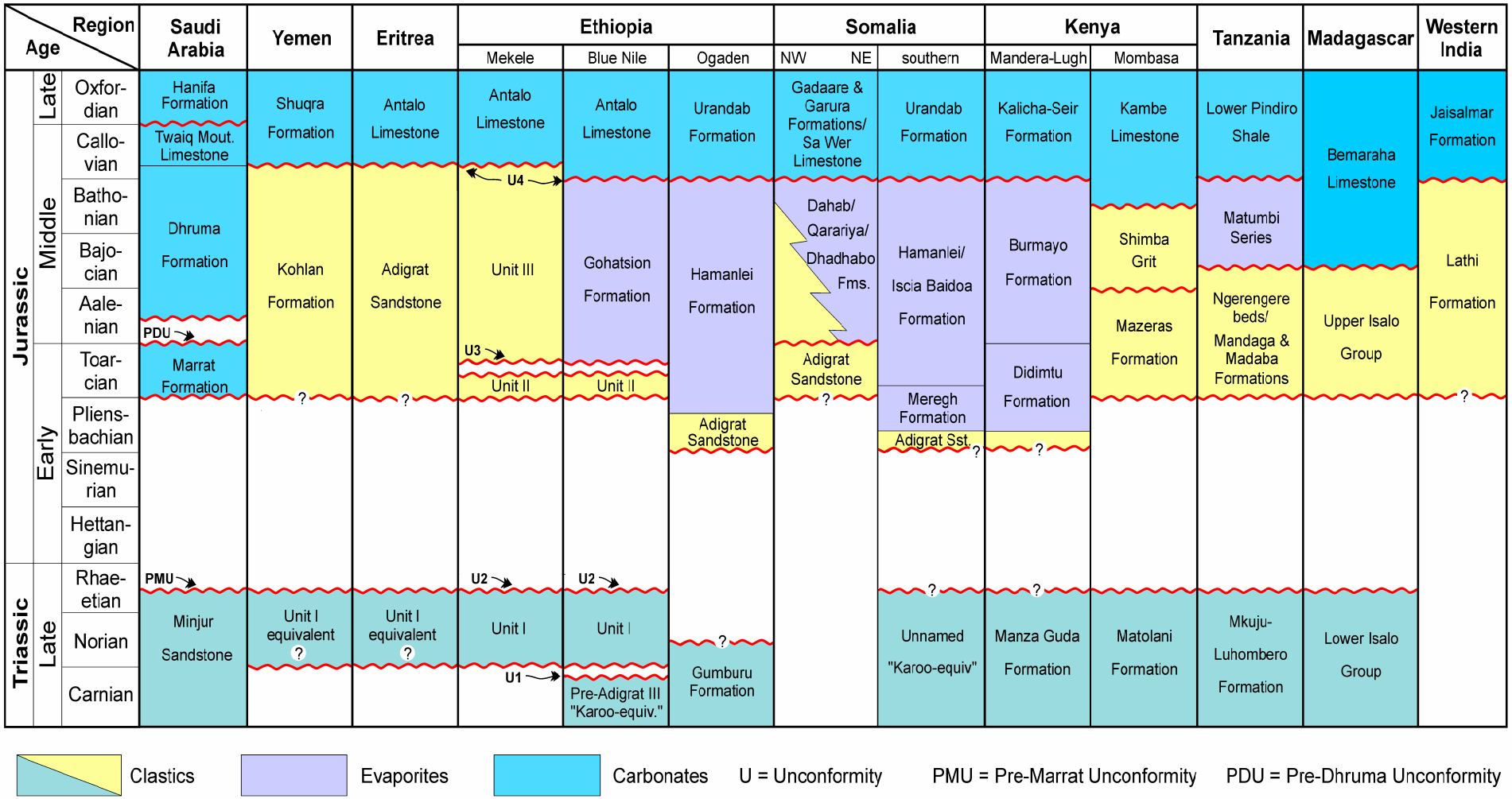


Fig. 9.1. Regional correlation chart for the Late Triassic to Middle Jurassic stratigraphic units of the Blue Nile and Mekele basins with equivalent units in East Africa and the Arabian platform. See text for main data sources.

In ***southern Somalia***, up to 120 m thick siliciclastic succession overlying the Karoo sediments was penetrated by wells drilled in the Mandera-Lugh and Mudugh basins. The succession was described to be composed of "well-sorted light grey quartzarenites" (Esso unpubl. rep. 1987, in Bosellini 1989). Based on lithologic similarity the succession can be correlated to *Unit II* of the Mekelle and Blue Nile basins. Other formations in southern Somalia that can be correlated with *Unit II* and *III* are the Meregh and Iscia-Baidoa formations. The apparent absence of the Late Triassic to Early Liassic in most localities of northern Somalia suggests that uplift and erosion might have been active across these areas during this time.

In ***Yemen*** a siliciclastic succession of up to 280 m thick, originally defined by Lamare (1930) as "Kohlan Formation", is supposed to be of Middle Jurassic age (Beydoun 1997). In the entire area of the Gulf of Aden, the formation is either missing or its thickness is fairly reduced. According to Bosellini (1989), sediment accumulation took place in a 200–300 km wide NE-trending depression representing probably an alluvial plain. The succession is not yet well-differentiated but might be broadly correlative to the Adigrat Sandstone of northern and central Ethiopia.

In ***central Saudi Arabia***, clastic and evaporitic shallow marine sediments that crop out in a north-south trend along the eastern margin of the Arabian Shield were reported to contain ammonoids and conodonts of Norian age (Le Nindre et al. 1990a, b). The succession is referred to as "Minjur Sandstone" (Enay et al. 1987, Sharland et al. 2001) and can be correlated to *Unit I* of the Mekelle and Blue Nile basins. Furthermore, the U2 unconformity recognised in the two basins can be correlated to the well-known Pre-Marrat Unconformity (Fig. 9.1) identified throughout the Arabian platform (Al-Husseini 2008). Uplift and widespread erosion during the Early Liassic (Hettangian–Plienbachian) is well-documented in the Arabian platform. This scenario seems to hold true for central and northern Ethiopia as well as Eritrea since Late Triassic deposits in these areas were also uplifted, partly eroded and extensively oxidised before the deposition of the overlying units. *Unit II* can be correlated to the Marrat Formation of central Saudi Arabia whereas *Unit III* is equivalent to the Dhruma Formation and the Twaiq Mountain Limestone. Moreover, the U3 unconformity can broadly be correlated to the Pre-Dhruma Unconformity (Enay et al. 1987, Sharland et al. 2001, Al-Husseini 2008).

In ***Kenya*** siliciclastic succession of probable continental origin overlying sediments of the Karoo strata have been reported by Cannon et al. (1981) and Rais-Assa (1988). The succession is referred to as the Mazeras Formation in the Mombasa Basin of southern Kenya. Based on the presence of microflora belonging to the *Callialasporites turbatus* zone this formation was dated as late Early Jurassic (Rais-Assa 1988, Hankel 1987, 1994). Thus, the Mazeras Formation is correlative to *Unit II* of the Mekelle and Blue Nile basins. The Manza Guda Formation in northeastern Kenya is not yet differentiated but numerous reports (e.g., Temperley 1952, Joubert 1963, Lundin Petroleum 2007, unpubl. rep.) suggested that it is equivalent to Karoo strata of other parts of Kenya. Stratigraphic units that are equivalent to *Unit III* are the Shimba Grit and the Kambe Limestone of the Mombasa basin (Hankel 1994).

In ***Tanzania*** successions equivalent to *Units II* and *III* are the Madaba and the Mandanga formations respectively, both of them in the Luwegu Basin (Hankel 1994). In the Mandawa basin of southeastern Tanzania, dinoflagellate and microfloral evidence suggest that the Ngerengere Beds and the Matumbi Series are of Toarcian to Bathonian age (Balduzzi et al. 1992). Hence, they can be taken as correlative equivalents of *Unit II* and *III* of the Mekelle and Blue Nile basins.

In ***Madagascar*** the presence palynological assemblages belonging to the *Callialasporites turbatus* and *Dictyotosporites complex* zones in the Upper Isalo Group of the Morondava Basin indicates a Toarcian to Early Bajocian age (Besairie 1971, Hankel 1994). Thus, the Upper Isalo Group can be correlated to *Unit II* and the lower part of *Unit III* of the

Mekelle basin whereas the Lower Beharama Limestone is considered to be equivalent to the upper part of *Unit III*.

In ***western India*** up to 300 m thick siliciclastic succession of deltaic to shallow marine origin (Lathi Formation) has been described from the Rajasthan Basin (Poddar 1964). Subsurface samples from the succession have yielded a rich microfloral assemblage indicative of latest Early to Middle Jurassic age (Srivastava 1966). Thus, the Lathi Formation can be broadly correlated to *Units II* and *III*.

In summary, according to the lithostratigraphic and biostratigraphic evidences reported above, it is striking to note that Early Liassic sedimentary records are absent in Somalia, Kenya, Tanzania, Madagascar and India, suggesting a major break of probable regional extent. This significant hiatus is most probably related to the regional crustal uplift that affected the whole East African margin and is accompanied by volcanic activities that were apparently documented, for example, in several parts of Somalia, Yemen, Tanzania and Madagascar (Beydoun 1970, Abbate et al. 1987, Elf Somalia unpubl. rep. 1972, in Bosellini 1989, Kainz 1990, Hankel 1994).

# 10. Palaeogeographic Evolution

## 10.1. Introduction

At the beginning of the Late Triassic, intraplate extensional deformation ceased in southeastern Gondwana and was replaced by a major crustal uplift and accompanied intraplate magmatic activity. In contrast, the northeastern part of East Africa and Arabia formed part of a stable and slowly subsiding Neotethyan passive margin. The onset of rifting in the Neotethys during the Early Jurassic terminated the period of relative tectonic quiescence that characterised the region during the Late Triassic, heralding the full separation of East and West Gondwana (Reynolds et al. 1997). Crustal extension and rifting that continued throughout the Middle Jurassic, enhanced by global eustatic sea level rise (Haq et al. 1987), caused marine transgressions that flooded wide areas of East Africa. Furthermore, the NE-inclined depositional dip was inverted towards the southeast, i.e., towards the developing rift between East and West Gondwana.

The Early to Middle Jurassic therefore represents a critical time interval for the development of the East Africa-Madagascar conjugate margins, when the transition from a very long and complex continental rifting to the development of oceanic spreading and passive margins took place. An overall continuous geodynamic evolution since the Permian has been proposed by some authors (e.g., Coffin & Rabinowitz 1987, Hankel 1994, Wopfner 1994) whereas others (Geiger et al. 2004; Geiger & Schweigert 2006) point to a significant interruption during the earliest Jurassic. The latter breakup model attributes the Permian–Triassic Basin to a pre-rifting stage of the Gondwana breakup whereas the effective breakup occurred as a short-lived rifting stage during the Toarcian–Aalenian. Drifting and oceanic spreading commenced during the Jurassic Magnetic Quite Zone (Callovian-Early Oxfordian) (Haq et al. 1987). The oceanic crust flanking Somalia and Madagascar is the oldest crust yet dated in the Indian Ocean (Rabinowitz et al. 1983, Coffin & Rabinowitz 1987). However, others (e.g., Hankel 1994, Geiger et al. 2004, Papini & Benvenuti 2008) dispute that the Early Bajocian flooding of the continental margins of East Africa and Madagascar is related to the initial phase of separation, which would imply that seafloor spreading started earlier than suggested previously.

Fig. 10.1. Late Triassic palaeogeography of East Africa and the southeastern part of the Arabian platform (modified after Schandelmeier et al. 1997).

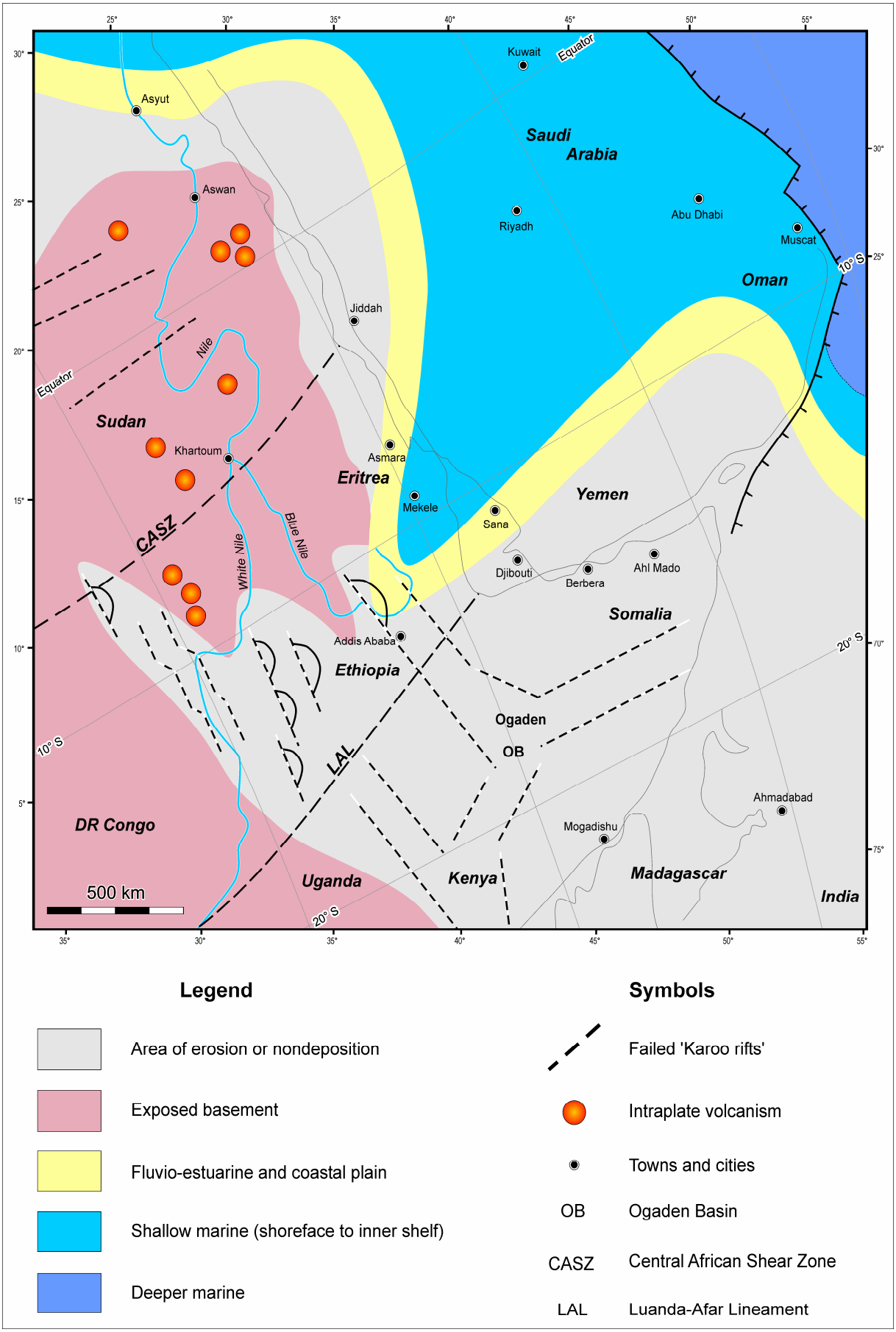
Kuwait
Equator
Asyut
Saudi Arabia
Aswan
Riyadh
Abu Dhabi
Muscat
10° S
Oman
Jiddah
Nile
Equator
Sudan
Khartoum
Asmara
Eritrea
Mekele
Sana
Yemen
CASZ
White Nile
Blue Nile
Djibouti
Berbera
Ahl Mado
Somalia
Addis Ababa
Ethiopia
20° S
Ogaden
OB
LAL
10° S
Ahmadabad
DR Congo
Mogadishu
Madagascar
Uganda
Kenya
India
500 km
20° S
Legend
Area of erosion or nondeposition
Exposed basement
Fluvio-estuarine and coastal plain
Shallow marine (shoreface to inner shelf)
Deeper marine
Symbols
Failed 'Karoo rifts'
Intraplate volcanism
Towns and cities
OB Ogaden Basin
CASZ Central African Shear Zone
LAL Luanda-Afar Lineament

This section outlines the tectonic-palaeogeographic evolution of East Africa and adjacent regions in the interval between the Late Triassic and Middle Jurassic periods. The major structures, depositional and nondepositional areas, and the distribution of intraplate magmatic events are illustrated in Fig. 10.1 & 2.

## 10.2. The Late Triassic (Norian-Rhaetian)

The northward drift of Gondwana which started in the Late Palaeozoic continued throughout the Triassic and the Neotethyan ocean thus started to grow on the expense of the closing Palaeotethys (Sengör et al. 1988, Schandelmeier et al. 1997). In the Norian times East Africa and the Arabian platform were situated between lat. 20°N and 25°S. The Karoo rifts, which were best developed in the southern part of the East African margin „failed“ and the region was subjected to crustal uplift (Hankel 1994, Geiger et al. 2004). The uplift was accompanied by intraplate magmatic activity as recorded by the alkaline igneous complexes of central and northern Sudan (Fig. 10.1, Vail 1990, Müller-sohnius & Horn 1994).

In contrast to the situation in southern part of the East African margin, the Arabian platform and the northeastern African margin, including central and northern Ethiopia, were characterised by relative tectonic quiescence and formed part of a stable and slowly subsiding passive margin to the Neotethyan ocean in the northeast. A shallow gulf encroached from the northeast onto wide areas of the Arabian platform and propagated as far southeast as central Ethiopia. In Saudi Arabia, shallow marine clastics and evaporites (Minjur Sandstone) croping out on the southeastern margin of the Arabian Shield contain ammonoids and conodonts of Rhaeto-Norian age (Le Nindre et al. 1990a, b). In the Mekelle and Blue Nile basins, the presence of northeast prograding estuarine to shallow marine siliciclastics (*Unit I*) of Rhaeto-Norian age indicates that the two areas might have been connected through an epicontinental seaway widening towards the northeast (Fig. 10.1). The presence of a marine connection between Ethiopia and Saudi Arabia implies that the Arabian shield might have not been emergent during that time.

## 10.3. The Early Jurassic (Hettangian-Pliensbachian)

Between the Late Triassic and the Early Jurassic, Gondwana rotated anticlockwise with East Africa and Arabia showing only insignificant changes in the palaeogeographic location. In the Early Jurassic, the two areas were situated between lat. 15°N and 25°S (Fig. 10.2). Regional crustal uplift continued in the East African margin during the Early Liassic, and this time affecting also the Arabian platform. The base of the Marrat Formation that unconformably overlies the Minjur Sandstone in central Saudi Arabia was dated as Toarcian (Enay et al. 1987). Moreover, the pre-Marrat unconformity and the Hettangian-Pliensbachian depositional hiatus can be traced throughout the Arabian platform (Sharland et al. 2001, Al-Husseini 2008). The Arabian Shield might most probably have started to rise during this uplift episode, which may probably be related to compressional deformation associated with the establishment of subduction system in the north that consumed the Neotethyan lithosphere (Sengör et al. 1988). In the East African margin crustal uplift is accompanied by widespread Early Liassic intraplate magmatism in Yemen, Somalia, Tanzania and Madagascar (see Fig. 10.2).

Renewed extensional deformation recommenced along the East African margin during the Pliensbachian, heralding this time the full separation of East and West Gondwana (Bosellini 1989, Reynolds et al. 1997). An epicontinental seaway had already been established during this time following the NE-trending axis of the evolving rift that started to propagate into the supercontinent from its Tethyan margin (Wopfner 1994). Synrift sedimentation has

already reconvened along an actively subsiding intracratonic margin of East Africa (southeastern Somalia and Ogaden) during the Pliensbachian, as indicated by the occurence of *Vidalina martana*, *Lingulina tenera and Orbitopsella praecursur* recovered from several wells in the Ogaden, Mandera-Lugh and Mudugh basins (Bosellini 1989, Geletu 1998). In contrast, northern and central Ethiopia as well as adjacent areas (i.e., southern Yemen, northern Somalia, Kenya, Tanzania and Madagascar) must have remained areas of erosion and/or nondeposition, since Early Jurassic biostratigraphic evidence older than Toarcian is apparently missing.

### 10.4. The latest Early to Middle Jurassic (Toarcian-Callovian)

The latest Early to Middle Jurassic represents a critical time interval for the development of the East African-Madagascar conjugate margins, when the transition from a complex intracontinental rifting and regional crustal uplift to the development of oceanic spreading and passive margin took place. During the Middle Jurassic Gondwana rotated clockwise such that East Africa and Arabia lay between lat. 5°N and 30°S. Crustal extension and rifting continued and the seaway (also referred to as the Mozambique Channel (Wopfner 1993, 1994)) which started to open in the Pliensbachian continued to widen and propagate southwestward. The newly developing Gulf was bounded from the northeast and the southwest by the Arabo-Ethiopian High and the Indian Shield respectively (Fig. 10.2) where its shorelines have reached northern and central western Ethiopia, as well as southern Madagascar.

Active rift subsidence enhanced by eustasy resulted in a marine transgression, which flooded wide areas of East Africa and the Arabian platform. South-directed palaeocurrents from the basal clastics of southern Yemen and northern Somalia indicate a nearby sediment source, most probably the Hadhramut Saddle in the north (Bruni & Fazzuoli, 1977, Bosellini 1989, Mette 1993). In the Ahl Mado Basin, the clastic succession grades upward into a mixed evaporate-carbonate succession containing ammonites (*Bouleiceras* sp. and *Hildaites* sp.) indicating an Early Toarcian age (Mette 1993). In the Mekelle Basin of northern Ethiopia, coarse alluvial to deltaic deposits of Toarcian age (*Unit II*) transported towards the southeast suggest the occurrence of structural highs in the nearby north and northwest that provided increased sediment supply (Fig 8.3b). In the Blue Nile Basin of central Ethiopia well-sorted coarse-grained white to light grey sandstones and conglomerates deposited in a coastal to shallow marine environment indicate a NW-SE oscillating tidal flow path. Lithologicaly similar deposits that are overlain by the Hamanlei Formation have been described from the Ogaden, Mudugh and Mandera-Lugh basins in southeastern Ethiopia (Bosellini 1989, Geletu 1998). The Mazeras Formation and the upper part of the Didimtu Formation of Kenya, as well as the Madaba Formation and Ngerengere Beds of Tanzania represent the equivalents of the basal clastics of Ethiopia and northern Somalia (Cannon et al. 1981, Rais-Assa 1988, Hankel 1987, 1994). Palaeocurrent directions from the fluvio-deltaic complex in the Diego and Majunga basins indicate a NW-directed progradation from Madagascan hinterland into the newly developed gulf (Besairie & Collignon 1972). Similar palaeocurrent pattern was reported from the deltaic to shallow marine Lathi Formation of western India (Poddar 1964).

Synrift sedimentation dominated by mixed evaporitic and carbonate ramp-type deposits continued throughout the Middle Jurassic whereas accumulation of coastal to shallow marine siliciclastics was restricted to marginal areas of the evolving gulf. The intensive lithological variation and the increase in sediment thickness towards the rift axis both suggest synsedimentary tectonic movements. In the Mekelle Basin of northern Ethiopia, siliciclastic succession deposited in a transgressive barrier-lagoon environment changes upwards into prograding open-coast tidal flat (*Unit III*). The succession was deposited in a semi-circular

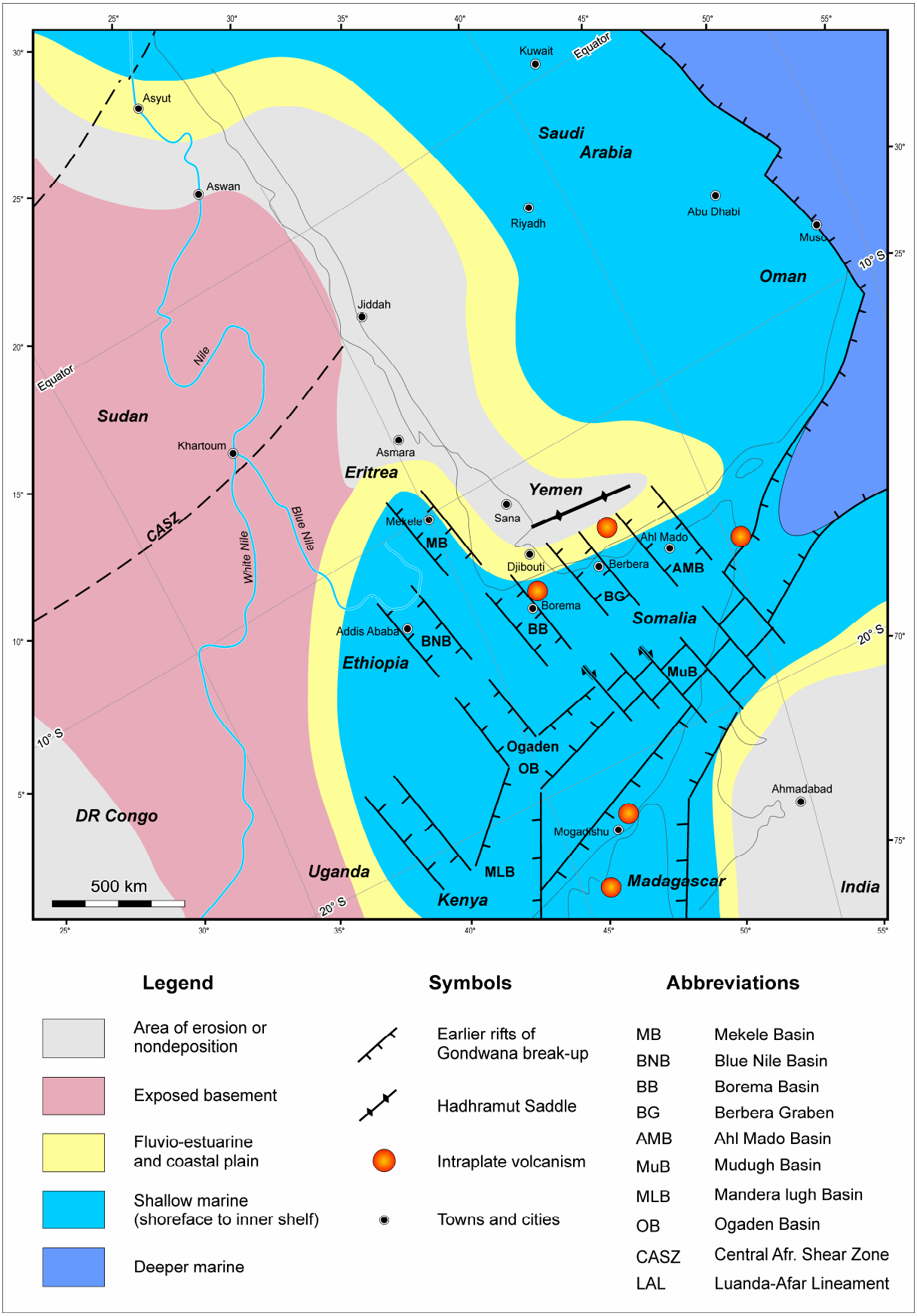


Fig. 10.2. Latest Early to Middle Jurassic (Toarcian–Early Callovian) palaeogeography of East Africa and the southeastern part of the Arabian platform (modified after Reynolds et al. 1997).

siliciclastic shoreline inclined to the southeast. In the Blue Nile Basin of central Ethiopia, however, evaporite accumulation continued until the Callovian, paralleled by mixed clastic-evaporite deposition in northern Somalia (Qarariye and Dahab formations) (Mette 1993). As deposition of mixed evaporites and carbonates was underway in the Ogaden Basin of southeastern Ethiopia, carbonate platforms had already been established in the Mandera-Lugh and Mogadishu basins of southern Somalia (Bruni & Fazzuoli 1977, Bosellini 1989). The gradual facies shift from mixed evaporite-carbonate to dominantly platform carbonates during the interval Toarcian-Bathonian is a widespread phenomenon in basins of East African margin, as evidenced by the Kambe Limestone of Kenya (Westermann, 1975), the Matumbi Limestone of Tanzania (Balduzzi et al. 1992) and, in Madagascar, by the '*Sonninia* and *Witchellia* bearing' beds of the Majunga and Diego Basin and the Lower Bemaraha Limestone of the Morondava Basin (Besairie, 1971).

## 11. Conclusions

1. *Stratigraphy*: The 'Adigrat Sandstone' succession in the Mekelle and Blue Nile basins consists of three unconformity bounded stratigraphic units that range in age from the Late Triassic to Middle Jurassic. *Unit I* (Late Carnian–Early Rhaetian) is composed of transgressive tide-dominated estuarine and prograding storm-dominated shoreface deposits. *Unit II* (Early Toarcian) is composed, in the Mekelle Basin, of fluvio-deltaic deposits whereas in the Blue Nile Basin the unit is of barrier/inlet-spit origin. *Unit III* (Late Toarcian to Early Callovian) in the Mekelle Basin is made up of transgressive barrier-lagoon, prograding open-coast tidal flat and fluvial deposits. The evaporite deposits of the Gohatsion Formation in the Blue Nile Basin represent the equivalent of *Unit III* in the Mekelle Basin.

2. *Basin evolution*: Based on comparison of the bio- and chronostratigraphic position of the 'Adigrat Sandstone' succession with the principal tectonic events that affected Gondwana during that time, five geodynamic stages of basin evolution have been identified: (a) post-rift thermal subsidence and the development of a stable passive margin-type basin during the Late Triassic; the two basins were structurally linked and represent parts of a vast shallow gulf which encroached from the northeast through the Arabian platform into northern and central Ethiopia; (b) regional crustal uplift during the Early Liassic that resulted in an extensive depositional hiatus in the sedimentary record of the region; (c) rifting and basin inversion during the Late Liassic; the basin evolved from a stable, northeast-facing passive margin to an active southeast-facing pericratonic downwarp that opens to the developing divergent margin between East and West Gondwana; (d) post-rift thermal subsidence during the early Middle Jurassic, which is most probably related to the continuous crustal thinning and subsidence along the evolving rift between East and West Gondwana; (e) rift-to-drift transition during the late Middle Jurassic which might correspond to the abandonment of previous irregular rift structures and their replacement with a laterally continouos depocenters prior to drifting in the Late Callovian.

3. *Palaeogeography implications*: During the Late Triassic northern and central Ethiopia were characterised by relative tectonic quiescence and formed part of a stable and slowly subsiding passive margin to the Neotethyan ocean in the northeast. A shallow gulf encroached from the northeast onto wide areas of the Arabian platform and propagated as far southeast as central Ethiopia. The presence of a marine connection between Ethiopia and Saudi Arabia implies that the Arabian shield was not emergent during that time. In the time between Late Rhaetian–Pliensbachian, northern and central Ethiopia as well as other adjacent areas (i.e., southern Yemen, northern Somalia, Madagascar) must have remained

areas of erosion and/or nondeposition since biostratigraphic evidence older than Toarcian is apparently missing. During the Toarcian an epicontinental seaway had already been established following the NE-trending axis of the evolving rift that started to propagate into the supercontinent from its Tethyan margin. The newly developing Gulf was bounded from the northeast and the southwest by the Arabo-Ethiopian High and the Indian Shield respectively where its shorelines have reached northern and central Ethiopia.

4. *Palynology*: The composition and upward distribution of palynomorphs from the 'Adigrat Sandstone' succession in the Mekelle and Blue Nile basins indicate a major sequential break separating two distinct and major microfloras. These include a lower *Falcisporites*-dominated microflora belonging to corystosperms and an upper *Callialasporites*-dominated microflora that apparently belongs to araucariacean and cheirolepidiacean conifers. The distribution allows proposing three informal palynological assemblage zones: namely, AZ I, Late Triassic (Late Carnian–Early Rhaetian); AZ II, latest Early Jurassic (Early Toarcian); and AZ III, latest Early–Middle Jurassic (Late Toarcian–Early Callovian). These palynological results allow for the first time a better biostratigraphic subdivision of the Adigrat Sandstone succession and its correlation with time equivalent units in the region.

5. In summary, the term 'Adigrat' as currently applied in the Horn of Africa incorporates sandstones of widely different ages and belonging to several separate depositional episodes. With regard to the Mekelle and Blue Nile basins, each of the three stratigraphic units identified within the Adigrat Sandstone succession may deserve a separate 'Formation' rank. The lowermost stratigraphic unit (*Unit I*) has nothing to do with the Gondwana break-up whereas the upper two units (*Unit II and III*) are directly related to this event. Consequentely, the introduction of new formation names appears to be useful to allow easier correlation of the sediments throughout the Horn of Africa and to better understand the tectonic and palaeogeographic evolution of the region. This, in turn, would significantly aid in locating potential reserviors and source rocks for possible sites of exploration in the region.

## 12. References


Abbate, E., Bruni, P. & Sagri, M. 1987. *The Mesozoic to Tertiary deposits. Int. Meeting on the Geology of Somalia and surrounding regions*, *Excursion B guidebook*: 12–22. Mogadishu.

Al-Subbary, A., Nichols, S. & Bosence, D. 1993. Cretaceous–Tertiary pre-rift fluvial/shallow marine sediments in Yemen. In E.R. Philobbos & B.H. Purser (eds.), *Geodynamics and Sedimentation of the Red Sea – Gulf of Aden Rift System. Geol. Soc. Egypt Spec. Publ.* 1: 383–407.

Alexander, C.R., DeMaster, D.J. & Nittrouer, C.A. 1991. Sediment accumulation in a modern epicontinental-shelf setting: the Yellow Sea. *Mar. Geol*. 98: 51–72.

Al-Husseini, M.I. 2008. The Middle East Geologic Time Scale. *GeoArabia* 13: 185–188.

Allen, G.P. 1991. Sedimentary processes and facies in the Gironde estuary: a recent model for macrotidal estuarine systems. In D.G. Smith, G.E. Reinson, B.A. Zaitlin & R.A. Rahmani (eds.), *Clastic Tidal Sedimentology*. *Can. Soc. Petrol. Geol. Mem*. 16: 29–40.

Allen, G.P. & Posamentier, H.W. 1993. Sequence stratigraphy and facies model of an incised valley fill: The Gironde estuary, France. *J. Sediment. Petrol*. 63: 378–391.

Allen, G.P. & Posamentier, H.W. 1994. Transgressive facies and sequence architecture in mixed tide- and wave-dominated incised valleys: an example from the Gironde estuary, France. In R.W. Dalrymple, B.A. Zaitlin & R. Boyd (eds.), *Incised Valley Systems: Origin and Sedimentary Sequences*. *SEPM Spec. Publ*. 51: 225–240.

Allen, J.R.L. 1964. Studies in fluviatile sedimentation: Six cyclothems from the Lower Old Red Sandstone, Anglo-Welsh Basin. *Sedimentology* 3: 163–198.

Allen, J.R.L. 1970. A quantitative model of grain size and sedimentary structures in lateral accretion deposits. *Geology* 7: 129–146.

Allen, J.R.L. 1981. Lower Cretaceous tides revealed by cross-bedding with mud drapes. *Nature* 289: 579–581.

Allen, J.R.L. 1982. *Sedimentary Structures: Their Character and Physical Basis. Vols. I and II.* Elsevier: Amsterdam.

Allen, J.R.L. 1984. *Sedimentary Structures: Their Character and Physical Basis. Development in Sedimentology 30*. Amsterdam: Elsevier.

Anderson, J.M. 1977. The biostratigraphy of the Permian and Triassic, part 3. A review of Gondwana Permian palynology with particular reference to the northern Karoo Basin, South Africa. *Bot. Surv. South Afr. Mem*. 41: 1–67.

Andrews, P. B. 1970. *Facies and Genesis of a Hurricane-washover St. Joseph Island, Central Texas Coast. Economic Geology Report 67*. Austin: University of Texas.

Archer, A.W. 1998. Hierarchy of controls on cyclic rhythmite deposition: Carboniferous basins of eastern and midcontinental U.S.A. In C.R. Alexander, R.A. Davis & V.J. Henry (eds.), *Tidalites: Processes and Products*. *SEPM Spec. Publ*. 61: 59–68.

Archer, A.W. & Feldman, H.R. 1994. Tidal influence in Carboniferous fine-grained limestones. *Geobios* 16: 283–291.

Archer, A.W., Feldman, H.R., Kvale, E.P. & Lanier, W.P. 1994. Pennsylvanian (Upper Carboniferous) fluvio- to tidal-estuarine coal-bearing systems: delineation of facies transitions based upon physical and biogenic sedimentary structures. *Palaeogeog. Palaeoclimatol. Palaeoecol*. 106: 171–185.

Archer, A.W. & Hubbard, M.S. 2003. Highest tides of the world. In M. Chan & A.W. Archer (eds.), *Extreme Depositional Environments: Mega End Members in Geological Time. Geol. Soc. Am. Spec. Pap*. 370: 151–173.

Arkin, Y., Beyth, M., Dow, D.B., Levitte, D., Haile, T. & Hailu, T. 1971. *Geological map of Mekelle, sheet area ND 37-11, Tigre Province*, *1:250.000*. Addis Ababa: Ethiopian Institute of Geological Survey.

Arnott, R.W. & Southard, J.B. 1990. Exploratory flow-duct experiments on combined flow bed configurations and some implications for interpreting storm-event stratification. *J. Sediment. Petrol*. 60: 211–219.

Ashley, G.M. & Sheridan, R.E. 1994. Depositional model for valley fills on a passive continental margin. In R.W. Dalrymple, R.J. Boyd & B.A. Zaitlin (eds.), *Incised-Valley Systems: Origin and Sedimentary Sequences*. *SEPM Spec. Publ*. 51: 285–301.

Assefa, G. 1979. Clay mineralogy of the Mesozoic sequence in the Upper Abay (Blue Nile) River valley region, Ethiopia. *Sinet Ethio. J. Sci*. 3: 37–65.

Assefa, G. 1981. Gohatsion Formation. A new Lias-Malm lithotratigraphic unit from the Abay River basin, Ethiopia. *Geosci. J*. 2: 63–68.

Assefa, G. 1988. Potential hydrocarbon-generating rock units within the Phanerozoic sequence of the Ogaden Basin, Ethiopia: a preliminary assessment using the Lopatin model. *J. Petrol. Geol.* 11: 461–472.

Assefa, G. (1991): Lithostratigraphy and environment of deposition of the Late Jurassic–Early Cretaceous sequences of the central part of the Northwestern Plateau, Ethiopia. *N. Jb. Geol. Paläont. Mh*. 182: 255–284.

Atnafu, B. 2003. Facies and diagenetic development of Jurassic carbonates (Callovian, Oxfordian, Kimmeridgian) in the Abay River Basin (Upper Blue Nile, Ethiopia). Ph.D. thesis, Friedrich Alexander Universität Erlangen, Nürnberg.

Aubry, A. 1886. Obsévations géologiques sur les pays Danakils, Somalis, le Royaume de Choa et les payes Gallas. *Bull. Soc. Geol. Fr*. 14: 201–222.

Ayalew, T. & Gichile, S. 1990. Preliminary U-Pb ages from southern Ethiopia. *15th Colloq. Afr. Geol*. *Extended abstracts*: 127–130. Nancy.

Ayalew, T., Bell, K., Moore, J.M. & Parrish, R.R. 1990. U-Pb and Rb-Sr geochronology of the western Ethiopian shield. *Geol. Soc. Am. Bull*. 102: 1309–1316.

Bahn, K.L & Fielding, C. 2004. An integrated ichnological and sedimentological comparison of non-deltaic shoreface and subaqueous delta deposits in Permian reservoir units of Australia. In D. McIlroy (ed), *The Application of Ichnology to Palaeoenvironmental and Stratigraphic Analysis*. *Geol. Soc. Lond. Spec. Publ*. 228: 273–307.

Balduzzi, A., Msaky, E., Trincianti, E. & Manum, S.B. 1992. Mesozoic Karoo and post-Karoo Formations in the Kilwa area, southeastern Tanzania: a stratigraphic study based on palynology, micropalaeontology and well-log data from Kizimbani Well. *J. Afr. Earth Sci*. 15: 405–427.

Balme, B.E. 1957: Spores and pollen grains from the Mesozoic of Western Australia. *CSIRO Aust. Coal Res. Sect. T.C*. 25: 1–48.

Balme, B.E. & Hennelly, J.P.F. 1956. Trilete sporomorphs from Australian Permian sediments. *Aust. J. Bot*. 4: 240–260.

Barrell, J. 1912. Criteria for the recognition of ancient delta deposits. *Geol. Soc. Am. Bull*. 23: 377–446.

Barwis, J.H. & Makurath, J.H. 1978. Recognition of ancient tidal inlet sequences: an example from the Upper Silurian Keyser Limestone in Virginia. *Sedimentology* 25: 61–82.

Bassoullet, J.P. Elmi, S., Poisson, A., Cecca, F., Bellion, Y., Guiraud, R. & Baudin, F. 1993. Middle Toarcian (184-182 Ma). In J. Dercourt, L.E. Ricou & B. Vrielynck (eds.), *Atlas Tethys Paleoenvironmental Maps*, *Explanatory Notes*: 63–80. Paris: Gauthier-Villars.

Bates, R.L. & Jackson, J.A. 1987. *Glossary of Geology, 3rd ed*. Verginia: American Geological Institute.

Beauchamp, J. & Lemoigne Y. 1974. Presence d'un basin de subsidence en Ethiopie centrale et essai de reconstruction paleogeographique de l'Ethiopie durant le Jurassique. *Bull. Geol. Soc. France* 7: 563–569.

Beauchamp, J. 1977. La série sédimentaire en Éthiopie centrale et orientale. Lyon: Thèse de Doctorat, Univ. Claude Bernard.

Beccaluva, L., Bianchini, G. Natali, C. & Siena, F. 2007. Continental Flood Basalts and Mantle Plumes: a Case Study of the Northern Ethiopian Plateau. *J. Petrology* 50: 1377–1403.

Beerbower, J.R. 1964. Cyclotherms and cyclic depositional mechanisms in alluvial plain sedimentation. *Kansas State Geol. Surv. Bull*. 169: 31–42.

Bennett, S.J. & Bridge, J.S. 1995. An experimental study of flow, bedload transport and bed topography under conditions of erosion and deposition and comparison with theoretical models. *Sedimentology* 42: 117–146.

Berhe, S.M., Desta, B., Nicoletti, M. & Teferra, M. 1987. Geology, geochronology and geodynamic implications of the Cenozoic magmatic province in W and SE Ethiopia. *J. Geol. Soc. Lond*. 144: 213–226.

Berné, S., Castaing, P., Le Drezen, E. & Lericolais, G. 1993. Morphology, internal architecture and reversal asymmetry of large subtidal dunes in the entrance to Gironde estuary (France). *J. Sediment. Petrol.* 63: 780–793.

Besairie, H. 1971. Geologie de Madagascar. I. Les terrains sedimentaires. *Ann. Geol. Madagascar* 35: 1–463.

Besairie, H. & Collignon, M. 1972. Géologie de Madagascar I, Les terrains sédimentaires. *Ann. Géol. Madagascar* 35: 1–463

Beydoun, Z.R. 1970. Southern Arabia and northern Somalia: comparative geology. *Phil. Trans. Roy. Soc. Lond.* A267: 267–292.

Beydoun, Z.R. 1997. Introduction to the revised Mesozoic stratigraphy and nomenclature for Yemen. *Mar. Pertrol. Geol*. 14: 617–629.

Beynon, B.M., Pemberton, S.G., Bell, D.D. & Logan, C.A. 1988. Environmental implications of ichnofossils from the Lower Cretaceous Grand Rapids Formation, Cold Lake Oil Sand Deposit. In D.P. James, & D.A. Leckie, (eds.), *Sequences, Stratigraphy, Surface and Subsurface*. *Mem. Can. Soc. Petrol. Geol*. 15: 275–290.

Beyth, M. 1972a. To the Geology of Central-Western Tigre. Ph.D. thesis, Friedrichs Wilhelms Universität, Bonn.

Beyth, M. 1972b. Paleozoic–Mesozoic sedimentary basin of Mekelle Outlier, Northern Ethiopia. *AAPG Bull*. 56: 2426–2439.

Beyth, M. 1973. Correlation of Palaeozoic–Mesozoic sediments in Northern Yemen and Tigre, Northern Ethiopia. *AAPG Bull*. 576: 2440–2443.

Bhattacharya, J.P. 2006. Deltas. In H. Posamentier & R.G. Walker (eds.), *Facies Models Revisited*. *SEPM Spec. Publ*. 84: 241–296.

Bhattacharya, J.P. & Giosan, L. 2003. Wave-influenced deltas: geomorphologic implications for facies reconstruction. *Sedimentology* 50: 187–210.

Bhattacharya, J.P., McLinjoy, K., MacEachern, J.A. & Davies, R.K. 2003. *Pennsylvanian adventures in Palo Pinto County, AAPG Annual Field Trip*: 1–38. Texas: Fort Worth.

Bhattacharya, J. & Walker, R.G. 1991. River- and wave-dominated depositional systems of the Upper Cretaceous Dunvegan Formation, northwestern Alberta. *Bull. Can. Petrol. Geol.* 39: 165–191.

Biggs, R.B. 1967. The sediments of Chesapeake Bay. In G.H. Lauff (ed.), *Estuaries*. *Am. Assoc. Adv. Sci*. 83: 239–260.

Blanford, W.T. 1869. On the Geology of a portion of Abyssinia. *J. Geol. Soc. Lond.* 25: 401–406.

Blanford, W.T. 1870. *Observations on the Geology and Zoology of Abyssinia, made during the British Expedition to that country in 1867-68. With Illustrations and a Geological Map*. London: Macmillan & Co.

Blum, M.D. & Tornqvist, T.E. 2000. Fluvial responses to climate and sea-level change: a review and look forward. *Sedimentology* 47: 2–48.

Boersma, J.R. & Terwindt, J.H.J. 1981. Neap-spring tide sequences of intertidal shoal deposits in a mesotidal estuary. *Sedimentology* 28: 151–170.

Boersma, J.R., Van de Meene, E.A. & Tjalsma, R.C. 1968. Intricated cross-stratification due to interaction of a mega ripple with its lee-side system of backflow ripples (upper point-bar deposits, Lower Rhine). *Sedimentology* 11: 147–162.

Boothroyd, J.C., Friedrich, N.E. & McGinn, S.R. 1985. Geology of microtidal coastal lagoons: Rhode Island. *Marine Geol.* 63: 35–76.

Bosellini, A. 1989. The continental margins of Somalia: their structural evolution and sequence stratigraphy. *Mem. Sci. Geol*. 41: 373–458.

Bosellini, A., Russo, A., Fantozzi, P.L., Assefa, G. & Tadesse, S. 1997. The Mesozoic succession of the Mekelle Outlier (Tigrai Province, Ethiopia). *Mem. Sci. Geol*. 49: 95–116.

Bourgeois, J. 1980. A transgressive shelf sequence exhibiting hummocky stratification: the Cape Sebastian Sandstone (Upper Cretaceous) southwestern Oregon. *J. Sediment. Petrol*. 50: 681–702.

Boyd, R., Dalrymple, R.W. & Zaitlin, B.A. 1992. Classification of clastic coastal depositional environments. *Sediment. Geol*. 80: 139–150.

Boyd, R., Dalrymple, R.W. & Zaitlin, B.A. 2006. Estuarine and Incised-Valley Models. In H. Posamentier & R.G. Walker (eds.), *Facies Models Revisited. SEPM Spec. Publ*. 84: 175–235.

Braathen, A., Grenne, T., Selassie, M.G. & Worku, T. 2001. Juxtaposition of Neoproterozoic units along the Baruda-Tulu Dimtu shear belt in the East African Orogen of western Ethiopia. *Precamb. Res*. 107: 215–234.

Brenchley, P.J. 1985. Storm influenced sandstone beds. *Modern Geology* 9: 369–396.

Bridges, P.J. 1982. Sedimentology of a tidal sea: the Lower Greensand of southern England. In A. H. Stride (ed.), *Offshore Tidal Sands*: 183–189. London: Chapman and Hall.

Bridge, J. & Best, J. 1997. Preservation of planar laminae due to migration of low-relief bed waves over aggrading upper-stage plane beds: comparison of experimental data and theory. *Sedimentology* 44: 253–262.

Broger, E.J., Syhlonyk, G.E. & Zaitlin, B.A. 1997. Glauconite sandstone exploration: A case study from the Lake Newell project, southern Alberta. In S.G. Pemberton & D.P. James (eds.), *Petroleum Geology of the Cretaceous Mannville Group, Western Canada. Can. Soc. Petrol. Geol. Mem*. 18: 140–168.

Bromley, R.G. & Ekdale, A.A. 1984. Chondrites – A trace fossil indicator of anoxia in sediments: *Science* 224: 872–874.

Bruni, P. & Fazzuoli, M. 1977. Sedimentological observation on Jurassic and Cretaceous sequences from Northern Somalia: Preliminary report. *Boll. Soc. Geol. Ital*. 95: 1571–1588.

Buatois, L.A. & Mangano, M.G. 2003. Sedimentary facies and depositional evolution of the Upper Cambrian–Lower Ordovician Santa Rosita Formation in northwest Argentina. *J. South Am. Earth Sci*. 16: 343–363.

Buatois, L.A., Gingras, M.K., MacEachern, J., Mangano, M.G., Zonneneveld, J.P., Pemberton, G., Netto, R.G. & Martin, A. 2005. Colonization of brackish water systems through time: Evidence from the trace fossil record. *Palaios* 20: 321–347.

Buatois, L.A., Mángano, M.G., Maples, C.G. & Lanier, W.P. 1997. The paradox of nonmarine ichnofaunas in tidal rhythmites: Integrating sedimentologic and ichnologic data from the late Carboniferous of eastern Kansas, USA. *Palaios* 12: 467–481.

Bussert, R. & Dawit, E.L. 2009a. Unexpected diversity: New results on the stratigraphy and sedimentology of Palaeozoic and Mesozoic siliciclastic sediments in northern Ethiopia. *Zbl. Geol. Paläont*. I(3/4): 181–198.

Bussert, R. & Dawit, E.L. 2009b. Upper Ordovician glacigenic sediments in northern Ethiopia: Depositional setting and ice sheet behavior in NE Africa during the Hirnantian glaciation. *6th Annual Conference SEPM-CES Sediment 2009*, *Abstracts*. Kraków, Poland.

Bussert, R. & Schrank, E. 2007. Palynological evidence for a latest Carboniferous–Early Permian glaciation in Northern Ethiopia. *J. Afr. Earth Sci*. 49: 201–210.

Cannon, R.T., Simiyu Siambi, W.M.N. & Karanja, F.M. 1981. The proto-Indian ocean and a probable Palaeozoic Mesozoic triradial rift system in East Africa. *Earth Planet. Sci. Lett*. 52: 419–426.

Cant, D.J. 1978. Development of a facies model for sandy braided river sedimentation: comparison of the South Saskatchewan River and the Battery Point-Formation. In A.D. Miall (ed.), *Fluvial Sedimentology*. *Mem. Can. Soc. Petrol. Geol.* 5: 627–640.

Canuti, P. & Pirini Radrizzani, C. 1975. Microfacies from the upper portion of the Antalo Limestones (Blue Nile sequence, Ethiopia). Proceedings of the 5th African Colloquium on Micropaleontology. *Rev. Espan. Micropaleont*. 7: 131–148.

Carling, P.A., Radecki-Pawlik, A., Williams, J.J., Rumble, B., Meshkova, L., Bell, P. & Breakspear, R. 2006. The morphodynamics and internal structure of intertidal fine-gravel dunes. *Sediment. Geol*. 183: 159–179.

Carter, C.H. 1978. A regressive barrier and barrier-protected deposit: depositional environment and geographic setting of the Late Tertiary Cohansey Sand. *J. Sediment. Petrol*. 48: 933–950.

Carter, R.W.G. & Woodroffe, C.D. 1994. Coastal evolution: an introduction. In R.W.G. Carter & C.D. Woodroffe (eds.), *Coastal Evolution*. Cambridge: Cambridge University Press.

Catuneanu, O. 2002. Sequence stratigraphy of clastic systems: concepts, merits and pitfalls. *J. Afr. Earth Sci*. 35: 1–43.

Catuneanu, O. 2006. *Principles of Sequence Stratigraphy*. Oxford: Elsevier.

Catuneanu, O., Hancox, P.J. & Rubidge, B.S. 1998. Reciprocal flexural behavior and contrasting stratigraphies: a new basin development model from the Karoo retroarc foreland system, South Africa. *Basin Res*. 10: 417–439.

Catuneanu, O. Khidir, A. & Thanju, R. 2003. External controls on fluvial facies: the Scollard sequence, Western Canada foredeep. Abstracts, *AAPG Ann. Conv*. 12: A27.

Catuneanu, O., Willis, A.J. & Miall, A.D. 1998. Temporal significance of sequence boundaries. *Sediment. Geol*. 121: 157–178.

Cheel, R.J. & Leckie, D.A. 1990. A tidal-inlet complex in the Cretaceous epeiric sea of North America: Virgelle Member, Milk River Formation, southern Alberta, Canada. *Sedimentology* 37: 67–81.

Cheel, R.J. & Leckie, D.A. 1993. Hummocky cross-stratification. *Sediment. Rev*. 1: 103–122.

Clifton, H.E. 1969. Beach lamination: nature and origin. *Mar. Geol.* 7: 553–559.

Clifton, H.E. 1982. *Estuarine deposits*. *AAPG Mem*. 31: 179–189.

Clifton, H.E. 2006. A reexamination of facies models for clastic shorelines. In H. Posamentier & R.G. Walker (eds.), *Facies Models Revisited*. *SEPM Spec. Publ*. 84: 297–341.

Clifton, H.E., Hunter, R.E. & Phillips, R.L. 1971. Depositional structures and processes in the non-barred high energy nearshore. *J. Sediment. Petrol*. 41: 651–670.

Coffin, M.F. & Rabinowitz, P.D. 1987. Reconstruction of Madagascar and Africa: evidence from the Davie Fracture Zone and western Somali Basin. *J. Geophys. Res*. 92: 9385–9406.

Collinson, J.D. 1970. Deep channels, massive beds and turbidity current genesis in the central Pennine basin, *Proc. Yorks. Geol. Soc.* 37: 495–519.

Colman, S.M. & Mixon, R.B. 1988. The record of major Quaternary sea level changes in a large coastal estuary, Chesapeake Bay, Eastern United States. *Palaeogeogr., Palaeoclimatol., Palaeoecol*. 68: 99–116.

Couper, R.A. 1958. British Mesozoic microspores and pollen grains. *Palaeontogr. Abt*. B 103: 75–119.

Courtillot, V., Hofmann, C., Manighetti, I., Kidane, T. & Tapponnier, P. 1997. Relations between plume birth and continental breakup: the case of the Ethiopian traps and Afar depression. *Terra Nova* 9: 521–522.

Curtis, P. & Lenz, H. 1985. Geological and geochronological investigation of selected alkali igneous complexes in the Nuba Mountains, southern Kordofan, Sudan. *Geol. Jb*. 69: 3–34.

Dainelli, G. & Marinelli O. 1912. *Risultati Scientifici Di Un Viaggio Nella Colonia Eritrea*. Firenze.

Dainelli, G., 1943. *Geologia dell'Africa orientale*. Rome: Real Accad. Italia.

Dainelli, G. 1970. Photogeology of the Debre markos-Blue Nile area, southern Gojam, Ethiopia. *Mem. Soc. Geol. Italia* 9: 779–791.

Dalrymple, R.W. 1992. Tidal depositional systems. In R.G. Walker & N.P. James (eds.), *Facies Models and Sea Level Changes*: 195–218. St John's: Geoscience Canada.

Dalrymple, R.W. 2006. Incised valleys in time and space: An introduction to the volume and an examination of the controls on valley formation and filling. In R.W. Dalrymple, D.A. Leckie & R.W. Tillman (eds.), *Incised Valleys in Space and Time*. *SEPM Spec. Publ*. 85: 5–12.

Dalrymple, R.W., Boyd, R. & Zaitlin, B.A. 1992. Estuarine facies models: Conceptual basis and stratigraphic implications. *J. Sediment. Petrol*. 62: 1130–1146.

Dalrymple, R.W., Boyd, R. & Zaitlin, B.A. 1994. History of research, valley types and internal organization of incised-valley systems: introduction to the volume. In R.W. Dalrymple, R. Boyd, & B.A. Zaitlin (eds.), *Incised-Valley Systems: Origin and Sedimentary Sequences*. *SEPM Spec. Publ*. 51: 3–10.

Dalrymple, R.W. & Choi, K.S. 2003. Sediment transport by tides. In G.V. Middleton (ed.), *Encyclopedia of Sediments and Sedimentary Rocks*: 606–609. Dordrecht: Kluver Acadamic Publishers.

Dalrymple, R.W., Knight, R.J., Zaitlin, B.A. & Middleton, G.V. 1990. Dynamics and facies models of a macrotidal sand-bar complex, Cobequid Bay-Salmon River estuary (Bay of Fundy). *Sedimentology* 37: 577–612.

Dalrymple, R.W. & Makino, Y. 1989. Description and genesis of tidal bedding in the Cobequid Bay-Salmon River estuary, Bay of Fundy, Canada. In A. Taira & F. Masuda (eds.), *Sedimentary Facies of the Active Plate Margin*: 151–177. Tokyo: Terra Publishing.

Dalrymple, R.W., Makino, Y. & Zaitlin, B.A. 1991. Temporal and spatial patterns of rhythmite deposition on mudflats in the macrotidal Cobequid Bay-Salmon River estuary, Bay of Fundy, Canada. In D.G. Smith, G.E. Reinson, B.A. Zaitlin & R.A. Rahmani (eds.), *Clastic Tidal Sedimentology*. *Can. Soc. Petrol. Geol. Mem*. 16: 137–160.

Dalrymple, R.W. & Rhodes, R.N. 1995. Estuarine dunes and barforms. In G.M. Perillo (ed.), *Geomorphology and Sedimentology of Estuaries*. *Dev. Sediment*. 53: 359–422.

Dalrymple, R.W. & Zaitlin, B.A. 1989. Tidal Sedimentation in the Macrotidal Cobequid Bay-Salmon River Estuary, the Bay of Fundy. *2nd Int. Res. Symposium of Clastic Tidal Deposits, A Field Guide*. Calgary: Can. Soc. Petrol. Geol.

Daly, M.C., Chorowicz, J. & Fairhead, J.D. 1989. Rift basin evolution in Africa: the influence of reactivated steep basement shear zones. In M.A. Cooper & G.D. Williams (eds.), *Inversion Tectonics*. *Geol. Soc. Spec. Publ*. 44: 309–334.

Davidson, A. & McGregor, C. 1976. Palynomorphs indicating Permian rocks in Ethiopia. *Nature* 262: 371–373.

Davis, R.A. 1994. Barrier island systems - a geologic overview. In R.A. Davis (ed.), *Geology of Holocene Barrier Island Systems*: 1–46. New York: Springer.

Davis, R.A. & Clifton, H.E. 1987. Sea level change and the preservation potential of wave-dominated and tide-dominated coastal sequences. In D. Nummedal, P.H. Orrin & J.D. Howard, (eds.), *Sea Level Fluctuation and Coastal Evolution*: *SEPM Spec. Publ.* 41: 167–178.

Davis, R.A., Fox, W.T., Hayes, M.O. & Boothroyd, J.O. 1972. Comparison of ridge and runnel systems in tidal and non-tidal environments. *J. Sediment. Petrol*. 42: 413–21.

Dawit, E.L. & Bussert, R. 2009. Latest Ordovician-Early Silurian post-glacial tide-dominated shelf sediments in northern Ethiopia. *6th Annual Conference SEPM-CES Sediment 2009*, *Abstracts*. Kraków, Poland.

De Boer, P.L., Oost, A.P. & Visser, M.J. 1989. The diurnal inequality of the tide as a parameter for recognizing tidal influences. *J. Sediment. Petrol*. 59: 912–921.

De Jersey, N.J. 1975. Miospore zones in the lower Mesozoic of southeastern Queensland. In K.S.W. Campbell (ed.), *Gondwana Geology*: 159–172. Canberra: A.N.U. Press.

De Raaf, J.F.M. & Boersma, J.R. 1971. Tidal deposits and their sedimentary structures. *Geol. Mijnbw*. 50: 479–504.

De Raaf, J.F.M., Boersma, J.R. & van Felder, A. 1977. Wave generated structures and sequences from a shallow marine succession, Lower Carboniferous, Cork County, Ireland. *Sedimentology* 24: 451–483.

Demarest, J.M. & Kraft, J.C. 1987. Stratigraphic record of Quaternary sea levels: Implications for more ancient strata. In D. Nummedal, P.H. Orrin & Howard, J.D. (eds.), *Sea Level Fluctuation and Coastal Evolution*. *SEPM Spec. Publ*. 41: 223–240.

Dolby, J.H. & Balme, B.E., 1976. Triassic palynology of the Carnarvon Basin, Western Australia. *Rev. Palaeobot. Palynol*. 22: 105–168.

Dominguez, J.M.L. 1996. The São Francisco standplain: a paradigm for wave-dominated deltas? In M. De Batist & P. Jacobs (eds.), *Geology of Siliclastic Shelf Seas*. *Geol. Soc. Lond. Spec. Publ*. 117: 217–231.

Dott Jr., R.H. & Bourgeois, J. 1982. Hummocky stratification: significance of his variable bedding sequences. *Geol. Soc. Am. Bull*. 93: 663–680.

Dow, D.B., Beyth, M. & Hailu, T. 1971. Palaeozoic glacial rocks recently discovered in northern Ethiopia. *Geol. Mag*. 108: 53–60.

Dumas, S. & Arnott, R.W.C. 2006. Origin of hummocky and swaley cross-stratification – The controlling influence of unidirectional current strength and aggradation rate. *Geology* 34: 1073–1076.

Dumas, S., Arnott, R.W.C. & Southard, J.B. 2005. Experiments on oscillatory-flow and combined-flow bed forms: implications for interpreting parts of the shallow-marine sedimentary record. *J. Sediment. Res*. 75: 501–513.

Ebinger, C.J., Yemane, T., Woldegabriel, G., Aronson, J.L. & Walter, R.C. 1993. Late Eocene–Recent volcanism and faulting in the southern main Ethiopian rift. *J. Geol. Soc. Lond.* 150: 99–108.

Ekdale, A.A., Bromley, R.G. & Pemberton, S.G. 1984. Ichnology; the use of trace fossils and stratigraphy. *Soc. Econ. Paleont. Miner. Short Course* 15: 1–317.

Elliot, T. 1986. Clastic shorelines. In Reading, H.G. (ed.), *Sedimentary Environments and Facies*: 143–177. Oxford: Blackwell Scientific Publishers.

El-Nakhal, H.A., Stephenson, M.H. & Owens, B. 2002. New Late Carboniferous–Early Permian palynological data from glacial sediments in the Kooli Formation, Republic of Yemen. *Micropaleontology* 48: 222–228.

Embry, A.F. 1995. Sequence boundaries and sequence hierarchies: problems and proposals. In R.J. Steel, V.L. Felt, E.P. Johannessen & C. Mathieu (eds.), *Sequence Stratigraphy of the Northwest European Margin*. *Norwegean Petrol. Soc. Spec. Publ*. 5: 1–11.

Embry, A.F. 2001. Sequence stratigraphy: what it is, why it works and how to use it. *Can. Soc. Petrol. Geol*. 28: 14–15.

Enay, R., Le Nindre, Y.M., Mangold, C., Manivit, J. & Vaslet, D. 1987. Le Jurassique d'Arabie Saoudite Centrale: nouvelles donnes sur la lithostratigraphie, les paléoenvironnements, les faunes d'ammonites, les âges et les corrélations. In R. Enay (ed.), *Le Jurassique d'Arabie Saoudite Centrale*. *Geobios Mém. Spéc*. 9: 13–65

Ethridge, F.G. 1985. Modern alluvial fans and fan deltas. Recognition of fluvial depositional systems and their resource potential. *SEPM Short Course* 19: 101–126.

Fairbridge, R.W. 1982. The fracturing of Gondwanaland. In R.A. Scrutton & M. Talwani (eds.), *The Ocean Floor*: 229–235. Chichester, John Wiley & Sons.

Farabee, M.J., Taylor, T.N. & Taylor, E.L. 1989. Pollen and spore assemblages from the Falla Formation (Upper Triassic), Central Transantarctic Mountains, Antarctica. *Rev. Palaeobot. Palynol*. 61: 101–138.

Ficcarelli G. 1968. Fossili giuresi della serie sedimentaria del Nilo Azzurro meridionale. *Riv. Italia Paleont. Stratigr*. 74: 23–50.

Filatoff, J.F. 1975. Jurassic Palynology of the Perth Basin, Western Australia. *Palaeontographica Abt*. B154: 1–113.

Finkelstein, K. & Ferland, M.A. 1987. Backbarrier response to sea level rise, eastern shore of Virginia. In D. Nummedal, P.H. Orrin & J.D. Howard (eds.), *Sea Level Fluctuation and Coastal Evolution*: *SEPM Spec. Publ*. 41: 145–155.

Forbes, D.L. & Taylor, R.B. 1987. Coarse-grained beach sedimentation under paraglacial conditions, Canadian Atlantic coast. In D.M. FitzGerald & P.S. Rosen (eds.), *Glaciated Coasts*: 51–86. San Diego: Academic Press.

Frey, R.W. & Pemberton, S.G. 1984. Trace fossil facies models. In R.G. Walker (ed.), *Facies Models, 2nd ed.*: 189-207. St' Johns: Geoscience Canada.

Frey, R.W., Pemberton, S.G. & Saunders, T.D.A. 1990. Ichnofacies and bathymetry: a passive relationship. *J. Paleont*. 64: 155–158.

Futterer, K.1894. Beiträge zur Kenntnis des Jura in Ostafrika. *Z. dtsch. geol. Ges.* 46: 1–49.

Galloway, W.E. 1975. Process framework for describing the morphologic and stratigraphic evolution of deltaic depositional systems. In M.L. Broussard (ed.), *Deltas*: 87–98. Texas: Houston Geological Society.

Galloway, W.E. 1989. Genetic stratigraphic sequences in basin analysis II: application to northwest Gulf of Mexico Cenozoic basin: *AAPG Bull*. 73: 143–154.

Galloway, W.E. & Hobday, D.K. 2006. *Terrigenous clastic depositional systems: Application to fossil fuel and groundwater resources. 2nd ed*. Heidelberg: Springer.

Galloway, W.E., Hobday, D.K. & Magara, K. 1982. Frio Formation of Texas Gulf Coastal Plain: depositional systems, structural framework, and hydrocarbon distribution. *AAPG Bull*. 66: 649–688.

Garland, C.R. 1980. Geology of the Adigrat area. *Geol. Surv. Ethiopia Mem.* 1: 1–51.

Garland, C.R., Beyth, M, Dow, D.B., Kazmin, V., Assefa, A., Abraham, A., Haile, T. & Hailu, T. 1978. *Geological map of the Adigrat area, Sheet ND37-7*, *Tigre Province, 1:250.000*. Addis Ababa: Ethiopian Institute of Geological Survey.

Garrison Jr., J.R. & van den Bergh T.C.V. 2006. Effects of sedimentation rate, rate of relative rise in sea level and sea level cycle duration on the filling of incised valleys: examples of "filled" and "over-filled" incised valleys from the Upper Ferron Sandstone Last Chance Delta, East-central Utah. In R.W. Dalrymple, A. Leckie & R.W. Tillman (eds.), *Incised Valleys in Time and Space*. *SEPM Spec. Publ*. 85: 239–279.

Gawthorpe, R.L. & Colella, A. 1990. Tectonic controls on coarse-grained delta depositional systems in rift basins. *IAS Spec. Publ*. 10: 113–127.

Geiger, M., Clark, D.N. & Mette, W. 2004. Reappraisal of the timing of the breakup of Gondwana based on sedimentological and seismic evidence from the Morondava Basin, Madagascar. *J. Afr. Earth Sci*. 38: 363–381.

Geiger, M. & Schweigert, G. 2006. Toarcian–Kimmeridgian depositional cycles of the south-western Morondava Basin along the rifted continental margin of Madagascar. *Facies* 52: 85–112.

Geletu, S. 1998. Biostratigraphy, depositional environment, basin evolution and hydrocarbon potential of the Late Triassic to Late Jurassic succession, Ogaden Basin, Ethiopia. Ph.D. thesis, Eberhard-Karls-Universität, Erlangen.

Geletu, S. & Wille, W. 1998. Middle Triassic palynomorphs from the Fincha-a river valley section, Horo Guduru, western central Ethiopia. *N. JB. Geol. Paläont. Mh*. 5: 257–268.

George, R., Rogers, N. & Kelley, S. 1998. Earliest magmatism in Ethiopia: evidence for two mantle plumes in one flood basalt province. *Geology* 26: 923–926.

Gilbert, G.K. 1885. The topographic features of lake shores. *U.S. Geol. Surv. Annu. Rep*. 5: 75–123.

Gilbert, G.K. 1890. *Lake Bonneville*. *U.S. Geol. Surv. Monogr. 1*.

Gilboy, C.F. 1970. The Geology of the Gariboro Region of Southern Ethiopia. Ph.D. thesis, University of Leeds.

Gingras, M.K., MacEachern, J.A. & Pemberton, S.G. 1998. A comparative analysis of the ichnology of wave- and river-dominated allomembers of the Upper Cretaceous Dunvegan Formation. *Bull. Can. Petrol. Geol*. 46: 51–73.

Gingras, M.K., Pemberton, S.G., Saunders, T. & Clifton, H.E. 1999. Ichnology of modern and Pleistocene brackish water deposits at Willapa Bay, Washington: variability in estuarine settings. *Palaios* 14: 352–374.

Goodwin, M.B., Clemens, W.A., Hutchison, J.H., Wood, C.B., Zavada, M.S., Kemp, A., Duffin, C.J. & Schaff, C.R. 1999. Mesozoic continental vertebrates with associated palynostratigraphic dates from the northwestern Ethiopian Plateau. *J. Vertebr. Paleont*. 19: 728–741.

Goubin, N. 1965. Description ét répartition des principaux pollenites Permiens, Triassiques et Jurassique des sondages du Basin de Morondava (Madagascar). *Revue. Inst. fr. Pétrole* 20: 1415–1461.

Glaeser, J.E. 1978. Global distribution of barrier islands in terms of tectonic setting. *J. Geology* 86: 283–297.

Grabowsky, G.J. & Norten, I.O. 1995. Tectonic controls on the stratigraphic architecture and hydrocarbon systems of the Arabian Plate. In M.I. Al-Husseini (ed). *Middle East Petroleum Geosciences, Geo'94*: 413–430. Bahrain: Gulf PetroLink.

Gvirtzman, G., Klang, A. & Rotstein, Y. 1992. Early Jurassic shield volcano below Mount Carmel: new interpretation of the magnetic and gravity anomalies and implication for Early Jurassic rifting. *Israel J. Earth Sci*. 39: 149–159.

Hallam, A. 1988. A reevaluation of Jurassic eustasy in the light of new data and the revised Exxon curve. In C.K. Wilgus, B.S. Hastings, C.G.S.C. Kendall, H.W. Posamentier, C.A. Ross & Van Wagoner, J.C. (eds.), *Sea-Level Changes: An Integrated Approach*. *SEPM Spec. Publ*. 42: 261–273.

Hampson, G.J. & Howell, J.A. 2005. Sedimentologic and geomorphic characterization of ancient wave-dominated deltaic shorelines: Upper Cretaceous Blackhawk Formation, Book Cliffs, Utah, U.S.A. In L. Giosan, & J.P. Bhattacharya (eds.), *River deltas: Concepts, Models and Examples*. *SEPM Spec. Publ*. 83: 133–154.

Hankel, O. 1987. Lithostratigraphic subdivision of the Karoo rocks of the Luwegu Basin (Tanzania) and their biostratigraphic classification based on microfloras, macrofloras, fossil woods and vertebrates. *Geol. Rdsch*. 76: 539–565.

Hankel, O. 1993. Depositional cycles and palynostratigraphy of the Permo–Triassic and Early to Middle Jurassic of East Africa and Madagascar. In U. Thorweihe & H. Schandelmeier (eds.), *Geoscientific Research in Northeast Africa*: 351–355. Rotterdam: Balkema.

Hankel, O. 1994. Early Permian to Middle Jurassic rifting and sedimentation in East Africa and Madagascar. *Geol. Rdsch*. 83: 703–710.

Haq, B.U., Hardenbol, J. & Vail, P.R. 1987. Chronology of the fluctuating sea level since the Triassic. *Science* 235: 1156–1167.

Harms, J.C. 1979. Primary sedimentary structures. *Ann. Rev. Earth Plan. Sci*. 7: 227–248.

Harms, J.C., Southard, J.B., Spering, D.R. & Walker, R.G. 1975. *Depositional Environments as Interpreted From Primary Sedimentary Structures and Stratification Sequences, Short Course 2*: 1–153. Dallas: SEPM, Elsavier.

Harms, J.C., Southard, J.B. & Walker, R.G. 1982. *Structures and Sequences in Clastic Rocks, Short Course 9*: 1–249:Dallas: SEPM, Elsavier.

Harris, P.T. & Collins, M.B. 1985. Bedform distribution and sediment transport paths in the Bristol Channel and Severn Estuary. *Marine Geol*. 62: 153–166.

Hautot S, Whaler, K., Gebru, W. & Desissa, M. 2006. The structure of a Mesozoic basin beneath the Lake Tana area, Ethiopia, revealed by magnetotelluric imaging. *J. Afr. Earth Sci*. 44: 331–338.

Hayes, M.O. 1975. Morphology of sand accumulation in estuaries. In L.E. Cronin (ed.), *Estuarine Research*, *Vol. 2*: 3–22. New York: Acadamic Press.

Hayes, M.O. 1980. General morphology and sediment patterns in tidal inlets. *Sediment. Geol*. 26: 139–156.

Helby, R., Morgan, R. & Partridge, A.D. 1987. A palynological zonation of the Australian Mesozoic. *Mem. Assoc. Aust. Paleont*. 4: 1–94.

Helby, R., Morgan, R. & Partridge, A.D. 2004. *Updated Jurassic–Early Cretaceous dinocyst zonation NWS Australia*. Geosci. Austr. Publ.

Hiroki, Y. & Terasaka, T. 2005. Wavy lamination in a mixed sand and gravel foreshore facies of the Pleistocene Hosoya Sandstone, Aichi, Central Japan. *Sedimentology* 52: 65–75.

Hobday, D.K. & Horne, J.C. 1977. Tidally influenced barrier island and estuarine sedimentation in the Upper Carboniferous of southern West Virginia. *Sediment. Geol*. 18: 97–122.

Hofmann, C., Courtillot, V., Feraud, G., Rochette, P., Yirgu, G., Ketefo, E. & Pik, R. 1997. Timing of the Ethiopian flood basalt event and implications for plume birth and global change. *Nature* 389: 838–841.

Holbrook, J.M. 1996. Complex fluvial response to low gradients at maximum regression: a genetic link between smooth sequence boundary morphology and architecture of overlying sheet sandstone. *J. Sediment. Res*. 66: 713–722.

Honig, C. & Boyd, R. 1992. Estuarine sedimentation on the Eastern Shore of Nova Scotia. *J. Sediment. Petrol*. 62: 569–583.

Howard J.D. 1972. Trace fossils as criteria for recognizing shorelines in stratigraphic record. In J.K. Rigby & K. Hamblin (eds.), *Recognition of Ancient Sedimentary Environments*. *SEPM Spec. Publ*. 215–225.

Howard, J.D. 1975. The sedimentological significance of trace fossils. In R.W. Frey (ed.), *The Study of Trace Fossils*: 131–146. New York: Springer.

Howard, J. D., Elders, C. A. & Heinbokel, J.F. 1975. Estuaries of the Georgia coast, U.S.A. - Sedimentology and biology, V - Animal-sediment relationships in estuarine point bar deposits, Ogeeche River-Ossabaw Sound, Georgia: *Senckenbergiana Maritima* 7: 181–203.

Howard, J.D. & Reineck, H.E. 1981. Depositional facies of high-energy beach-to-offshore sequence: a comparison with low energy sequence. *AAPG Bull*. 65: 807–830.

Hoyt, J.H. 1967. Barrier island formation. *Geol. Soc. Am. Bull*. 78: 1123–1137.

Hubbard, D.K. & Barwis, J.H. 1976. Discussion of tidal inlet sand deposits: examples from South Carolina Coast. In M.O. Hayes & T.W. Kana (eds.), *Terrigenous Clastic Depositional Environments: Some Modern Examples*. *AAPG Field Course*. *Tech. Rep.* 11: 128–142.

Hughes, C.M.W 1988. Stratigraphy and rock unit nomenclature in the oil-producing area of Interior Oman. *J. Petrol. Geol*. 11: 5–60.

Hunter, R.E. & Clifton, E.H. 1982. Cyclic Deposits and Hummocky Cross-Stratification of Probable Storm Origin in Upper Cretaceous Rocks of the Cape Sebastian Area, Southwestern Oregon. *J. Sediment. Petrol*. 52: 127–144.

Hutchinson, R.W. & Engels, G.G. 1970. Tectonic evolution in the southern Red Sea and its possible significance to older rifted continental margins. *Geol. Soc. Am. Bull*. 83: 2989–3002.

Jespen, D.H. & Athearn, M.J. 1961. *Geologic plan and section of the left bank of the Blue Nile canyon near crossing of Addis Ababa-Debre Markos road*. U.S. Dept. Interior, Addis Ababa: Ethiopia's Water Res. Dept.

Jespen, D.H. & Athearn, M.J. 1964. *Land and Water Resources of the Blue Nile Basin. Geol. App. II*. Addis Ababa: U.S Dept. Interior.

Johnson, H.D. & Baldwin, C.T. 1996. Shallow clastic seas. In H.G. Reading (ed.), *Sedimentary Environments: Processes, Facies & Stratigraphy*: 232–280. Berlin: Blackwell Science.

Johnson, H.D. & Levell, B.K. 1995. Sedimentology of a transgressive, estuarine sand complex: Lower Cretaceous Woburn Sands (Lower Greensand), southern England. In A.G. Plint (ed.), *Sedimentary Facies Analysis: A Tribute to the Research and Teaching of Harold G. Reading. IAS Spec. Publ*. 22: 17–46.

Joubert, P.1963. Geology of the Wajir-Wajir Bor area. *Rep. Geol. Surv. Kenya* 57: 1–34.

Kainz, W. 1990. The Jurassic of the southern margin of the Arabian Plate between Habban and Al Mukalla (Yemen). *Z. geol. Wiss*. 18: 1157–1158.

Katz, M.B. 1987. East African rift and northeast lineaments: continental spreading-transform system? *J. Afr. Earth Sci*. 6: 103–107.

Kazmin, V. 1973. *The Geological Map of Ethiopia*. Scale 1: 2000000. Addis Ababa: Ethiopian Institute of Geological Survey.

Kazmin, V. 1975. *Explanation of the Geological Map of Ethiopia. Ethiopian Geol. Surv. Bull*. 1: 1–14.

Kazmin, V., Shiferaw, A. & Balcha, T. 1978. The Ethiopian basement: Stratigraphy and possible manner of evolution. *Geol. Rdsch*. 67: 531–546.

Kazmin, V., Tefera, M., Berhe, S. & Chewaka, S. 1979. Precambrian structure and metallogeny of western Ethiopia. *Geol. Surv. Egypt* 9: 1–18.

Kemp, E.M., Balme, B.E., Helby, R.J., Kyle, R.A., Playford, G. & Price, P.L. 1977. Carboniferous and Permian palynostratigraphy in Australia and Antarctica, a review. *BMR J. Aust. Geol. Geophys*. 2: 177–208.

Kendall, E. 1988. Aspects of evaporite basin stratigraphy. In B.C. Schreiber (ed.), *Evaporites*: 11-15. New York: Colombia University Press.

Kendall, A.C. & Harwood, G.M. (1996). Marine evaporites: arid shorelines and basins – In H.G. Reading (ed.), *Sedimentary Enviroments: Processes*, *Facies and Stratigraphy. 3rd ed.*: 281–324. Oxford: Blackwell Science.

Klein, G. de V. 1971. A sedimentary model for determining paleotidal range. *Bull. Geol. Soc. Am.* 82: 2585–2592.

Klitzsch, E. 1983. Paleozoic formations and a Carboniferous glaciation from the Gilf Kebir-Abu Ras Area in southwestern Egypt. *J. Afr. Earth Sci*. 1: 17–19.

Klitzsch, E. 1986. Plate tectonics and cratonal geology in Northeast Africa (Egypt, Sudan). *Geol. Rdsch*. 75: 755–768

Kraft, J.C., Chrzastowski, M.J., Belknap, D.F., Toscano, M.A. & Fletcher, C.H. 1987. The transgressive barrier-lagoon coast of Delaware: Morphostratigraphy, sedimentary sequences and responses to relative rise in sea level. In D. Nummedal, O.H. Pilkey & J.D. Howard (eds), *Sea Level Fluctuation and Coastal Evolution*. *SEPM Special Publ*. 41: 129–145.

Kraft, J.C., Biggs, R.B. & Halsey, S.D. 1973. Morphology and vertical sedimentary sequence models in Holocene transgressive barrier system. In D.R. Coates (ed.), *Coastal Geomorphology*: 321–354. Binghamton: State Univ. New York.

Kraus, M.J. 1999. Paleosols in clastic sedimentary rocks: their geologic applications. *Earth Sci. Rev*. 47: 41–70.

Kraus, M.J. & Aslan, A. 1993. Eocene hydromorphic paleosols: significance for interpreting ancient floodplain processes. *J. Sediment. Petrol*. 63: 453–463.

Kraus, M.J. & Hasiotis, S.T. 2006. Significance of different modes of rhizolith preservation to interpreting paleoenvironmental and paleohydrologic settings: examples from Paleogene paleosols, Bighorn Basin, Wyoming, U.S.A. *J. Sediment. Res*. 76: 633–646.

Krenkel, E. 1925. *Geologie Afrikas*. Berlin: Gebrüder Bomträger.

Kruck, W., Schäfer, U. & Thiele, J. 1996. Explanatory Notes on the Geological Map of the Republic of Yemen – Western Part. *Geol. Jb*. B87: 1–105.

Kruck, W. & Thiele, J. 1983. Late Paleozoic glacial deposits in the Yemen Arab Republic. *Geol. Jahrbuch* B46: 3–29.

Kuehl, S.A., DeMaster, D.J. & Nittrouer, C.A. 1986. Nature of sediment accumulation on the Amazon continental shelf. *Cont. Shelf Res*. 6: 209–225.

Kulp, M., Penland, S., Williams, S.J., Jenkins, C., Flocks, J. & Kindinger, J. 2005. Geological framework and sediment resources for restoration of the Louisiana coastal zone. In C.W. Finkl & S. Khailil (eds.), *Saving America's Wetland: Strategies for Restoration of Louisiana's Coastal Wetlands and Barrier Islands*. *J. Coastal Res. Spec. Issue* 44: 56–71.

Kumar, N. & Sanders, J.E. 1974. Inlet sequence: a vertical succession of sedimentary structures created by lateral migration of tidal inlets. *Sedimentology* 21: 491–532.

Kumpulainen, R., Uchman, A., Woldehaimanot, B., Kreuser, T. & Ghirmay, S. 2006. Trace fossil evidence from the Adigrat Sandstone for an Ordovician glaciation in Eritrea, NE Africa. *J. Afr. Earth Sci*. 45: 408–420.

Kvale, E.P., Cutright, J., Bilodeau, D., Archer, A.W., Johnson, H.R., & Pickett, B. 1995. Analysis of modern tides and implications for ancient tidalites. *Cont. Shelf Res*. 15: 1921–1943.

Lamare, P. 1930. Nature et extension des depots secondaires dana I'Arabie, I'Ethiopie et lea pays Somalis. *Mem. Soc. Geol. Fr*. 14: 49–68.

Le Nindre, Y.M., Manivit, J. & Vaslet, D. 1990a. Le Permo-Trias d'Arabie Centrale. Histoire géologique de la bordure occidentale de la plate-forme Arabe. Orleans: *Doc. Bur. Rech. Géol. Minièr* 193: 1–290.

Le Nindre, Y.-M., Manivit, J., Manivit, H., Vaslet, D., 1990b. Géodynamique et Paléogéographie de la plate-forme Arabe du Permien au Jurassique. Histoire géologique de la bordure occidentale de la plate-forme Arabe. *Doc. Bur. Rech. Géol. Minièr*. 192: 1–280.

Leatherman, S.P. & Williams, A.T. 1977. Lateral textural grading in overwash deposits. *Earth Surface Processes* 2: 333–341.

Leckie, D.A. & Walker, R.G. 1982. Storm- and tide-dominated shorelines in Cretaceous Moosebar-Lower Gates Interval – outcrop equivalents of Deep Basin gas trap in Western Canada. *AAPG Bull*. 66: 138–157.

Leeder, M.R. 1983. On the interaction between turbulent flow, sediment transport and bedform mechanics in channelized flows. In J.D. Collinson & J. Lewin (eds.), *Modern and Ancient Fluvial Systems*. *IAS Spec. Publ*. 6: 5–18.

Leeder, M.R. & Gawthorpe, R.L. 1987. Sedimentary models for extensional tilt-block/halfgraben basins. In M.P. Coward, J.F. Dewey & P.L. Hancock (eds.), *Continental Extensional Tectonics*. *Geol. Soc. Lond. Spec. Publ*. 28: 139–152.

Leithold, E.L. 1994. Stratigraphical architecture at the muddy margin of the Cretaceous Western Interior Seaway, southern Utah. *Sedimentology* 41: 521–542.

Leithold, E.L. & Dean, W.E. 1998. Depositional processes and carbon burial on a Turonian prodelta at the margin of the Western Interior Seaway. In W.E. Dean & M.A. Arthur (eds.), *Stratigraphy and Paleoenvironments of the Cretaceous Western Interior Seaway, USA*. *SEPM Concepts Sediment. Paleont*. 6: 189–200.

Levitte, D. 1970. *The Geology of Mekelle. Report on the Geology of the Central Part of Sheet ND 37-11*. Addis Ababa: Ethiopian Institute of Geological Survey.

Luger, P., Gröschke, M., Bussmann, M., Dina, A., Mette, W., Uhmann, A. & Kallenbach, H. 1994. Comparison of the Jurassic and Cretaceous sedimentary cycles of Somalia and Madagascar: implications for the Gondwana breakup. *Geol. Rdsch*. 83: 711–727.

MacEachern, J.A. Zaitlin, B.A. & Pemberton, S.G. 1999. A sharp-based sandstone of the Viking Formation, Joffre Field, Alberta, Canada: criteria for recognition of transgressively incised shoreface complexes. *J. Sediment. Res*. 69: 876–892.

MacEachern, J.A. & Bann, K.L. 2008. The role of ichnology in refining shallow marine facies. In G.J. Hampson, R.J. Steel, P.M. Burgess & R.W. Dalrymple. (eds.), *Recent Advances in Models of Siliciclastic Shallow Marine Stratigraphy*. *SEPM Spec. Publ*. 90: 77–116.

MacEachern, J.A., Bann, K.L., Bhattacharya, J.P. & Howell Jr., C.D. 2005. Ichnology of Deltas: Organism Responses to the Dynamic Interplay of Rivers, Waves, Storms and Tides. In L. Giosan & J.P. Bhattacharya (eds.), *River Deltas – Concepts, Models, and Examples*. *SEPM Spec. Publ*. 49–85.

MacEachern, J.A. & Pemberton, S.G. 1992. Ichnological aspects of Interior Seaway of North America. In S.G. Pemberton (ed.), *Applications of Ichnology to Petroleum Exploration: A Core Workshop* 17: 57–84.

MacEachern, J.A. & Pemberton, S.G. 1994. Ichnological aspects of incised valley fill systems from the Viking Formation of the Western Canada Sedimentary Basin, Alberta, Canada. In R. Boyd, B.A. Zaitlin & R.W. Dalrymple (eds.), *Incised Valley Systems: Origin and Sedimentary Sequences*. *SEPM Spec. Publ*. 51: 129–157.

Maejima, W. 1982. Texture and stratification of gravelly beach sediments, Enju Beach, Kii Peninsula, Japan. *J. Geosci*. 25: 35–51.

Maheshwari, H.K. & Kumaran, K.P.N. 1979. Upper Triassic sporae dispersae from the Tiki Formation. 1. Miospores from the Son river section between Tharipatar and Ghaiar, South Rewa Gondwana basin. *Palaeontographica* B171: 137–164.

Marzo, M. & Anadón, P. 1988. Anatomy of a conglomeratic fandelta complex: the Eocene Montserrat Conglomerate, Ebro basin, northeastern Spain. In W. Nemfc & R.J. Steel (eds.), *Fan-Deltas: Sedimentology and Tectonic Settings*: 318–340. Glasgow: Blakie.

Matire, L., Clari, P. & Pavia, G. 2000. Discontinuities and sequence stratigraphy of the Antalo Limestone (Upper Jurassic, North Ethiopia). *GeoRes. Forum* 6: 333–334.

McClure, H.A. 1980. Permian-Carboniferous glaciation in the Arabian Peninsula. *Geol. Soc. Am. Bull*. 91: 707–712.

McGowen, J.H. & Scott, A.J. 1975. Hurricanes as geological agents on the Texas coast. In L.E. Cronin (ed.), *Estuarine Research II, Geology and Engineering*: 23–46. New York: Academic Press.

Mckee, E.D. & Sterrett, T.S. 1961. Laboratory experiments on the form and structure of longshore bars and beaches. In J.A. Peterson & J.C. Osmond (eds.), *Geometry of Sandstone Bodies*: 13–28. Tulsa: AAPG.

McPherson, J.G., Shanmugan, G. & Moiola, R.J. 1987. Fan-deltas and braid deltas: varieties of coarse-grained deltas. *Geol. Soc. Am. Bull*. 99: 331–340.

Merla, G. & Minucci, E. 1938. *Missione geologica nel Tigrai*. Roma: Regia Accademia Italiana.

Merla, G., Abbate, E., Azzaroli, A., Bruni, P., Canuti, P., Fazzuoli, M., Sagri, M. & Tacconi, P. 1979. *Geological Map of Ethiopia and Yemen*. 1/2,000,000. *Comment*. Italy: Consiglio Nazionale delle Ricerche.

Merla, G., Abbate, E., Canuti, P., Sagri, M. & Tacconi, P. 1973. *A geological map of Ethiopia and Somalia*. Cons. Naz. Ricerche Firenze.

Mesfen, A. 1989. Sedimentary succession and probable Paleozoic rocks in the Fincha River Valley. In *Proc. 1st Geoscience and Mineral Development National Congress, Abstracts*. Addis Ababa: Ethiopian Institute of Geological Survey.

Mette, W. 1993. Stratigraphie und Fazies des Jura von Nordsomalia. *Berliner Geowiss. Abh*. A149: 1–125.

Miall, A. 1987. Recent developments in the study of fluvial facies models. In F.G. Ethridge, R.M. Flores & M.D. Harvey (eds.), *Recent Developments in Fluvial Sedimentology*. *SEPM Spec. Publ*. 39: 1–9.

Miall A.D. 1996. *The Geology of Fluvial Deposits: Sedimentary Facies, Basin Analysis, and Petroleum Geology*. Berlin: Springer.

Middleton, G.V. 1991. A short historical review of clastic tidal sedimentology. In D.G. Smith, G.E. Reinson, B.A. Zaitlin & R.A. Rahmani (eds.), *Clastic Tidal Sedimentology*. *Mem. Can. Soc. Petrol. Geol*. 16: 9–15.

Middleton, G.V. & Southard, J.B. 1984. Mechanics of sediment movement. *SEPM Short Course* 3: 1–401.

Miller, N.R., Alene, M., Sacchi, R., Stern, R.J., Conti, A., Kröner, A. & Zuppi, G. 2003. Significance of the Tambien Group (Tigrai, Northern Ethiopia) for Snowball Earth events in the Arabian-Nubian Shield. *Precamb. Res*. 121: 263–283.

Miller, D.J. & Eriksson, K.A. 2000. Sequence stratigraphy of Upper Mississippian strata in the central Appalachians: a record of glacio-eustasy and tectono-eustasy in a foreland basin setting. *AAPG Bull*. 84: 210–233.

Mitchum Jr, R.M. 1977. Seismic stratigraphy and global changes in sea-level, part 11: Glossary of terms used in seismic stratigraphy. In C.E. Payton (ed.), *Seismic Stratigraphy: Application to Hydrocarbon Exploration*. *AAPG Mem*. 26: 205–212.

Mohr, P.A. 1962. *The geology of Ethiopia*. Addis Ababa: Addis Ababa University Press.

Mohr, P.A. 1963. Occurrence of Karoo System sediments in Ethiopia. *Nature* 199: 1086–1086.

Morton, R.A. 1979. Temporal and spatial variations in shoreline changes and their implications, examples from the Texas Gulf Coast. *J. Sediment. Petrol*. 49: 1101–1112.

Moslow, T. & Tye, R. 1985. Recognition and characterisation of Holocene tidal inlet sequences. *Marine Geol*. 63: 129–151.

Müller, J., Klein, N., Bussert, R. & Dawit, L.E. 2007. Mesozoic vertebrates from the Adigrat Sandstone of Northern Ethiopia. *67th Annual Meeting of the Society of Verterbrate Palaeontology, Abstracts*. Texas.

Müller-Sohnius, D. & Horn, P. 1994. K-Ar dating of ring complexes and fault systems in northern Kordofan, Sudan – evidence for independent magmatic and tectonic activity. In H. Schandelmeier, R.J. Stern & A. Kröner (eds.), *Geology of Northeast Africa*. *Geol. Rdsch*. 83: 604–613.

Mulder, T. & Syvitski, J.P.M. 1995. Turbidity currents generated at river mouths during exceptional discharges to the world oceans. *J. Geology* 103: 285–299.

Murris, R.J. 1980. The Middle East: Stratigraphic Evolution and Oil Habitat. *AAPG Bull*. 64: 597–618.

Mutti, E., Rosell, J., Allen, G.P., Fonnesu, F. & Sgavetti, M. 1985. The Eocene Baronia Tide Dominated-Delta Shelf System in the Ager Basin. *IAS 6th European regional meeting, Excursion Guide-book*: 579–600. Lerida.

Nara, M. 1995. Rosselia socialis – A dwelling structure of a probable terebellid polychaete. *Lethaia* 28: 171–178.

Nichol, S.L. 1991. Zonation and sedimentology of estuarine facies in an incised valley, wave-dominated, microtidal setting, New South Wales, Australia. *Can. Soc. Petrol. Geol. Mem*. 16: 41–58.

Nichols, M.M. 1989. Sediment accumulation rates and relative sea-level rise in lagoons. *Mar. Geol*. 88: 201–219.

Nichols, M.M. & Biggs, R.B. 1985. Estuaries. In R.A. Davis (ed), *Coastal Sedimentary Environments*: 77–186. New York: Springer.

Nio, S.D. & Yang, C.S. 1991. Diagnostic attributes of clastic tidal deposits: a review. In D.G. Smith, G.E. Reinson, B.A. Zaitlin & R.A. Rahmani (eds.), *Clastic Tidal Sedimentology*. *Mem. Can. Soc. Petrol. Geol*. 16: 3–28.

Nummedal, D. & Swift, D.J.P. 1987. Transgressive stratigraphy at sequence bounding unconformities: some principles derived from Holocene and Cretaceous examples. In D. Nummedal, O.H. Pilkey & J.D. Howard (eds.), *Sea-Level Fluctuation and Coastal Evolution*. *SEPM Spec. Publ*. 41: 241–260.

Open University Team. 1989. *Waves, Tides and Shallow-water Processes*. Oxford: Pergamon Press.

Papini, M. & Benvenuti, M. 2008. The Toarcian–Bathonian succession of the Antsiranana Basin (NW Madagascar): Facies analysis and tectono-sedimentary history in the development of the East Africa-Madagascar conjugate margins. *J. Afr. Earth Sci*. 51: 21–38.

Pattison, S.A.J. 1992. Recognition and interpretation of estuarine mudstones (central basin mudstones) in the tripartite valley fill deposits of the Viking Formation, central Alberta. In S.G. Pemberton (ed.), *Applications of Ichnology to Petroleum Exploration – A Core Workshop*. *SEPM Core Workshop* 17: 223–249.

Pemberton, S.G. & MacEachern, J.A. 1997. The ichnological signature of storm deposits – The use of trace fossils in event stratigraphy. In C.E. Brett & G.C. Baird (eds.), *Paleontological Events-Stratigraphic, Ecological, and Evolutionary Implications*: 73–109. New York: Columbia University Press.

Pemberton, S.G., MacEachern, J.A. & Frey, R.W. 1992. Trace fossil facies models Environmental and allostratigraphic significance. In R.G. Walker & N.P. James (eds.), *Facies Models – Response to Sea Level Change*: 47–72. St John's: Geoscience Canada.

Pemberton, S.G. & Wightman, D.M. 1992. Ichnological characteristics of brackish water deposits. In S.G. Pemberton (ed.), *Applications of Ichnology to Petroleum Exploration. SEPM Core Workshop* 17: 141–167.

Penland, S., Suter, J.R. & Boyd, R. 1988. The transgressive depositional systems of the Mississippi River delta plain: A model for barrier shoreline and shelf sand development. *J. Sediment. Petrol*. 58: 932–949.

Pierce, S.E. & Benton, M.J. 2006. Pelagosaurus Typus Bronn, 1841 (Mesoeucrocodylia: Thalattosuchia) from the Upper Lias (Toarcian, Lower Jurassic) of Somerset, England. *J. Vertebr. Paleont*. 26: 621–635.

Pik, R., Deniel, C., Coulon, C., Yirgu, G., Hofmann C. & Ayalew, D. 1998. The Northwestern Ethiopian plateau flood basalts: classification and spatial distribution of magma types, *J. Volcanol. Geotherm. Res.* 81: 91–111.

Pik, R., Deniel, C., Coulon, C., Yirgu, G. & Marty, B. 1998. Isotopic and trace element signatures of Ethiopian flood basalts: evidence for plume-lithosphere interactions, *Geochim. Cosmochim. Acta* 63: 2263–2279.

Playford, G., Rigby, J.F. Archibald, D.C. 1982. A Middle Triassic Flora from the Moola-yember Formation, Bowen Basin, Queensland. *Publs. geol. Serv. Qd*. 380: l–52.

Plink-Björklund, P. & Steel, R.J. 2005. Deltas on falling-stage and lowstand shelf margins, Eocene Central Basin of Spitsbergen: importance of sediment supply. In L. Giosan & J. Bhattacharya (eds.), *River Deltas: Concepts, Models and Examples*. *SEPM Spec. Publ*. 83: 179–207.

Plummer, P.S. 1994. Mesozoic source rocks and hydrocarbon potential of the Seychelles offshore. *J. Petrol. Geol*. 17: 157–176

Plummer, P.S. & Gostin, V.A. 1981. Shrinkage cracks: desiccation or syneresis? *J. Sediment. Petrol*. 51: 1147–1156.

Poddar, M.C. 1964. *Mesozoics of western India: their geology and oil possibilities*. *Proc. XXII Int. Geol. Congress, sect. 1, part 1*: 126–143. New Delhi.

Posamentier, H.W. 2001. Lowstand alluvial bypass systems: incised vs. unincised. *AAPG Bull*. 85: 1771–1793.

Posamentier, H.W. & Allen, G.P. 1999. Siliciclastic Sequence Stratigraphy – Concepts and Applications. *SEPM Concepts in Sediment. Palaeont*. 7: 1–216.

Posamentier, H.W., Jervey, M.T. & Vail, P.R. 1988. Eustatic controls on clastic deposition, I. Conceptual framework. In C.K. Wilgus, B.S. Hastings, C.G.St.C. Kendall, H.W. Posamentier, C.A. Ross and J.C. van Wagoner (eds.), *Sea-Level Changes: An Integrated Approach*. *SEPM Spec. Publ*. 42: 109–124.

Posamentier, H.W. & Morris, W.R. 2000. Aspects of the stratal architecture of forced regressive deposits. *Geol. Soc. Lond. Spec. Publ*. 172: 19–46.

Posamentier, H.W. & Vail, P.R. 1988. Eustatic controls on clastic deposition, II. Sequence and systems tract models. In C.K. Wilgus, B.S. Hastings, C.G.St.C. Kendall, H.W. Posamentier, C.A. Ross & J.C. van Wagoner (eds.), *Sea-Level Changes: An Integrated Approach. SEPM Spec. Publ.* 42: 125–154.

Postma, G. 1984. Mass-flow conglomerates in a submarine canyon: Abrioja fan-delta, Pliocene, SE Spain. In E.H. Kosler & R.J. Steel (eds.), *Sedimentology of Gravels and Conglomerates. Can. Soc. Petrol. Geol. Mem.* 10: 237–258.

Postma, G. 1990. Depositional architecture and facies of river and fan deltas: a synthesis. In A. Colella & D.B. Prior (eds.), *Coarse Grained Deltas. IAS Spec. Publ.* 10: 13–27.

Price, P.L. 1983. *A Permian palynostratigraphy for Queensland, Permian Geology of Queensland*: 155–212. Brisbane: Geol. Soc. Aust., Queensl. Division

Rabinowitz, P.D., Coffin, M.F. & Falvey, D. 1983. The Separation of Madagascar and Africa. *Science* 220: 67-69.

Rahmani, R.A. 1988. Estuarine tidal channel and nearshore sedimentation of a Late Cretaceous epicontinental sea, Drumheller, Alberta, Canada. In P.L. De Boer, A. Van Gelder & S.D. Nio (eds.), *Tide-Influenced Sedimentary Environments*: 433–471. Dordrecht: Reidel Publishers & Co.

Rais-Assa, R. 1988. Stratigraphy and geodynamics of the Mombasa Basin (Kenya) in relation to the genesis of the proto-Indian Ocean. *Geol. Mag.* 125: 141–147.

Rampino, M.P. & Sanders, J.E. 1980. Holocene transgression in South-Central Long Island, New York. *J. sediment. Petrol.* 50: 1063–1080.

Reading, H.D. & Collinson, J.D. 1996. Clastic coasts, In H.G. Reading (ed.), *Sedimentary Environments: Processes, Facies & Stratigraphy*: 154–231. Berlin: Blackwell Science.

Reineck, H.E. & Singh, I. 1986. *Depositional Sedimentary Environments. With Reference to Terrigenous Clastics*: Berlin: Springer.

Reineck, H.E. & Wunderlich, F. 1968. Classification and origin of flaser and lenticular bedding. *Sedimentology* 11: 99–104.

Reinson, G.E. 1984. Barrier-Island and associated strand-plain systems. In R.G. Walker (ed.), *Facies Models. 2nd ed.* 119–140. St John's: Geoscience Canada.

Reinson, G.E. 1992. Transgressive barrier island and estuary systems. In R.G. Walker & N.P. James (eds.), *Facies Models: Response to Sea Level Change*: 179–194. St'Johns: Geological Association of Canada.

Reinson, G.E., Clark, J.E., & Foscolos, A.E. 1988. Reservoir geology of Crystal Viking Field, Lower Cretaceous Estuarine Tidal Channel-Bay Complex, South-Central Alberta. *AAPG Bull.* 72: 1270–1294.

Reiser, R.F. & Williams, A.J. 1969. Palynology of the Lower Jurassic sediments of the northern Surat Basin, Queensland. *Publs. geol. Surv. Qd 339, Palaeont. Pap.* 15: l–24.

Retallack, G.J. 1984. Completeness of the rock and fossil record: some estimates using fossil soils. *Paleobiology* 10: 59–78.

Retallack, G.J. 1988. Field recognition of paleosols. In J. Reinhardt & W.R. Sigleo (eds.), *Paleosols and Weathering Through Geologic Time: Principles and Applications. Geol. Soc. Am. Spec. Pap.* 216: 1–20.

Retallack, G.J. 1990. *Soils of the Past – An Introduction to Paleopedology*. London: Unwin Hyman.

Reynolds, P.O., Schandelmeier, H. & Semtner, A.K. 1997. Chapter 8. The Early Jurassic (Toarcian, ca. 180 Ma). In H. Schandelmeier & P.O. Reynolds (eds.), *Palaeogeographic-Palaeotectonic Atlas of Northeastern Africa, Arabia, and Adjacent Areas*: 51–54. Rotterdam: Balkema.

Reyre, Y. 1973. Palynologie du Mézozoique Saharien. *Mém. Mus. Nat. Hist. Natur.* 27: 1–284.

Riccardi, A.C. 1991. Jurassic and Cretaceous marine connections between the southeast Pacific and Tethys. *Palaeogeogr., Palaeoclimatol., Palaeoecol.* 87: 155–189.

Richards, M.A., Duncan, R.A. & Courtillot, V.E. 1989. Flood basalts and hotspot tracks: plume heads and tails. *Science* 246: 103–107.

Roy, P.S. 1994. Holocene estuary evolution – stratigraphic studies from southeastern Australia. In R. Boyd, B.A. Zaitlin & R.W. Dalrymple (eds.), *Incised Valley Systems – Origin and Sedimentary Sequences*. *SEPM Spec. Publ*. 51: 241–263.

Roy, P.S., Thom, B.G. & Wright, L.D. 1980. Holocene sequences on an embayed high energy coast: an evolutionary model. *Sediment. Geol*. 26: 1–19.

Russo, A., Assefa, G. & Atnafu, B. 1994. Sedimentary evolution of the Abbay River (Blue Nile) Basin, Ethiopia. *N. Jb. Geol. Paläont. Mh*. 5: 291–308.

Rust, B.R. 1978. Depositional models for braided alluvium. In A.D. Miall (ed.), *Fluvial Sedimentology*. *Mem. Can. Soc. Petrol. Geol*. 5: 605–625.

SACS: South African Committee for Stratigraphy 1980. Lithostratigraphy of the Republic of South Africa. Part 1: Stratigraphy of South Africa, South West Africa/Namibia and the Republics of Bophuthatswana, Transkei and Venda. In L.E. Kent (ed.), *Handbook Geological Survey of South Africa* 8: South Africa.

Saka, Y. & Miyata, T. 1979. *Directional structures and paleocurrent of the Duruma Sandstones (Karroo System) near Mombasa, Kenya*: 41–61. 4th Prelim. Rep. Afr. Stud. Nagoya University.

Salomon, J.C. & Allen, G. 1983. Rôle sédimentologique de la marée dans les estuaires à fort marnage. *Notes Mém. C.F.P*. 18: 35–44.

Saxena, G.N. & Assefa, G. 1983. New evidence on the age of the glacial rocks of northern Ethiopia. *Geol. Mag*. 120: 549–554.

Schandelmeier, H., Bremer, F. & Holl, H.G. 2004. Kinematic evolution of the Morondava rift basin of SW Madagascar – from wrench tectonics to normal extension. *J. Afr. Earth Sci*. 38: 321–330.

Schandelmeier, H. & Pudlo, D. 1990. The Central African Fault Zone (CAFZ) in Sudan – a possible continental transform fault. *Berliner geowiss. Abh*. A120: 33–44.

Schandelmeier, H., Reynolds, P.O., Semtner, A.K., 1997. Chapter 8. The Late Triassic (Norian, ca. 220 Ma). In H. Schandelmeier, P.O. Reynolds, A.K Semtner (eds.), *Palaeogeographic-Palaeotectonic Atlas of Northeastern Africa, Arabia, and Adjacent Areas*. 45–50. Rotterdam: Balkema.

Schmidt. D. & Werner, C. 1998. Early Cretaceous coastal plain sediments of the Muger Mudstone Formation. Abay River Basin, Ethiopia. *Zbt. Geol. Palaont*. 1: 293–309.

Scholle P.A. & Spearing, D. 1982. *Sandstone Depositional Environments*. *AAPG Mem*. 31. Tulsa: AAPG.

Schumm, S.A. 1968. Speculations concerning paleohydrologic controls of terrestrial sedimentation. *Geol. Soc. Am. Bull*. 79: 1573–1588.

Schwartz, R.K. 1982. Bedform and stratification characteristics of some modern small-scale washover sand bodies. *Sedimentology* 29: 835–849.

Scotese, C.R. 1991. Jurassic and Cretaceous Plate Tectonic Reconstructions. *Palaeogeogr., Palaeoclimatol., Palaeoecol*. 87: 493–501.

Seilacher, A. & Aigner, T. 1991. Storm deposition at the bed, facies and basin scale: the geological perspective. In G. Einsele, W. Ricken & A. Seilacher (eds.), *Cycles and Events in Stratigraphy*. 249–267. Berlin: Springer.

Sengör, A.M.C., Altiner, D., Cin, A., Ustaomer, T. & Hsü, K.J. 1988. Origin and assembly of the Tethyside orogenic collage at the expense of Gondwana Land. In M.G. Audley-Charles & A. Hallam (eds.), *Gondwana and Tethys*. *Geol. Soc. Spec. Publ*. 37: 119–181.

Sestini, G. 1989. Nile Delta: a review of depositional environments and geological history. In M.K.G Whateley & K.T Pickering (eds), *Deltas: Sites and Traps for Fossil Fuels*. *Geol. Soc. Lond. Spec. Publ.* 41: 99–127.

Shanley K.W. & McCabe P.J. 1993. Alluvial architecture in a sequence stratigraphic framework - a case history from the Upper Cretaceous of southern Utah, USA. In S.S. Flint & I.D. Bryant (eds.), *Quantitative Modelling of Clastic Hydrocarbon Reservoirs and Outcrop Analogs*. *IAS Spec. Publ*. 15: 21–55.

Shanley, K.W. & McCabe, P.J. 1994. Perspectives on the sequence stratigraphy of continental strata. *AAPG Bull*. 78: 544–568.

Sharland, P.R., Archer, R., Casey, D.M., Davies, R.B., Hall, S.H., Heward, A.P., Horbury, A.D. & Simons, M.D. 2001. *Arabian Plate Sequence Stratigraphy*. *GeoArabia Spec. Publ*. 2. Bahrain: Gulf PetroLink.

Shumburo, M.M. 1968. The Amba Aradam Formation (formerly the Upper Sandstone). Mobile Petroleum Ethiopia Inc., Unpublished report.

Simpson, E.L. & Eriksson, K.A. 1991. Depositional facies and controls on parasequence development in siliciclastic tidal deposits from the early Proterozoic, upper Mount Guide Quartzite, Mount Isa Inlier, Australia. *Can. Soc. Petrol. Geol. Mem*. 16: 371–387.

Sloss, L.L. Krumbein, W.C. & Duples, E.C. 1949. Intergrated facies analysis. In C.R. Longwell (ed.), *Sedimentary Facies in Geologic History*. *Geol. Soc. Am. Mem*. 39: 91–124.

Smith, D.G. 1988. Modern point bar deposits: analogous to the Athabasca oil sands. In P.L. De Boer, A. Van Gelder & S.D. Nio (eds.), *Tide-Influenced Sedimentary Environments and Facies*, 417–432. Dordrecht: Reidel Publishers.

Sonu, C.J. & Van Beek, J. 1971. Systematic beach changes on the Outer Banks, North Carolina. *J. Geol*. 79: 416–425.

Srivastava, S.K. 1966. Jurassic microflora from Rajasthan, India. *Micropalaeont.* 12: 87–103.

Stephenson, M.H., Osterloff, P.L. & Filatoff, J. 2003. Palynological biozonation of the Permian of Oman and Saudi Arabia: progress and challenges. *GeoArabia* 8: 467–496.

Stern, R.J. 1994. Arc assembly and continental collision in the Neoproterozoic East African Orogen: implications for the consolidation of Gondwanaland. *Ann. Rev. Earth Planet. Sci*. 22: 319–351.

Stern, R.J. & Abdelsalam, M.G. 1998. Formation of juvenile continental crust in the Arabian-Nubian Shield: evidence from granitic rocks of the Nakasib suture, NE Sudan. *Geol. Rdsch* 87: 150–160.

Stern, R.J. & Dawoud, A.S. 1991. Late Precambrian (740 Ma) charnockite, enderbite, and granite from Jabel Moya, Sudan: a link between the Mozambique Belt and the Arabo-Nubian Shield? *J. Geol*. 99: 648–659.

Suter, J.R., Berryhill, H.L. & Penland, S. 1987. Late Quaternary sea-level fluctuations and depositional sequences, Southwest Louisiana Continental Shelf. In D. Nummedal, O.H. Pilkey & J.D. Howard (eds), *Sea Level Fluctuation and Coastal Evolution*. *SEPM Special Publ*. 41: 199–219.

Swift, D. 1975. Barrier-Island Genesis: Evidence from the central Atlantic shelf, eastern USA. *Sediment. Geol*. 14: 1–43.

Swift, D, Moir, R. & Freeman, G.L. 1980. Quaternary rivers on the New Jersey shelf: relation of seafloor to buried valleys. *Geology* 8: 276–280.

Swift, D. & Nummedal, D. 1987. Hummocky cross-stratification, tropical hurricanes and intense winter storms. *Sedimentology* 34: 338–344.

Tadesse, K & Keller, G.R. 2006. A new regional assessment of the petroleum potential in Ethiopia. Abstract. *AAPG Annual meeting, April 1–4, 2007*. Longbeach, California.

Tadesse, T., Hoshino, M., Suzuki, K. & Iisumi, S. 2000. Sm–Nd, Rb–Sr and Th–U–Pb zircon ages of syn- and post-tectonic granitoids from the Axum area of northern Ethiopia. *J. Afr. Earth Sci*. 30, 313–327.

Tefera, M., Chernet, T. & Haro, W. 1996. Explanation of the Geological Map of Ethiopia. Addis Ababa: *Ethiopian Geol. Surv. Bull*. 3: 36–40.

Tefera, M., Chernet, T. & Haro, W. 1996. *Geological Map of Ethiopia, 1: 2000000. 2nd ed.* Addis Ababa: Ethiopian Institute of Geological Survey.

Teklay, M., Kroner, A. & Oberhansli, R. 1993. Reconnaisance Pb-Pb zircon ages from Precambrian rocks in eastern and southern Ethiopia and an attempt to define crustal provinces. In U. Thorweihe & H. Schandelmeier (eds.), *Geoscientific Research in Northeast Africa*: 133–138. Rotterdam: Balkema.

Temperley, B.N. 1952. A review of Gondwana rocks of Kenya Colony. *19th Int. Geol. Congr. Gondwana Symposium*: 195–208. Paris.

Terwindt, J.H.J. 1981. Origin and sequences of sedimentary structures in inshore mesotidal deposits of the North Sea. In S.D. Nio, R.T.E. Shuettenhelm & T.C.E. Van Weering, (eds.), *Holocene Marine Sedimentation in the North Sea Basin. IAS Spec. Publ.* 5: 4–26.

Terwindt, J.H.J. 1988. Paleotidal reconstructions of inshore tidal depositional environments. In S.D. Nio (ed.), *Tide-influenced Sedimentary Environments and Facies*: 233–263. Dordrecht: D. Reidel.

Tessier, B. 1993. Upper intertidal rhythmites in the Mony-Saint-Michel Bay (NW France): perspectives from paleo-reconstruction, *Marine Geol.* 10: 355–367.

Tessier, B., Archer, A.W., Lanier, W.P. & Feldman, H.R. 1995. Comparison of ancient tidal rhythmites (Carboniferous of Kansas and Indiana, USA) with modern analogues (the Bay of Mont-Saint Michel, France). In B.W. Flemming & A. Bartholom (eds.), *Tidal Signatures in Modern and Ancient Sediments. IAS Spec. Publ.* 24: 259–271.

Thomas, R.G., Smith, D.G., Wood, J.M., Visser, J., Calverly-range, E.A. & Koster, E.H. 1987. Inclined heterolithic stratification: terminology, description, interpretation, and significance. *Sediment. Geol.* 53: 123–179.

Tripathi, A. 2001. Permian, Jurassic and Early Cretaceous palynofloral assemblages from subsurface sedimentary rocks in Chuperbhita Coalfield, Rajmahal Basin, India. *Rev. Palaeobot. Palynol.* 113: 237–259

Truswell, E.M., Dettmann, M.E. & O'brien, P.E. 1999. Mesozoic palynofloras from the Mac. Robertson shelf, East Antarctica: geological and phytogeographic implications. *Antarctic Sci.* 11: 239–255

Tye, R.S., Bhattacharya, J.P., Lorsong, J.A., Sindelar, S.T., Knock, D.G., Puls, D.D. & Levinson, R.A. 1999. Geology and stratigraphy of fluvio-deltaic deposits in the Ivishak Formation; applications for development of Prudhoe Bay Field, Alaska. *AAPG Bull.* 83: 1588–1623.

Tye, R.S. & Moslow, T.F. 1993. Tidal inlet reservoirs: insight from modern examples. In E.G., Rhodes & T.F. Moslow (eds.), *Marine Clastic Reservoirs*: 77–99. Berlin: Springer.

Tyler, N. & Ethridge, F.G. 1983. Fluvial architecture of Jurassic uranium-bearing sandstones, Colorado Plateau, western United States. In J.D. Collinson & J. Lewin (eds.), *Modern and Ancient Fluvial Systems. IAS Spec. Publ.* 6: 533–547.

Unrug, R. 1992. The supercontinental cycle and Gondwanaland assembly: component cratons and the timing of suturing events. *J. Geodynamics* 16: 215–240.

Vail, J.R. 1990. Geochronology of the Sudan. *Overseas Geol. Miner. Resources* 66: 1–58.

Van Wagoner, J.C. 1995. Sequence stratigraphy and marine to nonmarine facies architecture of foreland basin strata, Book Cliffs, Utah, U.S.A. In J.C. Van Wagoner & G.T. Bertram (eds.), *Sequence Stratigraphy of Foreland Basin Deposits. AAPG Mem.* 64: 137–224.

Van Wagoner, J.C., Mitchum, R.M., Campion, K.M. & Rahmanian, V.D. 1990. Siliciclastic sequence stratigraphy in well-logs, cores, and outcrops – Concepts for high-resolution correlation of time and facies. *AAPG Methods in Exploration Series* 7: 55p.

Veevers, J.J. & Powell, C.M.A. (eds.), 1994. *Permian–Triassic Pangean basins and foldbelts along the Panthalassan margin of Gondwana. Geol. Soc. Am. Mem.* 184: 331–353.

Visser, M.J. 1980. Neap-spring cycles reflected in Holocene subtidal large-scale bedform deposits – A preliminary note. *Geology* 8: 543–546.

Walker, R.G. 1967. Turbidite sedimentary structures and their relationship to proximal and distal depositional environments. *J. Sediment. Petrol*. 37: 25–43.

Walker, R.G. & Cant, D.J. 1984. Sandy fluvial systens. In R.G. Walker (ed.), *Facies Models, 2nd ed. Geosci. Can. Rep. Series* l: 71–90.

Walker, R.G. & Plint, A.G. 1992. Wave and storm-dominated shallow marine systems. In R.G. Walker & N.P. James (eds.), *Facies Models: Response to Sea Level Change*: 219–238. St John's: Geological Association of Canada.

Warren, A., Yates, A.M. Damiani, R.J., Goodwin, M.B., Wood, C.B. & Schaff, C.R. 1998. The first temnospondyl amphibian (Stereospondyli: Capitosauroidea) from Ethiopia. *N. J. Geol. Palaont*. 11: 694–704.

Weimer, R.J., Howard, J.D. & Lindsay, D.R. 1982. Tidal flats and associated tidal channels. In P.A. Scholle & S. Spearing (eds.), *Sandstone Depositional Environments*, *AAPG Rep. Series* 10: 191–245.

Weimer, P. 1998. Sequence stratigraphy of Pliocene and Pleistocene turbidite systems, northern Green Canyon and Ewing Bank (offshore Louisiana), northern Gulf of Mexico. *AAPG Bull*. 82: 918–960.

Werner, C. 1995. Neue Funde von Mesozoischen Wirbeltieren in Äthiopien. *Berliner Geowiss. Abh*. E16: 377–383.

Wescott, W.A. & Ethridge, F.G. 1990. The Yallas Fandeltas – alluvial fans in coastal settings. In A.H. Racchoki & M. Church (eds.), *Alluvial Fans*: 195–212. New York: John Wiley & Sons.

Westermann, G.E.G., 1975. Bajocian ammonoid fauna of Tethyan affinities from the Kambe Limestone Series of Kenya and implication to plate tectonics. *Newsl. Stratigr*. 4: 23–48.

Westphal, F. 1962. Die Krokodilier des Deutschen und Englischen Oberen Lias. *Palaeontographica Abt*. A 118: 23–118.

Wilkinson, B.H. 1975. Matagorda Island, Texas: the evolution of a Gulf Coast barrier complex. *Geol. Soc. Am. Bull*. 86: 959–967.

Willis, J.W. 2005. Deposits of tide-influenced river deltas. In L. Giosan & J.P. Bhattacharya (eds.) *River Deltas: Concepts, Models and Examples*. *SEPM Spec. Publ*. 83: 88–129.

Woldetinsae, G. 2005. Gravity field and isostatic state of Ethiopia and adjacent areas. *J. Afr. Earth Sci*. 41: 103–117.

Wolela, A.M. 1997. Sedimentology, diagenesis and hydrocarbon potential of sandstones in hydrocarbon perspective rift basins (Ethiopia, UK, USA). Ph.D. thesis, The Queen's University, Belfast.

Wolela, A.M. 2008. Sedimentation of the Triassic–Jurassic Adigrat Sandstone Formation, Blue Nile (Abay) Basin, Ethiopia. *J. Afr. Earth Sci*. 52: 30–42.

Wood, C.B., Goodwin, M.B. Schaff, C.R. & Assefa, G. 1993. First Mesozoic vertebrates from the Ethiopian Plateau, Blue Nile Gorge Region, East Africa. *J. Vertebr. Paleont*. 13: 63–64.

Woodroffe, C.D., Chappell, J., Thom, B.G. & Wallensky, E. 1989. Depositional model of a macrotidal estuary and flood plain. South Alligator River, Northern Australia. *Sedimentology* 36: 737–756.

Wopfner, H. 1993. Structural development of Tanzanian Karoo Basins and the break-up of Gondwana. In R.H. Findlay, R. Unrug, M.R. Banks & J.J. Veevers (eds.), *Gondwana Eight: Assembly, Evolution and Dispersal*: 531–539. Rotterdam: Balkema.

Wopfner, H. 1994. The Malagasy Rift, a chasm in the Tethyan margin of Gondwana. *J. SE-Asian Earth Sci*. 9: 451–461.

Wopfner, H. & Casshyap, S.M. 1997. Transition from freezing to subtropical climates in the Permo-Carboniferous of Afro-Arabia and India. In I.P. Martini (ed.), *Late Glacial and Postglacial Environmental Changes*: 192–212. Oxford: Oxford University Press.

Worku, H. 1996. Structural control and metamorphic setting of the shear zone-related Au vein mineralization of the Adola Belt (southern Ethiopia) and its tectono-genetic development. *J. Afr. Earth Sci.* 23: 383–409.

Worku, T. 1988. Sedimentology, diagenesis and hydrocarbon potential of the Karoo sediments (Late Palaeozoic to Early Jurassic), Ogaden Basin, Ethiopia. Unpublished M. Phil. Thesis, University of Reading.

Worku, T. & Astin, T.R. 1992. The Karoo sediments (Late Palaeozoic to Early Jurassic) of the Ogaden Basin, Ethiopia. *Sediment. Geol*. 76: 7–21.

Wright, L.D., Wiseman, W.J., Bornhold, B.D., Prior, D.B., Suhayda, J.N., Keller, G.H., Yang, Z.S. & Fan, Y.B. 1988. Marine dispersal and deposition of Yellow River silts by gravity-driven underflows. *Nature* 332: 629–632.

Yang, B.C., Gingras, M.K., Pemberton, S.G. & Dalrymple, R.W. 2008. Wave-generated tidal bundles as an indicator of wave-dominated tidal flats. *Geology* 36: 39–42.

Yang, C.S. & Nio, S.D. 1989. An ebb-tide delta depositional model, a comparison between the modern Eastern Scheldt Tidal Basin (SW Netherlands) and the Lower Eocene Roda Sandstone in the Southern Pyrenees (Spain). *Sediment. Geol.* 64: 175–196.

Ye, L.S. & Kerr, D. 2000. Sequence stratigraphy of the Middle Pennsylvanian Bartsville Sandstone, northeastern Oklahoma: a case of an underfilled incised valley. *AAPG Bull.* 84: 1185–1204.

Yibas, B., Reimold, W.U., Armstrong, R., Koeberl, C, Anhaeusser, C.R. & Phillips, D. 2002. The tectonostratigraphy, granitoid geochronology and geological evolution of the Precambrian of southern Ethiopia. *J. Afri. Earth Sci*. 34, 57–84.

Zaitlin, B.A., Dalrymple, R.W. & Boyd, R. 1994. The stratigraphic organization of incised-valley systems associated with relative sea-level changes. In R.W. Dalrymple, R.J. Boyd & B.A. Zaitlin (eds.), *Incised Valley Systems: Origin and Sedimentary Sequences*. *SEPM Spec. Publ*. 51: 45–60.

Zaitlin, B.A. & Shultz, B.C. 1990. Wave-influenced estuarine sand body, Senlac heavy oil pool, Saskatchewan, Canada; In J.H. Barwis, J.G. McPherson & J.R. Strudlick (eds.), *Sandstone Petroleum Reservoirs*: 363–387. New York: Springer.

Ziegler, P.A. 1989. *Evolution of Laurussia. A study in Late Palaeozoic plate tectonics.* Dordrecht: Kluwer Academic.

# Appendix

## Sedimentary Petrographic Plates

## Plates I and II

**Plate I: Thin section photomicrographs from the Mekelle Basin**

A. Well-developed, discrete heavy mineral (mainly opaque) concentrations in the form of laminae indicating extensive reworking and concentration of grains by density in beach foreshore sandstones. Agwe section, upper part of *Unit I*, sample Ag 09.

B. Scattered glauconite grains in the barrier-lagoon system in the middle part of *Unit I*, Samre section, sample Sa 07.

C. Well-sorted and well-rounded quartzarenites reflecting deposition by the swash and backwash mechanism of waves in the beach foreshore environment. Megab section, upper part of *Unit III*, Sample Me 41.

D. Poorly sorted and angular to sub-rounded distributary mouth bar sandstones from the river-dominated delta. Agwe section, middle part of *Unit II*, Sample Ag 15.

E. & F. Microhummocky cross-lamination from lower shoreface sandstones. Abiadi section, middle part of *Unit I*, Sample Ad 07.

G. A lateritic paleosol marking the unconformity between *Unit II* and *Unit III* with well-developed rootlet mottles (arrow). The paleosol developed on top of an abandoned delta plain. Abiadi section, Sample Ad 26.

H. A paleosol marking the unconformity between *Unit I* and *Unit III* with well-developed clay skin (argillan and illuviation cutan) (arrow). Samre section, Sample Sa 18.

**Plate II: Thin section photomicrographs from the Blue Nile Basin**

A. Pervasive iron oxide/hydroxide cementation that characterises the *Red Unit* (*Unit I*) in the Blue Nile Basin. Dejen section, lower part of *Unit I*, sample De 07.

B. An example from the *White Unit* (*Unit II*), which is unaffected by pervasive iron oxide and/or hydroxide cementation. Dejen section, upper part of *Unit II*, sample De 42.

C. Effective grain rounding reflecting deposition by the swash and backwash mechanism of waves in the beach foreshore environment. Jejube section, uppermost part of *Unit I*, sample Ye 22.

D. Angular to sub-rounded fluvial channel fill sandstones from the lowermost part of the Fincha section, sample Fi 01.

E. Greenish (glauconite?) cement (arrows) indicating subaerial exposure. Uppermost part of the Dedu section, sample Dd 15.

F. Microscopic view of mud drapes on foresets (arrow) from flaser bedded estuarine sandstones (see Fig. 5.1g in the text). Yejube section, lower part of *Unit I*, sample Ye 02.

G. A paleosol marking the unconformity at the base of *Unit I* with well-developed angular blocky ped structures. The paleosol developed between the Adigrat Sandstone and the underlying Karoo-equivalent unit. Dejen Section, sample De 01.

H. A paleosol marking the unconformity between *Unit I* and *Unit II* with well-developed branching rootlet traces (arrows). Dejen section (see Fig. 5.9f in the text), sample De 34b.

## PLATE I

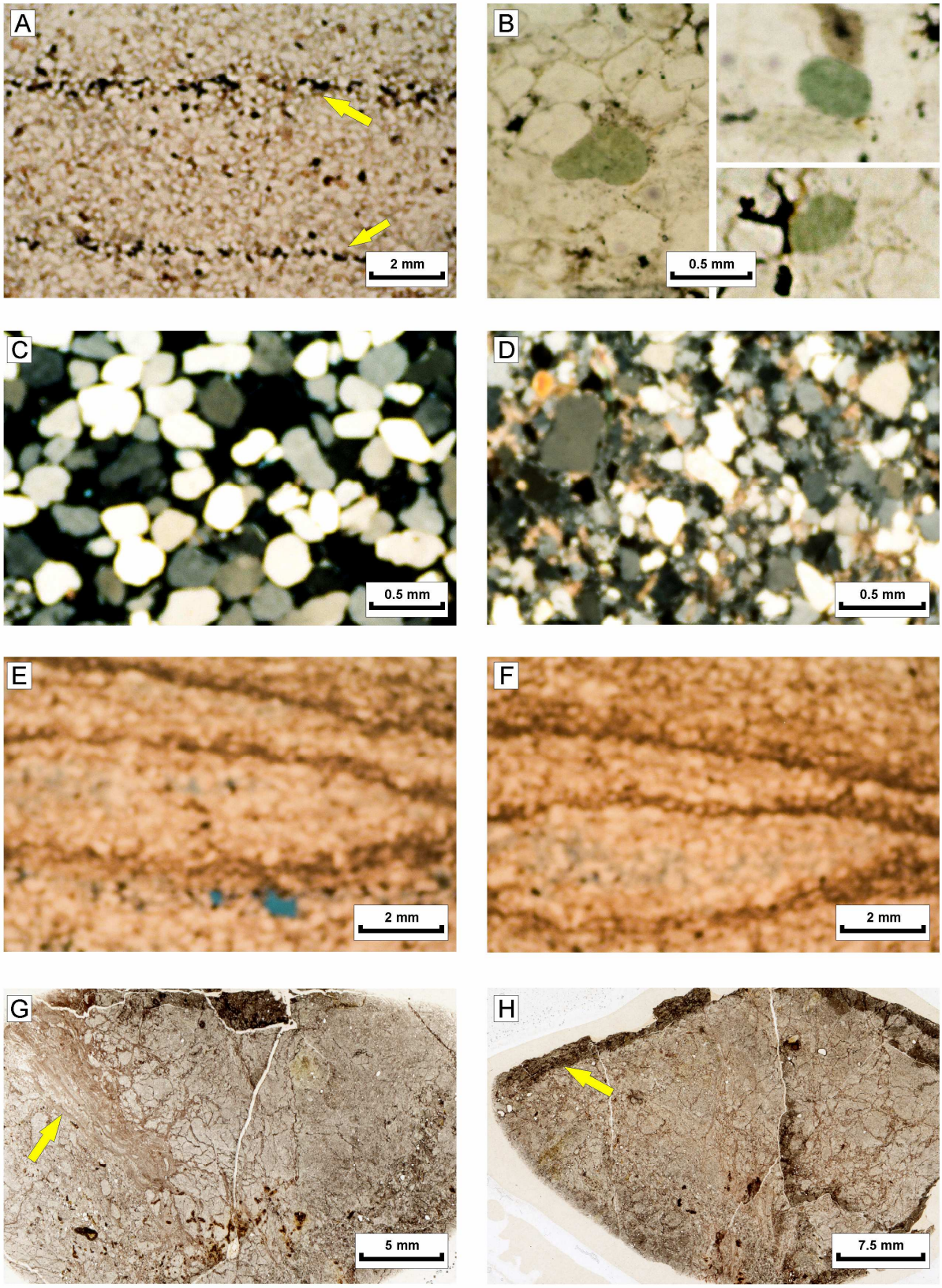

## PLATE II